Using artificial circulation for in-reservoir management of cyanobacteria and taste and odour metabolite production

(Alternative Format Thesis)

Slavin, Emily

Award date:
2021

Awarding institution:
University of Bath

Using artificial circulation for in-reservoir management of cyanobacteria and taste and odour metabolite production

Emily Slavin

A thesis submitted for the degree of

Doctor of Philosophy

University of Bath

Department of Architecture and Civil Engineering

April 2020

AUTHOR DECLARATIONS

This thesis contains my original work and no material previously published or written by another person except where referenced in the text. Contributions by others to the Journal article used in Chapter 4 of this thesis are clearly stated. The work presented in this thesis was carried out from the start of my Research degree at the University of Bath and does not include any other work submitted for another degree or diploma at any other institution.

The work in this thesis was financially supported by the Natural Environment Research Council (NERC) GW4+ Doctoral Training Partnership and CASE sponsored by Wessex Water.

COPYRIGHT

SUMMARY

The quality of raw water in reservoirs used for drinking water supply is projected to decline with the changing climate through prolonged thermal stratification and its associated water quality implications such as cyanobacterial blooms. To mitigate against water quality deterioration, in-reservoir artificial mixing techniques are often used to prevent the development of thermal stratification. Surface mixers are a relatively novel artificial mixing technique and are being increasingly installed in reservoirs to improve raw water quality, despite very limited observations of effectiveness. In this thesis, the hydrodynamics of surface mixer operation in a shallow, hypereutrophic reservoir was investigated using historical and in-reservoir measurements to assess their effects on cyanobacteria, taste and odour metabolite production, and soluble manganese concentrations. To understand the effects of surface mixers on taste and odour metabolite production in cyanobacteria, a greater understanding of the key trigger(s) of production was required. Here, water samples from the intakes of different reservoirs with varying trophic states were assessed using self-organising maps to determine the key trigger(s) in taste and odour metabolite production. The analysis revealed that high concentrations of ammonium relative to nitrate are important in the production of taste and odour metabolites in cyanobacteria. In-reservoir measurements of temperature, dissolved oxygen, and water velocities demonstrated that the range of influence of surface mixers were localised, but within the range of influence, temperature and dissolved oxygen gradients were reduced. Finally, despite the localised effects, surface mixer operation was found to decrease soluble manganese concentrations at the intake and increase cyanobacterial biomass. Although light penetration was low in the hypereutrophic reservoir, surface mixer operation did not effectively light-limit cyanobacteria to suppress photosynthesis as the water column depth was too shallow and mixing between light and nutrients created a beneficial growing environment for *Planktothrix*. Historical and in-reservoir observations showed that taste and odour metabolite concentrations were not affected by mixer operation but were susceptible to variable environmental conditions, such as heavy rainfall that can introduce a pulse of nutrients into the reservoir. Overall, surface mixer operation in a shallow, hypereutrophic reservoir poses a water quality management dilemma as the benefits of reduced soluble manganese concentrations at the intake need to be weighed against the cost of increased cyanobacterial biomass and greater risk of taste and odour event occurrence.

ACKNOWLEDGEMENTS

This PhD has opened doors for me that would otherwise have remained closed, so I thank everyone involved along the way, but there are some people who deserve specific recognition. Firstly, I would like to thank Chris for stepping into a supervisory role. Despite not being in his field of research, his help has been invaluable, and his motivation and positivity have been greatly received.

I would like to thank Danielle for the continuous support from across the pond and throughout the directional changes this project has taken. The project has changed since the original proposal she put forward, becoming more biologically focussed. Nonetheless, I need to thank her for pushing my boundaries to learn new things.

I would also like to thank Roo for the advice, keeping me focused, and for all the opportunities to meet industry experts. I have learnt a lot from him and hope to continue to work with him in the future.

Wessex Water enabled this project to happen. My thanks go to Steve for his help facilitating all the fieldwork and access to the laboratory. Thanks also to Mandy and Shrirunga, for teaching me new methods and keeping me sane through hours of phytoplankton identification. I would like to thank Tom and Paul for all their help at Durleigh and I hope this research helps with water quality management in the future.

Thank you to everyone who helped along the way, including Mahan, Yiyi, Annalise, Becca, and Stefano for help with fieldwork. Russell, for teaching me some German and Swedish. Andy B. for being the only person I can talk to about self-organising maps and their usefulness.

Although at times it was challenging, I am incredibly grateful for all the opportunities I have been given along the way and the chance to meet many brilliant people.

This research was supported by a GW4+ Doctoral Training Partnership studentship from the Natural Environment Research Council [NE/L002434/1] and additional funding was provided from CASE partner Wessex Water (YTL Group).

CONTENTS

LIST OF FIGURES

LIST OF TABLES

CHAPTER 1

INTRODUCTION

1.1 Research relevance: thermal stratification and artificial mixing to improve raw water quality

The changing climate threatens the production of drinking water for public supply, with the quality of surface water reservoirs predicted to decline (Delpla et al. 2009). Rising surface water temperatures are likely to prolong periods of thermal stratification (Komatsu et al., 2007) and decrease vertical mixing (Sahoo et al., 2011). More stable water columns favour cyanobacterial dominance (Reynolds et al. 1983) and internal loading of nutrients and soluble metals under thermal stratification (Wagner and Adrian, 2009; Paerl et al., 2016). Consequently, studies have predicted that the frequency and magnitude of cyanobacterial blooms will increase with climate change (O'Neil et al., 2012), which raises the risk of taste and odour (T&O) and toxin production (Bai et al., 2017). The perception of safe drinking water is largely based on aesthetic qualities, so customer complaints regarding T&O are a primary concern for water utilities (Webber et al., 2015). In drinking water reservoirs, cyanobacteria are considered one of the principal producers of T&O metabolites (Jüttner and Watson, 2007), and it has been suggested that the frequency of T&O events is increasing worldwide (Winter et al. 2011; Bai et al., 2017).

In-reservoir artificial mixing techniques are often used to address these water quality issues, although success has been mixed. For example, Visser et al. (2016) reviewed the effectiveness of continuous/intermittent operation of aeration techniques (e.g. bubble diffusers/curtains) at controlling cyanobacterial blooms from a range of case studies and reported decreased cyanobacterial biomass in seven cases, increases in two cases (one continuous and one intermittent), and no change in five cases. Moreover, Huisman et al. (2004) found that artificial mixing decreased cyanobacterial dominance by increasing turbulence and decreasing the buoyancy regulating advantage of some cyanobacteria species. However, some studies have indicated that cyanobacterial biomass does not always correlate with T&O or toxin concentrations over time (Graham et al., 2010; Watson et al., 2008), questioning the effectiveness of artificial mixing techniques for managing the risk of T&O events or toxin production in drinking water supply.

More recently, the use of surface mixers as a means of artificial circulation has been gaining traction with more being installed in drinking water reservoirs in England and Wales. However, aside from a white paper (Elliott and Swan, 2003) and a handful

of peer-reviewed papers (Lawson and Anderson, 2007; Morillo et al., 2009), there is limited literature regarding the effects of surface mixer operation on reservoir hydrodynamics. Consequently, how surface mixers affect the raw water quality in drinking water reservoirs is poorly understood.

1.2 Research objectives and thesis outline

This project uses historical data and in-reservoir observations to assess the effectiveness of surface mixers at mixing a shallow, hypereutrophic drinking water reservoir. Particular focus is given to the changes in hydrodynamics generated by the surface mixer, determining whether the range of influence covers a considerable area of the reservoir, or localised circulation cells as observed with the axial flow pumps in shallow Lake Elsinore (Lawson and Anderson, 2007). Once the effects of the mixers are determined, their effect on water quality can be examined. While Lawson and Anderson (2007) noted significant sediment resuspension and scouring of the bed from pump operation in Lake Elsinore, there have been no peer-reviewed studies reporting on whether raw water quality changed due to surface mixer operation. Therefore, in this PhD, the impact of surface mixers on phytoplankton and nutrient dynamics will be assessed for the first time. Using a shallow, hypereutrophic drinking water reservoir that has had surface mixers in operation since 2015 as a case study example, a measurement campaign was undertaken in 2018 to determine the effectiveness of surface mixers as an in-reservoir water quality management technique. To compare conditions during artificial mixing to natural mixing conditions only, the surface mixers were turned off twice during the measurement campaign, and monitoring during these shutdowns were considered as no mixing controls.

In the present work, particular focus is given to the effect of surface mixers on T&O metabolite production in cyanobacteria. Cyanobacteria are considered the primary source of T&O metabolites in drinking water reservoirs (Jüttner and Watson, 2007). Production occurs along the pathways of isoprenoid synthesis, but what triggers production along these pathways has not been elucidated. Therefore, in order to understand how surface mixers influence cyanobacteria and T&O production in drinking water reservoirs, the key trigger involved in T&O metabolite production needs to be identified.

To achieve these aims, the following research objectives and questions were created:

Objective 1. Understand how artificial circulation using surface mixers affects the raw water quality in a shallow, hypereutrophic drinking water reservoir

- Using historical data and in-reservoir observations from a case study example, can mixer operation be identified as the principal cause of changing raw water quality compared to other environmental factors?
- Are surface mixers an effective in-reservoir management technique for improving raw water quality in shallow drinking water reservoirs, and if so, how is raw water quality improved?
- Can the range of influence of the surface mixers be identified, and if so, is the entire target area mixed successfully?

Objective 2. Determine the key trigger in the production of taste and odour metabolites in cyanobacteria

- If T&O metabolite concentrations and cyanobacterial biomass are not always correlated over time, what triggers rapid production along the pathways of isoprenoid synthesis in cyanobacteria?
- Is the key trigger of T&O metabolite production in cyanobacteria the same across a range of sites?
- Can the trigger of rapid productivity be identified to enable more proactive management strategies for managing T&O events in drinking water reservoirs?

Objective 3. Ascertain whether artificial circulation with surface mixers effectively light-limits cyanobacteria in a shallow, hypereutrophic drinking water reservoir

- Is light-limitation the primary growth-limiting variable in a shallow, hypereutrophic drinking water reservoir?
- Can artificial circulation in a reservoir < 10 m suppress photosynthesis in cyanobacteria by increasing the time cells spend in darkness?
- Can artificial circulation reduce the internal loading of nutrients that can be utilised by phytoplankton, by increasing dissolved oxygen concentrations near the sediments?

Objective 4. Determine whether artificial circulation with surface mixers influences the production of taste and odour metabolites in cyanobacteria

- Has artificial mixing in a shallow, hypereutrophic drinking water reservoir decreased concentrations of T&O metabolites in the reservoir and entering the intake?
- Although elevated cyanobacterial biomass increases the risk of high T&O metabolite concentrations, they do not always correlate in time. So, is artificial circulation, which is designed to address cyanobacterial biomass, an effective management technique for controlling T&O events in drinking water reservoirs?

The research presented in this PhD combines historical data analysis and in-reservoir observations from Durleigh, a shallow, hypereutrophic drinking water reservoir. In the following chapter, the concepts associated with surface mixers are introduced and the limited number of existing surface mixer observations are discussed with observations from other artificial mixing techniques and consideration for shallow drinking water reservoirs (Section 2.2). In section 2.3 of Chapter 2, T&O metabolite production in cyanobacteria is examined and the potential triggers of metabolism along the pathways of isoprenoid synthesis are identified. The study site, equipment used, and 2018 measurement campaign are presented in Chapter 3. Data analysis methods are also described in Chapter 3, including self-organising maps, which are used in Chapter 4 to help identify the key trigger of T&O metabolite production in cyanobacteria. In Chapter 5, the effects of surface mixer operation on the hydrodynamics in a shallow, hypereutrophic reservoir are presented from the comprehensive 2018 measurement campaign. Chapter 6 combines historical water sample measurements from Durleigh with in-reservoir observations collected during the 2018 measurement campaign to determine whether surface mixer operation influences T&O metabolite production in cyanobacteria. Lastly, the findings from all results Chapters (4-6) are discussed in terms of water quality management in Chapter 7. Conclusions are made in relation to the objectives defined above and potential directions for future work are highlighted.

CHAPTER 2

LITERATURE REVIEW

2.1 Thermal stratification and raw water quality

The development of density layers within the water column affects the natural mixing regime of lakes and reservoirs (Elçi, 2008) and is referred to as thermal stratification. These layers are typically defined as the surface mixed layer (epilimnion) and the denser, more stagnant bottom waters (hypolimnion), which are often separated by a thermocline (Wetzel, 1983). Thermal stratification typically occurs during the summer in temperate water bodies, where heat inputs from solar radiation and warmer air temperatures limit the extent of vertical mixing driven by the wind and convection (McGinnis and Wüest, 2005). Reduced vertical mixing limits the vertical transport of oxygen to the hypolimnion, where demand for oxygen is typically highest (Zhang et al., 2015). The sediment oxygen demand (SOD) refers to both the demand for oxygen from biological and chemical processes in the sediments (Adams et al., 1982). For example, dissolved oxygen concentrations near the sediments decline due to microbial activity, which lowers redox potentials that can lead to the internal loading of metals (Davison, 1993; Boros et al., 2011; Munger et al., 2016) and nutrients (Kennedy and Walker, 1999). Internal loading of metals and nutrients from the sediments to the overlying water column impacts treatment requirements and can raise costs (Wagner, 2015). For example, increased internal loading of nutrients, such as orthophosphate, can promote algal growth. In addition, the increased stability of the water column promotes the dominance of cyanobacteria that have buoyancy regulating mechanisms (e.g. *Microcystis*, *Aphanizomenon*, and *Dolichospermum*), which can lead to blooms of cyanobacteria that have the potential to produce toxins or T&O metabolites (Visser et al., 2016; Chaffin et al., 2019). Water quality issues associated with thermal stratification are problematic for drinking water supply due to increased treatment costs and pressures to meet the drinking water quality standards defined by the relevant regulatory body.

Water quality issues associated with thermal stratification are predicted to increase with climate change. For example, Delpla et al. (2009) provide a comprehensive overview of how climate change is likely to influence the thermal regime of surface water supplies and the consequential impacts on drinking water production. Increasing surface water temperatures will not only prolong and strengthen stratification in reservoirs, but also promote microbial respiration that will enhance biological oxygen demand. Elevated microbial respiration is particularly pertinent for shallow reservoirs (Jöhnk et al., 2008), where hypolimnetic oxygen demand is typically

high (Kerimoglu and Rinke, 2013) and internal loading can make nutrients available directly to the photic zone (Welch and Cooke, 2005). As well as the effects of continuously increasing air temperatures, the frequency and magnitude of extreme events, such as floods and droughts, are predicted to increase as a consequence of climate change (Bates et al., 2008). An increase in extreme events will influence the concentrations of dissolved substances in water bodies (Delpla et al., 2009). For example, runoff from catchments following heavy rainfall events can increase turbidity and nutrient concentrations within reservoirs, and this has been shown to benefit cyanobacteria (Morabito et al., 2018). Therefore, to mitigate against the predicted water quality decline with climate change, artificial mixing solutions are increasingly used in drinking water supply reservoirs to prevent the development of thermal stratification and its associated water quality problems.

2.2 Artificial mixing and raw water quality

Many drinking water reservoirs worldwide have artificial mixing devices installed to mitigate raw water quality problems such as low dissolved oxygen (DO) concentrations (Wagner, 2015), internal loading of metals and nutrients (Abesser and Robinson, 2010), and high phytoplankton productivity (Visser et al., 2016). To diminish the negative effects of thermal stratification, artificial mixing devices are deployed to supply additional mixing energy to supplement naturally induced mixing via the wind, convection, and/or inflows that may otherwise be insufficient to uniformly mix the water column.

Artificial mixing systems aim to circulate or destratify the water body to homogenise the water column. The most common artificial mixing system used worldwide are bubble plumes/curtains (Sherman et al., 2000; Wagner, 2015), which are reported as having variable success for controlling cyanobacteria in lakes and reservoirs (Visser et al., 2016). Air-driven destratification systems move water using bubbles that are introduced in the deepest part of the reservoir, entraining bottom waters as they rise to the surface, where they mix with warmer, less dense surface waters, creating a fluid of intermediate density (Cooke et al., 1993). Upon reaching the surface, the mixed water detrains from the plume, sinks to a depth of neutral buoyancy and intrudes laterally away from the plume, which weakens stratification away from the plume (Sherman et al., 2000). However, McGinnis et al. (2004) reported localised destratification around a bubble plume in Lake Hallwil, Switzerland, where upon reaching the surface, the plume

water detrained and plunged downwards with little lateral propagation and was re-entrained into the plume. Additionally, Zic and Stefan (1994) suggested that the laterally intruding water did not substantially increase mixing between the epilimnion and hypolimnion in a stratified reservoir and in order for destratification to be successful, airflow rates needed to be higher. A range of different air flow rates were analysed by Lorenzen and Fast (1977), who concluded that 0.15 $m^3 s^{-1}$ per 1 km^2 of lake surface area should be sufficient to achieve stratification. The airflow rate proposed by Lorenzen and Fast (1977) has since been used in 'optimal' bubble diffuser design operation (Kortmann et al., 1994), but Visser et al. (2016) questioned the airflow rate, suggesting it may not be sufficient to entrain colonies of cyanobacteria and mix them out of the photic zone. Wagner (2015) suggests that having more diffusers over which the same airflow is distributed results in a larger volume of water moved, and Imteaz and Asaeda (2000) reported that increasing the number of diffusers is more effective for reducing chlorophyll-α concentrations. Some studies have suggested that air-driven destratification systems have successfully reduced surface bloom occurrence (Huisman et al., 2004; Visser et al., 2016), but others have reported increased cyanobacterial abundance, or no change (Knoppert et al., 1970; Oberholster et al., 2006; Tsukada et al., 2006). The introduction of air/oxygen into the water with bubbles increases the DO concentrations in the hypolimnion, which should reduce internal loading of soluble metals and nutrients from the sediments (Wagner, 2015). Sherman et al. (2000) observed slight DO concentration gradients during the summer with operation of bubble plumes in Chaffey Reservoir. The supply of DO from the surface layers (air-water exchange and photosynthesis) was maintained with mixing generated by the bubble plumes. However, Lindenschmidt and Hamblin (1997) reported that bubble plume/diffuser operation introduced phosphorus into the epilimnion, increasing the availability for phytoplankton and consequently leading to blooms.

Other techniques such as hypolimnetic oxygenation are used to improve raw water quality. Hypolimnetic oxygenation uses lower airflow rates that maintain stratification while increasing DO concentrations in the hypolimnion (Beutel and Horne, 1999). Hypolimnetic oxygenation is used for the indirect control of phytoplankton by increasing DO concentrations near the sediment-water interface (SWI) and subsequently decreasing the internal loading of reduced species (e.g. iron (Fe^{2+}), manganese (Mn^{2+}), phosphorus, and ammonia) from the sediments (Cooke et al., 1993; Beutel, 2006). Concentrations of soluble manganese were successfully reduced by hypolimnetic oxygenation in the bottom waters of Carvins Cove Reservoir (Bryant et al., 2011).

Bormans et al. (2016) reviewed case studies of hypolimnetic oxygenation for controlling phytoplankton and internal loading of nutrients from the sediments and reported that DO concentrations near the sediments generally increased, but a reduction in internal loading of nutrients was not always observed.

Recently, surface mixers have increasingly been used for the artificial circulation of lakes and reservoirs. The rise in surface mixer popularity is in part attributed to their claimed lower running and maintenance costs compared to bubble plumes/curtains (Elliott and Swann, 2003). Compared to air-driven destratification techniques, pumping systems are generally designed to move smaller volumes of the target volume each day and maintain mixed conditions rather than breaking down stratification (Wagner, 2015). Pumping systems generally either pump waters upwards or downwards. For example, surface mixers use an impeller situated at the surface of the water column, to pump surface waters downwards, where they mix with bottom waters (Wagner, 2015). On the other hand, updraft pumps use impellers to circulate bottom waters upwards to the surface to achieve the same results as surface mixers. However, observations of a solar-powered updraft pump in Falling Creek Reservoir revealed that the lateral circulation of waters around the pump was very weak, only extending up to 5 m from the pump (Upadhyay et al., 2013). Surface mixers are a relatively novel mixing technique, so the effectiveness of surface mixers at improving the raw water quality in lakes and reservoirs has not been widely researched.

2.2.1 Artificial circulation with surface mixers

Artificial circulation is a method of artificial mixing that aims to fully circulate the water column throughout the year, preventing thermal stratification and the subsequent water quality degradation. One increasingly common method is the use of surface mixers, where impellers situated near the surface of the water column rotate and push a plume of well-aerated water downward. The plume displaces bottom waters and causes upwelling away from the impeller, which creates a circulation cell (Punnett 1991; Figure 2.1a). In principle, the circulation of the water column sustains mixed conditions and prevents the development of stratification, therefore maintaining concentrations of DO throughout the water column preventing undesirable sediment-water interactions (Achmad, 2009; Wagner, 2015). The advective transport of DO through the water column is increased by the circulation (Elliott and Swan, 2003), facilitating aerobic microbial respiration and minimising the reduction of metals and

nutrients at the sediment-water interface and internal loading of reduced species (Beutel and Horne, 1999). However, there is limited peer-reviewed literature regarding the operation of surface mixers in lakes and reservoirs. Anecdotal and monitoring data from reservoirs with surface mixers highlight that complete mixing is uncommon as low DO concentrations near the sediments persist (Wagner, 2015), and the extent of destratification is often limited. For example, Lawson and Anderson (2007) assessed the range of influence of 20 axial flow pumps (type of impeller/surface mixer) in Lake Elsinore, California, where the mean depth ranged between 3 and 6.7 m. Pumps were arranged in groups of 4 with good coverage over the 10.5 - 13.1 km^2 lake basin, but results indicated local destratification occurred with a limited range of mixing, leading to the formation of localised circulation cells around the impellers.

Alternatively, Morillo et al. (2009) proposed that impeller operation produces a plume that descends to the depth of terminal penetration, where it rebounds and intrudes laterally away from the mixer at a depth of neutral buoyancy (Fischer et al., 1979; Figure 2.1b). The depth of terminal penetration is defined as the depth at which the negative upward buoyancy force overcomes the downward momentum of the plume (Fan, 1967). Laterally intruding water weakens stratification away from the mixer, in a similar manner to lateral intrusions generated by bubble plumes, this increases the effectiveness of natural mixing processes (Sherman et al., 2000), and enables the lateral transport of DO (Elliott and Swan, 2003). Monitoring data presented by Wagner (2015) showed that surface mixers increased the mixed layer depth without destratifying the water column, but low DO concentrations sometimes persisted near the sediments. However, these effects were typically observed in deeper water bodies, questioning whether the hydrodynamic effect of surface mixers varies between reservoirs of different depths.

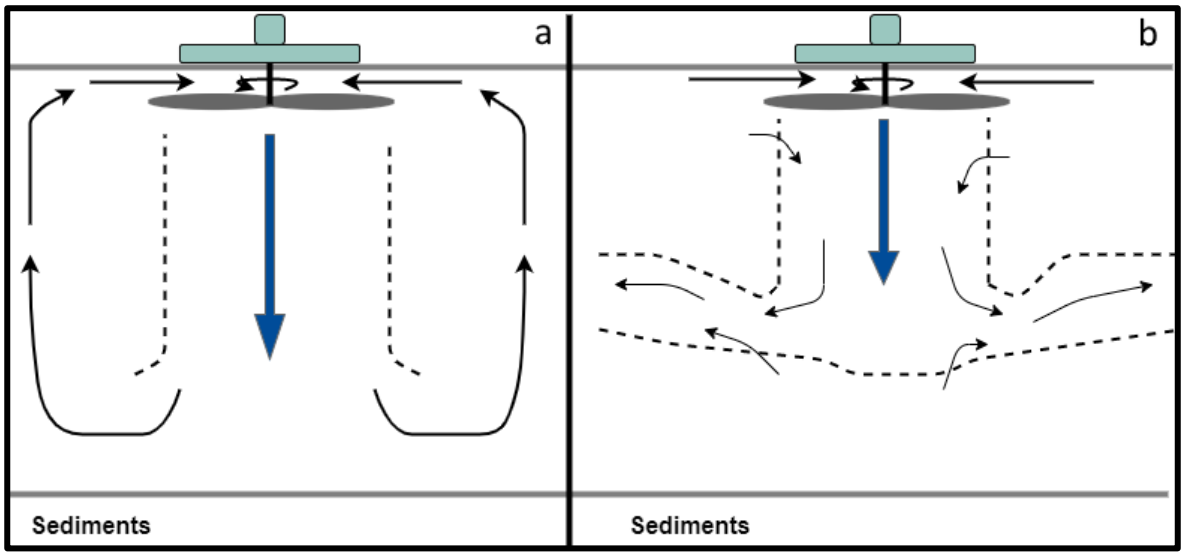

Figure 2.1a. Conceptual diagram of surface mixer operation in a shallow reservoir. The dashed line indicates the plume boundary. Rotation of the impeller draws in warmer, oxygen rich, surface waters and pushes these downwards. As the plume descends it entrains surrounding water. The momentum of the plume displaces bottom waters, which causes upwelling away from the impeller. Adapted from Gurney Environmental (2018). Figure 2.1b. Conceptual diagram of surface mixer operation, adapted from Morillo et al. (2009). Rotation of the impeller draws in warmer, oxygen rich, surface waters and pushes these downwards. The plume rebounds and intrudes laterally away from the impeller at a level of neutral buoyancy. As the intrusion spreads laterally, it weakens stratification away from the plume.

The amount of water moved by a surface mixer is proportional to the size and speed of the impeller. Therefore, correct sizing and operational design of impellers is essential to successfully mix the target area and optimise efficiency (Punnett, 1991). For instance, if the flow rate is too low, mixing will be insufficient to distribute DO through the water column or mix the target volume (Wagner, 2015). Conversely, if the flow rate is too high, there is a risk of sediment re-suspension, which is problematic for water supply as it leads to increased turbidity, and potential release of metals and nutrients into the water column (You et al., 2007; Chung et al., 2009; Matisoff et al., 2017). For shallow reservoirs, appropriate sizing and operational design of surface mixers is essential as there is a much greater risk that additional energy from mixers will cause sediment resuspension. However, mixing needs to be sufficient to provide oxygen to the bottom waters to satisfy the high SOD in shallow reservoirs. Lawson and Anderson (2007) observed notable sediment resuspension and scouring of the bed directly underneath the impellers in Lake Elsinore. However, a shallow reservoir in Illinois with one of the oldest reported surface mixers, was artificially mixed for 7 years in the 1980s. During this time, mixing led to typical DO concentrations >2 mg l^{-1} at the bed and metal concentrations decreased by around 95%, however total algae counts were

not effectively reduced (Wagner, 2015). The reservoir was also fitted with a deflection plate (a sheet of metal anchored to the bed) directly beneath the mixers, which may have aided the effectiveness of the mixing by reducing sediment resuspension in the immediate proximity of the mixer. Generally, there is a limited understanding of the extent of surface mixer influence, particularly in shallow reservoirs, and there is a need to better inform the operational design of surface mixers to reduce the risk of sediment resuspension (Objective 1, Chapter 1).

The response of a water body to naturally induced mixing depends on water body morphology and meteorological factors. Shallow reservoirs are less likely to maintain a stratified water column for the length of the summer as they are more sensitive to meteorological conditions (Kerimoglu and Rinke, 2013). For example, the mixing regime in shallow reservoirs can switch between stratified and mixed within the same day (Wallace et al., 2000; Stepanenko et al., 2013; Yang et al., 2018). When stratification does form in shallow eutrophic reservoirs, the small hypolimnetic to epilimnetic volume ratio can lead to high sediment oxygen demand (SOD) and nutrient release rates (Kerimoglu and Rinke, 2013). For example, microbial respiration and oxidative processes can deplete DO concentrations near the sediments can cause ammonification and reduction of iron (Fe^{3+} to Fe^{2+}) and manganese (MnO_2 to Mn^{2+}), with subsequent release of iron- or manganese-bound phosphorus (Wang et al., 2019). Nutrient release from the sediments can lead to increased phytoplankton productivity which, combined with metal release from the sediments, can be problematic for water treatment (Perkins and Underwood, 2001; Chowdhury et al., 2016; Tobiason et al., 2016). Theoretically, if correctly designed, surface mixer operation in shallow reservoirs should reduce the risk of ephemeral stratification and transport DO to the sediments, where demand is highest.

High phytoplankton biomass and productivity are common in shallow, eutrophic systems, and increase autochthonous sources of organic matters (OM). Decomposition of OM increases biochemical oxygen demand (BOD) and subsequently decreases DO concentrations in the bottom waters (Wetzel, 1983; Gons et al., 1992). The mineralisation of OM increases the bioavailability of nutrients such as ammonium (Fallon and Brock, 1979), phosphorus (Gao et al., 2013), and dissolved organic carbon (Li et al., 2018). Surface mixers are not primarily aerators/oxygenators; so surface mixers may not be the most suitable in-reservoir management solution if high BOD is a principal cause of water quality degradation. For example, a review determining which

artificial mixing or aeration system would be most suitable to improve water quality in the shallow, eutrophic, JC Boyle Reservoir (Oregon, USA) concluded that circulation was the least effective option (CH2M Hill, 2013). The primary water quality problem in the reservoir was low DO concentrations caused by loading of OM that elevated biochemical oxygen demand (BOD). Consequently, surface mixers were considered the least effective option as they are primarily mixing devices rather than aerators that introduce air/oxygen into the water column.

2.2.1.1 Summary

Generally, the influence of surface mixers on the hydrodynamics in reservoirs is not fully understood. Although a white paper (Elliott and Swan, 2003) suggests surface mixers have the capability to destratify, surface mixers are more commonly used to circulate the water column, preventing the development of stratification and transport DO to the bottom waters, where demand is highest (Wagner, 2015). Comparison between the observations from Lawson and Anderson (2007) and Morillo et al. (2009) demonstrate that surface mounted propellers can produce localised circulation cells around the pumps or deepen the mixed layer depth locally and the plume then intrudes laterally away from the pump, highlighting that the hydrodynamics of surface mixers may vary with basin morphology (shallow/deep). There is a need to improve understanding of the hydrodynamic effect of surface mixers and how they influence temperature and DO gradients within reservoirs (Objective 1), to better advise optimal operational design for improved raw water quality in drinking water reservoirs.

2.2.2 Artificial circulation and cyanobacteria

2.2.2.1 Cyanobacteria

Cyanobacteria are photosynthetic prokaryotes with an extensive evolutionary history that has enabled them to adapt and proliferate in a diverse range of environments, including aquatic systems (Whitton and Potts, 2012). In drinking water supply reservoirs, the production of secondary metabolites by cyanobacteria are a principal concern for water quality management as metabolites include toxins and T&O compounds, which can threaten the quality of water for consumers and toxins pose a risk public health (Falconer, 1999). The proliferation of cyanobacteria in lakes and reservoirs has been facilitated by climate change, with warmer water temperatures promoting optimal growth rates for cyanobacteria compared to other phytoplankton

groups (Paerl and Huisman, 2008). Increased water column stability and prolonged thermal stratification benefit bloom-forming cyanobacteria that use gas vesicles or other buoyancy mechanisms to regulate their position near the surface of the water column, often out-competing other phytoplankton through shading and limiting light penetration further into the water column (Paerl and Ustach, 1982). However, Richardson et al. (2019) recently acknowledged that extreme weather events may influence cyanobacterial growth, whereby heavy rainfall introducing a pulse of nutrients followed by prolonged, stable weather conditions may promote cyanobacterial growth (Paerl et al., 2016), whereas a turbid event following heavy rainfall may reduce light availability and limit growth (James et al., 2008). Despite consensus that cyanobacteria will continue to proliferate with increasing air and water temperatures, the increased unpredictability of extreme events and climate change introduce an element of uncertainty for controlling cyanobacteria in drinking water reservoirs. Consequently, strategies and techniques are sought by water quality managers to control the highly complex interacting factors that affect cyanobacterial productivity.

Anthropogenic nutrient enrichment has also been attributed to increased cyanobacterial dominance within drinking water reservoirs (Fernández et al., 2015). The cellular requirement of nitrogen and phosphorus is high relative to their availability, but excessive loading of these nutrients from allochthonous sources have been recognised as a cause of accelerated cyanobacteria proliferation (Lewis et al., 2011; Howarth et al., 2012). Successional nitrogen limitation has been reported in freshwater systems, where higher nutrient inputs lead to increased phytoplankton biomass during the spring and subsequent sedimentation of organic material. Decomposition of organic material and consumption of dissolved oxygen near the sediments leads to internal loading of phosphorus from the sediments (Karlson et al., 2015), making nitrogen the primary growth-limiting nutrient that benefits nitrogen-fixing cyanobacteria (Andersen et al., 2019). Some filamentous cyanobacteria have the capability to fix their own nitrogen using specialised heterocyst cells that create an anoxic environment, promoting nitrogenase enzyme activity (Golden and Yoon 2003). Nitrogenase enables the fixation of dinitrogen, providing nitrogen-fixing cyanobacteria with a competitive advantage during periods of nitrogen-limitation (Wolk et al., 1994). The various competitive adaptations of cyanobacteria enable different species to thrive under different conditions, which proves a nuisance for water quality management. Therefore, any in-reservoir artificial mixing techniques that aim to control cyanobacteria, should limit

internal loading of nutrients from the sediments by increasing dissolved oxygen availability near the sediments and preventing resuspension (Visser et al., 2016).

2.2.2.2 Artificial circulation effects on cyanobacteria

Although preventing the development of thermal stratification and improving DO distribution through the water column are the main aims of surface mixers, Elliott and Swan (2003) suggest that top-down circulation can also be used to control cyanobacterial biomass. Theoretically, the flow generated from surface mixer operation should entrain cells of cyanobacteria from the surface and transport them out of the photic zone for long enough to suppress photosynthesis and limit growth (Hobson et al., 2012). Furthermore, reduced water column stability minimises the buoyancy regulating advantage of some cyanobacteria that enable cells to maintain their position within the photic zone (Reynolds et al., 1987), which should reduce the risk of bloom formation and potentially shift phytoplankton community structure through competition (Visser et al., 2016). For example, Huisman et al. (2004) found that air bubble diffusers caused a shift away from a *Microcystis*-dominated phytoplankton assemblage to a diatom-dominated assemblage. This shift was attributed to increased turbulence generated by the bubble diffusers, which diminished the advantage of buoyant species such as *Microcystis* and entrained sinking phytoplankton, such as diatoms. Additionally, the case studies presented by Wagner (2015) suggested that artificial circulation had limited success at controlling cyanobacteria blooms. For example, one reservoir in the USA reported that copper sulphate still needed to be dosed despite surface mixer operation. Therefore, artificial mixing can manipulate competition between buoyant and sinking phytoplankton that could shift community dominance away from bloom-forming cyanobacteria, but if other treatments are still required, the artificial mixing cannot be considered successful.

In shallow, eutrophic systems, phytoplankton community composition is often driven by competition for the available light (Huisman et al., 2004), so even if buoyancy advantages are diminished, species that are low light-adapted may benefit from mixing. For instance, experiments by Reynolds et al. (1983) demonstrated that deep artificial mixing hindered the growth of buoyant *Microcystis* and *Dolichospermum* (then *Anabaena*) as cells were entrained and mixed out of the photic zone long enough to make them light-limited, but benefited low light-adapted *Oscillatoria agardhii* (now *Planktothrix agardhii*). Consequently, studies in shallow lakes have shown that artificial mixing frequently does not alter cyanobacterial biomass as the mixing is not deep

enough to limit light availability (Visser et al., 2016). Wagner (2015) suggests that in water columns <10 m deep, artificial circulation is unlikely to effectively reduce cyanobacterial biomass. Some shallow, eutrophic systems experience high turbidity due to suspended solids and high phytoplankton biomass through the water column, which limits light attenuation, suppressing phytoplankton productivity (Phlips et al., 1995). Although cells exposed to fluctuating light intensities may not experience significantly different growth rates compared to cells in continuous light intensity, the fluctuations may reduce the growth efficiency of cells (Köhler et al., 2017). Generally, mixing cyanobacteria out of the photic zone can be achieved with surface mixers in shallow reservoirs, but the shallow water column depth is unlikely to suppress photosynthesis long enough to light-limit cyanobacterial growth rates.

Typically, studies have determined the effectiveness of artificial mixing devices based on their ability to reduce cyanobacterial biomass (Heo and Kim, 2004; Visser et al., 2016), but T&O and toxin concentrations do not always correlate with biomass through time (Graham et al., 2010; Hollister and Kreakie, 2016; Beaver et al., 2018). Therefore, implementing artificial mixing solutions to reduce cyanobacterial biomass may not address the management concerns around secondary metabolite production.

2.2.2.3 Summary

Although studies of other artificial mixing techniques suggest that in shallow reservoirs, surface mixers will not effectively light-limit phytoplankton, there have been no direct observations of surface mixer operation as a technique for cyanobacterial control (Objective 3). Additionally, the effects of surface mixer and axial flow pump operation on nutrient dynamics in reservoirs has largely been overlooked (Objective 1). Therefore, understanding whether surface mixer operation in a shallow reservoir affects the light and nutrient availability through the water column is important for determining whether surface mixers will help mitigate against the rising frequency and magnitude of nuisance cyanobacterial blooms. Nevertheless, there is a need to verify whether managing cyanobacterial biomass effectively reduces the production of secondary metabolites, or whether these in-reservoir techniques are addressing a symptom (Objective 4).

2.2.3 Artificial circulation and metal concentrations

2.2.3.1 Iron and manganese in drinking water

Typical iron concentrations in drinking water are not considered harmful to public health and drinking water standards are instead defined for aesthetic reasons such as discolouration. For example, iron concentrations ~ 0.3 mg l^{-1} can cause reddish-brown discolouration to water supplies (Colter and Mahler, 2006). Elevated concentrations of manganese in drinking water are a worldwide public health concern. Exposure to high concentrations of manganese in drinking water has been reported to increase the risk of developing neurological health problems (Hafeman et al., 2007; Oulhote et al., 2014). The World Health Organisation (2004) defined 0.4 mg l^{-1} of manganese as the health-based upper limit for drinking water but is no longer used as the health-based standard is well above the standard for aesthetics of 0.1 mg l^{-1} (Frisbie et al., 2012; Munger et al., 2016). Manganese can cause discolouration (Kim and Jung, 2008), unfavourable tastes (Raveendran et al., 2001), and build up in network pipes (Sly et al., 1990; Tobiason et al., 2016) at > 0.1 mg l^{-1}. Therefore, drinking water standards are often considerably lower. For example, in England and Wales, the upper tolerable limit of manganese is 0.05 mg l^{-1} (Rumsby et al., 2014).

In drinking water reservoirs, the oxidation state of iron and manganese largely depends on microbial activity and concentrations of DO. Under oxidising conditions (higher redox potential), where DO concentrations are > 2 mg l^{-1}, manganese and iron occur as insoluble forms (Fe^{3+} and MnO_2) in sediments (Davison, 1993). In contrast, under reducing conditions (lower redox potential) the reductive dissolution of iron and manganese from the sediments into soluble forms (Fe^{2+} and Mn^{2+}) can occur (Davison, 1993). The accumulation of Fe^{2+} and Mn^{2+} in anoxic sediment pore waters drives diffusion along concentration gradients into the overlying water column and other processes such as sediment resuspension and bioturbation can also introduce Fe^{2+} and Mn^{2+} from the pore water in the overlying waters (Lesven et al., 2008). Oxidation of Fe^{2+} and Mn^{2+} in the water column depends on DO concentrations, pH, temperature, and microbial activity (Munger et al., 2016). For abiotic oxidation of Fe^{2+}, Davison (1993) reported a half-time (time taken for half of the initial mass of Fe^{2+} to be oxidised) of < 24 hours, whereas for Mn^{2+} the half-time is much longer, > 1 year (Munger et al., 2016). However, some studies have reported that manganese-oxidising organisms can accelerate the half-time of Mn^{2+} oxidation (Chapnick et al., 1982). For example,

Richardson et al. (1988) suggested that blooms of Microcystis facilitated manganese oxidation at high pH when photosynthesising, and Nealson and Saffarini (1994) state that the redox kinetics of iron and manganese are similar, so it is likely that many organisms have the metabolic ability to oxidise both. Nevertheless, removal of Mn^{2+} and MnO_2 from drinking water is required and different treatment options can be used for soluble and particulate forms, with particulate manganese generally being easier to remove (Tobiason et al., 2016). To ease treatment pressures, artificial mixing techniques are used to reduce the internal loading of soluble metals, like Mn^{2+}, in reservoirs and subsequently reduce concentrations entering the water treatment works.

2.2.3.2 Artificial circulation effects on metal concentrations

By increasing the concentrations of DO in the bottom waters through advective transport, artificial circulation aims to reduce internal loading of inorganic nutrients and soluble metals from the sediments (Wagner, 2015). Low DO concentrations near the sediment-water interface can lead to anoxic conditions near the sediments, promoting the reduction of Fe^{3+} to Fe^{2+} and of MnO_2 to Mn^{2+} and the subsequent diffusion of Fe^{2+} and Mn^{2+} into the overlying water (Zaw and Chiswell, 1999; Beutel et al., 2007). Moreover, the reduction to Fe^{2+} promotes the release of iron-bound phosphorus into the labile pool through diffusion or turbulent mixing, making it available for assimilation by phytoplankton (Wang et al., 2019). Although there are limited peer-reviewed studies into the effectiveness of surface mixers for reducing the internal loading of nutrients and metals from sediments, Wagner (2015) suggests that artificial circulation systems (e.g. surface mixers) are typically inadequate for maintaining mixed conditions during prolonged warm periods in the summer. Nevertheless, shallow reservoirs are more sensitive to meteorological conditions and are less likely to remain stratified throughout the summer (Kerimoglu and Rinke, 2013; Yang et al., 2018) Therefore, surface mixers may provide additional mixing energy reduce the likelihood of stratification developing in shallow reservoirs and maintain DO concentrations through the water column. However, Lawson and Anderson (2007) found a large area of anoxic sediments remained despite axial flow pump operation in shallow Lake Elsinore, suggesting that the advective transport of DO by artificial circulation may be insufficient to maintain DO concentrations in the bottom waters throughout the thermal stratification season. Trophic status may indirectly influence the oxidation state of metals in reservoirs. Eutrophic systems typically have higher concentrations of OM, which is most efficiently mineralised by microbes through aerobic respiration (den Heyer and Kalff,

1998). High rates of microbial decomposition deplete DO concentrations and lowers the redox potential, increasing the risk of internal loading of soluble manganese and iron into the overlying waters (Adams et al., 1982; Boros et al., 2011). Uncertainty remains around whether surface mixer operation can effectively transport DO through the water column to meet demand and minimise internal loading of soluble manganese and iron (and subsequently phosphorus) into the overlying water column.

2.2.3.3 Summary

Wagner (2015) suggests that surface mixer operation will likely be inadequate for maintaining DO concentrations near the sediments during thermal stratification. In shallower reservoirs, which are less likely to be stratified throughout the summer, surface mixer operation may maintain DO concentrations near the sediments, although sediment oxygen demand will be higher. However, observations by Lawson and Anderson (2007) suggest that despite axial flow pump operation, large areas of anoxic sediments remained, indicating that advective transport of DO is localised. However, concentrations of soluble metals were not reported. There is a need to better understand whether surface mixer operation can improve DO concentrations through the water column, and subsequently reduce internal loading of soluble metals from the sediments to reduce treatment pressures (Objective 1).

2.3 Taste and odour metabolite production in cyanobacteria

The perception of safe drinking water is largely based on aesthetic qualities, so customer complaints regarding T&O are a primary concern for water utilities (Webber et al., 2015). In this section, the two most common T&O metabolites, 2-methylisoborneol (2-MIB) and 1,10-dimethyl-trans-9-decalol (Geosmin), are introduced and their production by cyanobacteria, the most common source of these metabolites in drinking water reservoirs (Jüttner and Watson, 2007), is discussed.

2.3.1 Taste and odour metabolites

Typically, water utilities deem high cyanobacterial biomass to be a major problem in drinking supply reservoirs as they are known producers of T&O metabolites and toxins. Some studies have reported high concentrations of T&O metabolites and toxins at times of high cyanobacterial biomass, leading to the general assumption that high biomass causes high T&O concentrations. For example, Wnorowski and Scott (1990)

associated high Geosmin concentrations with the abundance of *Microcystis aeruginosa* in multiple reservoirs in South Africa as it was the dominant taxa in the phytoplankton community. However, it is now known that *Microcystis aeruginosa* is not a 2-MIB or Geosmin producer (Watson et al., 2016; Chong et al., 2018) and suggests that high biomass should not necessarily be used to infer high T&O concentrations (Watson et al., 2008).

Recently, Watson et al. (2016) highlighted the current reactive approach within the water industry for addressing T&O outbreaks in supply that tends to accept lower quality raw water due to algal metabolites and treat it accordingly. Reasons for this reactive approach include a lack of understanding of 2-MIB/Geosmin production, a lack of diagnostic tools, and the increasing magnitude of the problem (Harris et al., 2016; Watson et al., 2016). There is a need to understand the key trigger(s) in the production of 2-MIB and Geosmin in order to inform better management practices (Objective 2, Section 1.3). Therefore, current understanding of the metabolic pathways for T&O production in cyanobacteria and the possible factors triggering their production are discussed below.

2.3.1.1 Production of T&O Compounds in Water Supply Reservoirs

T&O events in drinking water supply associated with the secondary metabolites 2-MIB and Geosmin are increasing in frequency and magnitude worldwide (Winter et al., 2011; Bai et al., 2017). 2-MIB and Geosmin are naturally occurring tertiary alcohols that produce a musty (2-MIB) and earthy (Geosmin) odour (Rogers, 2001), and impart unfavourable tastes in drinking water. The thresholds of these metabolites in drinking water are very low at 6.3 ng l^{-1} for 2-MIB (molar mass: 168.28 g mol^{-1}) and 1.3 ng l^{-1} for Geosmin (molar mass: 182.33 g mol^{-1}; Wert et al., 2014). However, Webber et al. (2015) found that customers in Australia only deemed water ‘unacceptable’ when Geosmin concentrations were 30 ng l^{-1} and above, whereas the range of 2-MIB samples tested were not deemed ‘unacceptable’ (10 - 30 ng l^{-1}). Nevertheless, these compounds are one of the principal causes of customer complaints to water utilities worldwide (Bai et al., 2017) and over recent years the number of consumer complaints has been growing (Rogers, 2001). Biodegradation rates of 2-MIB and Geosmin are slow (Ho et al. 2007) and the removal of 2-MIB and Geosmin involves expensive treatment, such as ozonation and powdered/granulated activated carbon filtration (Greenwald et al. 2015), and these treatments are not always fully effective (Ashitani et al., 1988; Dunlap et al.,

2015). Therefore, understanding the trigger(s) of 2-MIB and Geosmin production in cyanobacteria can help to reduce the stress on treatment and aid water companies in meeting T&O compliance limits.

Producers of 2-MIB and Geosmin include fungi, actinomycetes, phytoplankton, and higher plants (Jüttner and Watson, 2007). Cyanobacteria are commonly reported as the source of T&O production in drinking water supply reservoirs (Jüttner, 1984; Suffet et al., 1996; Jüttner and Watson, 2007). T&O producing cyanobacteria can be planktonic or form benthic biofilms in shallow regions (Watson and Ridal, 2004). A review by Jüttner and Watson (2007) summarises all cyanobacteria known or reported to produce 2-MIB and Geosmin. However, Watson et al. (2008) state that even between closely related taxa there can be a large range in production capacity of 2-MIB and Geosmin.

2-MIB and Geosmin appear to be precursors for important cellular compounds such as sterols and pigments, although the biological use of 2-MIB and Geosmin within cells is not fully understood (Bentley and Meganathan, 1981; Watson, 2004). Production occurs along the metabolic pathways for isoprenoid synthesis: the 2-methylerythritol-4-phosphate isoprenoid (MEP) pathway, the mevalonate (MVA) pathway, and Leucine pathway (Figure 2.2; Jüttner and Watson, 2007). The MEP pathway is considered an alternate, or concomitant pathway to the MVA and Leucine pathways (Seto et al., 1996), all of which are found in cyanobacteria (Jüttner and Watson, 2007). Depending on the growth phase and environmental factors, cyanobacteria cells store or release 2-MIB and Geosmin (Watson et al., 2016). For example, Rosen et al. (1992) found that Geosmin was released by *Dolichospermum circinalis* during the stationary phase due to cell lysis, and intracellular Geosmin was greatest during the exponential growth phase. Watson (2003) states that release of intracellular pools of 2-MIB/Geosmin are most likely during the stationary phase or at the onset of senescence. Lysis of cells typically releases any remaining intracellular 2-MIB/Geosmin into the surrounding water (Watson et al., 2008; Lee et al., 2017), which explains why T&O concentrations can be associated with high biomass. During the rapid growth phase in actinomycetes, the MEP pathway was found to dominate (Seto et al., 1996), and high 2-MIB concentrations have been reported during periods of high Adenosine triphosphate (ATP) synthesis (Behr et al., 2014). Production of T&O compounds during periods of high productivity could explain why some studies fail to find a correlation between 2-MIB/Geosmin concentrations and biomass over time (Seto et al., 1996; Watson et al., 2008; Graham et al., 2010; Xuwei et al., 2019). Consequently, caution needs to be taken using water quality models, for example Chong

et al. (2018), which are based on cyanobacterial abundance to predict T&O outbreaks. Although it is generally accepted that 2-MIB and Geosmin are produced along the pathways of isoprenoid synthesis, what triggers productivity along these pathways has been less well studied.

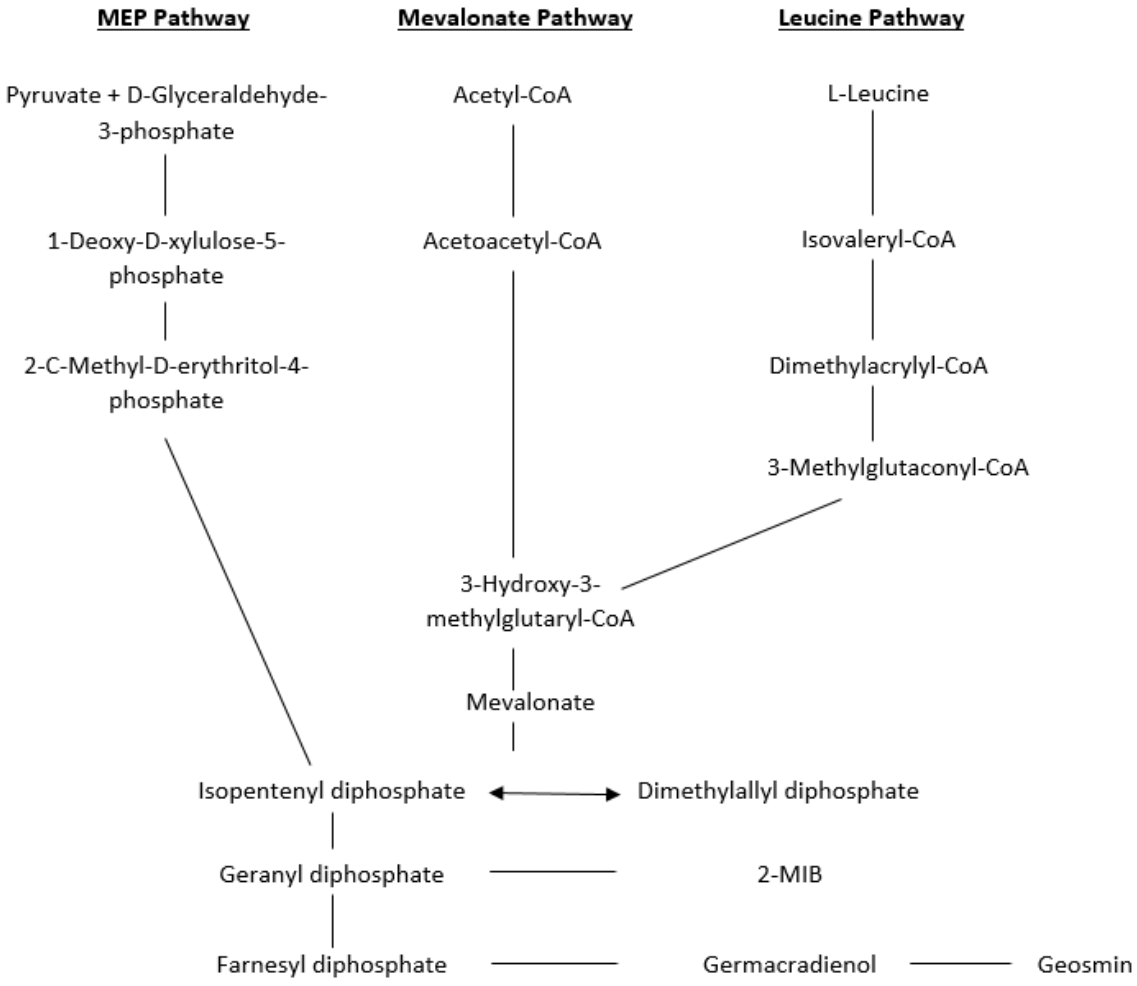

Figure 2.2 A simplified schematic of the 3 isoprenoid pathways that produce 2-MIB and Geosmin in cyanobacteria. Adapted from Jüttner and Watson (2007).

2.3.1.2 Nutrients and T&O metabolites

Nutrient ratios, for example total nitrogen to total phosphorus (TN:TP), have been used to monitor and predict when cyanobacterial dominance is more likely (Hall et al., 2005). A TN:TP threshold of 16:1 was defined by Redfield (1958), but Smith (1983) suggested that cyanobacteria dominance was likely at TN:TP ratios < 29. The TN:TP ratio has since been used to monitor and predict for T&O events and higher toxin

concentrations (Keene, 2002). However, in eutrophic systems where nutrients are abundant and phytoplankton are more light-limited, the TN:TP ratio is less predictive of cyanobacterial productivity (Huisman et al., 2004).

Ratios of different fractions of nitrogen, such as concentrations of ammonia (NH_3) relative to nitrate (NO_3), may also influence growth in cyanobacteria (Watson et al., 2008). For example, McCarthy et al. (2009) studied two shallow, eutrophic systems and found increased cyanobacterial dominance with decreasing TN:TP and increasing NH_4:NO_x ratios at Lake Okeechobee. At Lake Taihu, cyanobacterial dominance increased with decreasing TN:TP ratio but changes in the NH_4:NO_x did not appear to influence phytoplankton community structure. However, McCarthy et al. (2009) focussed on effects of these nutrient ratios on the dominance of cyanobacteria within the phytoplankton community and not the effects on production of T&O metabolites.

More recently, Harris et al. (2016) studied the TN:TP and NO_3:NH_3 ratios across a range of eutrophic reservoirs and found that higher 2-MIB, Geosmin, and Microcystin concentrations were more likely to occur at TN:TP ratios < 30. Higher concentrations of 2-MIB, Geosmin, and Microcystin were also associated with lower NH_3:NO_3 ratios. These associations suggest that phosphorus and more reduced forms of nitrogen are likely to influence the production of T&O metabolites in cyanobacteria. Experiments by Aubriot and Bonilla (2012) demonstrated that the uptake of phosphate in bloom-forming cyanobacteria is rapid (beginning within 15-25 minutes) and suggest that the elevated rates of uptake promote higher growth rates. Therefore, higher phosphate concentrations may cause rapid growth in cyanobacteria and potentially trigger production of T&O metabolites along the pathways of isoprenoid synthesis. Ammonium is the most reduced form of nitrogen and is the least energetically expensive nitrogen fraction that phytoplankton can assimilate (Flores and Herrero, 2005). Consequently, rates of assimilation of ammonium are faster than oxidised fractions of nitrogen (NO_3 and NO_2) because assimilation of these oxidised fractions requires the use of nitrate and/or nitrite reductase (Collos and Berges, 2009). Hence, faster assimilation of ammonium promotes more rapid growth in cyanobacteria.

Although both phosphorus and reduced forms of nitrogen have been suggested to promote rapid growth in cyanobacteria and been associated with higher concentrations of T&O and toxins, the trigger(s) of production along isoprenoid pathways in cyanobacteria remain unknown. In addition to nutrient concentrations, T&O production in cyanobacteria has also been suggested to be influenced by temperature, light, pH, and

turbulence (Wu and Jüttner, 1988; Rashash et al., 1995; Zhang et al., 2009; Watson et al., 2016). Therefore, a better understanding of key factors stimulating the production of T&O metabolites in cyanobacteria is needed to inform water quality management (Objective 2, Section 1.3).

Furthermore, there appears to be no peer-reviewed literature describing the effects of artificial circulation on the production of T&O metabolites in cyanobacteria (Objective 4). Research has predominantly focussed on using artificial circulation to reduce cyanobacterial biomass and reduce the frequency and magnitude of cyanobacterial blooms (Visser et al., 2016), which is assumed to be associated with T&O and toxin production in cyanobacteria. Therefore, continuing from section 2.2.2, artificial mixing techniques designed to address cyanobacterial biomass may reduce the risk of T&O events, but not directly address the triggers of T&O metabolite production in cyanobacteria.

2.3.1.3 Summary

Consensus within the literature is that 2-MIB and Geosmin are produced along the pathways of isoprenoid synthesis in cyanobacteria (Jüttner and Watson, 2007). Some research suggests that 2-MIB and Geosmin production is greatest during high productivity (Zimmerman et al., 1995), which is would explain why large 2-MIB concentrations have been reported at times of high ATP synthesis (Behr et al., 2014). The production of 2-MIB and Geosmin during high productivity also explains why some studies fail to see correlations between phytoplankton biomass and T&O concentrations over time (Graham et al., 2010). Jüttner and Watson (2007) state that cyanobacteria are the principal source of T&O compound production in drinking water reservoirs. Therefore, it is important to understand the key trigger(s) of T&O production to inform management of water supply reservoirs and determine if the trigger(s) is universal for all sites or differs depending on site characteristics (Objective 2, Section 1.3). In this thesis, Chapter 4 investigates the trigger(s) of T&O production in drinking water reservoirs.

CHAPTER 3

STUDY SITE, EQUIPMENT, AND METHODS

3.1 Introduction

Descriptions of the main study site (Section 3.2), measurement campaign (Section 3.3), and equipment (Section 3.4) referred to in Chapters 5 and 6 are detailed in this Chapter. Analysis using Self-Organising Maps, which is presented in Chapter 4, is discussed in detail in Section 3.5.2.

3.2 Study Site

The primary study site discussed in Chapters 5 and 6 is Durleigh Reservoir (Figure 3.1), which is owned and managed by Wessex Water. Other sites included in the statistical analyses described in Chapter 4 are: Blagdon Lake, Chew Valley Lake, Cheddar Reservoir (all owned and managed by Bristol Water and situated in the Mendips), Plas Uchaf and Dolwen reservoirs (managed by Dŵr Cymru Welsh Water and located in North Wales). A brief description of these study sites is included in Chapter 4, Section 4.2.1 and the historical data analysis is described in Section 3.6.

Figure 3.1. Photograph of Durleigh Reservoir (Source: Author).

3.2.1 Durleigh Reservoir, Somerset, UK

Durleigh reservoir is a small (0.33 km^2), shallow, lowland drinking water reservoir located near Bridgwater, Somerset (UK). At full capacity, the mean depth of the reservoir is 3.1 m and the maximum depth is 8.1 m (Figure 3.2). There are two main inflows, a natural river inflow from Durleigh Brook (tributary of the River Parrett) at the western end of the reservoir, and an intermittent pumped inflow with water taken

from the Bridgwater and Taunton canal that enters the reservoir on the south side (Figure 3.2).

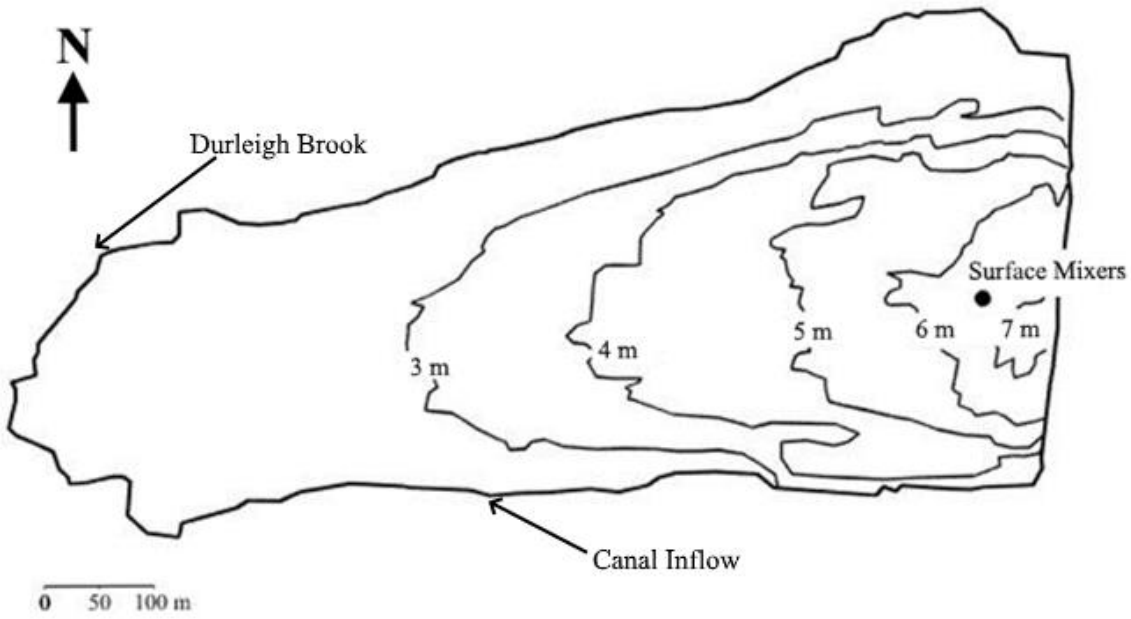

Figure 3.2. Bathymetry of Durleigh reservoir. Black circle indicates surface mixer location.

The reservoir was formed in 1938, when Durleigh Brook was dammed. Originally, the reservoir was only used to supply water to the British Cellophane factory (Appendix 1). The raw water was abstracted and filtered before use by the factory and Durleigh Brook was the only inflow into Durleigh Reservoir. Durleigh Brook has a catchment area of 17.21 km^2 (Figure 3.3) that largely consists of arable farmland with some livestock grazing. In the 1970's the reservoir was upgraded to a drinking water supply reservoir for the town of Bridgwater (Appendix 1). To deal with the greater drop in water level that accompanied increased abstraction from the reservoir to meet drinking water demand, a new inflow that pumped water from the canal was built. Water from the Bridgwater and Taunton canal is pumped into Durleigh to maintain higher water levels throughout the summer. Primarily, the canal is filled with water from the River Tone catchment, although there are multiple sources of canal water. Through the 1980's the trout fishery became less viable and by the early 1990's the reservoir became a coarse fishery, with an abundance of roach, carp, bream, perch, and pike. During this time, the water became more turbid, warmer, and macrophyte numbers declined, which led to the decline in trout numbers (Appendix 1). Currently, as well as being used as a source for drinking water, bank coarse fishing (for carp, roach, bream,

perch, and pike) is permitted on the reservoir and there are sailing and windsurfing facilities.

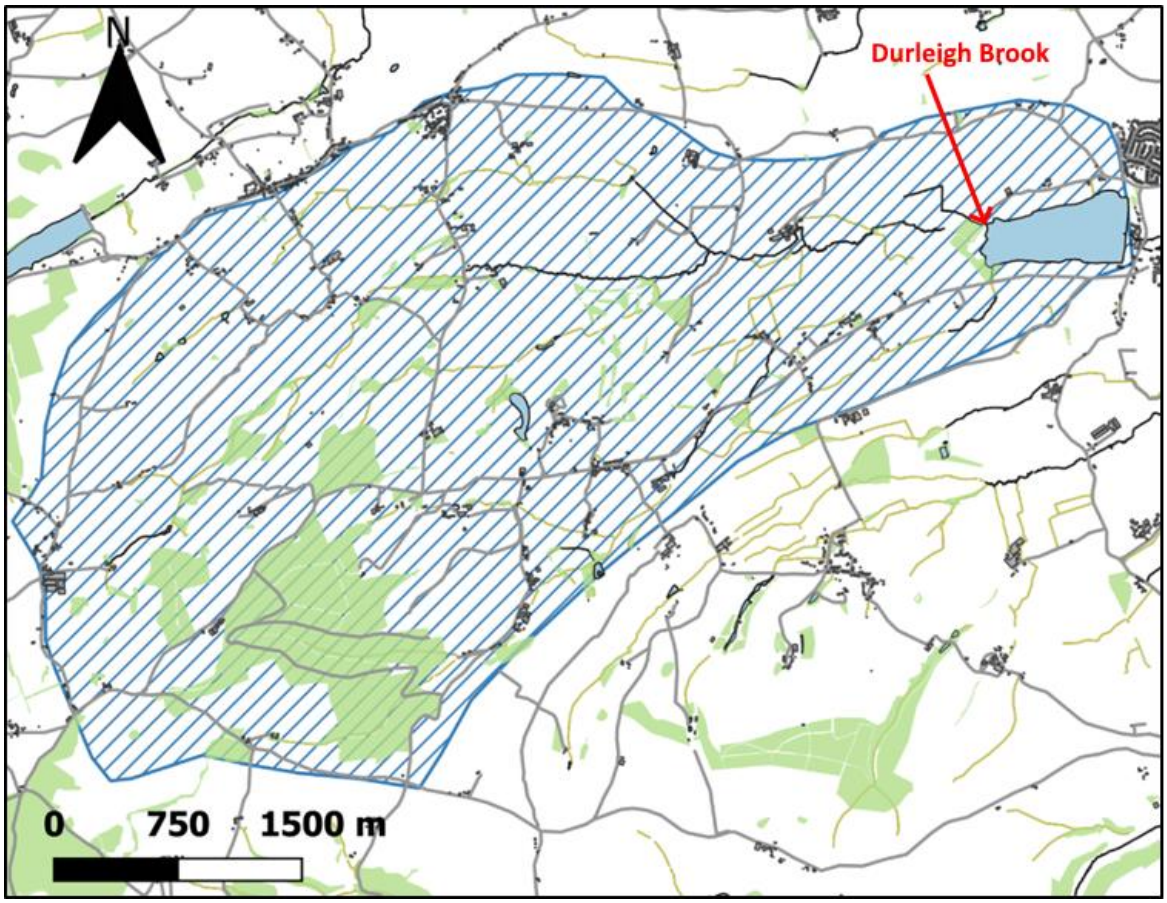

Figure 3.3. Catchment area for Durleigh Brook, the natural inflow for Durleigh Reservoir.

The reservoir is classified as eutrophic (Environment Agency, 2016) and has a history of water quality issues (Figure 3.4). In Chapter 4, Section 4.2.2, the trophic state index for Durleigh was calculated as 73.47 based on annual average chlorophyll-α concentrations. Generally, TSI values between 50 and 70 are considered eutrophic, and values > 70 are considered hypereutrophic and therefore designates Durleigh as hypereutrophic.

Figure 3.4. Photograph of Durleigh shoreline, August 2018 (Source: Author).

Durleigh has suffered from nutrient over enrichment. The Environment Agency Nitrate Vulnerable Zone (NVZ) Report (2016) states that high levels of total phosphorus (TP) are contained within the sediments and that Durleigh has accumulated phosphorus between 2010 and 2012 from external sources, but external loading is assumed to have occurred for longer (EA, 2016). Between 2010 and 2012, using estimated inputs and exports of TP, the reservoir was found to be accumulating TP at a rate of 130 kgTP yr^{-1} (EA, 2016). The principal source of TP was identified as the agricultural land use in the catchment, although the pumped canal inflow showed high TP loading (EA, 2016). Nitrogen loading from external sources is also high, with an estimated rate of 50920 kgN yr^{-1} (equivalent to 7.8 mg l^{-1}) leached from agricultural sources into the reservoir (EA, 2016). During the summer, total oxidised nitrogen concentrations in the reservoir decline to very low levels, indicating that nitrogen-limitation maybe occurring during the phytoplankton growth season. Cyanobacterial cell counts have exceeded 100,000 cells ml^{-1} every year since 2003 and are likely due to

the high levels of nutrient loading in the reservoir. Consequently, the reservoir and catchment were designated as an NVZ and the overall ecological status based on Water Framework Directive guidelines is considered bad (EA, 2016).

In-reservoir management techniques have been implemented to improve the raw water quality of the reservoir. In the 1980s or 1990s (date unknown), an air curtain was installed in the reservoir, consisting of a perforated pipe extended perpendicular from the intake tower across a third of the reservoir, which pumped compressed air into the reservoir. Although operated intermittently, the airline was very energy intensive and running costs were high, which is why it fell out of favour as an in-reservoir management technique. Therefore, in February 2015, the airline was turned off and 3 surface mixers were installed in the reservoir (Figure 3.5). When full (1,005,000 m^3), the water depth at the location of the surface mixers is ~6.6 m. The surface mixers at Durleigh have a variable flow rate but are typically operated continuously at 0.67 $m^3 s^{-1}$ (maximum volumetric flow rate for each mixer). Each mixer has a diameter of 2.4 m, an initial plume velocity of 0.15 m s^{-1}, and typically operates at 0.7 kW/hr (WEARS Australia, 2019).

At the beginning of 2018, the third mixer at Durleigh was moved closer to the intake and in June 2018 (Figure 3.6a), a standing silt curtain was installed around the intake and third mixer to prevent sediment entering the intake (Figures 3.6a and 3.8). A standing silt curtain acts as a filter with openings that are large enough that water can pass through, but small enough to trap suspended particles (Texas Boom Co., 2018). The curtain is anchored to the bed with heavy weights and kept in a vertical position with buoyancy aids (Radermacher et al., 2013). For a silt curtain to trap fine sediments suspended in the water, but allow water through, a very low permeability is required (Radermacher et al., 2013). The presence of the silt curtain is likely to influence the currents in the water column and so will likely have an impact on the currents induced by the mixers. For example, Particle Imaging Velocimetry (PIV) used in flume experiments by Vu and Tan (2010) revealed that silt screens can have a significant effect on local flow distribution either side of the silt screen. At Durleigh, the presence of the silt curtain is likely to alter the hydrodynamics locally, particularly within the range of influence of the mixer inside the silt curtain. However, the silt curtain is not expected to significantly influence the surface mixers positioned outside.

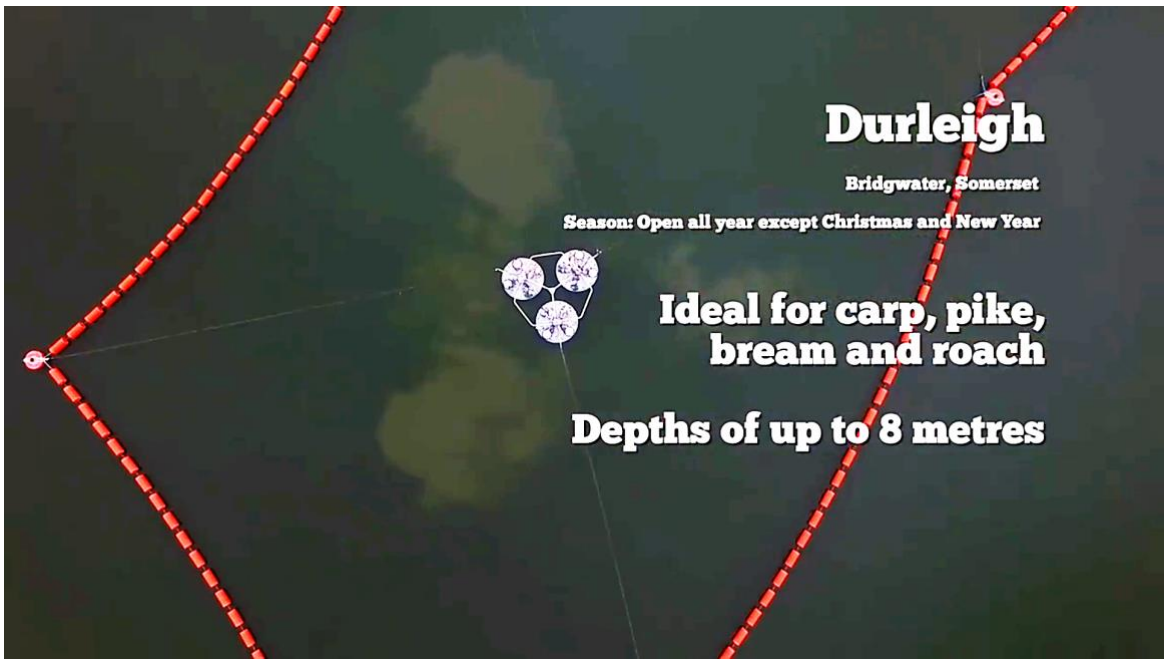

Figure 3.5. Aerial photograph of the 3 surface mixers at Durleigh and the clouds of sediment around each of the mixers that has been re-suspended due to mixer operation. Source: Wessex Water, 2016.

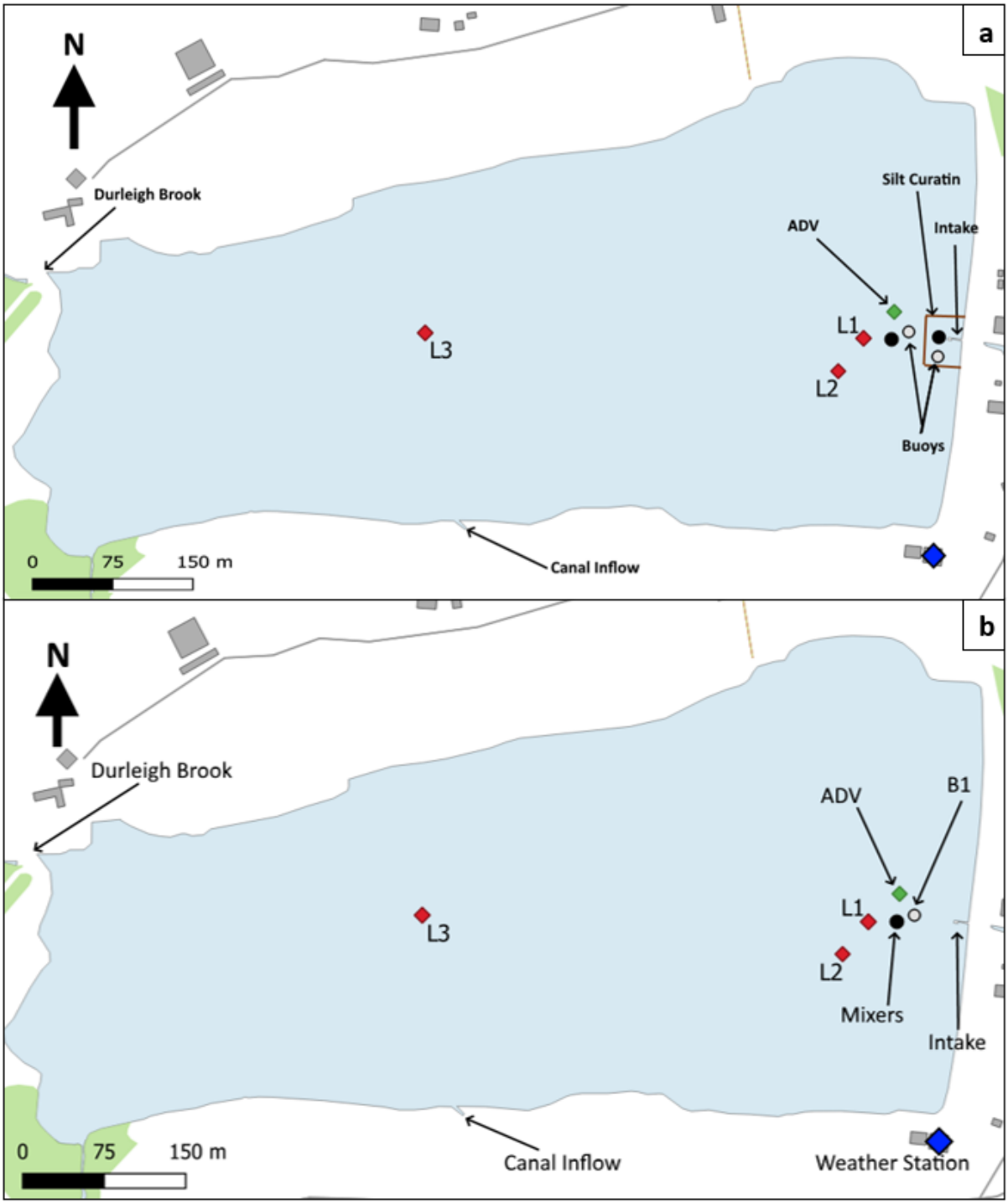

Figure 3.6. a). Map of Durleigh Reservoir with all features. The Durleigh Brook and canal inflow are highlighted. Black circles mark the locations of the mixers, two outside the silt curtain (brown line) and one inside, near the intake (marked). Grey circles show position of monitoring buoys installed by Wessex Water. Red diamonds mark the water sampling locations, green diamond shows ADV position between 20 and 24 August 2018, and blue diamond shows weather station position. b). Map of Durleigh Reservoir highlighting all the sites and equipment referred to during the 2018 measurement campaign (Chapters 5 and 6).

Figure 3.7. Photograph of the surface mixers and monitoring buoys in Durleigh in relation to the intake. Direction: facing east (Source: Author).

Figure 3.8. Photograph of the silt curtain. Taken from the dam, next to the intake. Direction: facing west (Source: Author).

3.3 Measurement Campaign

The results presented in Chapters 5 and 6 are based on a measurement campaign conducted at Durleigh reservoir between 22 February and 5 October 2018 (Figure 3.9), a towed ADCP survey conducted on 22 and 23 October 2019, and turbulence profiles from 11 September 2015. The details of the measurement campaign, ADCP survey, and turbulence measurements are described in this section.

3.3.1 Measurement Locations

Three study locations (L1, L2, and L3, Figure 3.6b) were chosen with increasing distance from the surface mixers to assess the spatial extent of artificially induced mixing. L1, L2, and L3 were positioned at 25, 60, and 435 m from the surface mixer, respectively. In addition, two moored buoys with surface and bottom mounted YSI EXO1 sondes were positioned near the mixers to collect temperature and DO data (Figure 3.6a). The monitoring buoy positioned inside the silt curtain reported obviously erroneous data during 2018 (for example, negative water temperature values) and therefore is not considered further.

3.3.2 Measurement schedule and mixer operation

A summary of the measurement campaign is presented in Figure 3.9. Continuous measurements of temperature at the surface and bottom of the water column were taken at B1, L2, and L3 (Figure 3.6b). DO measurements were taken at the surface and bottom of the water column at B1 and at the bottom of the water column at L2 and L3 (10-minute intervals). On-site water sampling and water quality profiling were conducted on 22 February, 5 April, 20 April, 30 May, 13 June, 27 June, 9 July, 24 July, 20 August, 21 August, 22 August, 23 August, 24 August, and 5 October 2018 at L1, L2, and L3 (Figure 3.9). Water samples were taken for nutrients, metals, T&O compounds, and phytoplankton cell counts. A weather station was installed on-site (Figures 3.6b and 3.12) on 5 April 2018 and was used to measure the weather conditions until the end of the measurement campaign. An Acoustic Doppler Velocimeter (ADV) was deployed ~ 30 m north of the mixers (Figure 3.6b) between 20 and 24 August 2018.

The surface mixers at Durleigh were shut down on 4 occasions in 2018, but adequate data was only collected during 2 of these shutdowns and these are presented in Chapter 5 (Figure 3.9). The shutdowns were considered as no-mixing controls, so that the effects of artificial circulation with surface mixers could be determined. The first of these, shutdown A occurred between 08:19 on 20 June 2018 and 12:22 on 22 June 2018. The second, shutdown B, occurred between 07:17 on 22 August 2018 and 16:42 on 23 August 2018. The ADV was only deployed during shutdown B (August 2018).

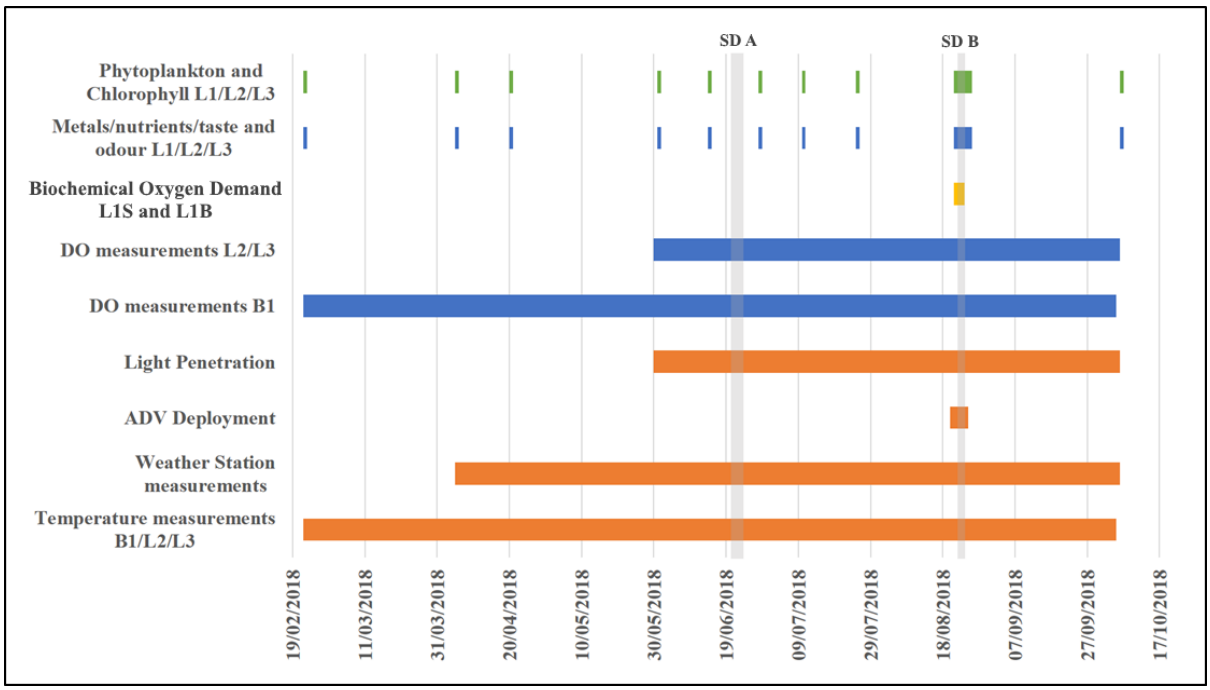

Figure 3.9. Gantt chart of the measurement campaign at Durleigh between 22/02/18 and 05/10/18. Orange indicates the physical parameters that were measured: weather, temperature, light penetration, Secchi depth, and ADV. Note that the ADV was only deployed for shutdown B. Blue marks the chemical parameters that were measured: Dissolved Oxygen, metals, nutrients, and T&O compounds. The yellow indicates biochemical oxygen demand, a biochemical parameter. Green indicates when the biological parameters were measured: phytoplankton samples and chlorophyll-α concentrations. Grey patches indicate mixer shutdowns A and B marked and SD A and SD B on the chart, respectively.

3.3.3 ADCP Measurement Campaign

In order to discern the spatial variability of the flow generated by the surface mixers, a towed ADCP survey was undertaken on 22 and 23 October 2019. Despite these measurements not being taken concurrently with other water quality data presented in this thesis, they are illustrative of expected flow patterns during the 2018 campaign.

On the 22 and 23 October 2019, velocity profiles in the vicinity of the mixers at Durleigh were acquired by towing a StreamPro ADCP from the side of a boat along three pre-defined transects (Figure 3.10) when the surface mixers were operating and turned off. Transect 1 ran east to west, south of the mixers (Figure 3.10a). Transect 2 ran east to west, starting 25 m away from the mixers (Figure 3.10b) and transect 3 ran south to north (Figure 3.10c). These transects were considered representative of the accessible area near the mixers at Durleigh.

ADCP transects were taken when all the mixers were operating, and average wind speeds were 3.53 m s^{-1} and the modal wind direction was 202.5° (Weather Underground) on 22 October 2019. On 23 October 2019, the mixers were turned off at 09:00 but transects were not acquired until 12:30. A period of 3.5 hours was considered sufficient time after the mixers were turned off for any suspended sediments to settle out of the water column. Weather conditions on 23 Oct were similar to the 22 Oct and average wind speeds were 2.68 m s^{-1} and the modal wind direction was 112.5°. At 14:15 on 23 Oct, the mixers were turned on and further transects were taken.

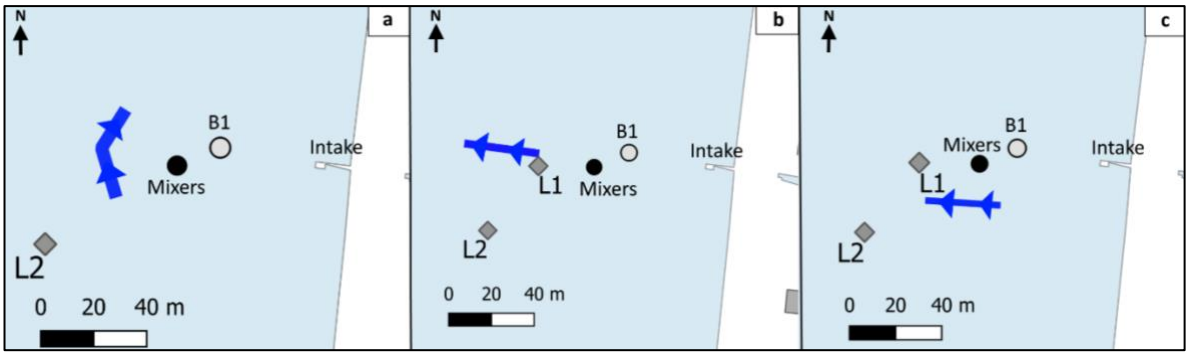

Figure 3.10. a.) Transect 1 (blue line with arrows) of the StreamPro ADCP moving S to N, 25 m away from the mixers (black circle). b.) Transect 2 moving west away from the mixers, starting 25 m W of mixers and finishing 55 m W of mixers. c.) Transect 3 moving away from the dam, starting 18 m SE of the mixers and finishing 25 m SW of the mixers. Grey diamonds indicate L1 and L2, and grey circle shows B1.

3.3.4 Turbulence and eddy diffusivity measurements

On 11 September 2015, water column turbulence at Durleigh was measured using a self-contained autonomous microprofiler (SCAMP, Precision Measurement Engineering Inc.). In this thesis, these profiles were processed, and water column turbulence was used to estimate turbulent diffusivity to assess whether turbulence from artificial circulation promoted the passive transport of phytoplankton cells through the

water column, reducing the advantage of species with buoyancy regulating mechanisms. Results of turbulence profiles are presented in Chapter 5.

Turbulence profiles were obtained at three locations (Figure 3.11) with increasing distance from the mixers (of which only 1 was operating) and decreasing depth. Five profiles were collected from each location (Figure 3.11), but to minimise the effects of sampling in the wake of the device, profiles were taken approximately 5 m apart and at 5-minute intervals. The vertical extent of each profile extended from the surface to ~ 0.5 m from the

bed as the sensor guard on the SCAMP (Figure 3.20, Section 3.4.7) prevented profiling right to the sediments.

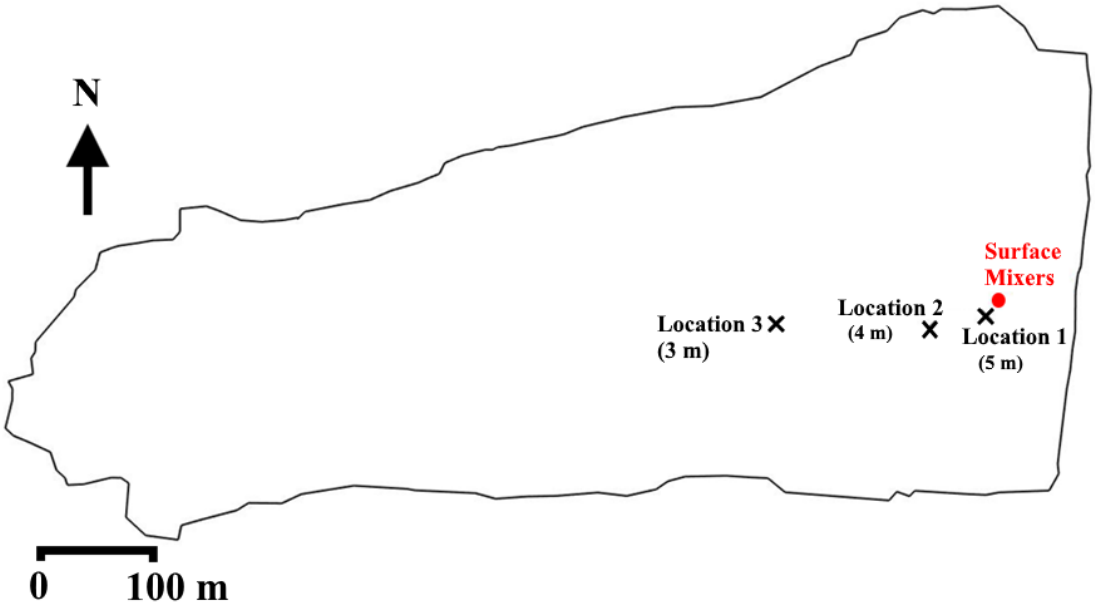

Figure 3.11. Map of the three locations for SCAMP profiles from 11th September (2015) with site depths relative to the water column depth at the time reported in brackets. Surface mixer location is highlighted in red, where only one mixer was operational. Location 1: 10 m from mixers, Location 2: 60 m, and Location 3: 190 m.

3.4 Equipment

The equipment used during the measurement campaign described in Section 3.3 and presented in Chapters 5 and 6 are described in this section.

3.4.1 Temperature

Temperature was measured at different locations to determine whether artificial circulation effectively reduced temperature gradients throughout Durleigh. The equipment used to measure temperatures at different locations in Durleigh is listed in Table 3.1. Thermistors (Figures 3.12) used at L2 and L3 were attached to a rope using a 10 kg kettle bell as an anchor and an A2 buoy as a float to keep the rope taut in the water column (herein referred to as moorings). The accuracy of the TidbiT v2 loggers is lower than that of the RBR SoloT thermistors, which introduces an element of uncertainty when interpreting and comparing temperature measurements between the different locations. The YSI EXO sondes (Figure 3.13) permanently moored at B1 provided temperature data every 15 minutes via a telemetry system used by Wessex Water and data from these buoys were made available for this thesis. Obvious erroneous data (e.g. negative water temperature values) were removed and water temperature measurements from B1, L2, and L3 were averaged hourly.

Table 3.1 Locations of temperature measurements (between 22 Feb and 5 Oct 2018) at Durleigh and the equipment, accuracy, and sampling interval for each location. (RBR Ltd.; Onset Computer; YSI).

Location	Equipment	Accuracy	Sampling Interval
B1 – Surface	YSI EXO1 sonde	± 0.01ºC	15 minutes
B1 – Bottom			
L2S	RBR SoloT thermistor	± 0.002ºC	10 minutes
L2B			
L3S	HOBO TidbiT v2 logger	± 0.21ºC	10 minutes
L3B			

Figure 3.12. a) Photograph of an RBR SoloT thermistor. b) Photograph of a HOBO TidbiT v2 logger. Pen used for scale.

Figure 3.13. Photograph of the YSI EXO3 multiparameter sonde used for water quality profiles and akin to the EXO1 sondes permanently moored at Durleigh.

3.4.2 Dissolved Oxygen

Dissolved oxygen (DO) was measured to assess whether artificial circulation effectively reduced DO gradients through the water column. Point measurements of DO were collected from the surface and bottom of the water column at B1 and the bottom of the water column at L2 and L3, while profiles were taken on the water sampling days to supplement the moorings data. Equipment availability limited measurements at the surface of L2 and L3. Instead the bottom of the water column at these locations was considered more important to capture as typical demand for DO is higher near the sediments, hence sensors were fitted to the bottom of the moorings.

At B1, DO was measured every 15 minutes at the surface and bottom of the water column using YSI EXO1 sondes, which record in percentage saturation (0 – 200%) and have an accuracy of ± 1%. The EXO measures DO using optical luminescence, where a blue light causes an immobilised dye to luminesce from which the lifetime of the dye

luminescence is measured by a photodiode on the probe. The lifetime of the luminescence is inversely proportional to the amount of oxygen present. During calibration and field sampling, DO measurements are corrected for temperature and salinity effects using measurements from additional sensors on the EXO1 and EXO3 sondes. Measurements of DO in % saturation at B1 were converted to mg l^{-1} using the temperature measurements from the EXO1 sondes.

At locations L2 and L3, miniDOT oxygen loggers and miniWIPER's (PME; Figure 3.14) were deployed on 30 May 2018 and DO measurements were taken every 10 minutes until the end of the campaign. Sensor fouling and deployment set up caused obviously erroneous data that was identified and removed prior to averaging. Data from L2 was only available for shutdown A (June 2018). For all locations, DO measurements were averaged hourly prior to analysis.

Additional water quality profiles were taken on water sampling days (Figure 3.9), using a YSI EXO3 sonde (Figure 3.13) at L1, L2, and L3. These profiles were collected to supplement the continuously monitored data and assess the homogeneity of DO through the water column at these sites, but also measured for: temperature, turbidity, chlorophyll-*α*, and pH (Section 3.4.8.1).

Figure 3.14. Photograph of a miniDOT dissolved oxygen logger (top) and miniWIPER (bottom) that was deployed at Durleigh to measure dissolved oxygen at the bottom of the water column at L2 and L3.

3.4.3 Weather Station

On-site meteorological data were measured to assess natural drivers of hydrodynamics and water quality at Durleigh. A Delta T WS-GP1 weather station was installed on-site (at 14:00 on 5 April 2018; Figure 3.15) to provide information on the local weather conditions throughout the measurement campaign. The weather station was equipped with sensors for measuring wind speed and direction, rainfall, humidity, solar radiation, and air temperature. Sensor range, accuracy, and measuring interval is reported in Table 3.2. The weather station was positioned on a 2 m vertical pole fixed to the fishing lodge at Durleigh at a height ~ 4m above the surface of the water on the South bank adjacent to the dam (Figure 3.6b). Data collected were averaged hourly for ease of comparison with other field observations.

Table 3.2. Delta T WS-GP1 weather station sensor ranges and accuracy. From Delta T Devices Ltd. (2019).

Sensor	**Range/Note**	**Accuracy**	**Measurement interval**
Wind Speed D-034B-CA (combined wind sensor)	0.4 to 75 m s^{-1}	± 0.1 m s^{-1}	Averaged over 10-minute intervals.
Wind Direction D-034B-CA (combined wind sensor)	0 to 360º	± 4 degrees	Averaged over 10-minute intervals.
Rainfall RG2+WS-CA	160 mm funnel diameter	0.2 mm / tip (sensitivity)	10-minutes
Humidity RHT3nl-CA (combined air temperature sensor)	5% to 95% RH at 23º	± 2% RH	Averaged over 10-minute intervals.
Temperature RHT3nl-CA (combined air temperature sensor)	-20ºC to 70ºC	± 0.3ºC	Averaged over 10-minute intervals.
Solar Radiation D-PYRPA-CA	0 to 1.1 kW m^{-2} 300 to 1100 nm	± 5%	Averaged over 10-minute intervals.

Figure 3.15. Photograph of the weather station installed on the fishing lodge at Durleigh Reservoir (Source: Author).

3.4.4 Acoustic Doppler Velocimeter

Near-bed flow velocities at Durleigh were measured with a Nortek Vector Acoustic Doppler Velocimeter (ADV) during shutdown B (20 and 24 August 2018) to assess the effects of artificial circulation on water velocities and sediment resuspension (inferred from acoustic backscatter signal strength). Installed in a stainless-steel frame (Figure 3.16), the ADV was deployed approx. 30 m north of the surface mixers (Figure 3.6b) in 4.5 m water depth. The sensor was positioned to measure velocities ~ 10 cm above the sediment, however variation in the height of the measurement may have occurred due to monitoring error or variation of the local bed elevation due to resuspension and/or deposition of sediment. Prior to deployment the ADV compass was calibrated and the instrument was set up to measure in the ENU directions. Velocities were measured using burst mode, measuring for 16 seconds every 10 minutes at a frequency of 64 Hz for 1024 samples.

Signal strength from the ADV was used to determine suspended particle concentrations. Studies have highlighted that a relationship exists between acoustic backscatter strength and suspended sediment concentrations (Chanson et al., 2008). For example, clear water typically returns a weaker signal, whereas turbid water produces a

stronger acoustic backscatter signal (Sontek, 1998). However, the strength of the relationship depends on sediment characteristics and equipment (Ha et al., 2009).

Figure 3.16. Photograph of the ADV fixed into a steel frame before it was deployed in Durleigh Reservoir (Source: Author).

3.4.5 Light Penetration

Water column transparency was measured using a Secchi disk (Figure 3.18) attached to a rope marked every 10 cm, the disk was lowered into the water column until it was no longer visible, and the depth at which it became visible again was taken as the Secchi depth, Z_{SD}. Secchi disk measurements were taken at L1, L2, and L3 on the water sampling days.

Light penetration through the water column has important implications for temperature stratification and primary productivity in reservoirs. Generally, the depth at which 1% of the photosynthetically active radiation (PAR) from the surface is available is regarded as the maximum depth at which photosynthesis can occur and referred to as the euphotic depth (Z_{eu}) and marks the limit of the euphotic zone (Scheffer, 2004; Reinart et al., 2000; Lee et al., 2007). PAR is the radiation within the 400-700 nm wavelength range (Kirk, 1994).

In September 2015, a Self-Contained Autonomous Microprofiler (SCAMP) was used to measure PAR and turbulence through the water column (Section 3.4.7). The SCAMP was fitted with a Li-Cor LT-192SA underwater radiation sensor mounted facing upwards. PAR profiles (W m^{-2}) were collected concurrently with temperature

microstructure profiles. Z_{eu} was identified for each of the profiles at the depth at which 1% of the PAR from the surface remained. Although using SCAMP PAR profiles gives a fairly accurate estimate of Z_{eu} for Durleigh, these were only collected over a few days in September 2015 and therefore are unlikely to be representative of the variability in Z_{eu} at Durleigh over the year.

Consequently, Z_{eu} was also estimated from the Secchi disk depth measurements that were taken at L1, L2, and L3 on the water sampling days. Using a Secchi Disk (Figure 3.18) attached to a rope marked every 10 cm, the disk was lowered into the water column until it was no longer visible, and the depth at which it became visible again was taken as the Secchi depth, Z_{SD}. Z_{SD} can be used as a proxy for Z_{eu} (Kirk, 2011; Luhtala and Tolvanen, 2013),

$$Z_{eu} = m \times Z_{SD} \quad (1)$$

where the conversion coefficient (m) is a constant. Several studies recommend different values for m (Højerslev, 1986, 1987; Lindenschmidt and Chorus, 1998; Dokulil and Teubner, 2003), for example, Holmes (1970) suggests that $m = 3$ is a suitable value for turbid waters. In this thesis, a range of values for the m constant in equation 1 were used to give a range of uncertainty. Z_{eu} was also estimated using the average, minimum, and maximum Secchi depth measurements from the water sampling days in 2018. All estimates of Z_{eu} are presented in Table 5.2 (Chapter 5) and the average of these is used as a general estimate of the Z_{eu} at Durleigh.

Figure 3.17. Photograph of the Secchi Disk with rope marked every 10 cm that was used to measured Secchi Disk depth at Durleigh.

3.4.6 Acoustic Doppler Current Profiler

A towed StreamPro ADCP (Teledyne RD Instruments, 2015) was used to measure vertical profiles of flow velocity at Durleigh on 22 and 23 October 2019 to assess the effects of artificial circulation on flow velocities. In this section, the instrument capabilities and setup are discussed and then the towed survey is described.

3.4.6.1 StreamPro ADCP

Mounted on a Riverboat SP float, the StreamPro ADCP (Figure 3.19) can be towed from a boat to measure velocity profiles, capturing velocities over a greater area than the ADV. Velocity profiles of up to 6 m in vertical extent can be acquired, with measured velocities in the range ± 5 m s^{-1}, to an accuracy of ± 1% of the flow velocity relative to the ADCP (± 2 mm s^{-1}). Using the bottom tracking feature, the StreamPro ADCP can correct velocity measurements for the boat speed relative to the bottom. Bottom tracking uses the Doppler Shift of the acoustic pulses reflected from the bed to determine the velocity of the boat (Mueller et al., 2007).

The StreamPro was set up to measure 30 bins with a 20 cm cell size, a 3 cm blanking distance and was configured using instrument-specific software (WinRiver II v. 2.21) to use the commands: CR1, TS, WF3, WM12, WN30, WS20, and WP6 (Table

3.3). In water profiling mode 12, velocity measurements are obtained by averaging the Doppler phase shift for the 6 pings and conducting a phase-velocity transformation to give velocities.

Table 3.3. Configured commands and description of commands for the StreamPro ADCP deployed on 22 and 23 Oct 2019.

Command	Description
CR1	The StreamPro will load into RAM the factory default settings.
TS	Sets real-time clock.
WF3	Blanking distance (3 cm).
WN30	Number of bins, 30.
WS20	Depth of each cell, 20 cm.
WM12	Water profiling mode 12 – default water profiling mode.
WP6	Pings per ensemble, 6 pings.

Figure 3.18. Photograph of the StreamPro ADCP set up at Durleigh Reservoir on 22nd October 2019.

3.4.6.2 Uncertainty

To maximise the accuracy of the velocity measurements, the boat was operated at < 0.5 m s^{-1} throughout all transects (accuracy 0.005 m s^{-1} ±0.002 m s^{-1}). Measurement uncertainty can be introduced from a range of sources including instrument resolution, instrument accuracy, boat speed, sampling time, near transducer error, flow angle induced error, and operational conditions (Lee et al., 2014). Studies suggest that when

measuring flow velocities below 0.25 m s^{-1}, the variability in StreamPro ADCP measurements increases and to minimise this effect, multiple transects (at least 8) should be taken over the target measurement area (Rehmel, 2006; USGS, 2011; Lee et al., 2014). However, due to time constraints with the equipment, spatial coverage was prioritised over repeated transects and therefore some uncertainty maybe introduced into the StreamPro measurements.

3.4.6.3 Data Processing

All data were exported from the StreamPro with the boat speed bottom track correction (REF BT) applied using WinRiver II v. 2.21. Subsequently, data were exported from WinRiver II v. 2.21 and processed in MATLAB.

3.4.7 Self-Contained Autonomous Microprofiler (SCAMP)

Artificial circulation may increase turbulence through the water column, which could increase vertical mixing. Mixing depends on the production of turbulent kinetic energy (*TKE*), which is a balance between buoyancy flux (b) and turbulent kinetic energy dissipation rate (ε) (Osborn, 1980; Ivey and Imberger, 1991),

$$TKE = b + \varepsilon \quad (2)$$

Temperature gradients from temperature microstructure measurements can be used to calculate (ε). The SCAMP (Figure 3.20) measures small-scale temperature variations with an accuracy of 0.05℃, using fast-response Thermometrics FP07 thermistors (7 ms response time). The profiling fall rate of the SCAMP is approximately 0.1 m s^{-1}, with a sampling frequency of 100 Hz.

Figure 3.19. Image of the SCAMP (PME Inc.).

Observed data were fitted to the theoretical Batchelor spectrum (Batchelor, 1959). Batchelor fitting was used to estimate turbulent kinetic energy dissipation following Ruddick et al. (2000), where segments that poorly fitted the spectra were removed from further analysis using the criteria proposed by Ruddick et al. (2000).

Rates of TKE dissipation are related to vertical mixing (b) using the eddy diffusivity coefficient (K) proposed by Osborn (1980):

$$K = b/N^2 = \Gamma \cdot \varepsilon / N^2 \quad (3)$$

where $N = [-\left(\frac{g}{\rho}\right)\frac{\partial \rho}{\partial z}]^{1/2}$ is the buoyancy frequency that defines the strength of stratification depending on the gravitation acceleration (g), water density (ρ), and the density gradient $\left(\frac{\partial \rho}{\partial z}\right)$. The parameter Γ estimates how much turbulent kinetic energy dissipation (ε) is converted to mixing (b) and here the typical value of Γ = 0.2 was used (Huisman et al., 2004; Ivey et al., 2008) although Γ varies depending on how turbulence is generated and the strength of stratification (Ivey and Imberger, 1991).

3.4.8 Water Sampling

In Chapters 5 and 6, in-reservoir water samples were analysed for biological, chemical, and physical parameters to understand the in-reservoir processes and help determine the effects of artificial circulation on nutrient, metal, and phytoplankton dynamics. These measurements were supplemented with weekly raw water samples

from the intake, provided by Wessex Water, to highlight any changes in water quality since surface mixers were installed (Chapter 6). Samples collected from the intake at Durleigh were measured for: nutrient concentrations, turbidity, total and soluble metal concentrations, pH, phytoplankton cell counts, and T&O metabolites. Wessex Water provided historical intake water quality measurements from 2010 – 2019.

With permission from Wessex Water, Welsh Water, and Bristol Water, the author statistically analysed the historical water sample data from Blagdon, Cheddar, Chew, Durleigh, Dolwen, and Plas Uchaf reservoirs, which is reported in Chapter 4 and published in Perkins and Slavin et al. (2019). The methods used to collect the historical data are reported in Section 4.2.3 and summarised in Table 4.4 (Chapter 4), where differences between laboratories are highlighted.

3.4.8.1 In-Reservoir Sampling

Water samples were collected at Durleigh on water sampling days in 2018 from L1, L2 and L3 (Figure 3.6b). Samples were taken from the surface, middle, and bottom of the water column. A Van Dorn water sampler (Figure 3.21) was used to collect samples from the middle and bottom of the water column, while surface samples were collected directly into sample bottles. All water samples collected were processed and analysed at the Wessex Water Scientific Centre (Section 3.4.8.2). They were analysed for total oxidised nitrogen (TON), ammonium, nitrate, nitrite, orthophosphate, silica, total and soluble manganese, total and soluble iron, 2-MIB, geosmin, chlorophyll-α, phytoplankton cell counts, and turbidity. Water samples to assess biochemical oxygen demand (BOD) were collected in 1L PET bottles, where the bottle was filled with no head space, from the surface and bottom of the water column at L1 on the mornings of 21, 22, and 23 August 2018 (Section 3.4.8.3).

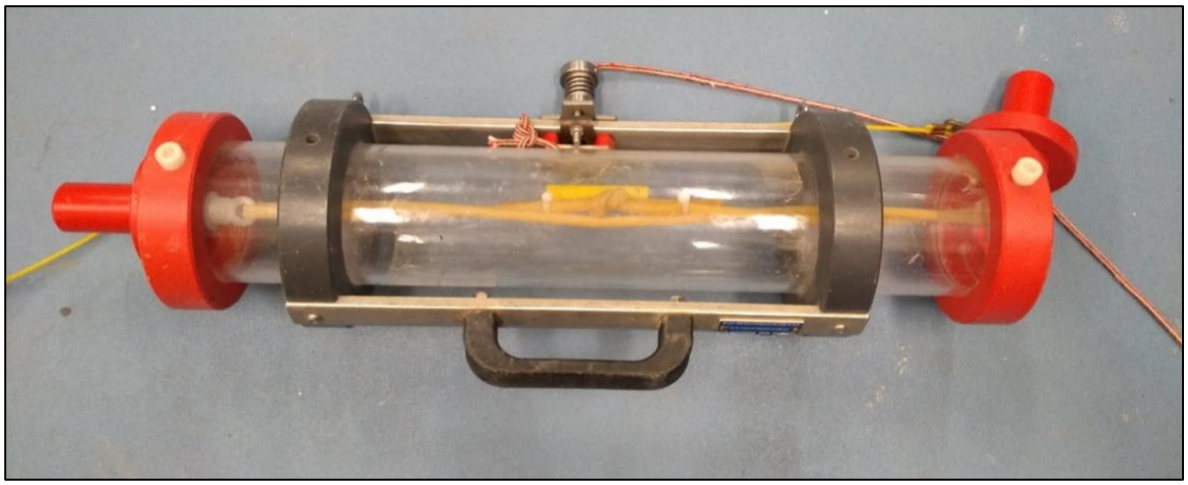

Figure 3.20. Photograph of the Van Dorn water sampler used to collect water samples from the middle and bottom of the water column at Durleigh.

Water quality profiles were acquired using an EXO3 profiling sonde (Figure 3.13), which measures temperature, DO, turbidity, and pH (sensor accuracy: ± 0.2 pH units). Three-point calibration of the pH senor was conducted prior to fieldwork as per Xylem (2019). The EXO3 turbidity sensor uses near-infrared light to measure turbidity and was calibrated to record in nephelometric turbidity units (NTU).

3.4.8.2 Laboratory Methods

To determine nitrite concentrations the sulphanilamide/N-1-napthylethylene-diamine dihydrochloride method was used. Nitrite ions react with sulphanilamide and N-1-napthylethylene-diamine in an acidic medium, producing a pink dye, the intensity of which is proportional to the nitrite concentration present. Subsequently, the pink dye was measured spectrophotometrically at 540 nm using a Thermo Scientific Aquakem 600 spectrophotometer. For TON concentrations the same method was followed but nitrate was reduced first. Nitrate was determined as the TON concentration minus nitrite concentration. Ammonium concentrations were determined using the sodium salicylate/sodium nitroferricyanide method and then measured spectrophotometrically at 660 nm.

Orthophosphate concentrations were determined using the ascorbic acid method, where orthophosphate reacts with ammonium molybdate and antimony potassium tartrate to produce an antimony-phospho-molybdate complex, which is reduced by ascorbic acid and forms a blue-coloured complex, proportional to the orthophosphate concentration. The blue complex was then measured spectrophotometrically using a Thermo Scientific Aquakem 600 spectrophotometer at 880 nm. Total phosphorus (TP)

was determined using Inductively Coupled Plasma Mass Spectrometry (ICP-MS) using an Agilent 7700 ICP-MS. Iron and manganese (total and soluble) concentrations were also measured using ICP-MS. Turbidity was measured using a HACH 2100AN Turbidimeter and results were presented as Nephelometric Turbidity Units (NTU).

2-MIB and Geosmin concentrations were determined using Gas Chromatography and Mass Spectrometry (GC/MS/MS). Samples were extracted using solid phase extraction (SPE) and eluted from the SPE cartridge using Dichloromethane. Calibration standards, analytical quality control and blank samples are extracted and analysed alongside test samples. Analysis is performed on a Thermo Trace 1310 Gas Chromatograph with a TSQ 8000 triple quadrapole. The internal standard, Geosmin-D5 was used in the method to compensate for variations in recovery due to matrix effects and ion suppression in the MS. The method described here determines total Geosmin/2-MIB concentrations and does not distinguish between the dissolved and protein-bound fractions of Geosmin (Wu and Jüttner, 1988). Current methods are also thought to underestimate the protein-bound fraction (Jüttner and Watson, 2007).

Chlorophyll-*α* was measured using *in vivo* fluorometric quantification using a bbe AlgaeLabAnalyser, which is not a UKAS accredited method. A six coloured light emitting diode (LED) was used at wavelengths 370, 430, 470, 525, 590, and 610 nm. The excitation wavelengths were adapted to the absorption wavelengths of the fluorescent pigments: phycocyanin, phycoerythrin, fucoxanthin, peridinin, and chlorophyll. Frequently, these *in vivo* fluorescence measurements were checked against chlorophyll-*α* measurements extracted using methanol and determined spectrophotometrically, for quality assurance.

For phytoplankton cell counts, water samples were collected in 1L PET bottles and fixed with Lugol's iodine solution (1%). Due to the high chlorophyll-*α* concentrations of the water samples from Durleigh, 5 ml of each sample was extracted for filtration prior to identification and enumeration. Samples were then concentrated by membrane filtration, using 47 mm diameter cellulose acetate membranes with a pore size of 0.45 µm. The filtered membranes were then dried in an oven at 35 ± 5 °C. Filters were mounted onto microscope slides and identification and enumeration was conducted using an Olympus BH2 light microscope, which has 10x, 20x, 40x, and 100x objectives. The 40x objective was used for enumeration. During identification and enumeration, the average colony and filament size were noted. A minimum of 30 fields of view (FOV) were counted per sample, or at least 500 cells for the most abundant

genera. A FOV was considered as the total area observed through the eyepiece without moving the stage. For the in-reservoir samples collected in 2018, 15 FOVs were counted per sample, which reduces the accuracy of the results, but was necessary due to the volume of samples that required processing. Phytoplankton cell counts from 2018 were carried out by the author to reduce reader error between samples. For all historical data and samples from the intake at Durleigh, a minimum of 30 FOVs were counted. The laboratory method used for phytoplankton identification and enumeration is not a UKAS accredited method. Nevertheless, Lund et al. (1958) suggest that the cell count presented is within the range of ± 20% when more than 300 cells are counted.

3.4.8.3 Biochemical Oxygen Demand

Biochemical oxygen demand (BOD) is a measure of the mass of dissolved oxygen consumed per unit volume of water sample and is reported in mg O_2 l^{-1}. BOD refers to the oxygen consumption by micro-organisms to decompose organic matter present in a given water sample at a certain temperature and over a set time period. The higher the BOD, the more rapidly oxygen is depleted.

Prior to incubation, the concentration of dissolved oxygen (DO) was measured using the Rohasys robotic BOD system, Hach Lange LDO101 probes, and a HQ40d Portable Meter, and 0.5 ± 0.1 ml of allythiourea (atu) was added to suppress nitrification (reported as BOD (atu)). Samples were incubated at 20 ± 0.5 °C in the dark for 5 days (117.5 ± 4.5 hours). After incubation, the concentration of DO was measured again and the difference between the 2 readings was used to calculate the BOD(atu) of the sample, which was reported in mg O_2 l^{-1} (the amount of oxygen consumed per litre or sample over 5 days incubation at 20˚C).

The presence of algal cells in the samples may cause oxygen super-saturation and lead to a falsely high BOD result due to the decay of dead cells during incubation. To reduce this interference, samples were passed through a stainless-steel sieve with a fine mesh to remove large algal cells and other plants and animals in the sample.

3.5 Data Analysis

3.5.1 Natural generation of turbulent kinetic energy

Natural mixing energy input can be generated through wind-driven or convective mixing. The combination of both sources constitutes the total naturally-driven mixing in

a reservoir and can be compared to the artificial energy input. The input of turbulent kinetic energy (TKE) from wind-driven and convective mixing was calculated for Durleigh reservoir between 5 of April and 5 October 2018 in Chapter 5 in order to compare the input of TKE from natural sources with that from the surface mixers.

Collected data were averaged daily and input into Lake Heat Flux Analyzer (LHFA; Woolway et al., 2015) to estimate derived meteorological quantities necessary to compute the input of turbulent kinetic energy (TKE) from wind and convective heat transfer (e.g. Saber et al., 2018). TKE input from the wind (TKE_{wind}) was calculated as

$$TKE_{wind} = \frac{1}{2}\rho_w(C_N u_*^3) \quad (4)$$

where C_N = 1.33 and $u_* = \sqrt{\tau/\rho_w}$ is the wind shear velocity, where τ is the surface shear stress (from LHFA) and ρ_w is the density of the surface layer. TKE input from convection (TKE_{conv}) was calculated as

$$TKE_{conv} = \frac{1}{2}\rho_w w_*^3 \quad (5)$$

where w_* is the velocity of vertical thermals in the water column due to surface heat loss and estimated as (Fischer et al., 1979),

$$w_* = \left(\frac{\alpha g h Q_{net}}{C_{\rho,w}\rho_{mld}}\right)^{1/3} \quad (6)$$

- α is the coefficient of thermal expansion of water (°C^{-1});
- g is gravitational constant (9.81 m s^{-2});
- h is the depth of the surface mixed layer (m);
- Q_{net} is the net heat flux into the surface of the lake and was calculated using LHFA (W m^{-2});
- $C_{\rho,w}$ is the specific heat of water (4.18 kJ kg^{-1}°C^{-1});
- ρ_{mld} is the density of the water in the mixed layer (kg m^{-3}).

In this study, considering that stratification was defined as a temperature difference of 2 °C through the water column, the temperature threshold of 1°C difference to the surface was used to define the MLD, following Mackay et al. (2011). There is uncewrtainty around defining the surface mixed layer as discussed in Gray et al (2020) but due to the differences in accuracy between temperature measurements from

the different thermistors used in this study, a difference of 1°C from the surface was considered the most applicable.

The u*:w* ratio was calculated following Read et al. (2012) and the threshold of 0.75 (Imberger, 1985) was used to define the equal input of both components.

3.5.2 Turbulent kinetic energy from surface mixers

The theoretical TKE input into the water column from a surface mixer can be calculated using Imboden (1980),

$$TKE_{mix} = \frac{Q_p (U_p)^2 \rho_w}{2A_0} \quad (7)$$

- TKE_{mix} is the TKE input from the operation of the surface mixers (W m^{-2});
- Q_p is the flow rate from the mixers (m^3 s^{-1});
- U_p is the flow velocity generated by the mixers (m s^{-1}) and was calculated following Punnett (1991);
- ρ_w is the water density (kg m^{-3});
- A_0 is the surface area of the mixers (4.5 m^2).

This value is constant while the mixers are in operation.

3.6 Statistical Analysis

3.6.1 Cross Correlation

Cross correlation analysis was carried out (Chapter 4, Section 4.3.4) on the historical intake data from Blagdon, Chew, Cheddar, and Durleigh reservoirs (2014 - 2017), to discern whether lags between nutrient availability and increased concentrations of 2-MIB and Geosmin were present. The analysis was performed in MATLAB using the 'xcorr' function. Variables included in analysis were: ammonium, 2-MIB, Geosmin, NH_4:NO_3 ratio, nitrate, orthophosphate, TP (in Durleigh), temperature (Chew/Cheddar/Blagdon), TN:OP (Chew/Cheddar/Blagdon), and TN:TP (Durleigh).

3.6.2 Self-Organising Maps

Self-Organising Maps (SOMs) are used to analyse historical data in Chapter 4. SOMs are a relatively novel method for large data set analysis and visualisation and can be considered as a non-linear generalisation of principal component analysis (PCA), which enables lags within time series data to be recognised. SOMs are artificial neural networks that employ unsupervised, competitive learning to transform high-dimensional data into a discrete lattice of neurons/nodes, referred to as a 'map' (Uriarte and Martín, 2005; Skupin and Agarwal, 2008).

A SOM trains itself using input data, where output neurons compete against each other to represent a given input vector (competitive learning). The best matching unit (BMU), or winning neuron, is the neuron whose weight vector most closely matches the input vector based on the Euclidean distance between them (Kohonen and Honkela, 2007). The BMU weighting is iteratively updated and hence neurons surrounding the BMU are updated respectively (self-organisation), but to a lesser extent as the competitive learning process. The process is based on how neurons in the brain function, where the neighbours of an excited neuron also get excited but to a lesser extent and creates a topological neighbourhood that decays with distance (Beale and Jackson, 1990). In SOMs, a similar topological neighbourhood is defined around the BMU. Self-organisation is completed once the updated weights for neurons stabilise with respect to the input vector, creating the topologically ordered map where the spatial location of a neuron in the output space corresponds to a particular feature of the input space (Bullinaria, 2004; Uriarte and Martín, 2008). The process is repeated for randomly selected inputs over many training epochs. The preservation of neighbourhood relations from the input data in the output map topology makes SOMs a good visualization tool for dimensionality reduction.

In Chapter 4, prior to analysis by SOM, all data were normalised to values between 0-1. SOMs were used for clustering and dimension reduction to identify the principal variables in T&O production. There are two phases of data abstraction/dimension reduction that can be employed in a SOM (Figure 3.22). Firstly, a SOM topology was created from the prototype vectors formed from the input data, then clustering of the nodes in the SOM topology creates the second abstraction level.

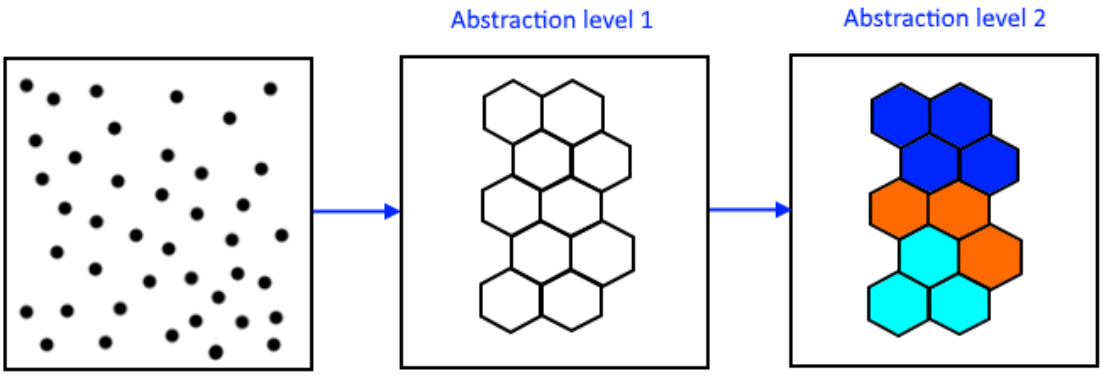

Figure 3.21. Conceptual diagram showing the first phase of abstraction by creating a set of prototype vectors from the input data (left) using the SOM. Then the second phase of abstraction is achieved by clustering of the SOM (shown by coloured groups, right).

Using the SomToolbox MATLAB package from the Helsinki University of Technology (Vestano and Alhoniemi, 2000), each SOM was trained with the batch-training algorithm som_make. In the SOM topology, patterns of the input variables are displayed on component planes of a 5x2 hexagonal-node grid, which was selected as the optimal size when considering the topographic and quantization errors (Uriarte and Martín, 2005). SOM component planes can be regarded as an analogue of PCA loading plots. Each node represents a certain position in the map space and are consistent across all component plots. Colours in the component plots show the values that variables have in the map structure, with yellow indicating higher values and blue lower (Chapter 4, Section 4.3.5). The similarity between neighbouring nodes was highlighted in the U-matrix, which was weighted according to Euclidean distance and indicated by colours on the map (Park et al., 2004), where blues designate smaller distances (similarity) and yellows larger (difference). The som_barplane function with 'varwise' scaling, was used to visualise the distribution of parameters for each weight vector in the output map. The bar plane plots rank the variables according to their perceived relative importance for each node. Clustering was performed using the k-means algorithm for each SOM topology (kmeans_clusters function). K-means is a standard partitive clustering approach that minimises the sum-of-squared-error between points in the clusters and their corresponding cluster centroids (Selim and Ismail, 1984). The best matching unit (BMU) for each input is identified using the som_bmus function. The input data was then assessed for significant differences between clusters (based on BMU identification and cluster analysis) using single-factor ANOVA and post hoc Tukey's test in PAST statistical software package (Hammer et al. 2001).

Selecting the size of the SOM is important in overall SOM performance. There are two error measurements that can help to inform the analyst of the quality of different sizes of SOM tested prior to selecting a final size: the topographic error and quantization error (Uriarte and Martín, 2005). Table 3.4 shows the quantization error and topographic error for all sites studied. The quantization error is the average distance (Euclidean) between the data points in the SOM and the nodes onto which they are mapped (Breard, 2017). Quantization error evaluates how well neurons in the trained network adapt to input vectors (Stefanovič and Kurasova, 2011), the smaller the value, the better the quantization (Sun, 2000). Quantization error is affected by the size of the lattice (number of neurons) and similarly to Uriarte and Martín (2005), we found that Quantization Error generally decreased with number of nodes (Figure 3.23).

Table 3.4. Quantization and topographic error for each SOM topology.

Dataset for SOM	Quantization Error	Topographic error
Durleigh	0.262	0.006
Blagdon	0.333	0.060
Cheddar	0.321	<0.001
Chew Valley	0.424	0.407
SPT1 (Plas Uchaf)	0.313	<0.001
SPT2 (Plas Uchaf)	0.381	0.019
SPT3 (Plas Uchaf)	0.272	<0.001
SPT4 (Plas Uchaf)	0.322	<0.001
SPT5 (Plas Uchaf)	0.315	<0.001
Dolwen	0.431	<0.001

The topographic error evaluates how well the SOM preserves the structure of the input data (Breard, 2017). Topographic error was measured by finding the number of all data vectors where the first and second BMUs are not adjacent vectors (Uriarte and Martín, 2005). When the first and second BMUs are not adjacent it is considered an error, which is why hexagonal nodes are generally preferred over rectangular nodes. The total number of errors divided by the total number of data points produces the topographic error for the SOM (Breard, 2017). Despite this, a large grid enables better interpretation. But for the SOMs presented in Chapter 4, the topographic error was 0 for 9 nodes (3x3) and 10 nodes (5x2). The quantization error was lower for larger grid sizes, so SOMs with 10 nodes in a 5x2 hexagonal lattice were selected.

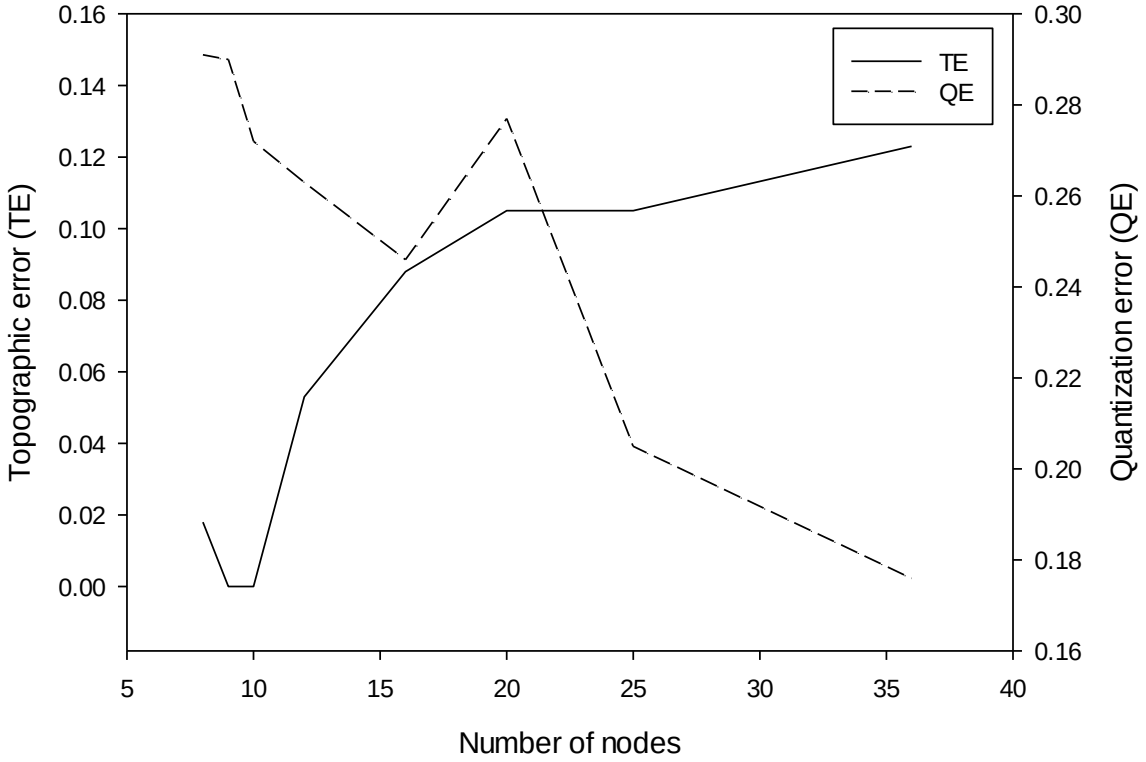

Figure 3.22. The change in Topographic Error (TE) and Quantization Error (QE) of the SOM for SPT3 (Plas Uchaf) according to number of nodes.

CHAPTER 4

STATISTICAL ANALYSIS OF TASTE AND ODOUR METABOLITE PRODUCTION IN DRINKING WATER RESERVOIRS

Declaration of contribution:

The work presented in this chapter is based on the research article published in the Journal of Environmental Management, “Managing taste and odour metabolite production in drinking water reservoirs: The importance of ammonium as a key nutrient trigger”, which is available in open access. R. Perkins and E. Slavin are listed as joint first authors.

In this thesis a traditional chapter format is used to better highlight the contribution made by the author of this thesis to the work published in the paper. The in-reservoir data from Plas Uchaf and Dolwen were collected and analysed by R. Perkins and T. Andrade. These data were used to hypothesise that increased ammonium concentrations could trigger the production of T&O in cyanobacteria. The author of this thesis took the hypothesis and designed an analysis methodology to test the hypothesis over a wider range of sites for improved robustness. All analysis using self-organising maps and subsequent statistical analysis were conducted by the author of this thesis. These findings confirmed the hypothesis and demonstrated that high ammonium relative to nitrate is a trigger for T&O production in all reservoirs analysed. Historical data were provided from Welsh Water, Wessex Water, and Bristol Water, who are recognised in this chapter for data collection and sharing accordingly. The in-reservoir data from the Welsh Water reservoirs in Perkins and Slavin et al. (2019) is cited, indicating the contribution of collaborators to the work. The percentage contribution for different aspects of the paper are defined in Table 4.1.

Table 4.1. Statement of authorship with regard to the paper: "Managing taste and odour metabolite production in drinking water reservoirs: The importance of ammonium as a key nutrient trigger."

This declaration concerns the article entitled:	Managing taste and odour metabolite production in drinking water reservoirs: The importance of ammonium as a key nutrient trigger.
Publication Status	Published
Publication Details (reference)	Perkins, R.G., Slavin, E.I., Andrade, T.M.C., Blenkinsopp, C., Pearson, P., Froggatt, T., Godwin, G., Parslow, J., Hurley, S., Luckwell, R., Wain, D.J. 2019. Managing taste and odour metabolite production in drinking water reservoirs: the importance of ammonium as a key nutrient trigger, *Journal of Environmental Management*, 244, 276-284. https://doi.org/10.1016/j.jenvman.2019.04.123.
Candidate's contribution to the paper (given as a percentage)	Plas Uchaf/Dolwen in-reservoir data collection: Welsh Water* (100%) Formulation of hypothesis: R. Perkins and T.M.C. Andrade Data provided by Bristol Water: R. Luckwell (100%) Data provided by Wessex Water: S. Hurley (100%) Welsh Water (Plas Uchaf) in-reservoir data analysis: R. Perkins (100%) Self-organising map analysis of all reservoirs: E. Slavin (100%) Preparation of manuscript: E. Slavin (75%), R. Perkins (25%) Preparation of supplementary data: E. Slavin (100%) * Andrade, T.M.C., C., Pearson, P., Froggatt, T., Godwin, G., Parslow.
Statement from Candidate	See Declaration of contribution
Signed	E. Slavin
Date	17th February 2020

4.1 Introduction

Chapter 2, Section 2.3, identified that the triggers of T&O metabolite production along isoprenoid pathways in cyanobacteria are poorly understood and there is a need to distinguish triggers to better inform water quality management. Therefore, the aim of this chapter is to investigate the potential trigger(s) of 2-MIB and Geosmin production in water supply reservoirs and advise the water industry on monitoring and management to mitigate T&O events (Objective 2, Chapter 1). Historical abstraction data from four different drinking water reservoirs, located in Somerset, UK, were analysed using Self-Organising Map (SOM) analysis. These data combined with SOM analysis of five sites in Plas Uchaf and one site in Dolwen, North Wales, UK, enabled investigation into what triggers production of T&O in a range of reservoirs across a trophic gradient.

4.2 Study Sites and methods

4.2.1 Study sites

All sites included in this chapter have separate, primarily agricultural catchments (livestock grazing and arable). Table 4.2 lists key characteristics of the different reservoirs studied. The inset of Figure 4.1 shows the locations of all study sites. Plas Uchaf is an upland reservoir managed by Dŵr Cymru Welsh Water (DCWW). It is fed by Dolwen reservoir (Figure 4.1), which is in turn fed by groundwater supply and from three small tributaries. There are no other point source inflows to Plas Uchaf, other than the primary pumped input abstracted from the River Aled, 1.5 km to the west. Five locations within Plas Uchaf and one site in Dolwen Reservoir (Figure 4.1) were sampled by DCWW regularly between 2015 and 2016, enabling spatial and temporal analysis of T&O production in the reservoir.

The four Somerset reservoirs (Figure 4.2; inset Figure 4.1) are Chew, Cheddar, Blagdon, and Durleigh. Chew Valley (51°21’3.67”N, 2°37’7.68”W) and Blagdon (51°20’15.82”N, 2°42’45.40”W) are both managed by Bristol Water. Both are river fed, Chew from multiple small rivers, and Blagdon mainly from the River Yeo with multiple smaller inflows (Figure 4.2, top panel). Cheddar reservoir (51°17’0.58”N, 2°48’30.66”W) is pumped with water taken from the Cheddar Yeo river and is also

managed by Bristol Water (Figure 4.2, top panel). Durleigh is a lowland reservoir (managed by Wessex Water) fed by a small stream and occasionally pumped with water from the Bridgwater and Taunton Canal, which enters the reservoir via a culvert on the southern bank (Figure 4.2, bottom panel). Water samples from the Somerset reservoirs were collected by their respective water companies.

Table 4.2. The morphological and catchment characteristics of the 6 study sites.

Reservoir	**Mean Depth (m)**	**Max Depth (m)**	**Surface Area (km^2)**	**Catchment Area (km^2)**	**Volume (ML)**	**Altitude (m A.O.D.)**	**Primary Catchment land use**
Blagdon	4.8	11.5	1.65	21.79	8260	45	Improved Grassland
Cheddar	5.9	13.6	0.92	4.80	6186.39	12	Improved Grassland
Chew	4.8	12.9	4.65	57.90	20714.22	52	Improved Grassland
Durleigh	3.1	8.1	0.33	17.31	1005	22	Arable and Horticulture
Plas Uchaf	6.3	-	0.04	3.58	133.38	148	Improved Grassland
Dolwen	2.8	-	0.06	2.28	204.46	168	Improved Grassland

All four Somerset reservoirs are artificially mixed. Blagdon, Chew, and Cheddar have bubble plumes to destratify the water column during the summer months and Durleigh has three surface mixers (ResMix 1000 units) installed, which are designed to circulate the water column all year round. Plas Uchaf and its feeder reservoir Dolwen are not mixed artificially. By including a range of artificially mixed and non-mixed reservoirs in this chapter we can investigate whether environmental factors influencing the production of T&O metabolites is different between mixed and non-mixed sites.

Figure 4.1. Map of Plas Uchaf and Dolwen reservoirs, North Wales, UK, showing sample points (SPT) 1-6 used in this chapter and the two main inflows into Plas Uchaf (Dolwen surface flow and River Aled pumped input). Inset: Location of all reservoirs in SW England and Wales, UK. Plas Uchaf (green) is located in North Wales and the other four reservoirs are located in Somerset, UK.

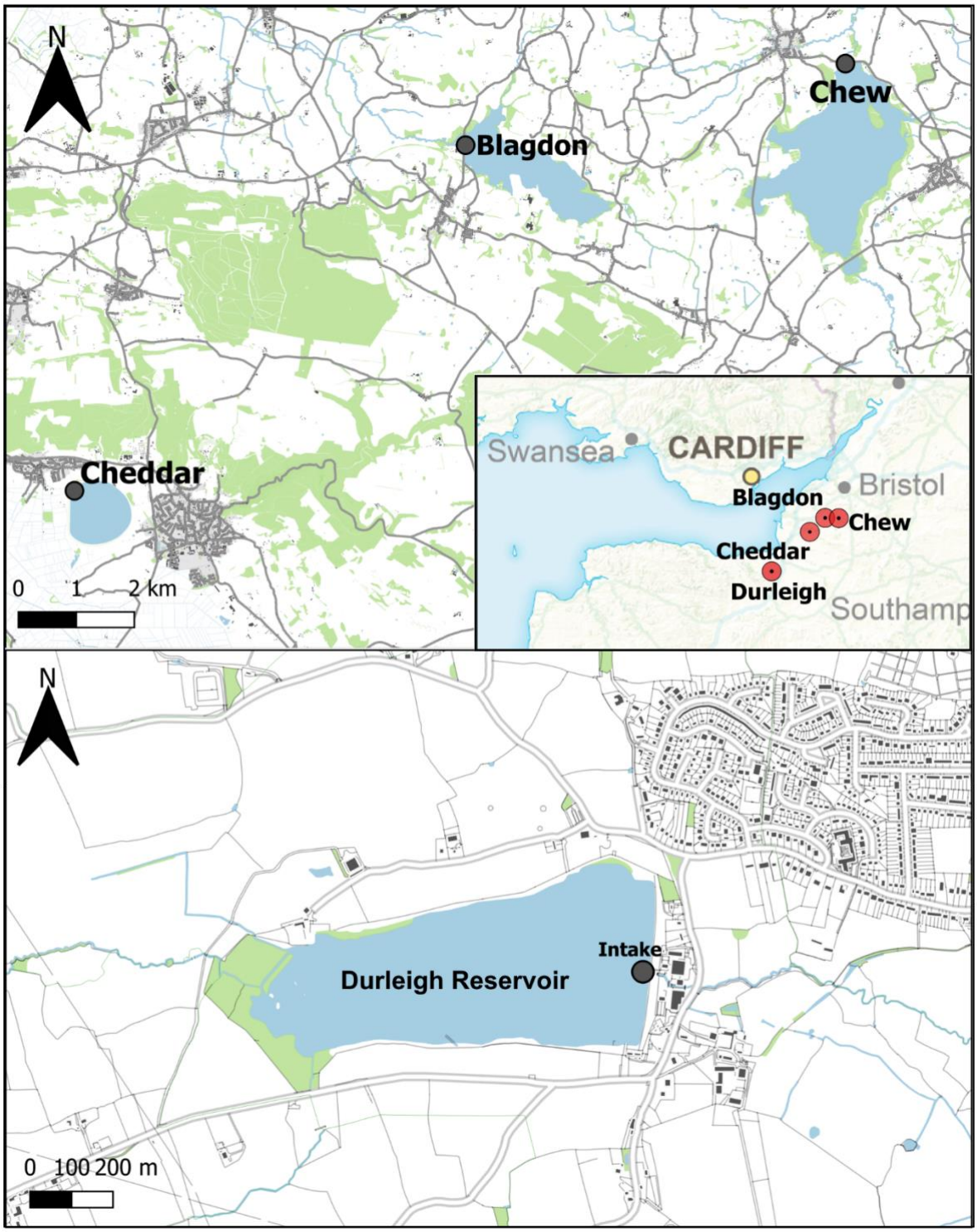

Figure 4.2. Top panel: Schematic of Cheddar, Chew, and Blagdon reservoirs, Somerset, UK and the location of the intake for each reservoir (grey circle). Bottom panel: Map of Durleigh reservoir, Somerset, UK. The intake is marked with a grey circle. Inset: Location of the reservoirs within the South West of England and South East Wales region.

4.2.2 Trophic State Index

The sites included in this chapter cover a range of trophic states (mesotrophic to hypereutrophic) and different locations to provide evidence for trigger(s) of T&O production more generally than at specific sites. The values of Trophic State Index (TSI) were calculated from the annual average chlorophyll-α values for each reservoir (Table 4.3) based on the method proposed by Carlson (1977):

$$TSI(chl) = 9.81 \ln(chl) + 30.6$$

For this chapter, the TSI values calculated from chlorophyll-α were chosen over Secchi depth (not measured) or total phosphorus (not available for all reservoirs) TSI indices. A trophic gradient from the mesotrophic Cheddar reservoir to the hypereutrophic Durleigh reservoir is observed, with Blagdon, Chew, and Plas Uchaf all categorised as eutrophic (Table 4.3).

Table 4.3. Trophic state index (TSI) values for each reservoir calculated from annual average chlorophyll-α values.

Reservoir	TSI (CHLA)	Nomenclature
Chew	56.49	Eutrophic
Blagdon	55.13	Eutrophic
Cheddar	47.18	Mesotrophic
Durleigh	73.47	Hypereutrophic
Plas Uchaf	51.28	Eutrophic

4.2.3 Sampling Methods

Raw water abstracted from the intake (draw off) of each reservoir was sampled weekly for analysis of biological, physical and chemical variables. Historical data were analysed for 2-MIB, Geosmin, nitrate, Total Nitrogen (TN) and orthophosphate (total phosphorus in Durleigh) for the period 2014 to the end of 2017.

In 2015, routine monthly water sampling within Plas Uchaf and Dolwen reservoirs was initiated by DCWW and data are presented comparing 2015 and 2016. Sampling consisted of obtaining surface water samples (in triplicate, 1 litre volume), collected in acid washed polyethylene plastic bottles. These samples were analysed for the same suite of variables as for the abstracted raw water samples.

Water samples from Plas Uchaf and Dolwen were processed at the DCWW Glaslyn laboratories, and all samples for Chew, Cheddar, and Blagdon were analysed by ALS environmental. Raw water samples abstracted from Durleigh Reservoir were processed at the Wessex Water (WW) Scientific Centre. All laboratories and methods listed in Table 4.4 are UKAS (United Kingdom Accreditation Service) accredited, and all laboratories follow quality assurance procedures, so comparability of data between laboratories is considered reliable. All measured parameters, and the methods and equipment used in analysis are listed in Table 4.4. Further detail of the sampling and processing (statistical) methods used for this chapter can be found in Chapter 3, Section 3.4.8 and Perkins and Slavin et al. (2019).

Table 4.4. List of measured parameters with the methods and equipment used for each. Reference for different laboratories: ALS Environmental (ALS), Welsh Water (DCWW), and Wessex Water (WW).

Parameter	**Method**	**Equipment**
Total Oxidised Nitrogen (TON) Ammonium Orthophosphate Nitrite	Colorimetry	Thermo Scientific Aquakem 600 spectrophotometer
Nitrate	Colorimetry then TON minus nitrate	As above
2-MIB Geosmin	Extracted using solid phase extraction (SPE) and eluted using Dichloromethane. Analysed by Gas chromatography and mass spectrophotometry (GC/MS/MS)	
Chlorophyll-*α*	Extracted using methanol and analysed spectrophotometrically (DCWW and ALS) *In vivo* fluorescence (WW)	Spectroquant Pharo 300 spectrophotometer bbe AlgaeLabAnalyser
Total Phosphorus (TP)	Inductively coupled plasma mass spectrometry (ICP-MS)	Agilent 7700 ICP-MS
Algal cell counts	Fixed with Lugol's and placed in sedimentation chamber. Identification and enumeration using an inverted microscope (DCWW and ALS) Fixed with Lugol's and concentrated by membrane filtration. Identification and enumeration using microscopy (WW)	Inverso 3000 (TC-100) inverted microscope Olympus BH2 microscope
Turbidity	Turbidimeter	Cyberscan Turbidimeter TB 1000 nephelometer (DCWW) HACH 2100AN Turbidimeter (ALS and WW)

4.2.4 Statistical Analysis

4.2.4.1 Cross correlation

Cross correlation analysis was carried out on the historical intake data from Blagdon, Chew, Cheddar, and Durleigh reservoirs (2014-2017), to discern whether lags between increased nutrient availability and increased concentrations of 2-MIB and Geosmin were present. Cross correlation analysis was performed in MATLAB using the 'xcorr' function. Variables included in analysis were: ammonium, 2-MIB, Geosmin, NH_4:NO_3 ratio, nitrate, orthophosphate, TP (in Durleigh), temperature (Chew/Cheddar/Blagdon), TN:OP (Chew/Cheddar/Blagdon), and TN:TP (Durleigh).

4.2.4.2 Self-Organising Map Analysis

A comprehensive overview of analysis using Self-Organising Maps (SOMs) is given in Chapter 3, Section 3.6.2. This comparatively recent addition to large dataset analysis methods can be considered a non-linear generalization of principal component analysis. Here, the historical abstraction data (2014-2017) from all studied reservoirs were normalised to values between 0-1, and for each site, a Self-Organising Map (SOM) was used to identify the principal variables in T&O production. Using the SomToolbox MATLAB package from the Helsinki University of Technology (Vestano and Alhoniemi, 2000), each SOM was trained with the batch-training algorithm `som_make.` The `som_barplane` function with 'varwise' scaling, was used to visualise the distribution of parameters for each weight vector in the output map. Clustering was performed using the k-means algorithm for each SOM topology (`kmeans_clusters` function). The best matching unit (BMU) for each input is identified using the som_bmus function. The input data is then assessed for significant differences between clusters (based on BMU identification and cluster analysis) using single-factor ANOVA and post hoc Tukey's test in PAST statistical software package (Hammer et al. 2001).

4.3 Results

In this section, time series of historical T&O and cyanobacteria cell count data are presented from all sites. Then nutrient concentrations are shown as time series and used in ratios regarding T&O concentrations. The Plas Uchaf in-reservoir measurements from Perkins and Slavin et al. (2019) are presented to help explain the hypothesis development. Results from cross correlation analysis are presented and discussed to show why Self-Organising Map (SOM) analysis was considered a better method of analysis. SOM results for all sites are shown and a summary table (4.6) of the main findings is given at the end of this section.

4.3.1 2-MIB and Geosmin concentrations

2-MIB and Geosmin concentrations show a clear seasonal pattern at Cheddar and to a lesser extent, Blagdon and Chew (Figure 4.3). Geosmin concentrations at Chew peaked on 10 August 2015 at 243 ng l^{-1} and 2-MIB concentrations peaked at 89.8 ng l^{-1} on 11 September 2017 (Figure 4.3a). At Blagdon, 2-MIB peaked at 266 ng l^{-1} on 29 September 2014 and Geosmin peaked at 317 ng l^{-1} on 15 August 2017 (Figure 4.3b). 2-MIB concentrations at Durleigh followed a seasonal pattern, peaking in autumn each year (Figure 4.3c). However, Geosmin concentrations at Durleigh continued to rise through the winter of 2016-7 before peaking at 516 ng l^{-1} on 4 June 2017 (Figure 4.3c). At Plas Uchaf, a significant decrease in both 2-MIB and Geosmin concentrations were observed between 2015 and 2016 at all sampling locations within the reservoir (Figure 4.4.; Perkins and Slavin et al., 2019).

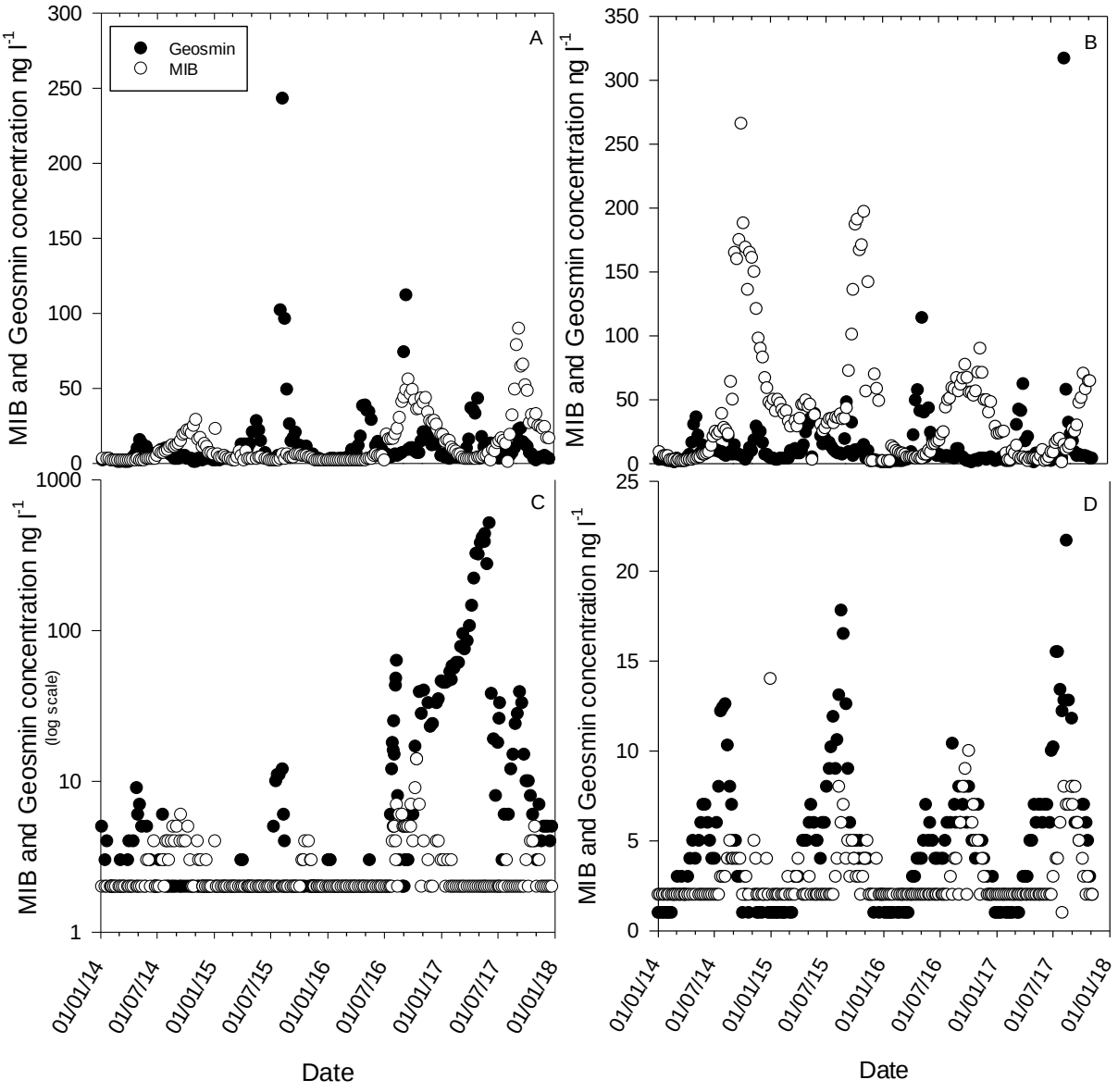

Figure 4.3. The 2-MIB and Geosmin concentrations in raw water abstracted from a) Chew, b) Blagdon, c) Durleigh (note the log scale), and d) Cheddar from 1 Jan 2014 – 1 Jan 2018.

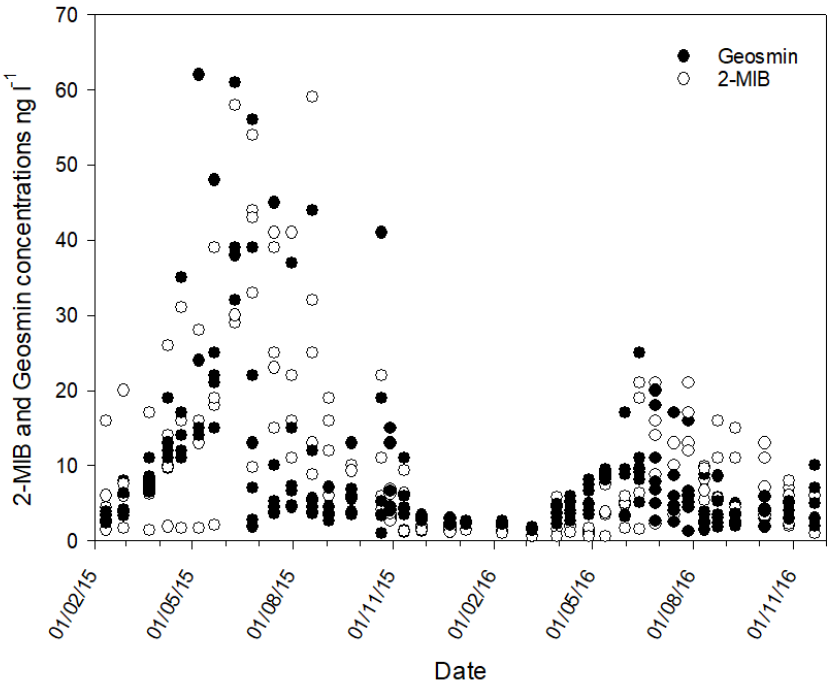

Figure 4.4. The 2-MIB and Geosmin concentrations from all sample points in Plas-Uchaf and the intake at Dolwen between 11 Feb 2015 and 21 Nov 2016. Data provided by Welsh Water.

4.3.2 Cyanobacteria Cell Counts

Cyanobacteria were present in all studied reservoirs, with Cheddar (Figure 4.5a) having the lowest overall cell counts of cyanobacteria and Durleigh (Figure 4.5d) having the highest, which follows the TSI(chl) values (Table 4.2). In 2017, cyanobacterial cell counts peaked on 16 April at Durleigh (Figure 4.5d). At Cheddar (Figure 4.5a), Chew (Figure 4.5b), and Blagdon (Figure 4.5c) counts were highest in 2014. Perkins and Slavin et al. (2019) observed higher cyanobacterial cell counts in 2015 compared to 2016 at all sites studied in Plas Uchaf and Dolwen (Figure 4.6).

In Plas Uchaf, *Dolichospermum* spp. (formerly *Anabaena* spp.) were the dominant cyanobacteria taxa, with low counts of *Oscillatoria* spp. and *Microcystis* spp. as the only other cyanobacteria taxa recorded (Perkins and Slavin et al., 2019). Cyanobacteria cell counts accounted for over 95% of the total algal cell counts in 2015 and 2016. *Dolichospermum* were also the most dominant cyanobacterial taxa observed in Blagdon (132 observations between 2014-7), followed by *Aphanizomenon* (56) and *Microcystis* (44). The largest peak in a cyanobacteria taxon at Blagdon was *Gloeotrichia* at 107926

cells ml^{-1}, with *Dolichospermum* being only the fourth highest after *Microcystis* and *Oscillatoria* (data not shown). The peak in *Gloeotrichia* cell counts (Figure 4.5c) coincided with the Geosmin peak at 317 ng l^{-1} (Figure 4.3b). In-reservoir observations at Blagdon between 26 June and 15 August 2017 revealed that the bloom of *Gloeotrichia* that was first observed in the reservoir on 25 July 2017 (author observations), suggesting that the high Geosmin concentrations at the intake in August were possibly due to the remnants of the bloom in the reservoir with the lysis of cells and subsequent release of intracellular Geosmin being responsible for the high concentrations observed at the intake. In Durleigh, *Planktothrix* were the most frequently observed taxa (305 times since 2010), but many other known T&O producing taxa have been observed including, but not limited to: *Dolichospermum*, *Aphanizomenon*, and *Aphanocapsa*. In 2017, *Planktothrix* accounted for on average 75% of the total algal cell counts in Durleigh (data not shown).

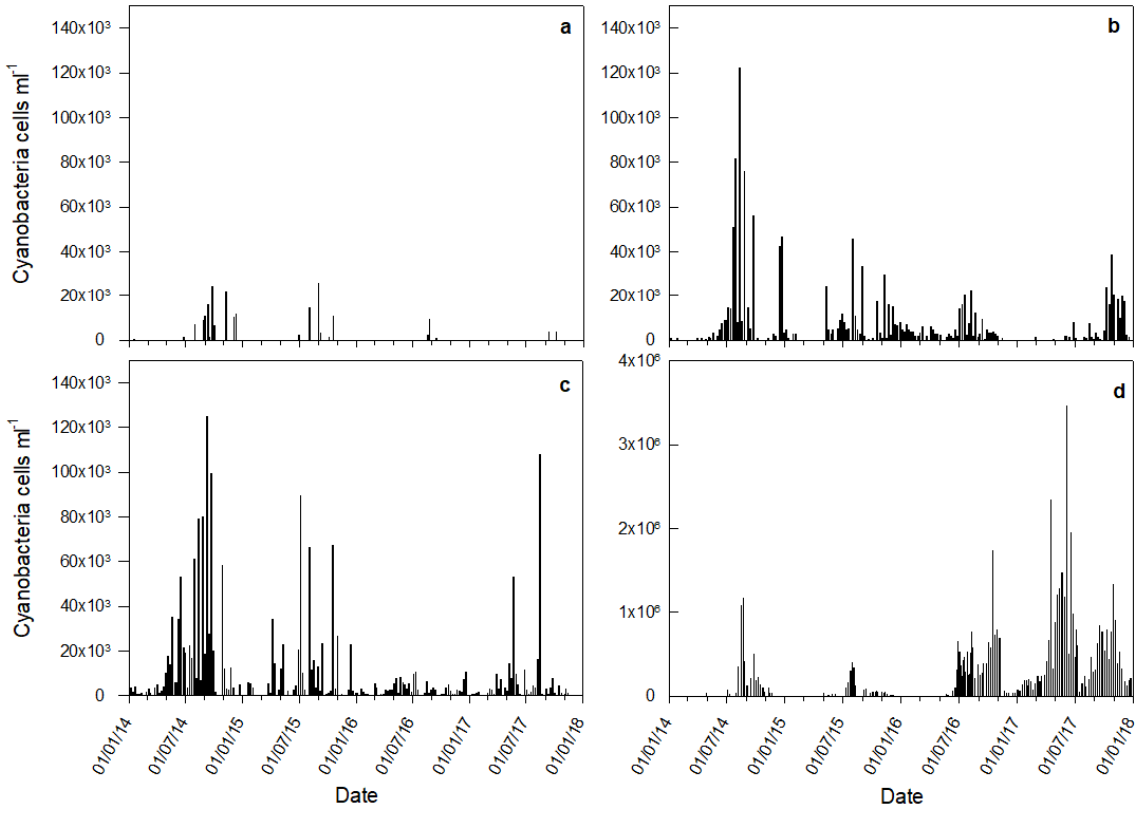

Figure 4.5. Historical cyanobacteria cell counts from the intake of a) Cheddar, b) Chew, c) Blagdon, and d) Durleigh between 1 Jan 2014 and 1 Jan 2018. Note the different scale on the y-axis of d. Data provided by Bristol Water (a-c) and Wessex Water (d).

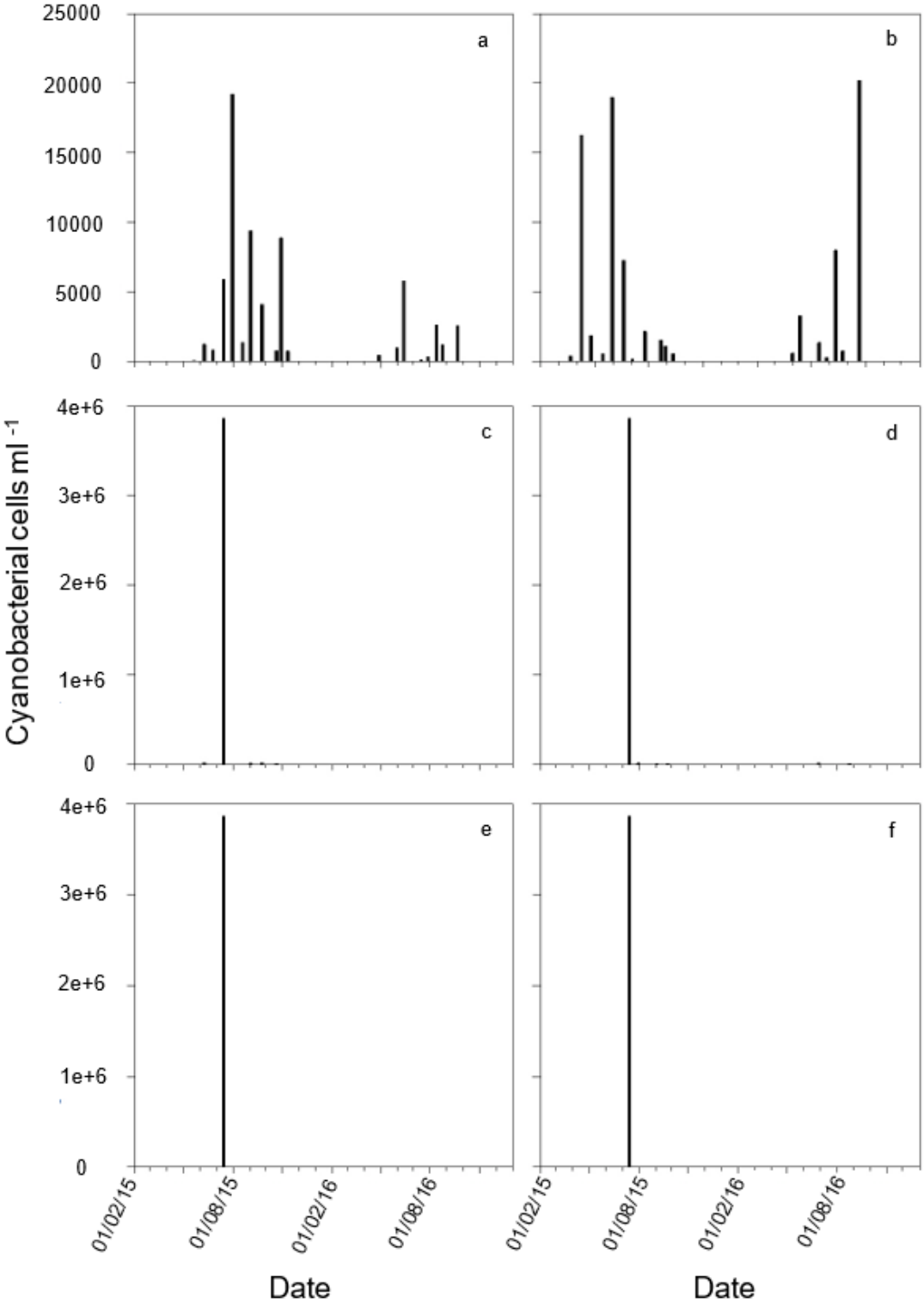

Figure 4.6. Historical cyanobacteria cell counts from sampling points in Plas Uchaf Reservoir a) SPT1, b) SPT2, c) SPT3, d) SPT4, e) SPT5, and f) Dolwen Reservoir intake between 1 Feb 2015 and 1 Jan 2017. Data provided by Welsh Water.

4.3.3 Nutrients and nutrient ratios

4.3.3.1. Phosphorus and nitrogen

Time series of orthophosphate (OP) and total phosphorus (TP) intake concentrations for all sites are presented in Figures 4.7 and 4.8, and total nitrogen intake concentrations are presented in Figures 4.9 and 4.10. Concentrations of TP at Plas (Figure 4.8a; Perkins and Slavin et al., 2019) were higher in 2016 compared to 2015 and typically increased between August and October both years. OP concentrations show a seasonal pattern at Chew (Figure 4.7b) and Blagdon (Figure 4.7c), with increases occurring around early July each year. Lower OP concentrations were observed at Cheddar (Figure 4.7a) and Durleigh (Figure 4.7d). However, TP at Durleigh (Figure 4.8b) shows similar seasonal patterns to OP at Chew and Blagdon, suggesting that internal loading of phosphorus is occurring in the late summer at these sites. The low concentrations of OP at the Durleigh intake could be due to the rapid assimilation of OP by cyanobacteria (Aubriot and Bonilla, 2012) when it is made available.

Total nitrogen (TN) concentrations show a clear seasonal pattern at the Somerset reservoirs (Figure 4.9), where decreases in concentrations occur during the summer. Additionally, TN concentrations at the Plas Uchaf intake show decreases in the summer of 2015 and 2016 (Figure 4.10). The declines in TN at all sites are primarily attributed to summer decreases in nitrate concentrations. Nitrate concentrations can decline in the summer due to increased denitrification (Hill, 1988; David et al., 2006), assimilation (Chaffin et al., 2013), and reduced runoff from the external sources (Ke et al., 2008). Nitrite concentrations at all sites studied were frequently below the level of detection, with values always less than 5% of total oxidised nitrogen (nitrate and nitrite) when recorded, so were not considered further. Ammonium concentrations are low compared to nitrate (Section 4.3.3.3). Therefore, based on these observations we suggest that the seasonal changes in TN concentration are primarily driven by a decline in nitrate.

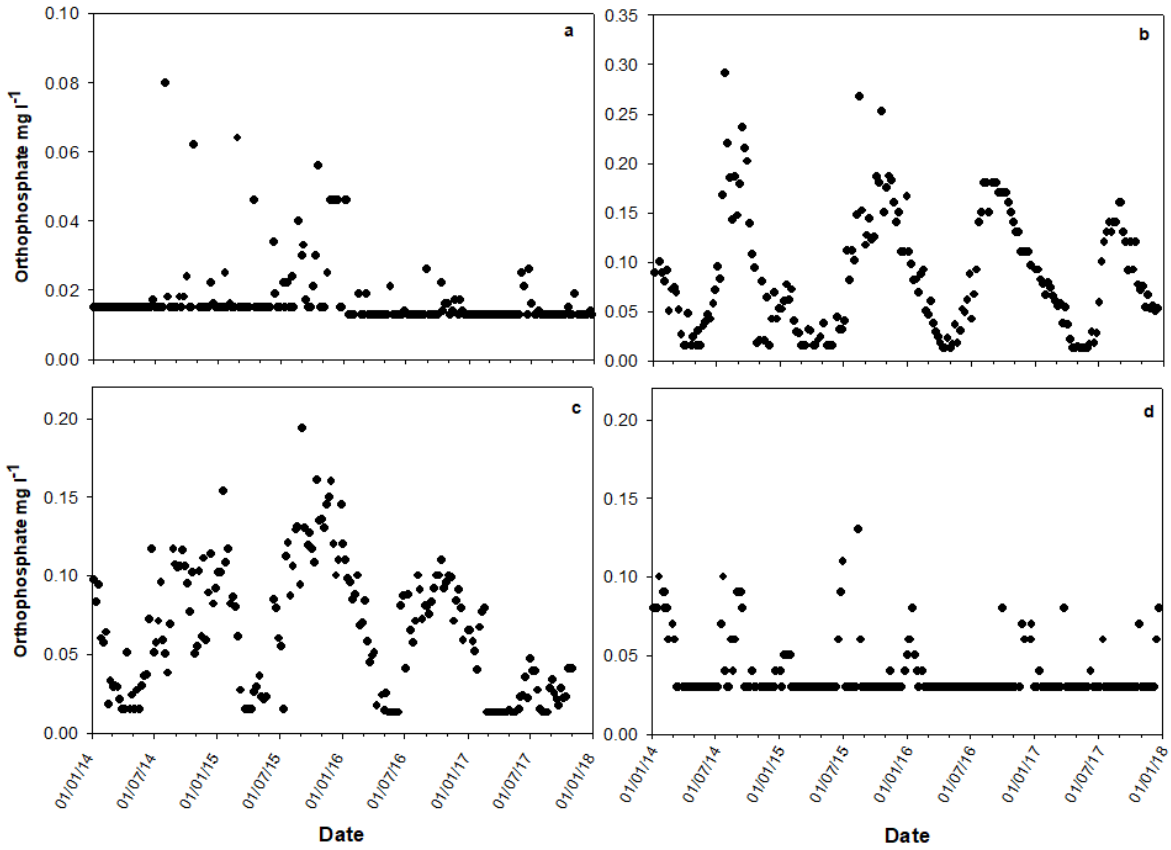

Figure 4.7. Concentrations of orthophosphate from the intake at a) Cheddar, b) Chew, c) Blagdon, and d) Durleigh, between 1 Jan 2014 and 1 Jan 2018. Data provided by Bristol Water (a-c) and Wessex Water (d).

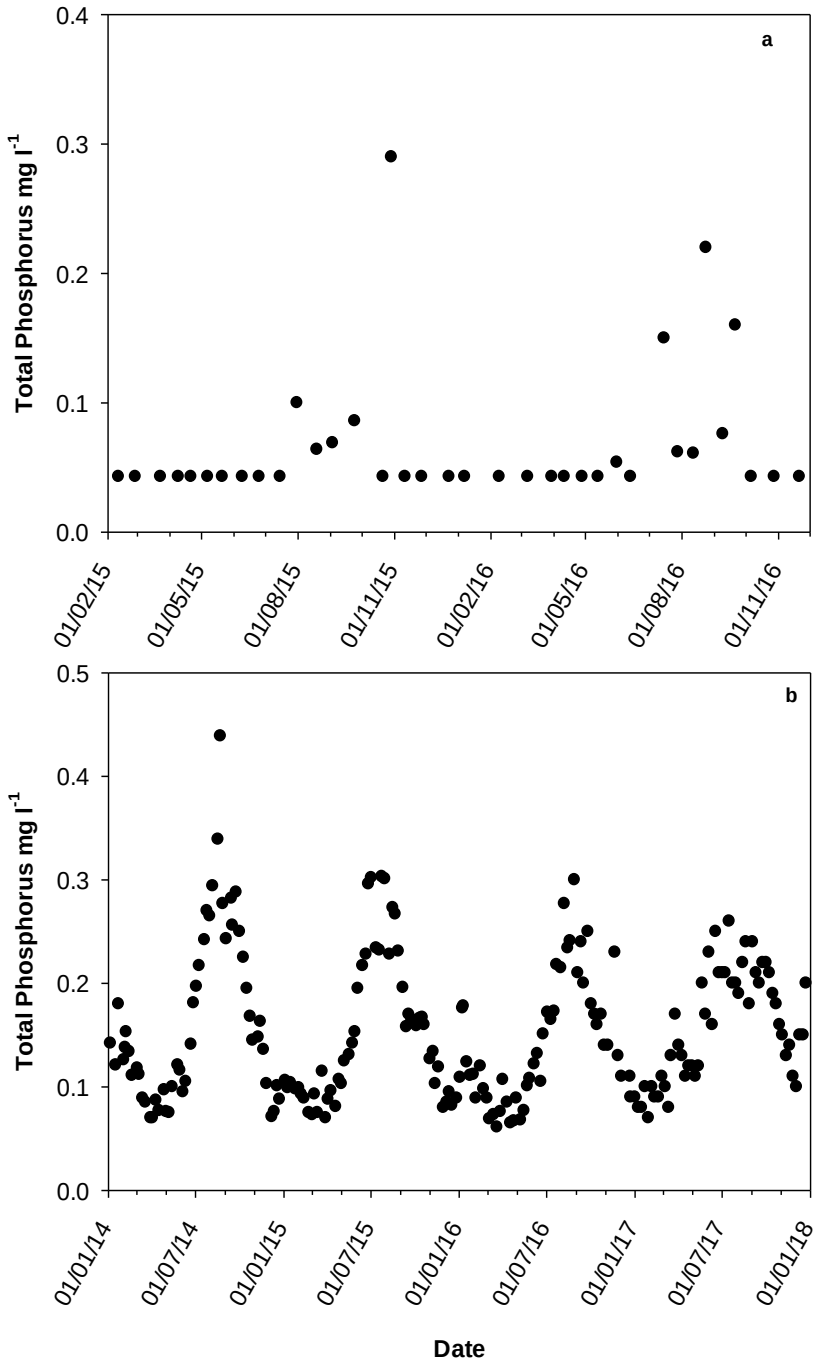

Figure 4.8. Concentrations of total phosphorus from the intake at a) Plas Uchaf (between 1 Feb 2015 and 21 Nov 2016) and b) Durleigh (between 1 Jan 2014 and 1 Jan 2018). Data provided by Welsh Water (a) and Wessex Water (b).

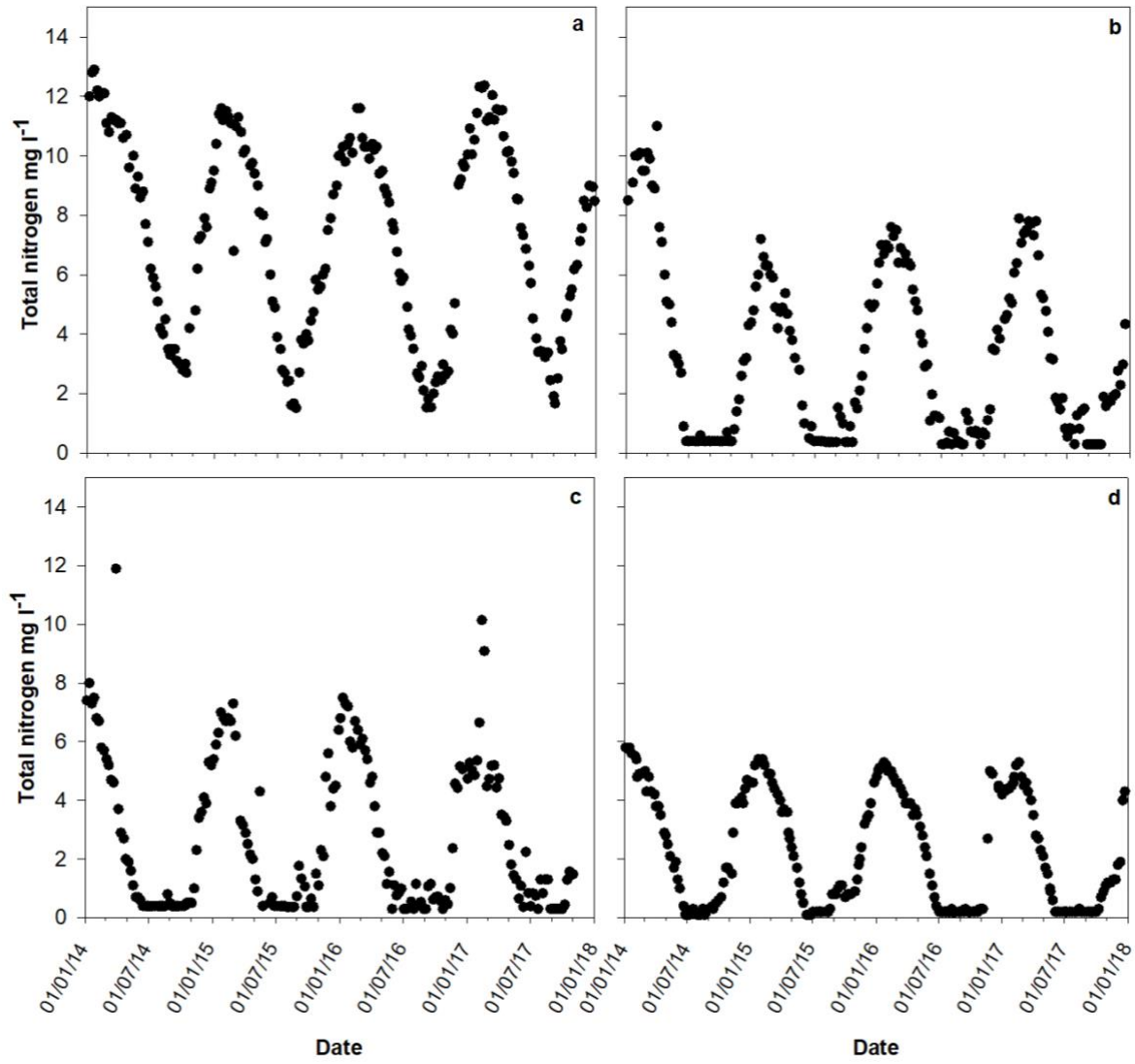

Figure 4.9. Concentrations of total nitrogen from the intake at a) Cheddar, b) Chew, c) Blagdon, and d) Durleigh, between 1 Jan 2014 and 1 Jan 2018. Data provided by Bristol Water (a-c) and Wessex Water (d).

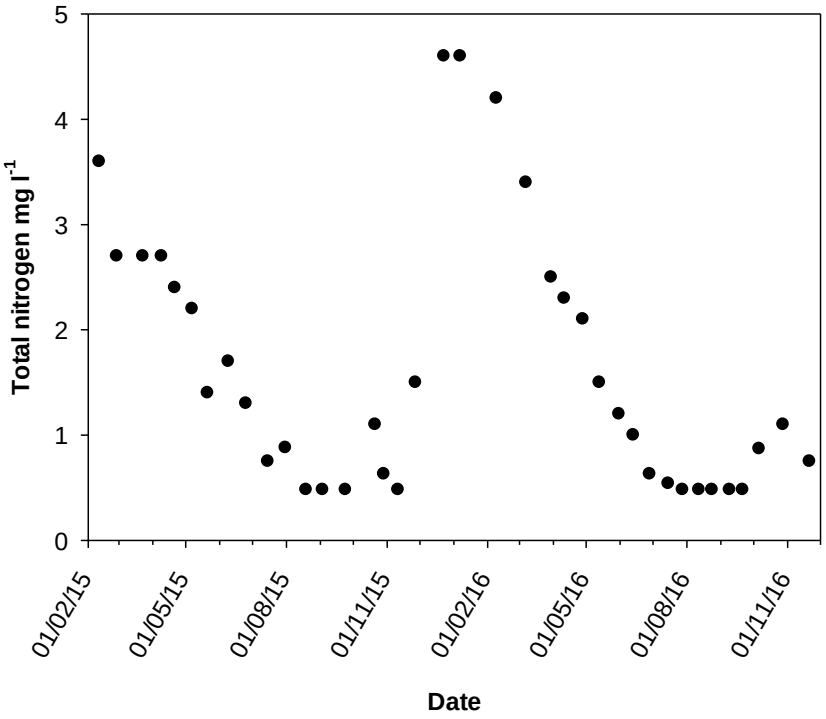

Figure 4.10. Concentrations of total nitrogen from the intake at Plas Uchaf between 1 Feb 2015 and 21 Nov 2016.

4.3.3.2. TN:TP ratio and T&O metabolites

The TN:TP ratio is frequently reported as a cause of increased cyanobacterial productivity (Bormans et al., 2016) and low ratio values have been associated with higher T&O metabolite concentrations (Watson, 2003; Winston et al., 2014; Harris et al., 2016). An inverse relationship is observed between the TN:OP ratio and 2-MIB/Geosmin concentrations at Chew, Cheddar, Blagdon, and Plas Uchaf (Figures 4.11a-c and 4.12) and between the TN:TP ratio and 2-MIB/Geosmin at Durleigh (Figure 4.11d). The observed relationship is generally clearer for 2-MIB concentrations compared to Geosmin. Changes in the TN:TP ratio appear to primarily be driven by the summer decline in nitrate and, to a lesser extent, a concomitant increase in TP/OP (section 4.3.3.1).

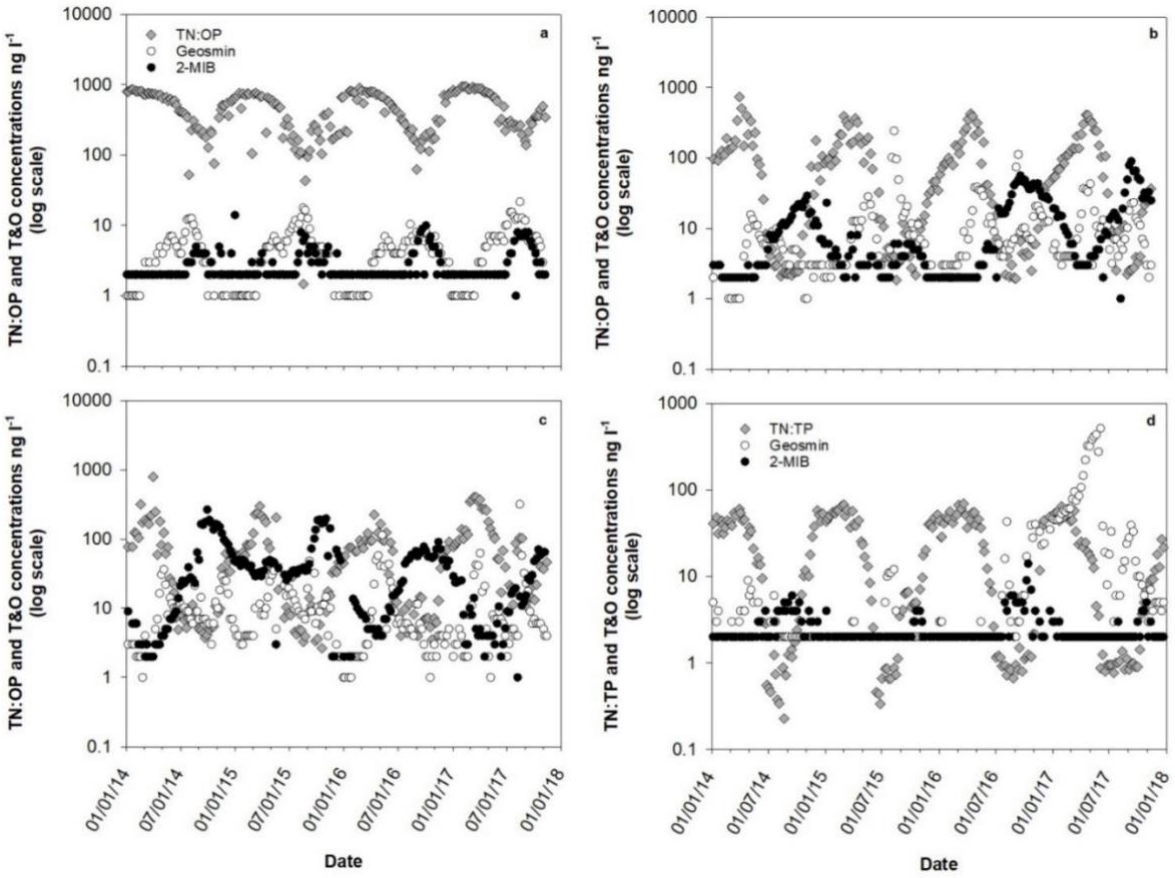

Figure 4.11. The TN:OP ratio and Geosmin/2-MIB concentrations between 2014-2018 at a) Cheddar, b) Chew, and c) Blagdon. d) the TN:TP ratio and Geosmin/2-MIB concentrations between 2014-2018 at Durleigh.

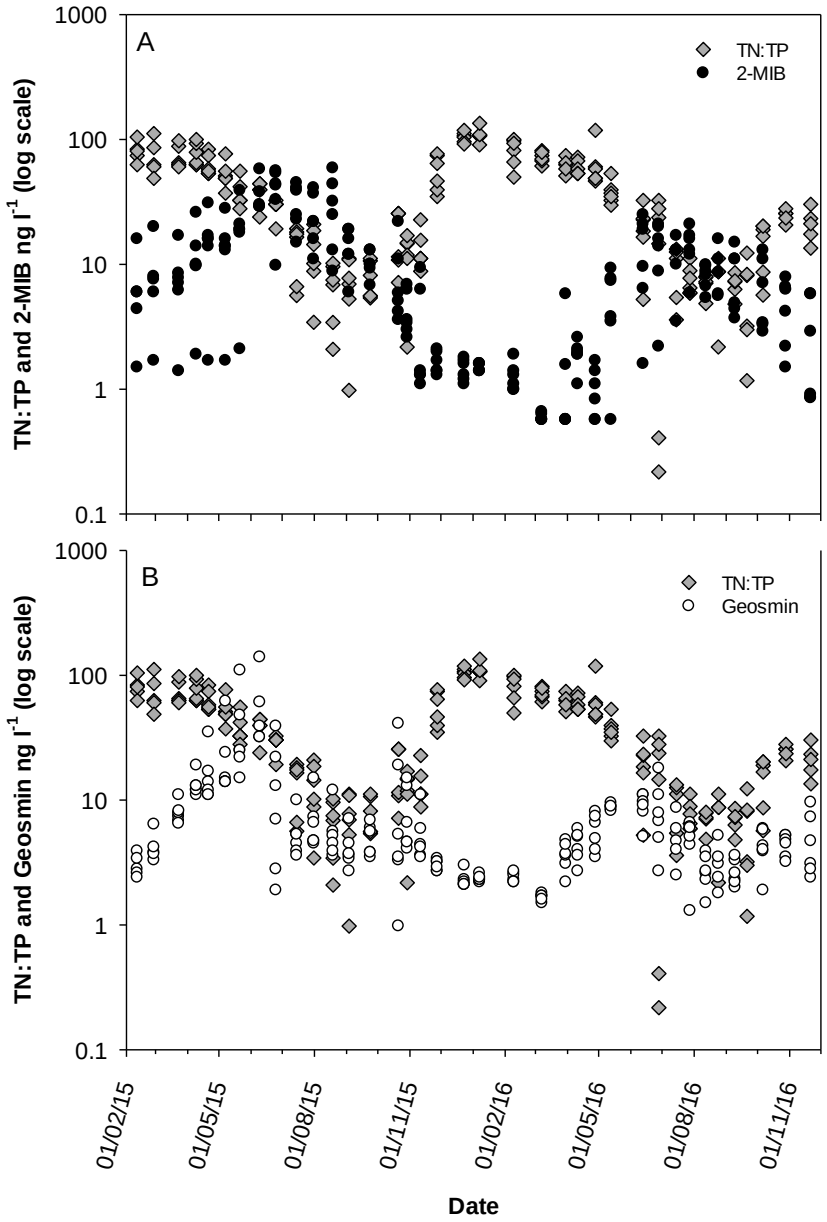

Figure 4.12. The TN:TP ratio and 2-MIB concentrations (A) and Geosmin concentrations (B) for 2015 and 2016 at Plas Uchaf Reservoir. Data points refer to absolute values from measurement taken at all 5 sample locations in Plas Uchaf and the Dolwen intake, hence showing the range of values at the time of measurement. From Perkins and Slavin et al. (2019).

4.3.3.3. Ammonium concentrations

Ammonium concentrations from the intakes of the Somerset reservoirs show seasonal variation (Figure 4.13). Both Cheddar (Figure 4.13a) and Durleigh (Figure 4.13d) show summer increases in ammonium, which may be caused by increased ammonification. Summer increases in ammonium are less apparent at Chew (Figure 4.13b) and Blagdon (Figure 4.13c). The summer increases in ammonium coincide with declining nitrate concentrations, which is responsible for the increased NH_4:NO_3 ratios in the summer observed in section 4.3.3.4.

At Plas Uchaf reservoir, the average ammonium concentrations decreased significantly at all five sample points between 2015 and 2016 and a decrease of 85% was observed at the Dolwen intake (Figure 4.14; Perkins and Slavin et al., 2019). The significant decrease in ammonium concentrations between 2015 and 2016 coincided with a significant decrease in both 2-MIB and Geosmin concentrations (Figure 4.4). No other measured water chemistry variable showed significant decrease between 2015 and 2016 (Perkins and Slavin et al., 2019). Therefore, Perkins and Slavin et al. (2019) suggested that ammonium may be an important trigger for production of T&O metabolites in cyanobacteria at Plas Uchaf.

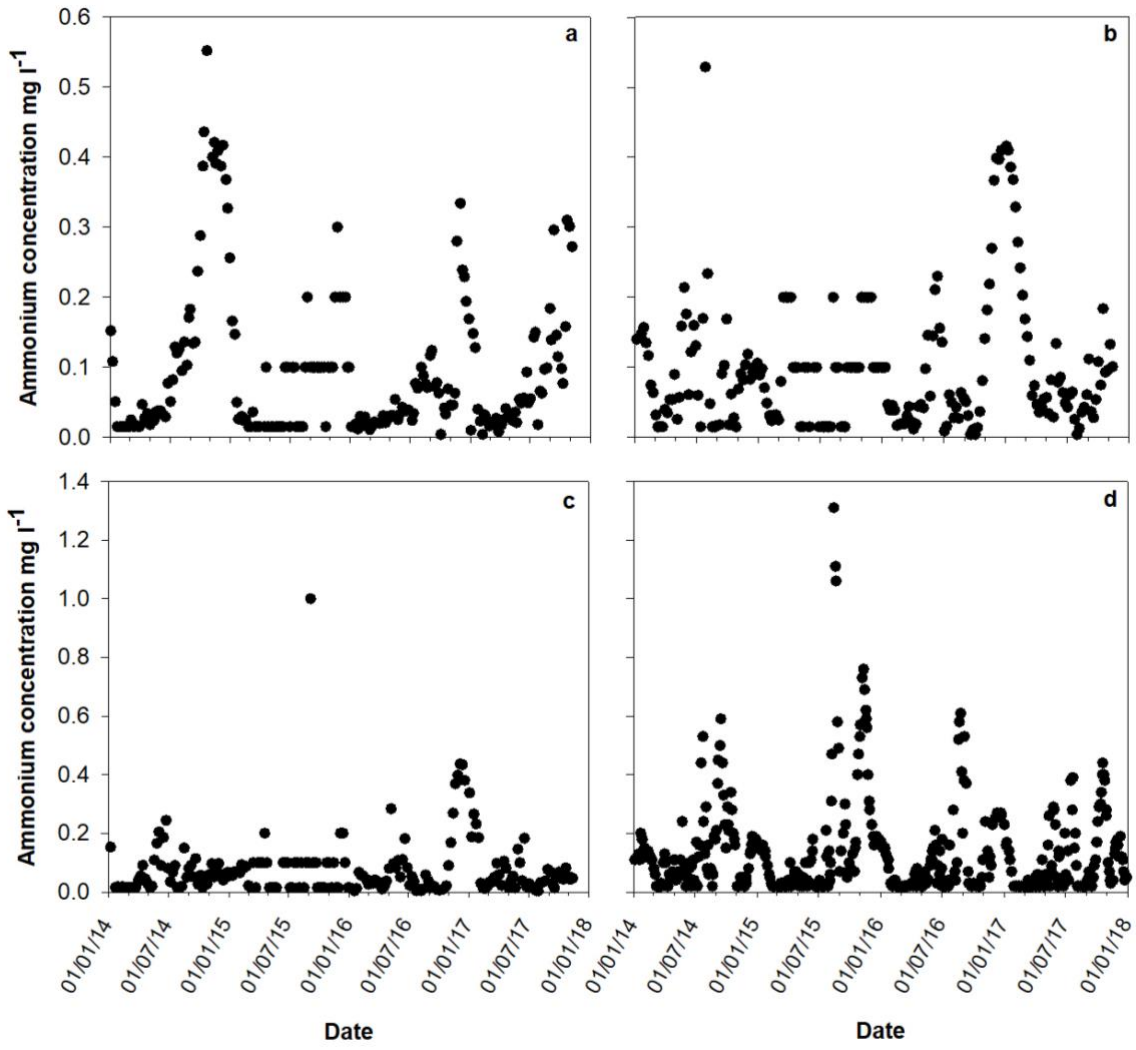

Figure 4.13. Ammonium concentrations from the intake at a) Cheddar, b) Chew, c) Blagdon, and d) Durleigh between 1 Jan 2014 and 1 Jan 2018.

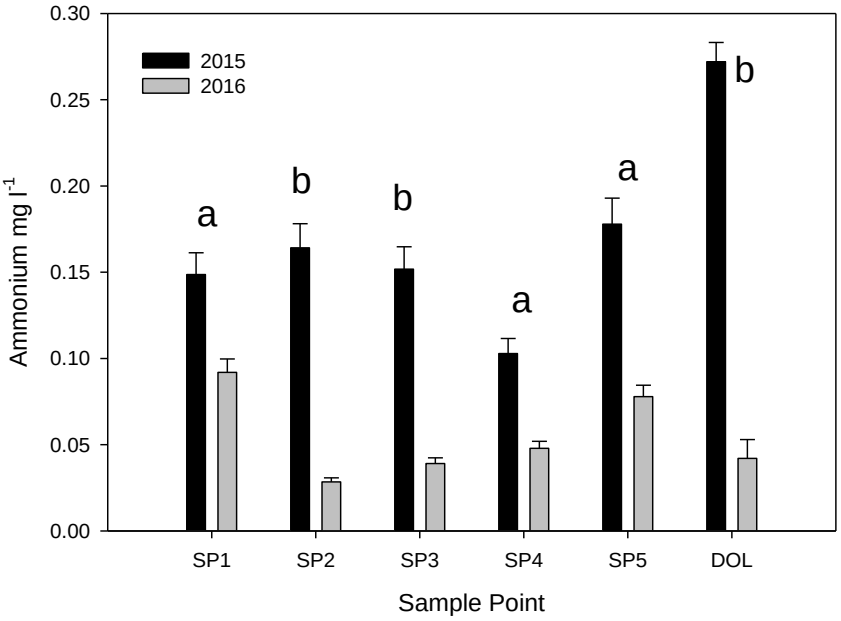

Figure 4.14. Ammonium concentrations in water samples from sample points 1 to 5 in 2015 and 2016. Mean values with standard error bars. Significant difference (ANOVA, two factor, df = 1, 24 for factor 1 (year) and 4, 24 for factor two (site), significant differences identified by post hoc Tukey's test) for each sample point are indicated at a significance level of $p < 0.05$ (a) and $p < 0.01$ (b). From: Perkins and Slavin et al. (2019).

4.3.3.4. NH_4:NO_3 ratio and T&O metabolites

Harris et al. (2016) found an association between high ammonia (NH_3) concentrations relative to nitrate (NO_3) and T&O and toxin concentrations, suggesting that the NH_3:NO_3 ratio may be important when considering the production of T&O metabolites. Here, we report ammonium concentrations relative to nitrate (NH_4:NO_3) instead of ammonia, based on the available data.

The NH_4:NO_3 increases in the summer at the Somerset reservoirs (Figure 4.15). Maximum values of NH_4:NO_3 appear to occur at similar times to peaks in T&O metabolites concentrations (Figure 4.15). Generally, the NH_4:NO_3 peaks slightly before maximum concentrations of 2-MIB are reached, whereas Geosmin concentrations peak just before, or at the time of high NH_4:NO_3 values. However, at Cheddar (Figure 4.15a), Geosmin concentrations start to increase around two months before increases in NH_4:NO_3 are observed. Both summer decline in nitrate (Figure 4.9) and increase in ammonium concentrations (Figure 4.13) are considered to cause the increase in NH_4:NO_3 values during the summer.

Although some association between T&O metabolite concentrations and both the TN:TP and the NH_4:NO_3 ratios is demonstrated, the cause and effect has not been identified. However, the in-reservoir observations at Plas Uchaf (Perkins and Slavin et al., 2019) demonstrate a significant decrease in ammonium concentrations (Figure 4.14) were associated with a significant decrease in T&O concentrations (Figure 4.4), while no other water chemistry variable exhibited such a decrease between 2015 and 2016 (Perkins and Slavin et al., 2019). These observations highlight that ammonium may be an important trigger in the production of T&O metabolites in cyanobacteria. The following sections describe statistical analysis on multiple parameters at the Somerset reservoirs and Plas Uchaf/Dolwen reservoirs to determine whether ammonium is a key trigger in T&O metabolite production across a trophic gradient of multiple different reservoirs, and to verify the broader applicability of the proposed theory.

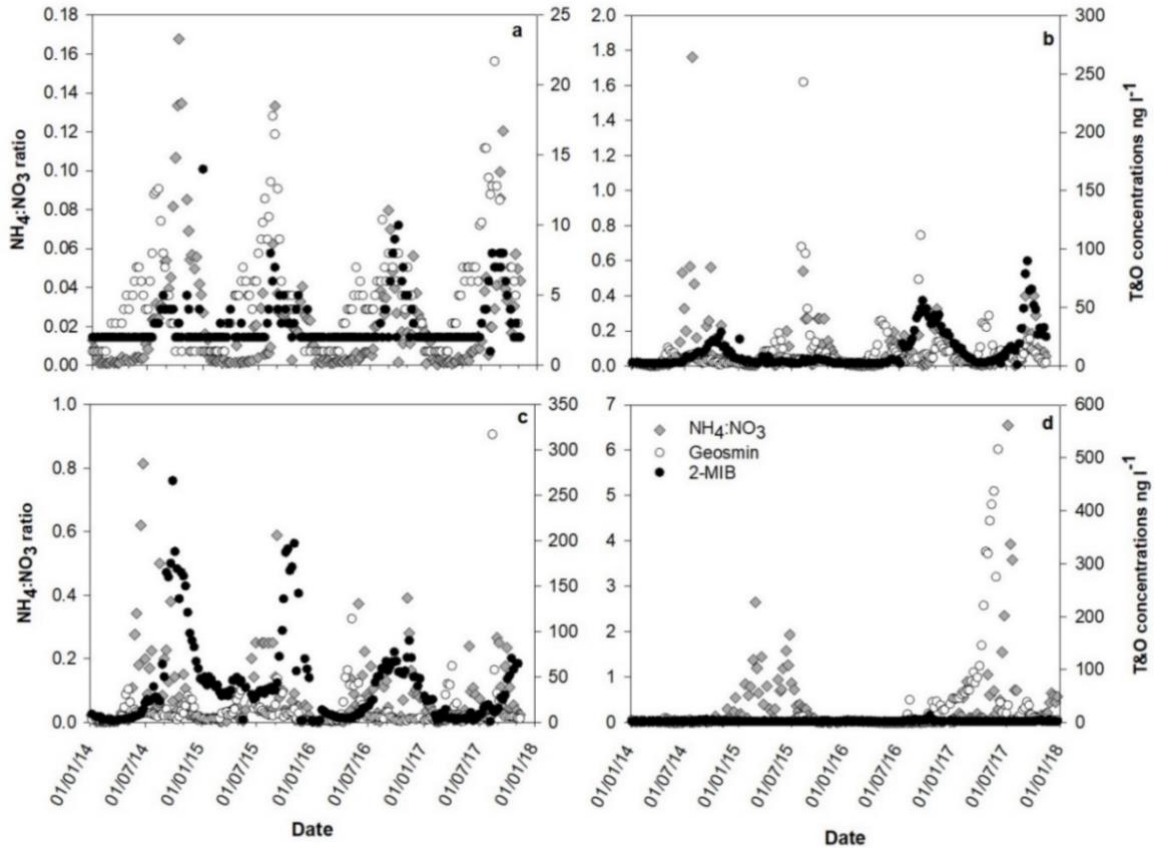

Figure 4.15. The NH_4:NO_3 ratio with 2-MIB and Geosmin concentrations for a) Cheddar, b) Chew, c) Blagdon, and d) Durleigh between 1 Jan 2014 and 1 Jan 2018.

4.3.4 Cross correlation analysis

Cross correlation analysis was used to identify whether increase in particular nutrient concentrations precede increases in T&O metabolite concentrations in data from the intakes of Cheddar, Chew, Durleigh, and Blagdon (Chapter 3, Section 3.6.1). In this section, only lags that demonstrated a short time delay between one peak and another are considered. Although lags > 10 days are still considerable when referring to T&O metabolite production in cyanobacteria (Naes et al., 1985).

Cross correlation results for Blagdon show 2-MIB concentrations tend to reach their maximum two weeks after orthophosphate (OP) concentrations and Geosmin peaks three weeks before maximum temperatures are reached (Table 4.5). Both OP and NH_4:NO_3 ratio increase one week prior to peaks in 2-MIB at Cheddar. At Cheddar, Geosmin concentrations peak before temperatures but only by one week. At Chew, no lag is observed between Geosmin and temperatures and all other lags are too large to consider as factors influencing 2-MIB and Geosmin production. At Durleigh, 2-MIB concentrations reach their maximum three weeks after total phosphorus and ammonium, and OP peaks two weeks before 2-MIB (Table 4.5).

Despite these lags being within the reported phytoplankton response range, increases in growth rates can occur within hours of increased nutrient availability (Örnólfsdóttir et al. 2004). Therefore, due to the frequency of water sample measurements (weekly), any observed lags are considered too long to relate to phytoplankton response. For example, Rukminasari and Redden (2011) found increases in phytoplankton biomass within 2 to 6 days following nutrient addition, which may be missed in weekly samples, whereas Heath et al. (2016) found exponential growth rates in *Phormidium* occurred within 3 to 9 days. Cross correlation is a useful method if more frequent water samples were collected, particularly if in-reservoir measurements are collected rather than at the intake. However, daily in-reservoir monitoring of nutrient concentrations would be expensive for utilities to undertake in all drinking water supply reservoirs subject to T&O outbreaks. Therefore, an alternate method of statistical analysis was sought to examine these data, the results of which are presented in the next section.

Table 4.5. Cross correlation lags (in weeks) for intake data (between 1 Jan 2014 and 1 Jan 2018) from Cheddar, Chew, Blagdon, and Durleigh.

Reservoir	Parameters	Lag 2-MIB	Lag Geosmin
Cheddar	NH_4	0	-15
	NO_3	0	+19
	OP	-1	0
	TN:OP	+28	+19
	Temperature	+7	+1
	NH_4:NO_3	-1	-10
Chew	NH_4	+38	-13
	NO_3	+31	+31
	OP	+14	-13
	TN:OP	-24	-70
	Temperature	-11	0
	NH_4:NO_3	-110	-53
Blagdon	NH_4	+60	-100
	NO_3	-35	-16
	OP	-2	-35
	TN:OP	+27	+22
	Temperature	-11	+3
	NH_4:NO_3	-14	-39
Durleigh	NH_4	-3	+79
	NO_3	+32	+67
	OP	+2	+166
	TN:OP	-32	-111
	Temperature	-8	-36
	NH_4:NO_3	-8	-93
	TP	-3	-136
	TN:TP	-34	-112

4.3.5 Self-organising map results

The Self-Organising Map (SOM) component plots (Figures 4.16a – 4.21a) show the topology of the SOM for each of the input variables and are the first phase of dimension reduction in a SOM. A 5x2 hexagonal-node grid was selected as the optimal map size when considering the topographic and quantization errors (Chapter 3, Section 3.6.2). Each node (hexagon) of the component plane represents a certain position in map space and is consistent across all component plots for all input variables. Colours in the component plots show the values that variables have in the map structure, with yellow indicating higher and blue lower. The similarity between neighbouring nodes is highlighted by the U-matrix, which is weighted according to Euclidean distance and indicated by colours on the map, with blues designating shorter distances (similarity) and yellows longer distances (difference). SOM component plots can be regarded as an analogue of PCA loading plots. The bar plane plots (Figures 4.16-4.21b) rank the input

variables according to their perceived relative importance for each node. The minimum and maximum loading values for the bar planes are based on weight scales in the component plots. The second phase of dimension reduction in a SOM is clustering the nodes based on similar characteristics from all the input variables. Figures 4.16c – 4.21c show the clusters defined using the k-means algorithm.

In this chapter, the SOM results for all Somerset reservoirs are presented (Figures 4.16-4.19 and Table 4.6) with SOMs for SPT1 (Plas Uchaf) and Dolwen. Here, Dolwen and SPT1 sites were selected as these sites are closest to the intake in both Dolwen and Plas Uchaf, so most comparable to the intake sites in the Somerset reservoirs. Sites close to the intake are of interest to water treatment and quality managers. The SOM results for SPT2, SPT3, SPT4, and SPT5 are reported in Perkins and Slavin et al. (2019). The main findings of the SOM analysis are discussed below, and a summary is presented in Table 4.6.

The SOM component plots for Durleigh (Figure 4.16a), Cheddar (Figure 4.17a) and SPT1 in Plas Uchaf (Figure 4.20a) show nitrate to correlate against all other variables as the high weightings (yellow) occur mainly in the first 2 nodes in the plot, opposite to the high weightings for all other variables. Visual analysis of the bar planes reveal that as weightings of nitrate decrease, weightings of ammonium, 2-MIB, and Geosmin increase (Figure 4.16b, 4.17b and 4.20b), indicating that low nitrate concentrations and high ammonium concentrations are associated with higher 2-MIB and Geosmin concentrations at these three different reservoirs.

Clustering by k-means and single factor ANOVA showed that cluster 1 (C1) of the Durleigh SOM (Figure 4.16c) has significantly higher ammonium and total phosphorus (TP) concentrations than cluster 2 (C2, all $p < 0.01$) and cluster 3 (C3, NH_4: $p = 0.02$; TP: $p < 0.01$) and has significantly lower nitrate concentrations than C2 ($p < 0.01$) and C3 ($p < 0.01$). No significant differences were observed in 2-MIB or Geosmin concentrations between clusters, however, C1 and C3 had higher concentrations of 2-MIB and Geosmin. The Durleigh SOM results indicate that 2-MIB and Geosmin concentrations are associated with higher ammonium and TP concentrations, and lower nitrate concentrations.

Similarly, for SPT1 in Plas Uchaf, clustering analysis (Figure 4.20c) and ANOVA indicate nitrate concentrations were significantly higher in C1 ($p < 0.01$). Chlorophyll-α concentrations, cyanobacteria, and pH were all significantly higher in C3 compared to

other clusters (pH and chlorophyll-α: $p < 0.01$; Cyanobacteria: $p < 0.05$). Concentrations of 2-MIB and Geosmin were significantly higher ($p < 0.01$) in C2 (Figure 4.20c), and although higher in C2, no significant differences were observed between clusters for ammonium and TP concentrations.

Component plots for Blagdon (Figure 4.18a) show that 2-MIB and Geosmin correlate with cyanobacteria, pH, temperature, and OP. The bar plane plots (Figure 4.18b) show that as the weightings of 2-MIB and Geosmin increase, the weighting for nitrate decreases. Single-factor ANOVA revealed that C1 had significantly higher (all $p < 0.01$) nitrate, 2-MIB, and OP concentrations than C2 (Figure 4.18c), whereas temperature ($p < 0.01$), Geosmin ($p = 0.01$), pH ($p < 0.01$), cyanobacteria ($p = 0.02$), and chlorophyll-α concentrations ($p < 0.01$) were all significantly higher in C2 compared to C1. Although ammonium loads highly in node 1 (Figure 4.18b), no significant difference was found in ammonium concentrations between clusters (Figure 4.18c).

SOM results for Chew revealed Geosmin correlated with OP and cyanobacteria, while 2-MIB correlated with ammonium (Figure 4.19a). The bar plane plots show that as the weightings of 2-MIB and ammonium increase, the weighting of nitrate decreases (Figure 4.19b). Cluster analysis and ANOVA revealed that cyanobacteria, pH, temperature, OP, and chlorophyll-α concentrations were significantly higher in C1 (Figure 4.19c) compared to C2 (temperature, pH, and chlorophyll-α: $p < 0.01$; OP: $p = 0.03$). Ammonium concentrations were significantly higher in C2 ($p < 0.01$). There were no significant differences in nitrate, cyanobacteria, 2-MIB, or Geosmin concentrations between clusters, although Geosmin concentrations and cyanobacteria were higher in C1 and 2-MIB and nitrate concentrations were higher in C2.

Component plots of the Dolwen SOM show that nitrate and Geosmin correlate together (Figure 4.21a). The bar planes revealed that weightings of ammonium increase with increasing weightings of 2-MIB and TP and decreasing weightings of nitrate (Figure 4.21b). Clustering and single-factor ANOVA revealed C3 (Figure 4.21c) has significantly higher nitrate and Geosmin concentrations ($p < 0.05$), whereas C1 had significantly higher ammonium concentrations ($p < 0.05$).

Overall, the SOM bar plane plots reveal that as the weighting of nitrate decreases, the weightings of ammonium, 2-MIB and Geosmin increase (Figures 4.16b – 4.21b). Generally, SOM component plots for all reservoirs, except Chew and Dolwen, show

that nitrate correlates against all other variables. Cluster analysis of the Cheddar and Durleigh SOMs show significantly lower nitrate concentrations where ammonium, 2-MIB, and Geosmin concentrations are significantly higher. However, Geosmin in Chew loads highly with OP and cyanobacteria (Figure 4.19b), and in Dolwen, Geosmin and nitrate load highly together (Figure 4.21b). A summary of the results from SOM analysis presented here can be found in Table 4.6.

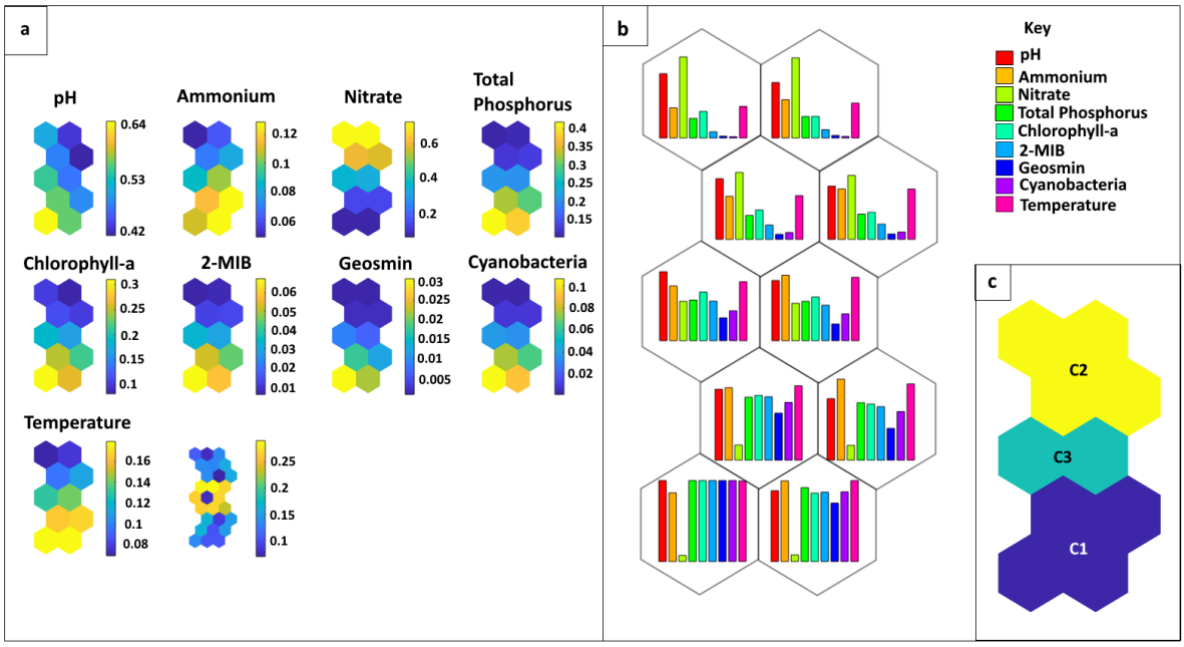

Figure 4.16. **Durleigh Reservoir** (a) SOM component planes and U-matrix for the 2014-2017 historical data from the intake. Each map unit (hexagon) represents a certain position in the map space, which is consistent across all component plots. Colours in the component plots show the values that variables have in the map structure, with yellow indicating higher values and blue lower. The U-matrix indicates similarity between map units (hexagons) based on Euclidean distance, with blue = shorter distance, and yellow = larger distance. (b) Bar planes show the weights for each input variable (see key) in each map unit (hexagon). Minimum and maximum values are based on weight scales in the component plots (a). (c) The three defined clusters from k-means cluster analysis. Clustering groups these data points according to similarity based on Euclidean distance between points in the clusters, and their corresponding cluster centroids.

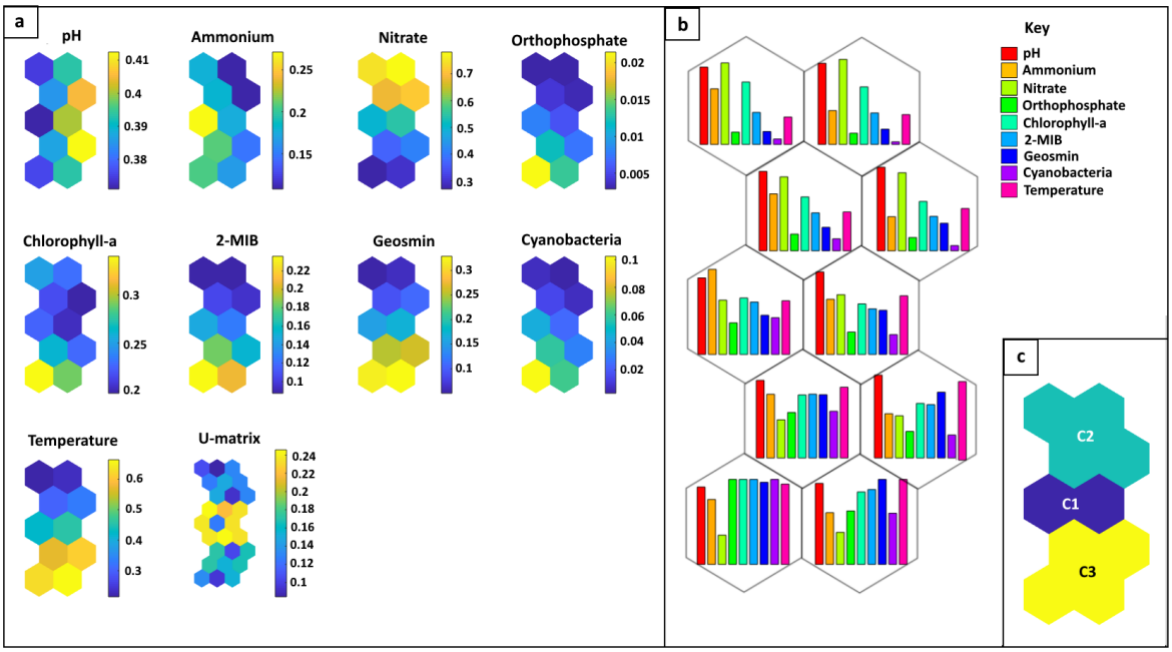

Figure 4.17. **Cheddar Reservoir** (a) SOM component planes and U-matrix for the 2014-2017 historical data from the intake. Each map unit (hexagon) represents a certain position in the map space, which is consistent across all component plots. Colours in the component plots show the values that variables have in the map structure, with yellow indicating higher values and blue lower. The U-matrix indicates similarity between map units (hexagons) based on Euclidean distance, with blue = shorter distance, and yellow = larger distance. (b) Bar planes show the weights for each input variable (see key) in each map unit (hexagon). Minimum and maximum values are based on weight scales in the component plots (a). (c) The three defined clusters from k-means cluster analysis. Clustering groups these data points according to similarity based on Euclidean distance between points in the clusters, and their corresponding cluster centroids.

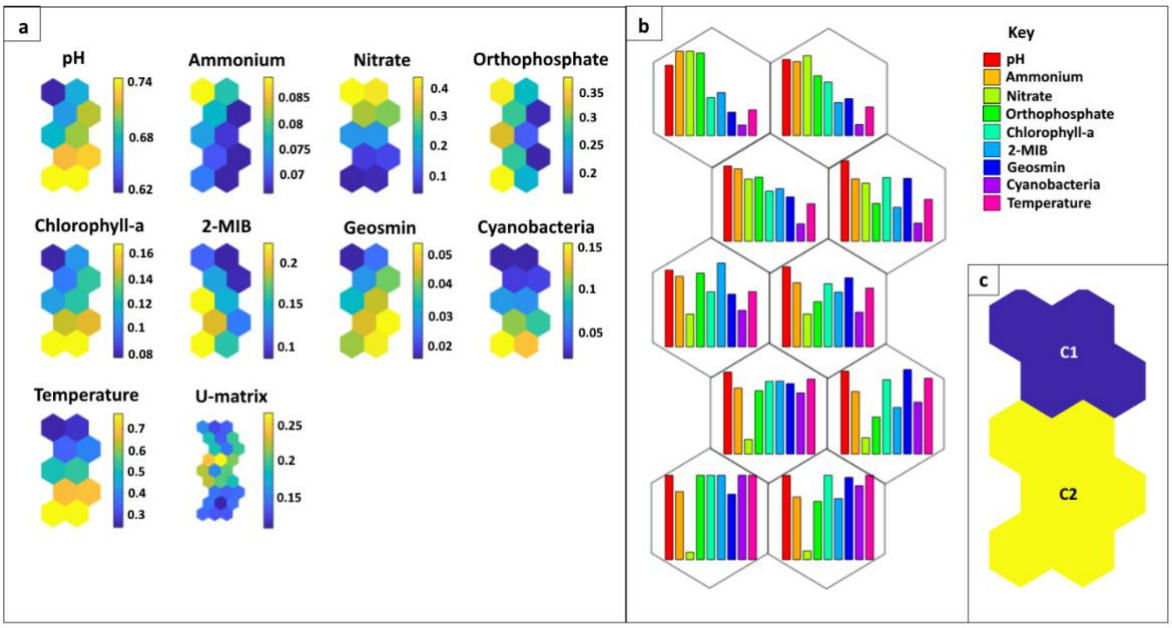

Figure 4.18. **Blagdon** (a) SOM component planes and U-matrix for the 2014-2017 historical data from the intake. Each map unit (hexagon) represents a certain position in the map space, which is consistent across all component plots. Colours in the component plots show the values that variables have in the map structure, with yellow indicating higher values and blue lower. The U-matrix indicates similarity between map units (hexagons) based on Euclidean distance, with blue = shorter distance, and yellow = larger distance. (b) Bar planes show the weights for each input variable (see key) in each map unit (hexagon). Minimum and maximum values are based on weight scales in the component plots (a). (c) The three defined clusters from k-means cluster analysis. Clustering groups these data points according to similarity based on Euclidean distance between points in the clusters, and their corresponding cluster centroids.

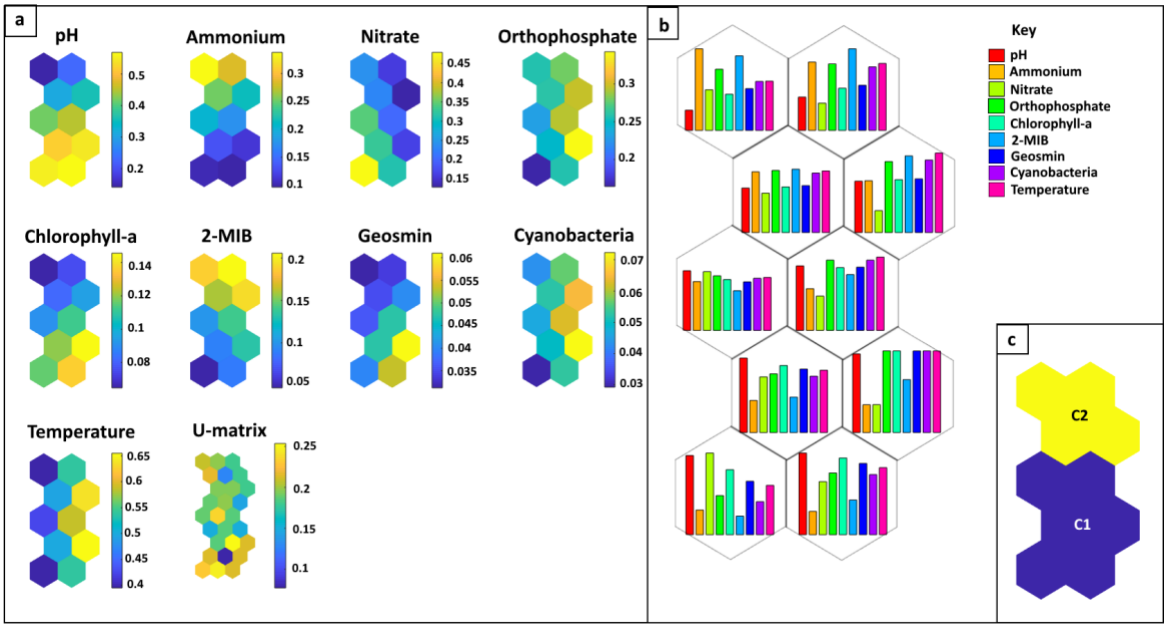

Figure 4.19. **Chew Valley** (a) SOM component planes and U-matrix for the 2014-2017 historical data from the intake. Each map unit (hexagon) represents a certain position in the map space, which is consistent across all component plots. Colours in the component plots show the values that variables have in the map structure, with yellow indicating higher values and blue lower. The U-matrix indicates similarity between map units (hexagons) based on Euclidean distance, with blue = shorter distance, and yellow = larger distance. (b) Bar planes show the weights for each input variable (see key) in each map unit (hexagon). Minimum and maximum values are based on weight scales in the component plots (a). (c) The three defined clusters from k-means cluster analysis. Clustering groups these data points according to similarity based on Euclidean distance between points in the clusters, and their corresponding cluster centroids.

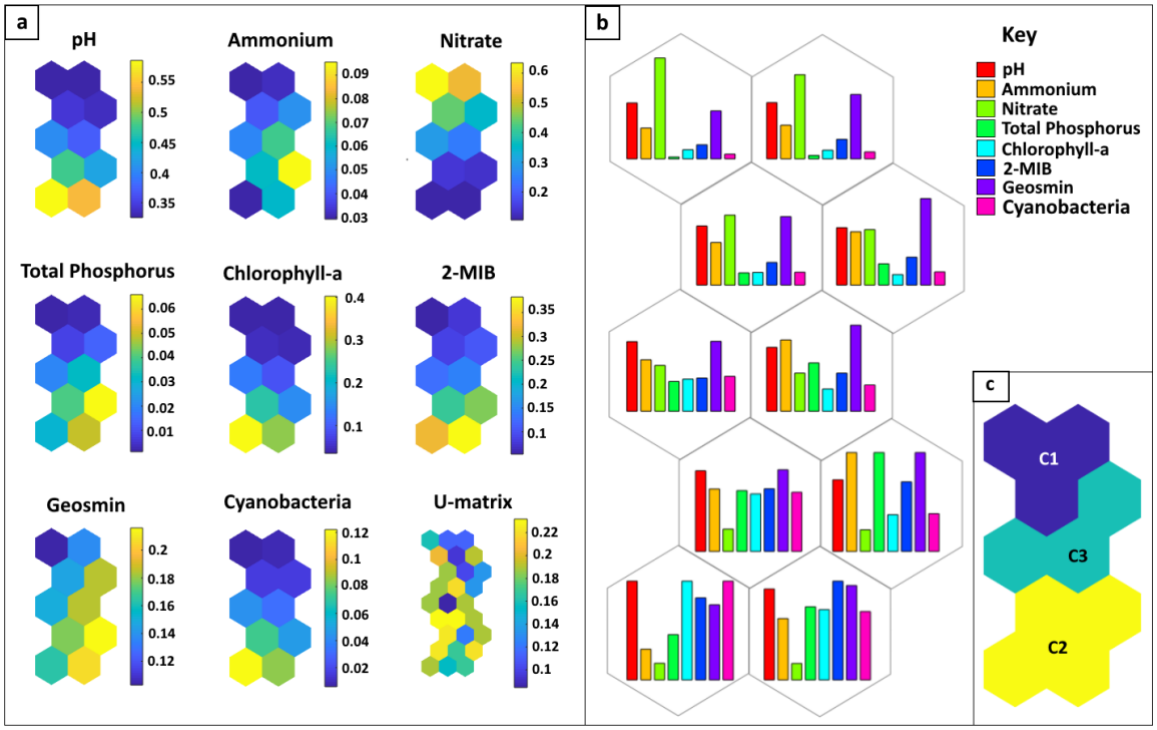

Figure 4.20. **Plas Uchaf Reservoir** (a) SOM component planes and U-matrix for SPT1, near the intake. Each map unit (hexagon) represents a certain position in the map space, which is consistent across all component plots. Colours in the component plots show the values that variables have in the map structure, with yellow indicating higher values and blue lower. The U-matrix indicates similar map units (hexagons) based on Euclidean distance, with blue=shorter distance, and yellow=larger distance. (b) Bar planes show the weights for each input variable (see key) in each map unit (hexagon). Minimum and maximum values are based on weight scales in the component plots (a). (c) The three defined clusters from k-means cluster analysis. Clustering groups these data points according to similarity based on Euclidean distance between points in the clusters, and their corresponding cluster centroids.

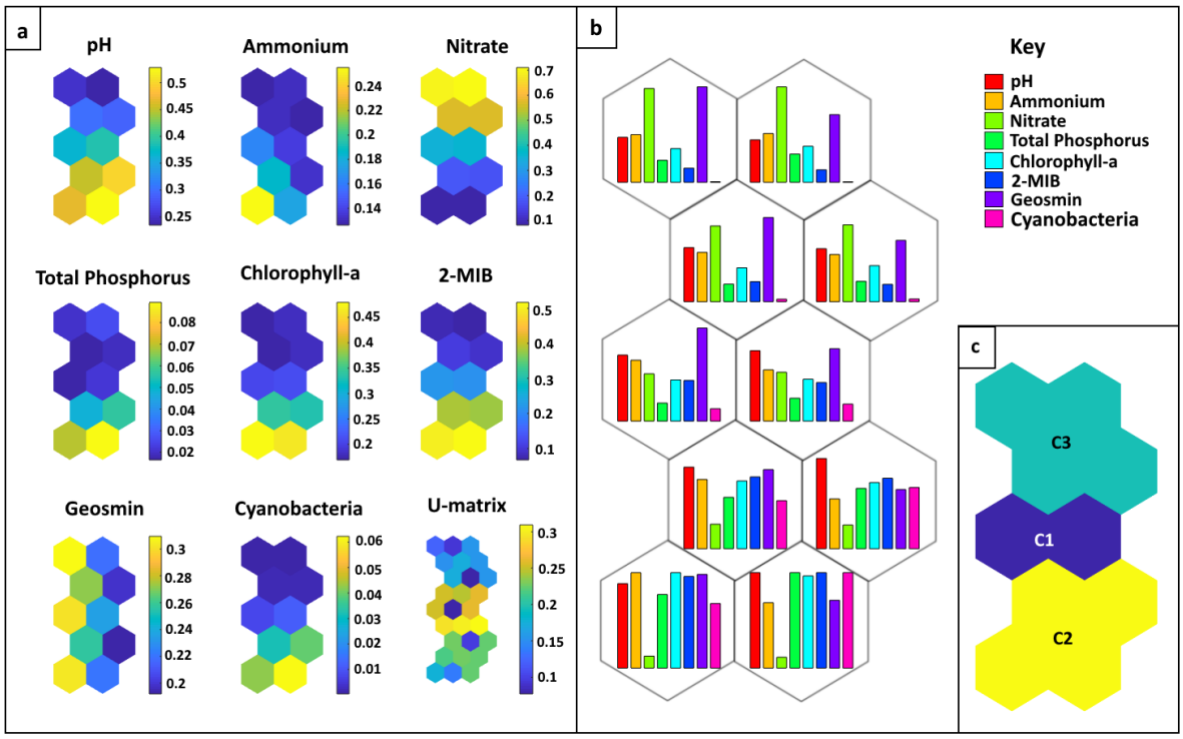

Figure 4.21. **Dolwen Reservoir** (feeder reservoir for Plas Uchaf). (a) SOM component planes and U-matrix for the intake. Each map unit (hexagon) represents a certain position in the map space, which is consistent across all component plots. Colours in the component plots show the values that variables have in the map structure, with yellow indicating higher values and blue lower. The U-matrix indicates similarity map units (hexagons) based on Euclidean distance, with blue = shorter distance, and yellow = larger distance. (b) Bar planes show the weights for each input variable (see key) in each map unit (hexagon). Minimum and maximum values are based on weight scales in the component plots (a). (c) The three defined clusters from k-means cluster analysis. Clustering groups these data points according to similarity based on Euclidean distance between points in the clusters and their corresponding cluster centroids.

Table 4.6. Summary of SOM results for the Somerset reservoirs, SPT1 in Plas Uchaf, and the Dolwen inflow.

Reservoir	SOM Result Summary
Blagdon	*Component plots* • NH_4 and NO_3 correlate together. • 2-MIB and OP correlate together. • Geosmin, cyanobacteria, pH, temperature, and chl-α correlate together. *Bar planes* • pH loads highly in all nodes. • NH_4, NO_3, and OP load highly in nodes 1-4. • In nodes 5-10 chl-α, 2-MIB, and Geosmin weightings are higher, while NO_3 weightings decrease. • NO_3 weightings decrease relative to weightings of NH_4.
Cheddar	*Component plots* • NO_3 correlates against OP, chl-α, 2-MIB, Geosmin, cyanobacteria, and temperature. • NH_4 correlates against pH. *Bar planes* • Nodes 1-4 have high weightings of pH and NO_3 and low weightings of OP and cyanobacteria. • Nodes 5 and 6 have high weightings of NH_4 and pH. • Nodes 7-10 have high weightings of temperature, OP, Geosmin, chl-α, and 2-MIB. • pH loads highly in all nodes. • In nodes 5-10 NH_4 loads higher than NO_3, whereas in nodes 1-4 NO_3 loads higher than NH_4.
Chew	*Component plots* • NH_4 correlates with 2-MIB. • NO_3 and pH correlate together. • OP, chl-α, Geosmin, cyanobacteria, and temperature correlate together. *Bar planes* • Nodes 1-3 weightings of NH_4, 2-MIB, and OP are high, whereas weights of NO_3 and pH are low. • Nodes 7-10 weightings of NH_4, OP, and 2-MIB decrease as weightings of Geosmin, chl-α, temperature, and cyanobacteria increase.
Durleigh	*Component plots* • NO_3 correlates against all other variables. *Bar planes* • NO_3 loads highly in nodes 1-4. • As weightings of NO_3 decrease in nodes 5-10, weightings of other variables increase.
Plas Uchaf SPT1	*Component plots* • NO_3 correlates against all other variables. *Bar planes* • In nodes 1-3 NO_3 load highly • In node 8 weightings of TP, Geosmin and NH_4 are high. • Geosmin weightings are high in nodes 4, 5, and 6. • NH_4 weights increase as NO_3 weights decrease.
Dolwen	*Component plots* • NO_3 and Geosmin correlate together and against all other variables. *Bar planes* • NH_4 weights increase as NO_3 weights decrease.

	• Nodes 1-4 have high weightings of NO_3 and Geosmin. • As weightings of NO_3 decrease in nodes 5-10, weightings of other variables increase.

4.4 Discussion

The rising frequency and magnitude of T&O outbreaks in drinking water reservoirs is an ever-increasing issue for the water industry. Determining the trigger(s) of T&O production in cyanobacteria is essential for management of raw water quality. The SOM results presented from six reservoirs with different trophic status, morphologies, mixing strategies, and catchments all indicate that concentrations of ammonium relative to nitrate are important for 2-MIB and Geosmin production. In combination with the in-reservoir findings in Plas Uchaf (Perkins and Slavin et al., 2019) these findings support the theory that ammonium stimulates cyanobacterial productivity, which in turn stimulates the synthesis of 2-MIB and Geosmin along isoprenoid pathways in cyanobacteria (Perkins and Andrade, see declaration). Although it is well recognised that adequate availability of phosphorus is required for rapid growth in cyanobacteria, and hence should still be considered in management decisions, it is suggested that monitoring sources and concentrations of ammonium is important for managing T&O outbreaks in drinking water reservoirs.

Cyanobacteria are present at all study sites (Figures 4.5 and 4.6) and the SOM results for all sites indicate that 2-MIB and Geosmin are associated with higher cyanobacteria counts (Figures 4.16 - 4.21). Generally, concentrations of 2-MIB and Geosmin in aquatic systems have been linked to high cyanobacteria biomass (Peter et al., 2009). However, a recent study by Xuwei et al. (2019) found that *Oscillatoria* were responsible for T&O production in the 'non-blooming' area of Lake Taihu, China, and Graham et al. (2010) failed to find correlations between T&O concentrations and biomass. The presence high cyanobacterial biomass is not always associated with 2-MIB and Geosmin concentrations. Here, despite the SOM components plots (Figures 4.16a - 4.21a) showing an association between 2-MIB/Geosmin and cyanobacteria, the clustering and ANOVA analysis reveal that the association of cyanobacteria and 2-MIB/Geosmin is not the most heavily weighted. Although sources of 2-MIB and Geosmin at all sites studied could be produced by other means, such as actinomycetes (Park et al., 2014), Jüttner and Watson (2007) state that cyanobacteria are the primary

source of T&O compounds in drinking water reservoirs. The known Geosmin producer *Dolichospermum*, dominated cyanobacterial counts in both Plas Uchaf (Perkins and Slavin et al. 2019) and Blagdon. Therefore, the presence of T&O producing cyanobacteria at all study sites suggest they are an important source of T&O compound production.

Thermal stratification can result in lower dissolved oxygen conditions near the sediments and is a common feature of reservoirs in the summer. The Somerset reservoirs are all artificially mixed by either bubble plumes (Chew, Cheddar, Blagdon) or surface mixers (Durleigh). Despite artificial mixing in these reservoirs, incomplete mixing may occur in areas of the reservoir (Chapter 5), or if air temperatures are warm enough and mixing is insufficient (wind and artificial), then thermal stratification could persist, which could explain why SOM analysis of the mixed and non-mixed reservoirs generally showed the same results. Low dissolved oxygen near the sediments can promote the reduction of iron (Fe^{3+} to Fe^{2+}) and subsequent release of iron bound phosphate into the labile pool (Boström et al., 1988; Wang et al., 2019). Turbulent mixing and sediment resuspension lead to diffusion of labile phosphate into the overlying water column. Internal loading of phosphorus from the sediments can alter the TN:TP ratio. Increased production of T&O compounds has been linked to the TN:TP ratio, with Harris *et al.* (2016) finding higher concentrations of 2-MIB and Geosmin associated with lower TN:TP ratios. In this chapter, the TN:TP (TN:OP) ratio shows an inverse relationship with 2-MIB concentrations (Figures 4.11 and 4.12). However, the inverse relationship with Geosmin is less clear (Figures 4.11 and 4.12), which indicates that phosphorus availability may not be the key trigger for T&O production in cyanobacteria. Generally, the SOM results show TP/OP to correlate with 2-MIB and Geosmin. It is evident that phosphorus is required for cyanobacterial productivity and needs to be considered in management, although it does not appear to be the key trigger for 2-MIB and Geosmin production.

In Durleigh the changes in TN:TP are attributed to both a decline in nitrate and an increase in TP in the summer, which indicates TP is entering the system either through internal loading or from the catchment/pumped canal inflow. Durleigh is a eutrophic reservoir with high algal biomass in general, so decomposition of organic matter and low dissolved oxygen conditions are likely to occur near the sediments. Both respiration and decomposition of cyanobacteria during a bloom can contribute to anoxic conditions and provide a carbon source for denitrifying bacteria (Chen et al., 2012). Furthermore,

anaerobic conditions in hypolimnetic waters can suppress nitrification and lead to accumulation of ammonium in the benthic sediments (Beutel, 2006), which can enter the water column through diffusion or turbulent mixing. The summer decline in nitrate is observed in all reservoirs and all sites in Plas Uchaf and is attributed to a combination of denitrification, assimilation by phytoplankton, and reduced external loading. Reduced pumping from the canal inflow in Durleigh combined with decreased runoff results in lower external loading of nitrate during the summer. Warmer temperatures and increased residence times are linked to increased denitrification rates (Hill, 1988; Ke et al. 2008), which are typical conditions of reservoirs in summer.

Furthermore, summer decline in nitrate concentrations affects the NH_4:NO_3 ratio (Figure 4.15). The increase in NH_4:NO_3 values during the summer can also be attributed to increases in ammonium during the summer (Figure 4.13), which is likely due to increased ammonification (Jørgensen, 1989). Changes in the NH_4:NO_3 ratio appear to more closely match changes in 2-MIB and Geosmin concentrations (Figure 4.15) than the TN:TP/OP ratio (Figures 4.11 and 4.12), suggesting that concentrations of different fractions of nitrogen are more closely associated to production of T&O metabolites in cyanobacteria compared to concentrations of nitrogen relative to phosphorus. Nevertheless, in-reservoir observations at Plas Uchaf and Dolwen reservoirs clearly demonstrated that a significant decrease in T&O metabolite concentrations was associated with a significant decrease in ammonium concentrations between 2015 and 2016 (Perkins and Slavin et al., 2019), highlighting the importance of ammonium in T&O metabolite production.

The SOM results for all reservoirs (Figures 4.16 - 4.21) showed that 2-MIB and Geosmin loaded highly with higher ammonium relative to nitrate, which is in accordance with a study by Saadoun et al. (2001), who found maximal Geosmin synthesis in *Dolichospermum* (then *Anabaena*) correlated with high ammonium concentrations (R^2=0.89) and low nitrate concentrations. Ammonium is the most reduced form of nitrogen in aquatic systems that can be assimilated by phytoplankton (Flores and Herrero, 2005; Harris et al., 2016; Gilbert et al., 2016). Cyanobacteria have been found to assimilate ammonium more efficiently than nitrate (Blomqvist et al., 1994; Hampel et al., 2018; Andersen et al., 2019). For example, Saadoun et al. (2001) reported that Geosmin production in *Dolichospermum* is inhibited by nitrate and promoted by ammonium. However, there is a large range in ability between cyanobacteria taxa to uptake and assimilate NO_3^- and NH_4^+ (Scanlan and Post, 2008;

Gilbert et al., 2016), which subsequently affects productivity and the production of T&O compounds. When nitrate is assimilated into the cells, it requires a 2-step reduction to ammonium, which uses cellular energy. Harris et al. (2016) reported increased 2-MIB and Geosmin concentrations during periods of high ammonium concentrations relative to nitrate, and Uwins et al. (2007) found significant correlation between ammonia concentrations and 2-MIB concentrations in Hinze Dam, Australia. High ammonium concentrations relative to nitrate likely stimulates higher productivity in cyanobacteria along the MEP pathway (Seto et al., 1996), which leads to increased production of T&O compounds and could explain why some studies fail to find a correlation between 2-MIB/Geosmin concentrations and biomass (Watson et al., 2008; Graham et al., 2010).

Other factors such as pH, temperature (Figures 4.16 - 4.19) and chlorophyll-α were associated with 2-MIB and Geosmin in the SOM results (Figures 4.16 - 4.21). High photosynthetic activity decreases dissolved CO_2 in the water column and leads to increased pH in the water (Visser et al., 2016) and cyanobacteria are known to remain productive in more alkaline environments (da Silva Brito et al., 2018). In this chapter, the higher pH values are likely caused by increased cyanobacterial productivity and not a direct factor in 2-MIB and Geosmin production. Cyanobacterial productivity is affected by water temperature. A recent study by Kim *et al.* (2018) showed that maximal secondary metabolite productivity (amount of secondary metabolite per unit biomass) occurred at 15°C when biomass was lowest and Van der Ploeg et al. (1995) found 2-MIB production and maximal growth rates in *Oscillatoria* cf. *chalybea* to be greatest at 28°C. However, Saadoun et al. (2001) found no correlation between Geosmin concentration in *Dolichospermum* and temperature. Similarly, Alghanmi et al. (2018) found no relationship between light intensity and temperature for 2-MIB and Geosmin production in two isolated cyanobacteria. The SOM results for the Somerset reservoirs (Figures 4.16 – 4.19) show that 2-MIB and Geosmin correlate with temperature, but this could be a relic of the summer decline in nitrate. Nevertheless, in UK reservoirs, warmer temperatures are likely to promote higher productivity in cyanobacteria. Although temperature may influence the production of 2-MIB and Geosmin in cyanobacteria, our results suggest that it is not the most important factor in production.

Although the SOM results presented here do not provide mechanistic proof, these findings corroborate with an *in-situ* study at Plas Uchaf reservoir, North Wales, where

an 85% reduction in ammonium supply from Dolwen to Plas Uchaf between 2015 and 2016 resulted in a decrease in both 2-MIB and Geosmin concentrations at all sites within the reservoir (Perkins and Slavin et al., 2019). A likely hypothesis is that enhanced ammonium supply stimulates a rapid increase in productivity, which stimulates synthesis of metabolites such as 2-MIB and Geosmin. If 2-MIB and Geosmin are synthesised in excess, then during less favourable periods they are released into the surrounding water column, which causes the T&O outbreaks reported by the water industry. This mechanism requires further study, but the findings presented from six different reservoirs in this chapter combined with those reported Perkins and Slavin et al. (2019) are a strong starting point from which to advise the management and monitoring of water supply reservoirs. In order to address T&O outbreaks in drinking water reservoirs, the source(s) of ammonium (internal and external) need to be identified. External sources of ammonium and nitrate can be from river or stream inflows, surface flows, and groundwater, particularly within agricultural catchments with livestock or arable crops where N-rich fertilisers are used (Jeppesen et al., 2011). Anaerobic conditions in hypolimnetic waters can suppress nitrification and lead to accumulation of ammonium in the benthic sediments (Beutel, 2006). Subsequent internal loading of ammonium into the overlying water column can occur through diffusion or turbulent mixing.

4.5 Conclusions

The results presented in this chapter show that 2-MIB and Geosmin production in six different drinking water reservoirs is associated with high concentrations of ammonium relative to nitrate despite an observed trophic gradient. Based on these findings and observations from literature and *in situ* (Perkins and Slavin et al., 2019), it is hypothesised that high ammonium concentrations trigger increased productivity in cyanobacteria and subsequent elevated production of 2-MIB and Geosmin along pathways of isoprenoid synthesis. It is recognised that further research into this mechanism is required, particularly into how the metabolisms of different cyanobacteria taxa respond to changes in nutrient availability and produce 2-MIB and Geosmin. Results indicate that certain factors can be important for specific sites but ammonium availability relative to nitrate is found consistently across all sites. The sites included in the analysis vary in morphological and catchment characteristics, and some sites are artificially mixed, but T&O production across all sites were consistently associated with

high ammonium to nitrate ratio. Combined with the in-reservoir observations at Plas Uchaf (Perkins and Slavin et al., 2019), these results suggest that ammonium is a key trigger in T&O production compared to all other variables. For management of 2-MIB and Geosmin production in drinking water supply reservoirs, it is advised that sources of ammonium (internal and external) are identified alongside the traditional approach of managing and monitoring phosphorus supply. A reduction in ammonium concentrations from all sources is essential for reservoir and catchment management in order to reduce the growing issues associated with T&O compounds in drinking water.

CHAPTER 5

THE PHYSICAL EFFECTS OF SURFACE MIXERS IN A SHALLOW, HYPEREUTROPHIC RESERVOIR

5.1 Introduction

Understanding how surface mixers influence hydrodynamics and water quality in a shallow drinking water reservoir is fundamental for aiding future management and investment decisions (Objective 1, Chapter 1; Section 2.2, Chapter 2). In this chapter, the work aims to assess the range of influence of surface mixers in a shallow reservoir and over a stratification season (Mar – Oct) to examine how effective mixers are spatially and temporally. In addition, we present an *in-situ* assessment of the effects turning surface mixers off has on water quality and to better identify the range of influence of mixers on the hydrodynamics, turbidity, and DO concentrations within the reservoir. The effects of artificial circulation on mixing phytoplankton cells through the water column is examined. Between February and October 2018 an in-reservoir monitoring campaign was carried out with data collected at 4 different sites within the reservoir. During the campaign, the surface mixers were shut down 4 times. Data collected during 2 of these shutdowns were assessed as a control for no artificial mixing, providing contrast between an artificially mixed environment and a more natural environment (wind-driven and convective mixing), enabling determination of the effects of artificial circulation on temperature, DO concentrations, turbidity, and phytoplankton cell distribution in a shallow, hypereutrophic drinking water reservoir.

5.2 Methods and Study Site

The results presented in this chapter are based around a measurement campaign conducted at Durleigh reservoir between 22 February and 5 October 2018 (Figure 3.9; Section 3.3, Chapter 3), a towed ADCP survey conducted on 22 and 23 October 2019 (Section 3.3.3, Chapter 3), and turbulence profiles from 11 September 2015 (Section 3.3.4, Chapter 3). A description of the study site and more detailed information about the measurement campaign can be found in Sections 3.3 and 3.2.1 (Chapter 3), respectively. In this section the measurement campaign is briefly described, and terminology only referred to in this chapter is introduced.

5.2.1 Measurement Campaign

In this chapter, four study locations are referred to: B1, L1, L2, and L3, which are located 15, 20, 60, and 435 m from the surface mixers, respectively (Figure 3.6, Chapter 3). During the measurement campaign, the mixers were turned off and data collected

during 2 shutdowns are presented in this chapter. The first of these, shutdown A, occurred between 08:19 on 20 June 2018 and 12:22 on 22 June 2018. The second, shutdown B, occurred between 07:17 on 22 August 2018 and 16:42 on 23 August 2018. The shutdowns were considered as no-mixing controls, so that the effects of artificial circulation with surface mixers on hydrodynamics, turbidity, DO concentrations, and cyanobacteria cell distributions could be determined. To determine the influence of the surface mixers on these parameters the pre-shutdown (hereafter ON1), shutdown (OFF), and post-shutdown (ON2) periods are compared. Each period is the same length and over the same hours to aid comparability. Hereafter, the first shutdown period (shutdown A) will be referred to as ON1A (pre-shutdown), OFFA (shutdown), and ON2A (post-shutdown), while the second shutdown period (shutdown B) will be referred to as ON1B, OFFB, ON2B.

5.2.2 Water Quality Parameters and Equipment

The water quality parameters considered in this chapter are highlighted in table 5.1, which also refers to the relevant sections of Chapter 3 for descriptions of the equipment and analysis methods used.

Table 5.1 Parameters measured for in-reservoir water quality assessment at Durleigh in 2018 that are presented in this chapter. Reference to full methods found in relevant sections in Chapter 3.

Parameter	Equipment Used	Dates Sampled	Method
Temperature	YSI EXO1 sonde RBR SoloT thermistor HOBO TidbiT v2 logger	22 Feb – 5 Oct 2018	Section 3.4.1, Chapter 3
Dissolved oxygen	YSI EXO1 sonde MiniDOT oxygen loggers	22 Feb – 5 Oct 2018 30 May – 5 Oct 2018	Section 3.4.2, Chapter 3
Weather	Delta T WS-GP1 Weather Station	5 Apr – 5 Oct 2018	Section 3.4.3, Chapter 3
Light penetration	Secchi Disk HOBO Pendant Temperature/Light 8K Data Loggers (L2 only)	Water sampling days Permanently moored at 0.5, 1.5, and 2.5 m 30 May – 5 Oct 2018	Section 3.4.5, Chapter 3
Water velocities and sediment resuspension	Nortek Vector Acoustic Doppler Velocimeter (ADV)	20 – 24 Aug 2018	Section 3.4.4, Chapter 3

	StreamPro Acoustic Doppler Current Profiler (ADCP)	22 and 23 Oct 2019	Section 3.4.6, Chapter 3
Turbulence	Self-contained autonomous microprofiler (SCAMP)	11 Sep 2015	Section 3.4.7, Chapter 3
Phytoplankton cell counts	Van Dorn water Sampler	Water sampling days	Section 3.4.8, Chapter 3

5.3 Data Analysis

5.3.1 Turbulent kinetic energy from wind-driven and convective mixing

The amount of turbulent kinetic energy (TKE) input by the wind can be calculated from the wind speeds and density of the water at the water surface. The daily average TKE_{wind} input at Durleigh was calculated using equation 4 and the daily average TKE_{conv} input was calculated using equation 5 in Section 3.5.1 (Chapter 3).

5.3.2 Turbulent kinetic energy from surface mixers

The theoretical TKE input into the water column from the surface mixer (TKE_{mix}) was calculated using equation 7 from Section 3.5.2 (Chapter 3). The TKE_{mix} value is constant while the mixers are in operation.

5.3.3 Statistical Analysis

Data were analysed using PAST statistical software (Hammer et al., 2001). Normality was assessed using the Shapiro-Wilk test. Normally distributed data were assessed for significant differences using single-factor ANOVA and post hoc Tukey's test. The Kruskal-Wallis test followed by Dunn's multiple comparison test were used for non-normally distributed data. Prior to statistical analysis, autocorrelation was conducted using the autocorrelation function (ACF) in MATLAB to determine the independence of observations in the time series. Autocorrelation determined that when data were averaged over 4-hour intervals there was no autocorrelation (within 95% confidence intervals). Therefore, the statistical analysis of the shutdowns was conducted

on the time series data averaged at 4-hour intervals to minimise uncertainty in the statistical analysis.

5.4 Results

In this section, the results from the 2018 measurement campaign are presented, before focussing in more detail on the two mixer shutdowns. Then results from the towed ADCP survey are presented. The turbulence profiles, which are used to inform levels of mixing through the water column, are presented after the phytoplankton cell counts. A summary of all the main results is given at the end of this section.

5.4.1 Weather

Between 5 Apr and 5 Oct 2018, the hourly average air temperatures at Durleigh ranged between 2.15 - 29.3˚C and the hourly average wind speeds ranged between 0.3 and 9.4 m s^{-1} (Figure 5.1). The predominant wind direction was from the North West (between 300 - 310˚). August was the wettest month with 63.6 mm of rainfall, whereas June was the driest with only 1.6 mm (data not shown). Shutdown A and B experienced different weather conditions. During shutdown A, air temperatures were warmer and peak daytime solar radiation was higher than shutdown B, but wind speeds were generally higher during shutdown A. Therefore, comparison of the two shutdowns enables assessment of mixer operation during different meteorological conditions.

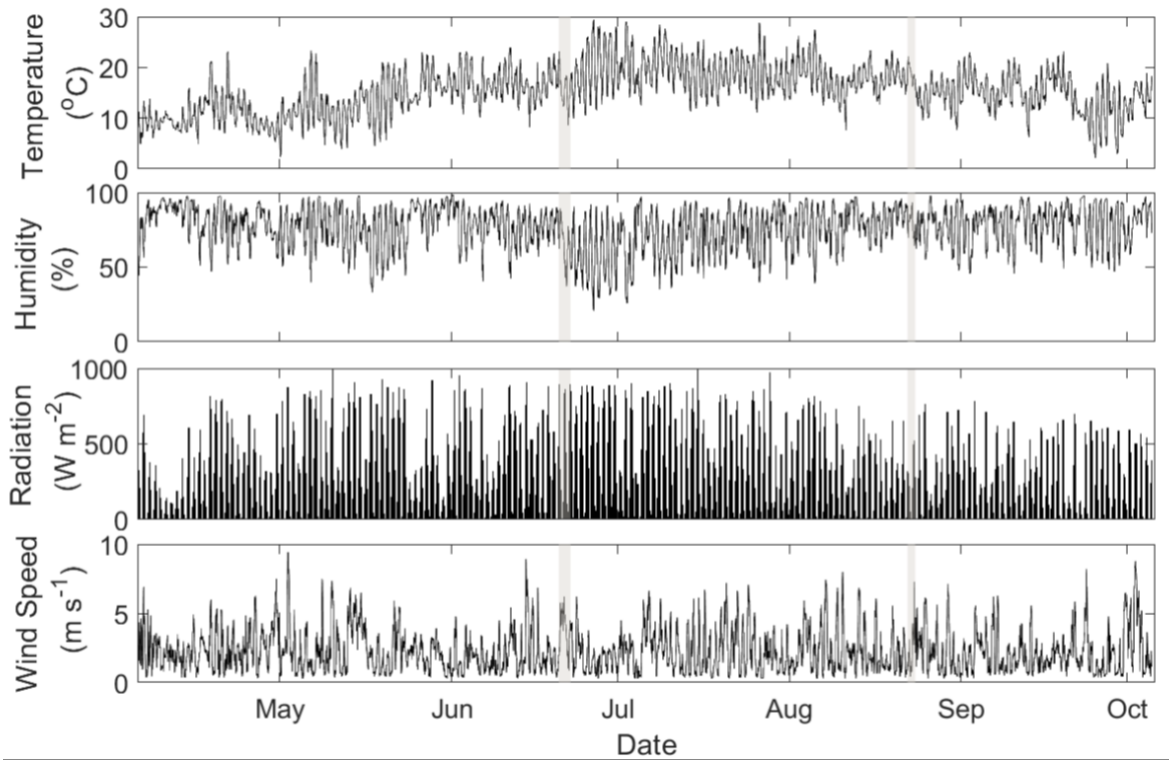

Figure 5.1. Hourly average weather data on site at Durleigh between 5 April and 5 October 2018. Surface air temperatures, humidity, surface radiation, and wind speeds. Grey shading indicates shutdowns A and B when the surface mixers were turned off.

5.4.2 TKE Inputs

Net surface heat flux was calculated using Lake Heat Flux Analyser, where air temperatures and solar radiation measurements were input to calculate the surface heat flux. Generally, the net surface heat flux is positive in the first half of the field investigation and negative from July onwards (Figure 5.2a). Latent heat flux was the main heat loss mechanism (evaporative losses) from July 2018 and contributed to the negative net surface heat flux values.

The daily average TKE_{wind} and TKE_{conv} were calculated using equations 4 - 7 in Chapter 3. The mean TKE_{wind} was 5.26 x 10^{-5} W m^{-2} and ranged between 2.95 x 10^{-6} and 4.34 x 10^{-4} W m^{-2}. The maximum TKE_{wind} occurred on 3 October 2018, when the daily average wind speeds were highest (5.59 m s^{-1}). The mean TKE_{conv} through the study period was 6.93 x 10^{-5} W m^{-2}, with a maximum of 2.85 x 10^{-4} W m^{-2} observed on 24 August 2018. Both TKE_{conv} and TKE_{wind} were variable, dependent on the net surface heat flux and wind speeds, respectively (Figure 5.2). Between April and the end of June, TKE_{conv} was intermittent and from July onwards, the net heat flux was generally

negative (Figure 5.2a) and consequently the TKE_{conv} was higher (Figure 5.2c). TKE_{wind} patterns reflect the wind speeds (Figure 5.2b and c). The u*: w* ratio over the study period shows that generally convection was the larger source of TKE into the reservoir, with many values < 0.75 (Figure 5.3). Together, the natural TKE inputs (TKE_{wind} and TKE_{conv}) averaged 1.22 x 10^{-4} W m^{-2}, with a maximum of 5.3 x 10^{-4} W m^{-2} on 2 October 2018.

The TKE from the mixers was calculated using equation 7. For one pump at Durleigh, TKE_{mix} is 1.67 W m^{-2}. The TKE_{mix} value is the energy input over the area of one mixer. The Watts produced by each mixer at Durleigh was calculated at 7.5 W. There were 2 mixers positioned outside of the silt curtain at Durleigh, giving a TKE_{mix} of 3.34 W m^{-2}. The input from each mixer is considerably larger than the maximum TKE from the combined wind and convective inputs.

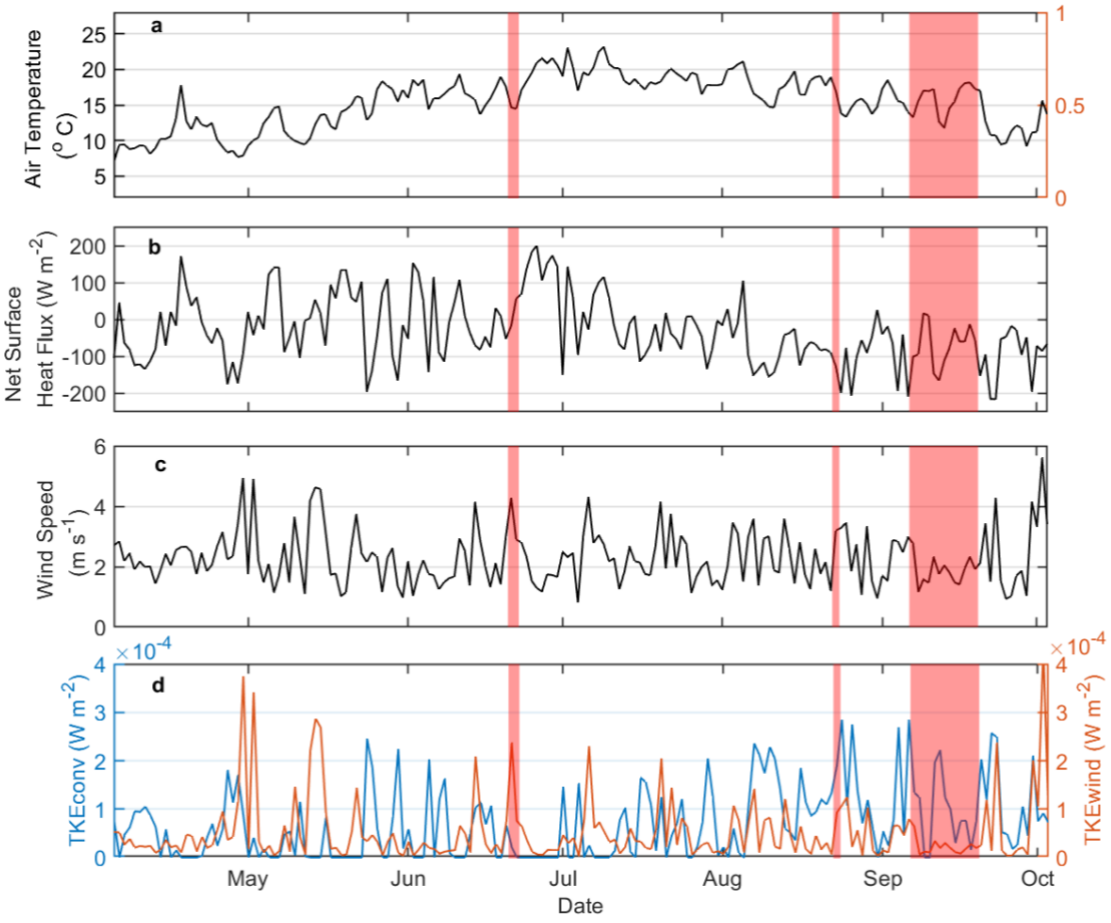

Figure 5.2. a.) Daily average air temperature, b.) daily average net surface heat flux at Durleigh between 5 April and 4 October 2018. c.) Daily average wind speeds at Durleigh. d.) Daily average TKE_{conv} (eqn. 5) and TKE_{wind} (eqn. 4) at Durleigh. red patches indicate the two shutdowns.

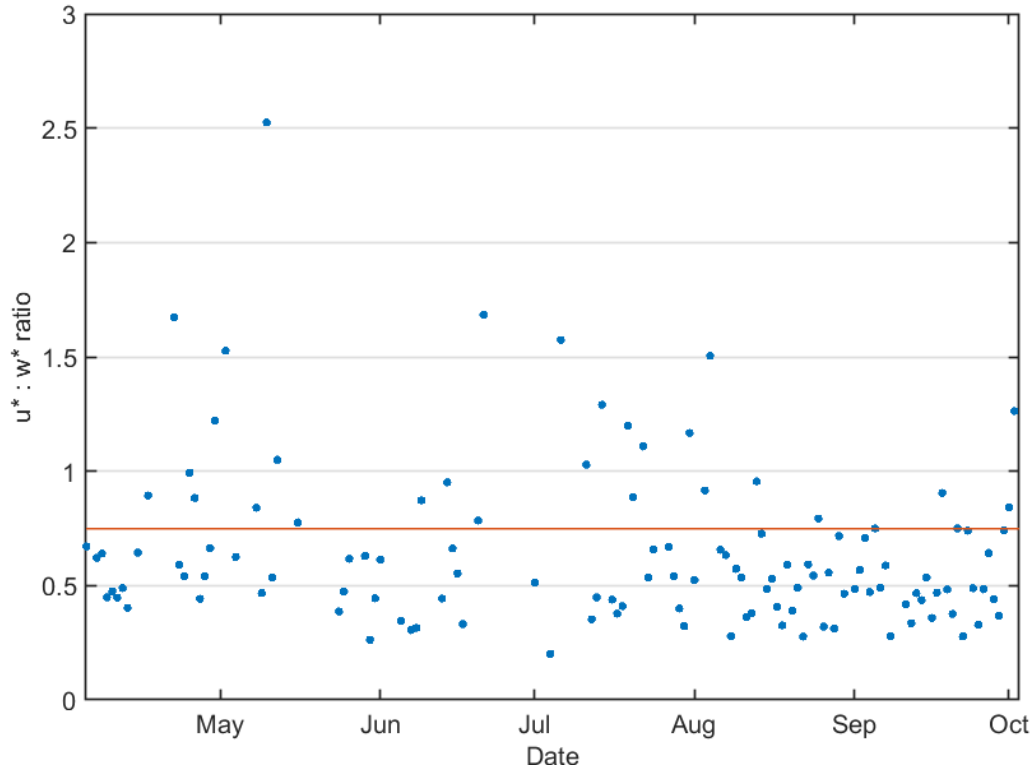

Figure 5.3. The u:w* ratio from daily values of u* and w* at Durleigh. The red line indicates 0.75, the threshold for equal inputs from wind-driven and convective mixing (Imberger, 1985).*

5.4.3 Light Penetration

Over the measurement campaign, the Secchi depths ranged from 0.2 to 0.7 m (average: 0.4 ± 0.15 m) and very little spatial variation was observed on sampling days, suggesting that reservoir turbidity is high throughout the reservoir. Subsequently, the euphotic depth estimated from Z_{SD} was generally low, ranging between 0.46 and 1.89 m (Table 5.2). Similarly, 2015 SCAMP PAR sensor data was used to estimate Z_{eu}. These were averaged to give an estimated Z_{eu} at of 1.55 m ± 0.1 m (standard deviation) and a range of 1.44 – 1.72 m (Table 5.2). Taking an average across all the estimates used for Z_{eu} gives an average of 1.15 m ± 0.28 m, which will be used herein as an estimate of Z_{eu}. Therefore, if phytoplankton cells were being entrained by the downwards flows induced from the mixers, they are likely to be transported out of the photic zone. Low light availability for phytoplankton can alter the community structure and productivity of different species, which will be discussed in further detail in Chapter 6.

Table 5.2.) Calculations of Euphotic Depth (Z_{eu}) from 2015 SCAMP PAR sensor data and Secchi disk measurements (water sampling days).

Method	Average	Minimum	Maximum
Z_{eu} from PAR profiles	1.55 ± 0.1	1.44	1.72
Z_{eu} from Secchi Depth where *m* = 2.3	0.95	0.46	1.61
Z_{eu} from Secchi Depth where *m* = 2.5	1.00	0.50	1.75
Z_{eu} from Secchi Depth where *m* = 2.7	1.08	0.54	1.89
Average	1.15 ± 0.28	0.74 ± 0.47	1.74 ± 0.12

5.4.4 Phytoplankton cell counts

Cyanobacterial cell counts (Figure 5.5) constituted a large proportion (always > 50%) of the total phytoplankton cell counts (Figure 5.4). The lowest cell counts were generally recorded at L3, except on 22 Feb and 13 Jun. The distribution of cells through the water column appeared most uniform at L3 and was likely due to the shallow depth, making it easily mixed by natural processes. At L1 and L2, cell distribution through the water column was more varied (Figures 5.4 and 5.5). Generally, L1 had the highest cyanobacterial and total phytoplankton cell counts. Single factor ANOVA and post hoc Tukey's test revealed no significant differences between cyanobacteria cell counts at the surface, middle, and bottom of the water column at all locations (L1 ($F_{(2,31)} = 0.29$, $p = 0.75$); L2 ($F_{(2,29)} = 0.17$, $p = 0.84$); L3 ($F_{(2,28)} = 0.09$, $p = 0.91$)). There were no significant differences between counts from the same depth (surface ($F_{(2,32)} = 0.67$, $p = 0.52$); middle ($F_{(2,27)} = 0.13$, $p = 0.88$); bottom ($F_{(2,29)} = 0.39$, $p = 0.68$)) at different locations.

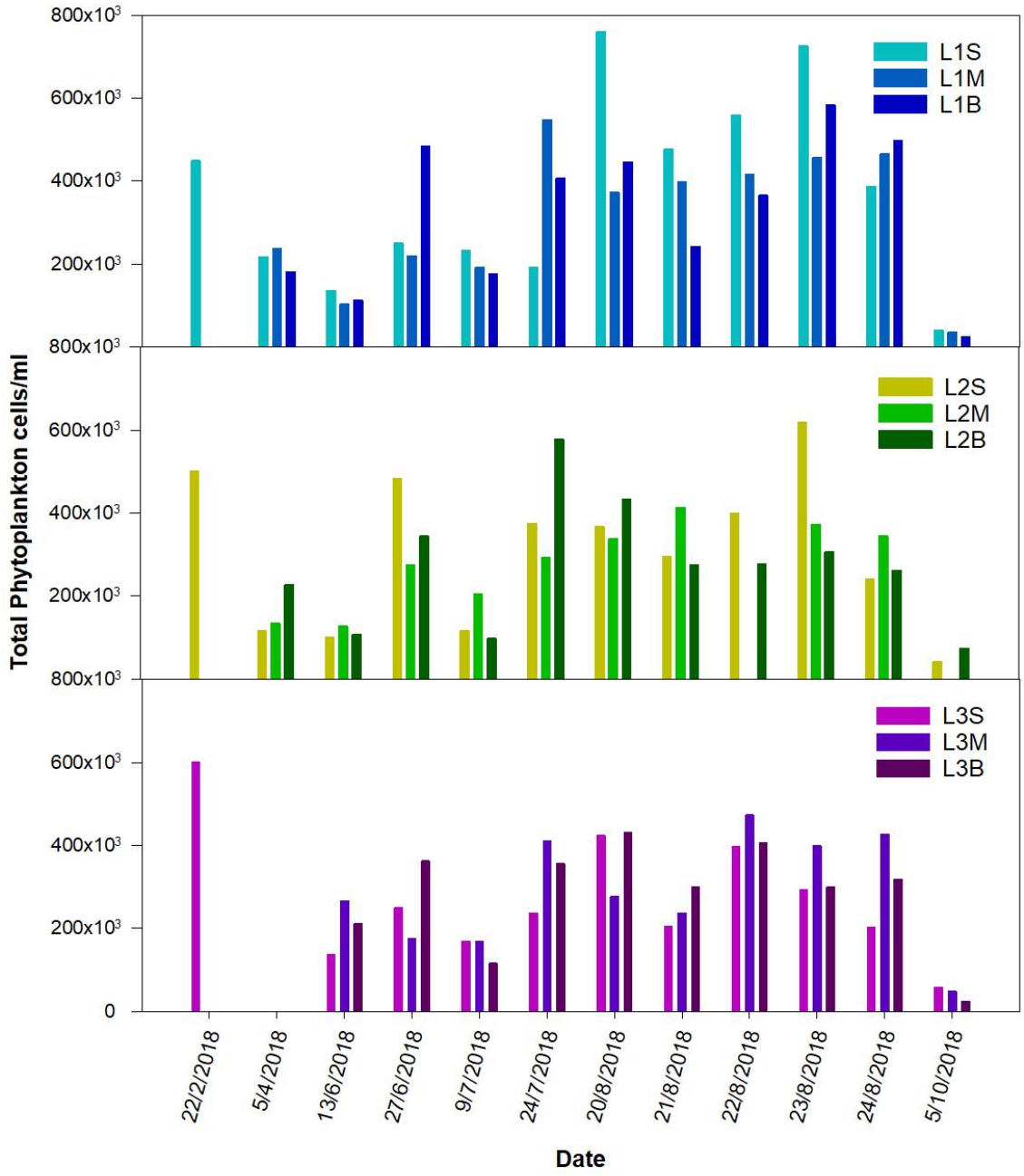

Figure 5.4. Total phytoplankton cells counts at the surface (S), middle (M), and bottom (B) of sites L1, L2, and L3 at Durleigh reservoir on the water sampling dates shown. Only one measurement from each site was taken due to the length of processing time for each sample. Missing values are due to sample loss or failing to get collected due to adverse weather conditions.

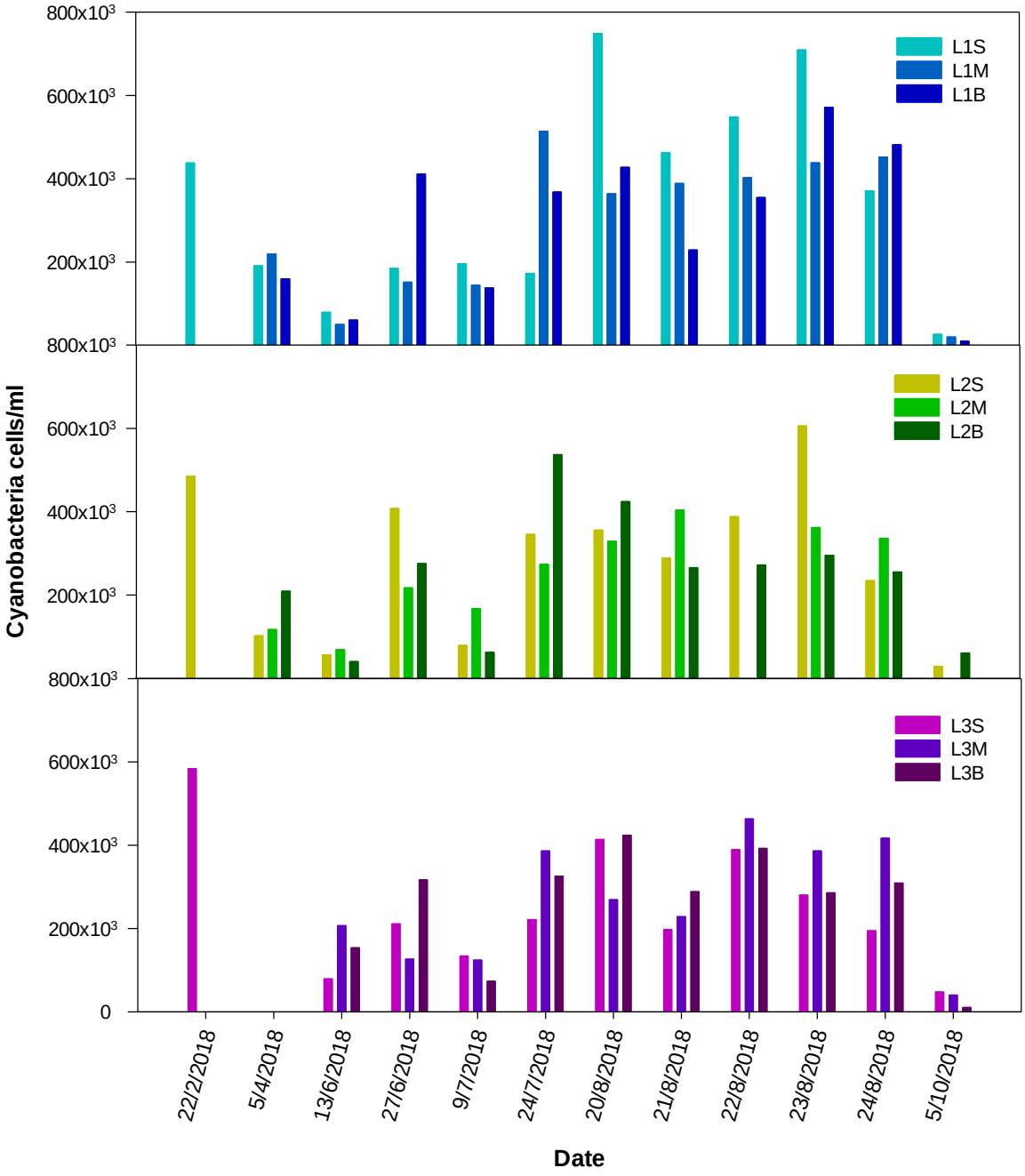

Figure 5.5. Cyanobacterial cell counts at the surface (S), middle (M), and bottom (B) of sites L1, L2, and L3 at Durleigh reservoir on the water sampling dates shown. Only one measurement from each site was taken due to the length of processing time for each sample. Missing values are due to sample loss or failing to get collected due to adverse weather conditions.

5.4.5 Turbulence and eddy diffusivity

Direct measurements of turbulence were not made during the 2018 campaign, but previous measurements made in September 2015 can help determine if the mixing was high enough to promote passive transport of phytoplankton cells through the water column and reduce the advantages of species with buoyancy regulating mechanisms. Assuming that nutrients are not limiting, McGinnis and Wüest (2005) suggest that typical values for turbulent kinetic energy dissipation are approximately 10^{-7} m^2 s^{-3} and 10^{-9} m^2 s^{-3} at the lake surface and interior, respectively. At Durleigh, the SCAMP profiles revealed high values of turbulent kinetic energy dissipation at all sites, generally exceeding 10^{-7} m^2 s^{-3} near the sediments and 10^{-6} m^2 s^{-3} at the surface (Figure 5.6). Profiles from location 1 and 2 (Figures 5.6 and 5.7) showed similar profiles that could signify the influence of the mixers on turbulent diffusivities. However, wind speeds on 11 September 2015 exceeded 5 m s^{-1} when profiles were taken (data not shown), which make it difficult to conclusively discern the effects of the mixers from naturally induced mixing in the profiles.

Values of eddy diffusivity have been used in the competition model proposed by Huisman et al. (2004) to determine how changes in turbulent mixing induced by bubble curtains changes competition for light between buoyancy regulating and non-buoyancy regulating phytoplankton. The average turbulent diffusivity without artificial mixing reported by Huisman et al. (2004) was 1.7 x 10^{-5} m^2 s^{-1} and 5.1 x 10^{-4} m^2 s^{-1} with artificial mixing. At Durleigh, when only one mixer was operational, turbulent diffusivities ranged between 10^{-5} and 10^{-3} m^2 s^{-1} (Figure 5.7) at all 3 locations. Location 1 and 2 showed similar profiles, which could signify the influence of the mixers on the turbulent diffusivities, however relatively high wind speeds (> 5 m s^{-1}) on the day of sampling make it difficult to discern the effects of the mixers from naturally induced mixing.

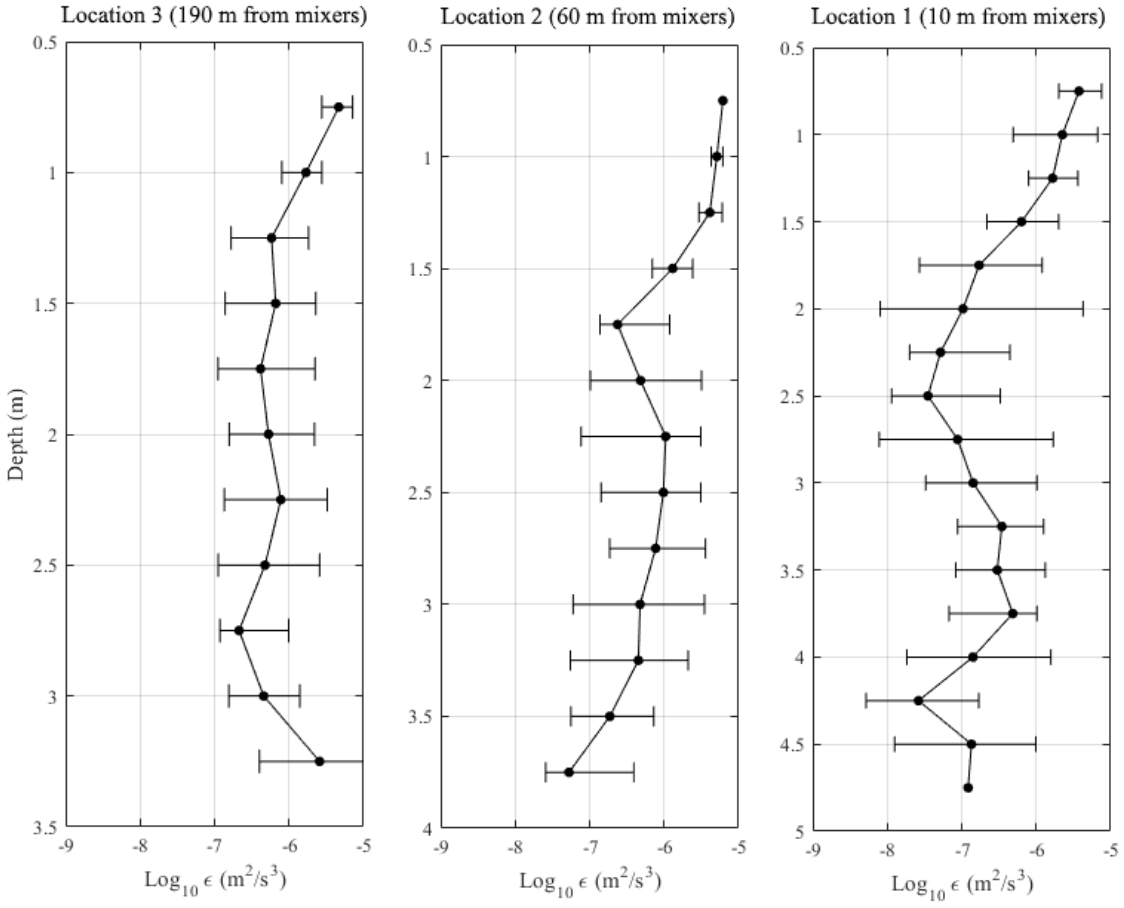

Figure 5.6. Averaged profiles of turbulent kinetic energy dissipation from SCAMP profiles collected on 11 September 2015 at 3 locations in Durleigh with increasing distance from the mixers.

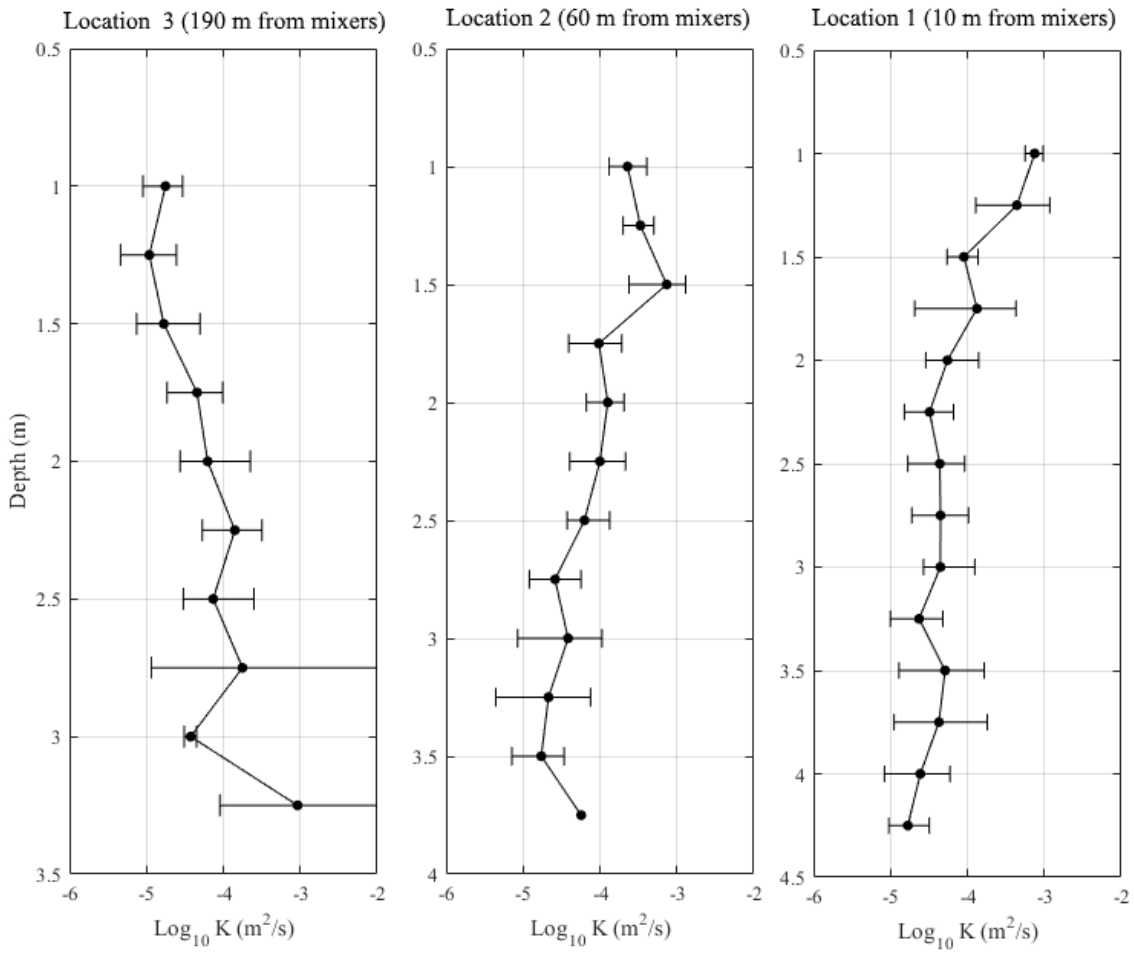

Figure 5.7. Averaged eddy diffusivity profiles estimated from SCAMP profiles collected on 11 September 2015 at 3 locations of varying depth in Durleigh with increasing distance from the mixers. Estimated using Osborn (1980).

5.4.6 Water Temperature

Hourly average water temperature measurements and differences (ΔT) are presented from surface and bottom measurements at B1, L2, and L3 (Figures 5.8 and 5.9) to demonstrate the variability in temperature measurements at below daily resolution. At L2 and L3, the hourly average surface and bottom temperatures were well-matched until May, which reflects lower air temperatures and solar radiation (Figure 5.1). In May, the hourly average surface and bottom temperatures at L2 and L3 began to diverge (Figure 5.8), indicating that the water column was becoming increasingly resistant to mixing, with maximum ΔT reaching 6.1℃ at L3 and 4.3℃ at L2 (Figure 5.9). The hourly average surface temperatures at L3 were the most variable (Figure 5.8), exhibiting a strong diurnal cycle. In May and early June 2018, ΔT at B1

and L2 were similar (Figure 5.9). However, from mid-June onwards, hourly average ΔT at L2 increased while ΔT at B1 remained lower.

Daily average temperature measurements were used in the statistical analysis (Kruskal Wallis test and Dunn's post-hoc test) instead of hourly averages to reduce the uncertainty of dependence between points. Daily average surface and bottom water temperatures between 9 May 2018 and 5 October 2018 were not significantly different between locations (Tables 5.3 and 5.4). However, over the same period, daily average ΔT was significantly different between each location. Daily average ΔT at B1 was significantly lower than L2 and L3, while daily average ΔT at L2 was significantly lower than ΔT at L3. Therefore, daily average ΔT increased with increasing distance from the mixers, indicating that during the summer, mixer operation maintained a more uniform water column (at B1) but the effects were localised as larger temperature differences were observed at L2 or L3.

Lorenzen and Fast (1977) suggest that artificial mixing can be deemed successful if ΔT is maintained at less than or equal to 2℃ and this metric has been used in many studies since as a measure of mixing success (e.g. Ashby and Kennedy, 1993). At all sites through 2018, the frequency of ΔT exceeding 2℃ increases with increasing distance from the mixers. ΔT at B1 exceeds 2℃ the least, which is likely due to the local impact of mixer operation, whereas at L3, ΔT exceeds 2℃ the most due to diurnal heating and cooling effects of a shallower water column. Nevertheless, ΔT at B1 does exceed 2℃ on numerous occasions, typically during periods of sustained warmer air temperatures and higher solar radiation (Figure 5.1), suggesting that despite mixer operation, sufficient mixing may not be achieved when warm weather conditions persist for prolonged periods.

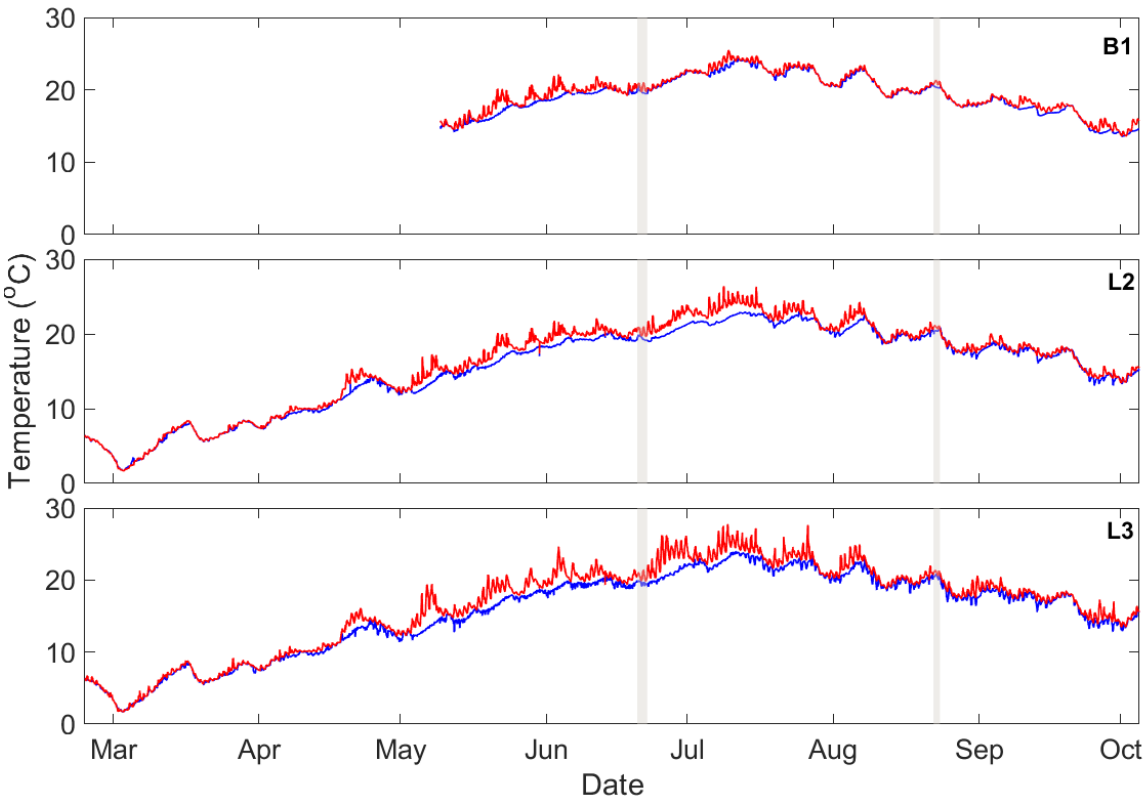

Figure 5.8. Hourly average temperatures at the surface (red) and bottom (blue) of the water column for all 3 study sites between 22 Feb and 5 Oct. Obvious erroneous data at B1 before 9th May was removed. Grey shading indicates shutdowns A and B.

Table 5.3. Results of the Kruskal-Wallis test and Dunn's post hoc test for daily average temperature measurements from B1, L2, and L3 between 9 May and 5 October 2018 at Durleigh.

	Significant difference	P value	Comments
Surface temperatures			
B1 and L2	N	0.99	H = 2.49, df = 2
B1 and L3	N	0.17	H = 2.49, df = 2
L2 and L3	N	0.17	H = 2.49, df = 2
Bottom temperatures			
B1 and L2	N	0.17	H = 1.92, df = 2
B1 and L3	N	0.39	H = 1.92, df = 2
L2 and L3	N	0.59	H = 1.92, df = 2
ΔT			
B1 and L2	Y	< 0.001	H = 81.49, df = 2
B1 and L3	Y	< 0.001	H = 81.49, df = 2
L2 and L3	Y	0.003	H = 81.49, df = 2

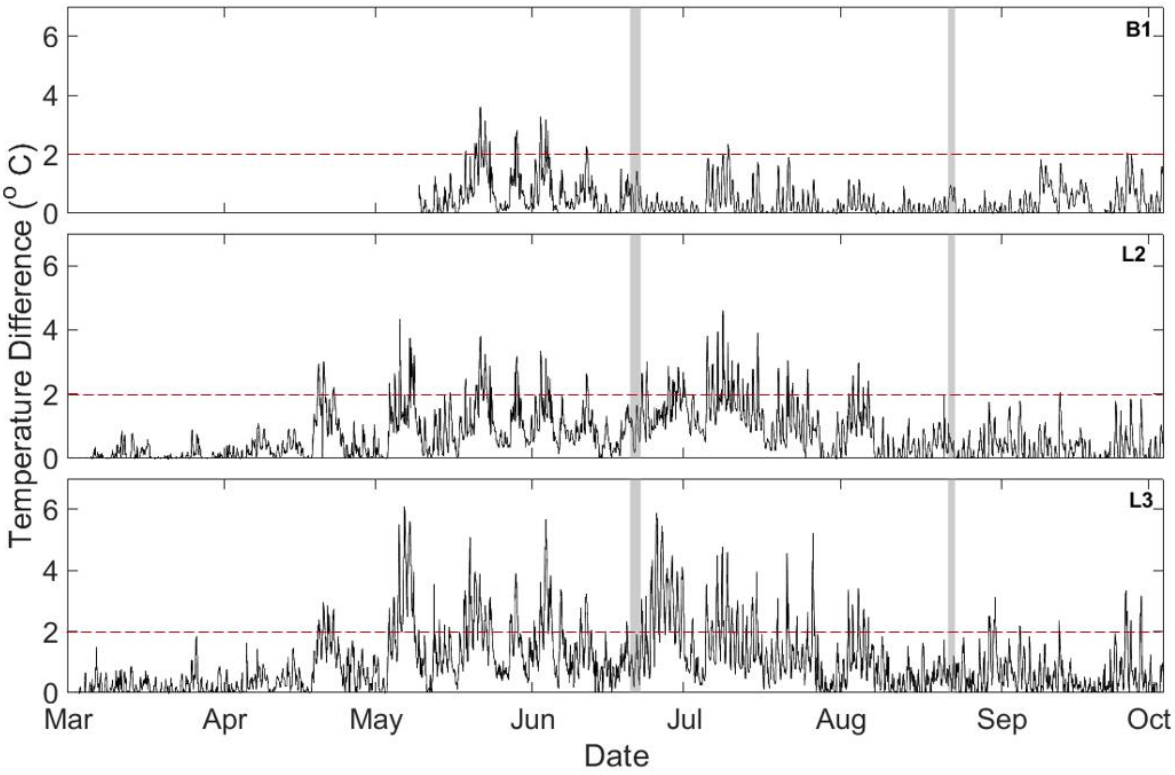

Figure 5.9. Temperature difference (ΔT) between the hourly average surface and bottom temperatures from Figure 5 for B1, L2, and L3. Obvious erroneous data at B1 before 9th May was removed. Grey shading indicates shutdowns A and B. Red dashed line indicates the 2 °C metric suggested by Lorenzen and Fast (1977).

Table 5.4. Descriptive statistics for daily average temperature measurements from B1, L2, and L3 between 9 May and 5 October 2018 at Durleigh.

	Mean	Median	Standard Deviation
Surface Temperatures			
B1	19.63	19.89	2.64
L2	19.62	19.92	2.74
L3	20.06	20.11	2.88
Bottom Temperatures			
B1	19.19	19.53	2.71
L2	18.79	19.21	2.45
L3	18.95	19.26	2.59
Δ*T*			
B1	0.43	0.28	0.45
L2	0.83	0.70	0.61
L3	1.11	0.91	0.79

5.4.7. Dissolved Oxygen

Hourly average dissolved oxygen differences (ΔDO) between surface and near-sediment (bottom) concentrations were calculated for B1 (Figures 5.10 and 5.11). The average ΔDO for periods when the mixers were operating between May and October 2018 was 2.3 mg l^{-1}, whereas for periods when the mixers were not operating ΔDO was 7.2 mg l^{-1}, suggesting that ΔDO observed during the shutdowns was unusual compared to when the mixers were operating (Figure 5.11). Therefore, the DO measurements demonstrate that mixer operation is important for locally reducing ΔDO.

ΔDO for each mixing period and shutdown was averaged and ΔDO was significantly larger during the shutdowns ($t_{(5)} = 3.4$, $p = 0.02$) compared to the periods when the mixers were operating, which suggests that the mixers had a local effect on dissolved oxygen distribution through the water column. In addition, between the shutdown's significant differences in ΔDO were explored using the Kruskal Wallis test and Dunn's post hoc test. ΔDO during the August shutdown (mean ΔDO: 10.2 mg l^{-1}) was significantly higher than the September (mean ΔDO: 6.6 mg l^{-1}) and June (mean ΔDO: 4.8 mg l^{-1}) shutdowns ($H = 42.9$, $p < 0.01$, df = 2), and the September shutdown had significantly higher ΔDO than the June shutdown ($H = 42.9$, $p < 0.01$, df = 2).

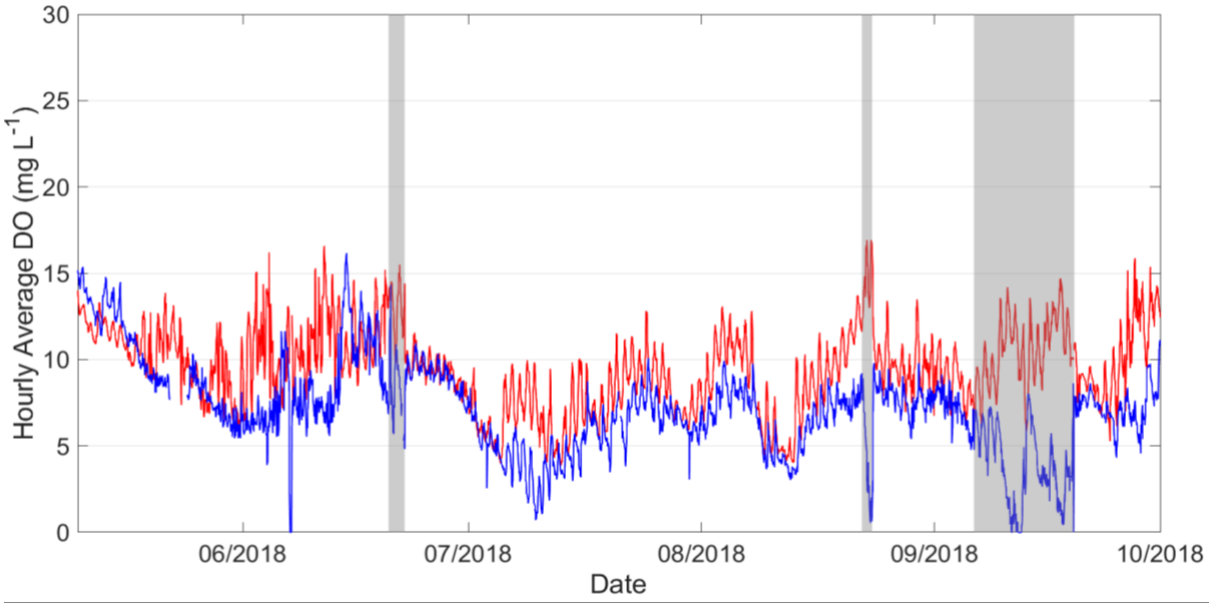

Figure 5.10. Dissolved Oxygen measurements from the surface (red line) and from the bottom (blue line) of the water column at B1. Grey shading indicates the mixer off periods, with the first two grey patches showing SD-A and SD-B, respectively.

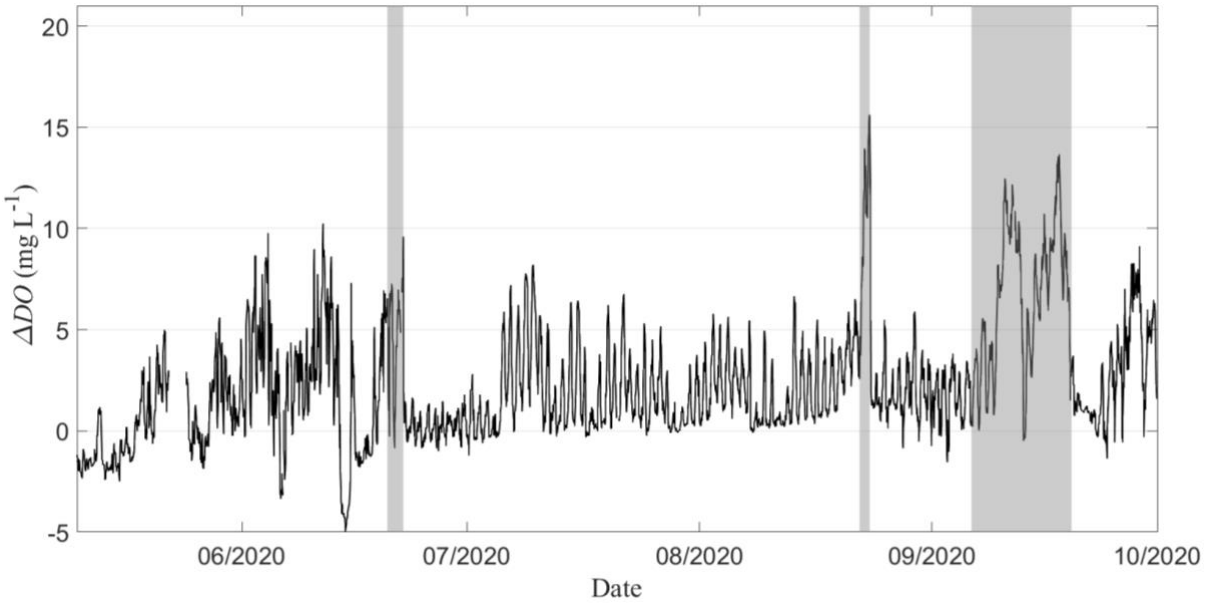

Figure 5.11. Dissolved Oxygen difference (ΔDO) between the hourly average surface and bottom measurements from B1. Grey shading indicates the mixer off periods, with the first two grey patches showing SD-A and SD-B, respectively.

5.4.8 Shutdown A

During shutdown A, hourly average temperature measurements from B1, L2, and L3 were taken. Hourly average surface and bottom DO (mg l^{-1}) from B1 and the difference between surface and bottom DO (Δ*DO*) are compared between ON1A, OFFA, and ON2A in this section. All data were averaged over 4-hour intervals prior to statistical analysis as the autocorrelation determined that at this averaging interval the time series observations were statistically independent of each other. These data were tested for significant differences using the Kruskal-Wallis test and Dunn's post hoc test.

Δ*T* at B1 was significantly higher during OFFA than both ON1A and ON2A, which is denoted by the superscript letters in Table 5.5. The significantly lower Δ*T* during ON1A and ON2A was likely due to mixer operation as Δ*T* at B1 was significantly lower than Δ*T* at L2 and L3, whereas during OFFA there was no significant difference between Δ*T* at all three locations. The average TKE from both convective (TKE_{conv}) and wind (TKE_{wind}) inputs during ON1A was 5.11 x 10^{-5} W m^{-2}, compared to 1.59 x 10^{-4} W m^{-2} during OFFA and 3.66 x 10^{-5} W m^{-2}. Despite natural TKE inputs being highest during OFFA Δ*T* at B1 was significantly higher than during ON1A and ON2A, indicating that at B1 mixer operation had a stronger influence on mixing than natural mixing processes. The higher Δ*T* at sites away from the mixers

during ON1A and ON2A suggest that the influence of the mixers was less pronounced and natural mixing processes may have a stronger influence. Net surface heat flux during averaged -10.8 W m^{-2}, -3.4 W m^{-2}, and 130.3 W m^{-2} during ON1A, OFFA, and ON2A, respectively, indicating that between 17 and 25 June, the heat content of the water column increased. As surface heat flux increased, ΔT at both L2 and L3 increased, which suggests that the flux of heat into the water column likely promoted the larger ΔT at sites away from the mixers (L2 and L3). The DO data further corroborates that mixer operation influences B1 as the ΔDO was significantly higher during OFFA compared to ON1A and ON2A, whereas the ΔDO during ON1A and ON2A were not significantly different (Table 5.5).

*Table 5.5. Mean (± SD) and median temperature difference (ΔT) (°C), dissolved oxygen difference (ΔDO) between the surface and bottom of the water. For surface mixer on/off periods in June 2018. Taken from observations averaged over 4-hour intervals as determined using autocorrelation. Results from the Kruskal-Wallis and Dunn's post hoc tests are indicated with superscripts. For the same period but different locations (by column) * marks locations that are not statistically different from each other. Between periods (across rows) values followed by the same letter (e.g. both followed by superscript a) were not found to be significantly different from each other (p > 0.05).*

	ON1A (17/06/18 09:00 – 19/06/19 12:00)	OFFA (20/06/18 09:00 – 22/06/18 12:00)	ON2A (23/06/18 09:00 – 25/06/18 12:00)
B1 median ΔT	0.14[a]	0.62*[b]	0.11[a]
B1 mean ΔT (°C)	0.26 ± 0.34	0.65 ± 0.39	0.17 ± 0.16
L2 median ΔT	0.57[a]	0.8*[b]	0.97*[b]
L2 mean ΔT (°C)	0.57 ± 0.27	0.86 ± 0.43	1.21 ± 0.61
L3 median ΔT	0.90[a]	0.95*[a]	1.78*[b]
L3 mean ΔT (°C)	0.97 ± 0.48	0.88 ± 0.33	2.06 ± 1.09
B1 median ΔDO	0.31[a]	5.74[b]	0.01[a]
B1 mean ΔDO (mg l^{-1})	0.47 ± 1.76	4.79 ± 2.61	0.09 ± 0.67

Prior to the June shutdown, on 19 June 2018, ΔDO increased during the day largely due to increased surface DO concentrations and in part due to decreased bottom water concentrations (Figure 5.12). Surface DO concentrations continued to increase over night on 19 June 2018, when the mixers were still operational. The mixers were turned off at 08:19 on 20 June 2018 and ΔDO remained low until 14:00, when it increased, peaking at 7.4 mg l^{-1} at 16:15. Overnight, ΔDO remained stable, generally between 5-7 mg l^{-1}, until 02:30 (21 June). At 06:30 ΔDO reached almost 0 and was negative between 07:15 and 09:15. From then on ΔDO increased and peaked at 10.2 mg l^{-1} at 12:15. The mixers were turned back on at 12:22 and ΔDO declined to 0.5 mg l^{-1} by

14:45. Generally, over this period, operation of the mixers appeared to increase dissolved oxygen concentrations through the water column.

DO at the bottom of the water column was also measured at L2 and L3 and showed that DO was generally lower than B1 and no obvious differences were observed between ON1A, OFFA, and ON2A. During OFFA bottom DO at B1 declined to levels similar to those observed at the bottom of the water column at L2 and L3, indicating that mixer operation may locally increase bottom DO concentrations.

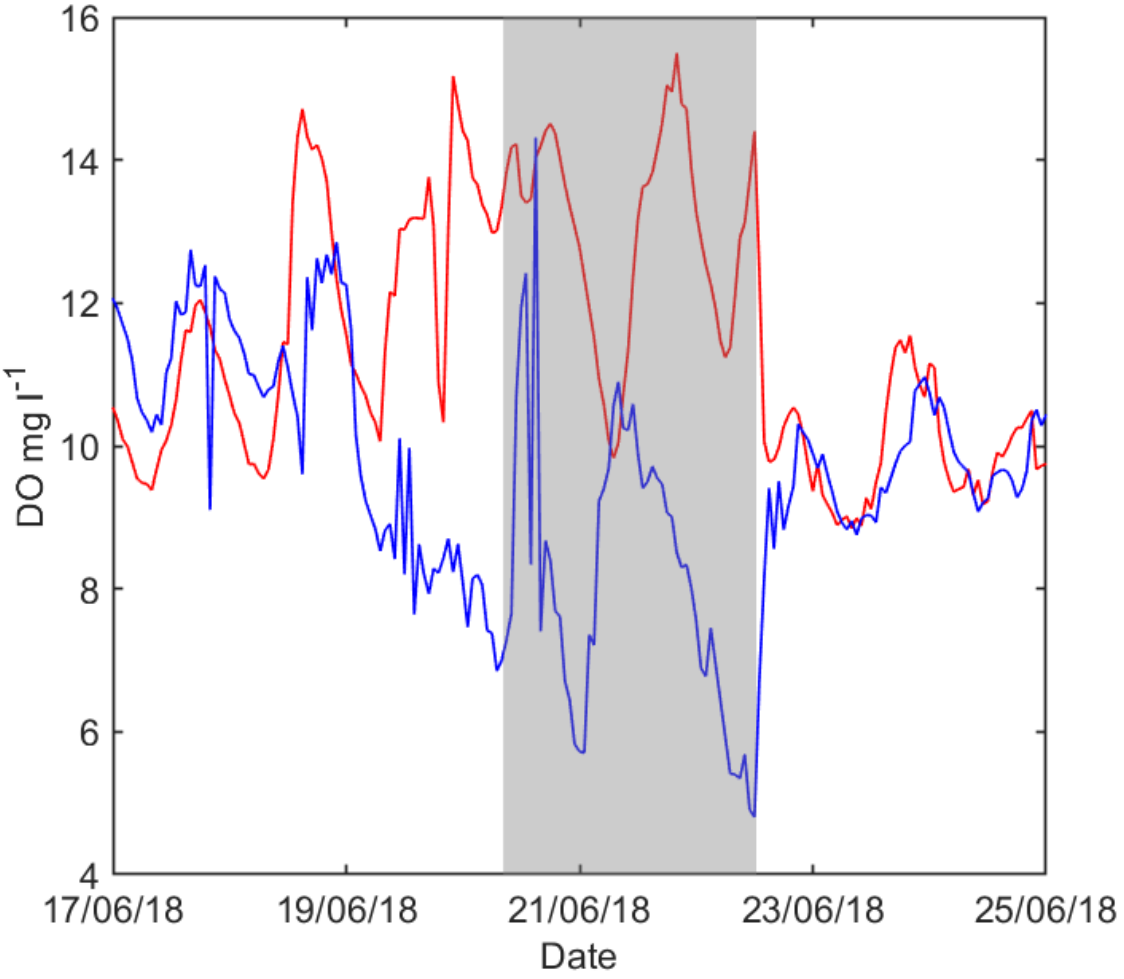

Figure 5.12. Hourly average dissolved oxygen (mg l^{-1}) at the surface (red line) and bottom (blue line) at B1 measured between 17-25 June (Shutdown A). The grey shading indicates OFFA, the period during which the surface mixers were not operational.

5.4.9 Shutdown B

Hourly average temperature measurements from B1, L2, and L3 were taken and hourly average surface and bottom DO (mg l^{-1}) from B1 and ΔDO were collected. All listed parameters were compared between ON1B, OFFB, and ON2B. Additionally, between 20 - 24 August 2018, the acoustic Doppler velocimeter (ADV) was deployed north of the mixers and measured near bed velocities and backscatter. All data were averaged over 4-hour intervals prior to statistical analysis as the autocorrelation determined that at this averaging interval the time series observations were statistically independent of each other. These data were tested for significant differences using the Kruskal-Wallis test and Dunn's post hoc test

At B1, Δ*T* during OFFB was significantly higher than Δ*T* during ON1B or ON2B (Table 5.6), indicating that turning the mixers off increased temperature differences between the surface and bottom of the water column close to the mixers. During OFFB, Δ*T* at B1 was significantly higher than Δ*T* at L2 (Table 5.6). At L2 and L3, Δ*T* significantly decreased during OFFB compared to ON1B. Net surface heat flux during averaged -81.5 W m^{-2}, -107.2 W m^{-2}, and -137.9 W m^{-2} during ON1B, OFFB, and ON2B, respectively, indicating that between 20 and 25 August the heat content of the water column decreased. Therefore, the results in Table 5.6 suggest that for L2 and L3, the net surface heat flux and TKE inputs from convection and wind-driven mixing likely influenced the thermal gradients to a greater extent than the operation of the mixers.

Δ*DO* at B1 significantly increased during OFFB (Table 5.6), indicating that when the mixers were turned off the circulation of DO through the water column reduced locally. Generally, the manipulation of the mixers over the shutdown had no discernible effect on thermal gradients at L2 or L3, but locally reduced temperature and dissolved oxygen differences through the water column at B1.

On 21 August, *ΔDO* increased to 6.6 mg l^{-1} at 18:15 due to increased surface DO concentrations. Overnight *ΔDO* declined slightly due to decreased DO concentrations at the surface (Figure 5.13). The mixers were turned off at 07:17 on 22 August and at this time *ΔDO* was 3.3 mg l^{-1}. *ΔDO* increased to 9.2 mg l^{-1} at 18:30 due to both decreased bottom DO concentrations and increased surface DO concentrations. Overnight, DO concentrations at the bottom of the water column decreased, resulting in increased *ΔDO.* From 09:00 onwards on 23 August, surface DO concentration increased and bottom DO

concentrations remained below 2 mg l^{-1}. At 15:00 on 23 August, the maximum *ΔDO* was reached at 15.7 mg l^{-1}, with 17 mg l^{-1} at the surface and < 1.3 mg l^{-1} at the bottom of the water column. The mixers were turned on at 16:42 on 23 August and *ΔDO* declined to 2.6 mg l-1 by 20:30 and 1.1 mg l-1 by 22:45. The rapid decline in *ΔDO* was caused by both decreased surface DO concentrations and increased bottom water DO concentrations. Overall, mixer operation appear to have a marked effect on DO distribution at B1.

*Table 5.6. Mean (± SD) and median temperature difference (ΔT) (ºC), dissolved oxygen difference (ΔDO) between the surface and bottom of the water. For surface mixer on/off periods in August 2018. Taken from observations averaged over 4-hour intervals as determined using autocorrelation. Results from the Kruskal-Wallis and Dunn's post hoc tests are indicated with superscripts. For the same period but different locations (by column) * marks locations that are not statistically different from each other. Between periods (across rows) values followed by the same letter (e.g. both followed by superscript a) were not found to be significantly different from each other (p > 0.05).*

	ON1B (20/08/18 08:00 – 21/08/18 16:00)	OFFB (22/08/18 08:00 – 23/08/18 16:00)	ON2B (24/08/18 08:00 – 25/08/18 16:00)
B1 median Δ*T*	0.15^{a}	0.66^{b}	0.01^{*a}
B1 mean Δ*T* (ºC)	0.18 ± 0.12	0.65 ± 0.23	0.06 ± 0.13
L2 median Δ*T*	0.78^{*a}	0.41^{*b}	0.13^{*c}
L2 mean Δ*T* (ºC)	0.78 ± 0.36	0.41 ± 0.21	0.13 ± 0.09
L3 median Δ*T*	0.83^{*a}	0.54^{*a}	0.72^{a}
L3 mean Δ*T*(ºC)	0.80 ± 0.40	0.53 ± 0.27	0.71 ± 0.59
B1 median Δ*DO*	4.10^{a}	11.16^{b}	1.44^{c}
B1 mean Δ*DO* (mg l^{-1})	4.10 ± 0.95	10.33 ± 3.81	1.99 ± 1.23

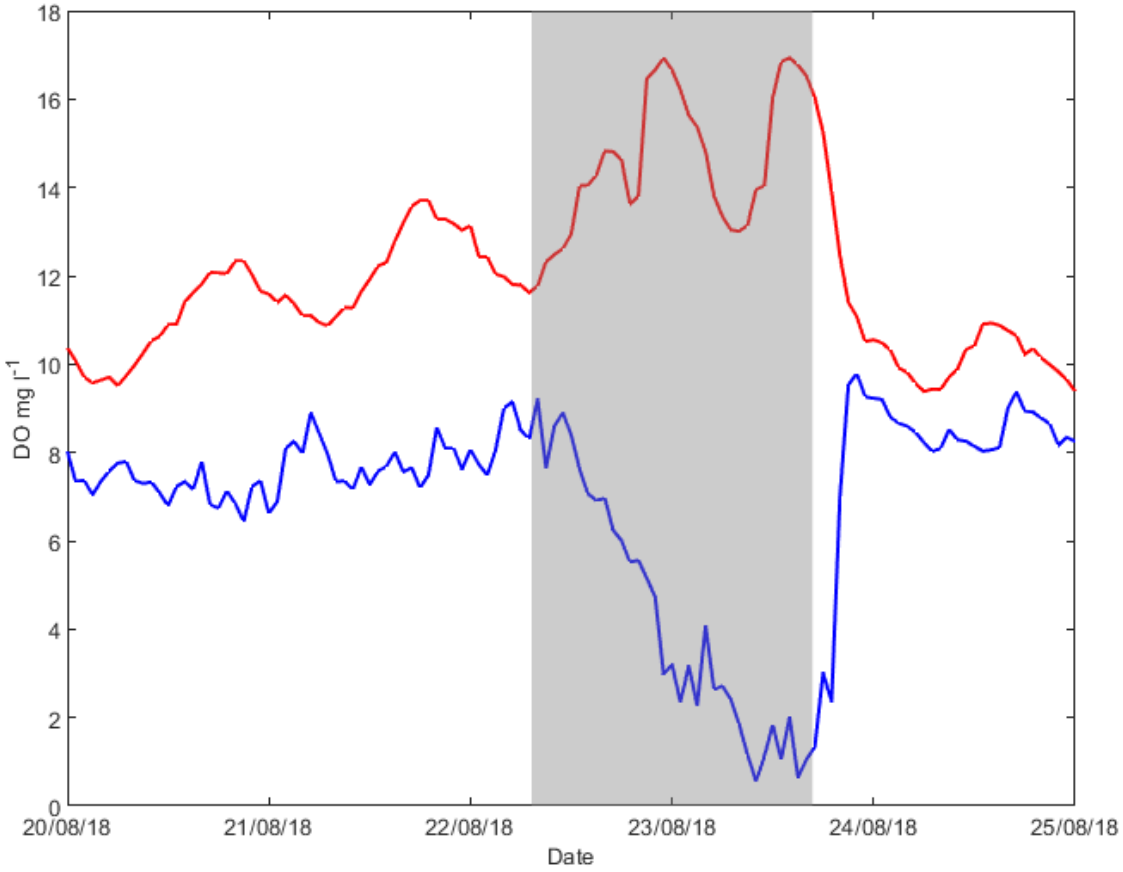

Figure 5.13. Hourly average dissolved oxygen (mg l^{-1}) at the surface (red line) and bottom (blue line) at B1 measured between 20-25 August 2018 (Shutdown B). The grey shading indicates OFFB, the period during which the surface mixers were not operational.

5.4.10 Acoustic Doppler Velocimeter

An acoustic Doppler velocimeter (ADV) was deployed ~ 30 m north of the mixers to measure near-bed velocities and signal amplitude (dB) for shutdown. Due to the length of ADV deployment the defined periods are different: ADV_ON1B, ADV_OFFB, and ADV_ON2B. The ADV_ON1B period refers to ADV measurements taken between 15:00 on 20 August and 07:10 on 22 August. The ADV_OFFB period refers to the mixer shutdown between 07:20 on 22 August and 16:40 on 23 August, and the ADV_ON2B period refers to measurements collected after the mixers were turned back on between 16:50 on 23 August and 09:30 on 24 August. Therefore, the ADV data is not directly comparable to the periods defined for other parameters during shutdown B. Nevertheless, data presented in this section provides insight into the hydrodynamics of surface mixers and the short-term effects of turning surface mixers off in a shallow reservoir.

The Kruskal-Wallis test and Dunn's multiple comparison test revealed that during every period (ADV_ON1B, ADV_OFFB, and ADV_ON2B), the velocities, magnitude, and amplitude averaged every 4 hours (to ensure no autocorrelation) were significantly different from each other (Table 5.7). During ADV_OFFB E decreased significantly and N increased significantly during ADV_ON2B (Figure 5.14b, Table 5.7), suggesting that the mixers strongly influence the near-bed velocities at least up to at least 30 m away. Each mixer has an initial flow velocity of 0.15 m s^{-1} (over an area of 9.05 m^2); compared to the initial flow velocity, the horizontal velocities 30 m north of the mixers are very small.

Magnitude of the velocities was significantly lower during ADV_OFFB than both ADV_ON1B and ADV_ON2B (Figure 5.14c), suggesting that when the mixers are turned off, the near-bed velocities ~ 30 m north of the mixers decrease. However, velocities largely remained below 0.05 m s^{-1} when the mixers were operating, and during ADV_OFFB velocities typically dropped below 0.02 m s^{-1}. The magnitude during ADV_ON2B is significantly higher than during ADV_ON1B, which likely a reflects the higher wind speeds during ADV_ON2B (Figure 5.14a; Table 5.7).

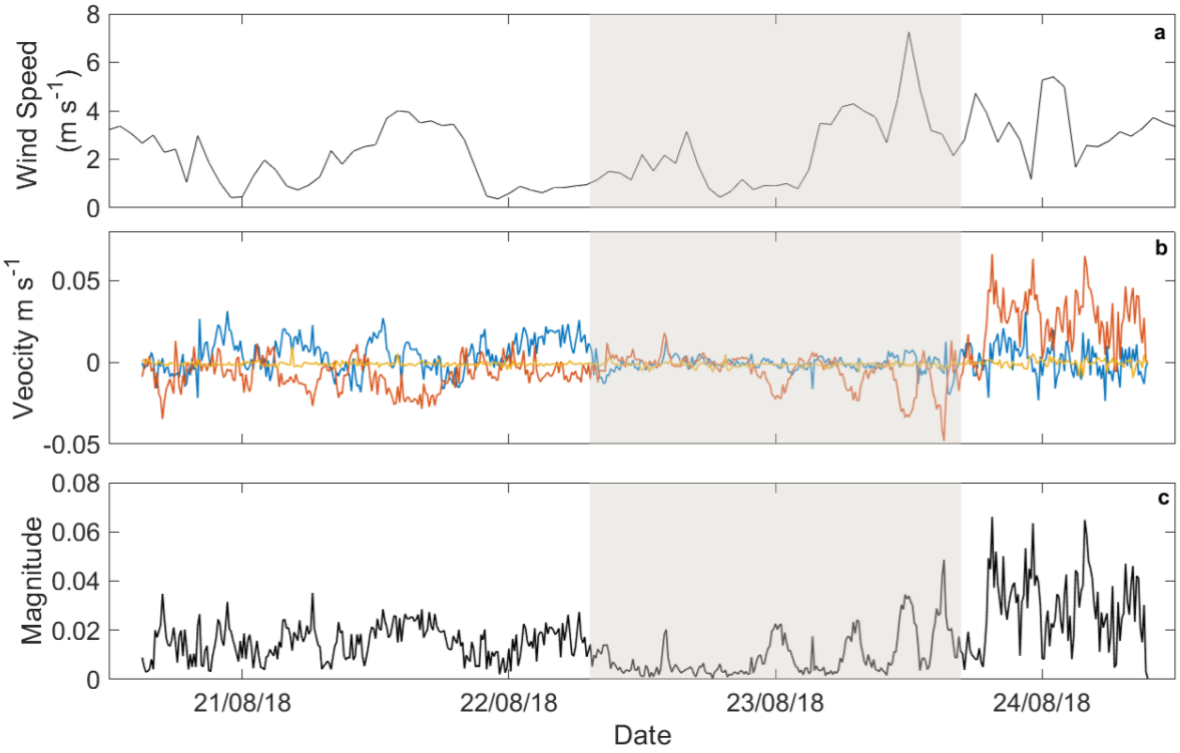

Figure 5.14. a.) Hourly average wind speeds at Durleigh between 20 and 24 August 2018. b.) The E, N, and Up velocities from the ADV, ~ 30 m north of the mixers, between 20 and 24 August 2018. c.) The magnitude of the velocities from ADV over the same time period. The grey shading indicates ADV_OFFB.

The ADV amplitude during ADV_OFFB was significantly lower than ADV_ON1B or ADV_ON2B, indicating a reduction in suspended material in the water column (Figure 5.15; Table 5.7). In addition, the amplitude during ADV_ON2B increased significantly, suggesting that the increased magnitude of near-bed velocities from the mixers being turned on caused increased suspension of sediments ~30 m from the mixers. Wind speeds increased on the morning of 23 August (Figure 5.14a), which likely caused the increased amplitude before the mixers were turned on. Therefore, the decreased amplitude and magnitude during ADV_OFFB cannot be solely attributed to the mixers not operating.

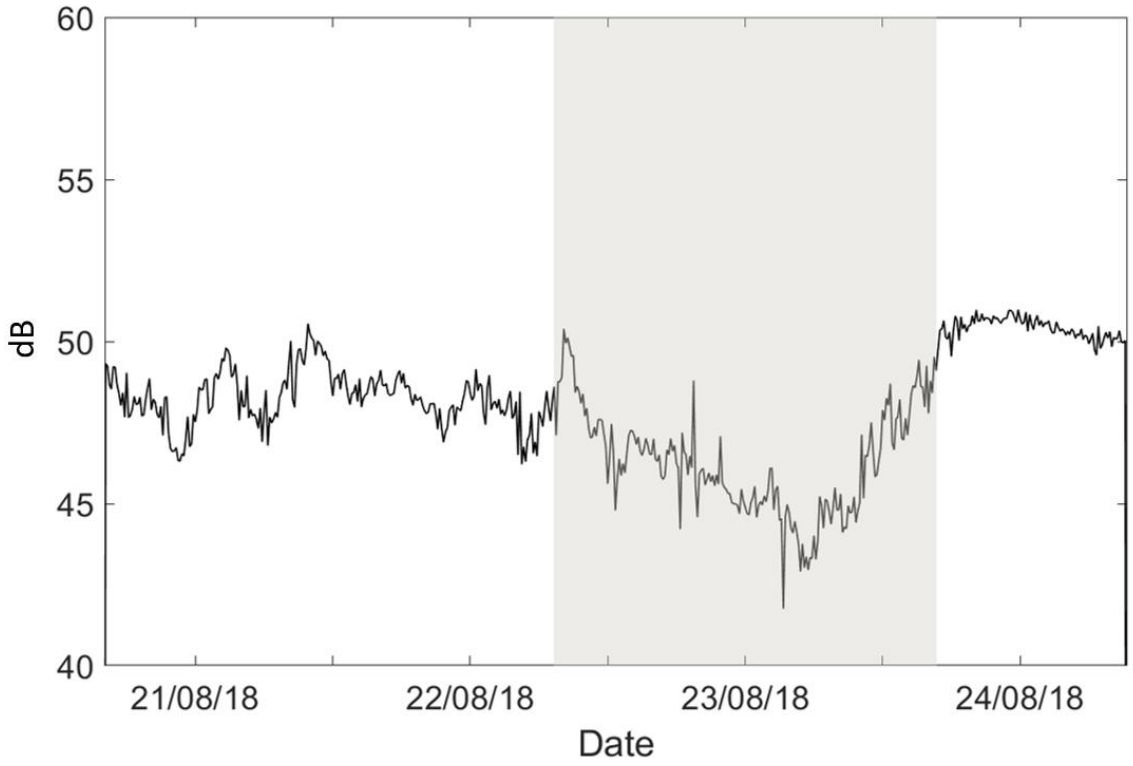

Figure 5.15. Amplitude of the received signal (measured in dB) from the ADV between 20 and 24 August 2018. The grey shading indicates ADV_OFFB.

Table 5.7. Median of amplitude, magnitude, and velocities recorded by ADV for surface mixer on/off periods in August 2018. Taken from hourly average measurements. Results from the Kruskal-Wallis and Dunn's post hoc tests are indicated with superscripts. Between periods (across rows) values followed by the same letter were not found to be significantly difference from each other (p > 0.05).

	ADV_ON1B 20/08/18 15:00 – 22/08/18 07:10	ADV_OFFB 22/08/18 07:20 – 23/08/18 16:40	ADV_ON2B 23/08/18 16:50 – 24/08/18 09:30
Median amplitude (dB)	48.24[a]	46.26[b]	50.39[c]
Mean amplitude (dB)	48.25 ± 0.83	46.11 ± 1.63	50.41 ± 0.32
Magnitude	0.046[a]	0.007[b]	0.104[c]
E (east)	0.526[a]	0.415[b]	0.465[c]
N (north)	0.356[a]	0.400[b]	0.657[c]
U (up)	0.438[a]	0.425[b]	0.486[c]

5.4.11 Acoustic Doppler Current Profiler

The StreamPro ADCP was towed for multiple transects to determine the range of influence of the mixers at Durleigh. Generally, the horizontal velocities and vertical velocities measured by the ADCP were small and for all transects, there were no obvious differences between the mixers operating and not operating. The closest the ADCP was towed to the mixers was 15 m at transect 3 (Figure 3.10c; Chapter 3), but water column velocities were small compared to the initial flow velocity of each mixer (0.15 m s^{-1}), with no obvious effects of the mixers operating compared with when they were turned off (data not shown).

The N-S velocities along transect 1 (data not shown; Figure 3.10a, Chapter 3) ranged between -0.106 and 0.107 m s^{-1} when the mixers were on and between -0.071 and 0.076 m s^{-1} when the mixers were off. Up velocities on the same transect ranged between -0.037 and 0.015 m s^{-1} when the mixers were on and between -0.014 and 0.027 m s^{-1} when the mixers were off. However, no significant difference was found between N-S or up velocities when the mixers were operating and not operating (p = 0.93 and 0.17, respectively).

Transect 2 moved E to W away from the mixers, starting 25 m west of the mixers (Figure 3.10b, Chapter 3). When the mixers were on, the E-W velocities ranged between -0.09 and 0.09 m s^{-1} compared to between -0.09 and 0.057 m s^{-1} when the mixers were off (not significantly different, p = 0.53). Up velocities (not significantly different, p = 0.49) ranged between -0.023 and 0.008 m s^{-1} when the mixers were on and between -0.046 and 0.007 m s^{-1} when the mixers were off (Figures 5.16 - 5.19). Lee et al. (2014) highlight that when measuring water velocities below 0.25 m s^{-1}, there is high variability in velocity measurements, even if 8 or more of the same transect are collected. Due to time constraints with the equipment, multiple transects could not be collected, so uncertainty may have been introduced into the StreamPro measurements. Overall, transect data from the StreamPro ADCP measurements show no obvious currents that could be produced by the mixers at distances > 15 m when they are operating compared to the measurements taken when the mixers were turned off. Although the ADCP data does not indicate evidence of mixer influence at distances > 15 m from the mixers, their influence beyond this distance cannot be disregarded.

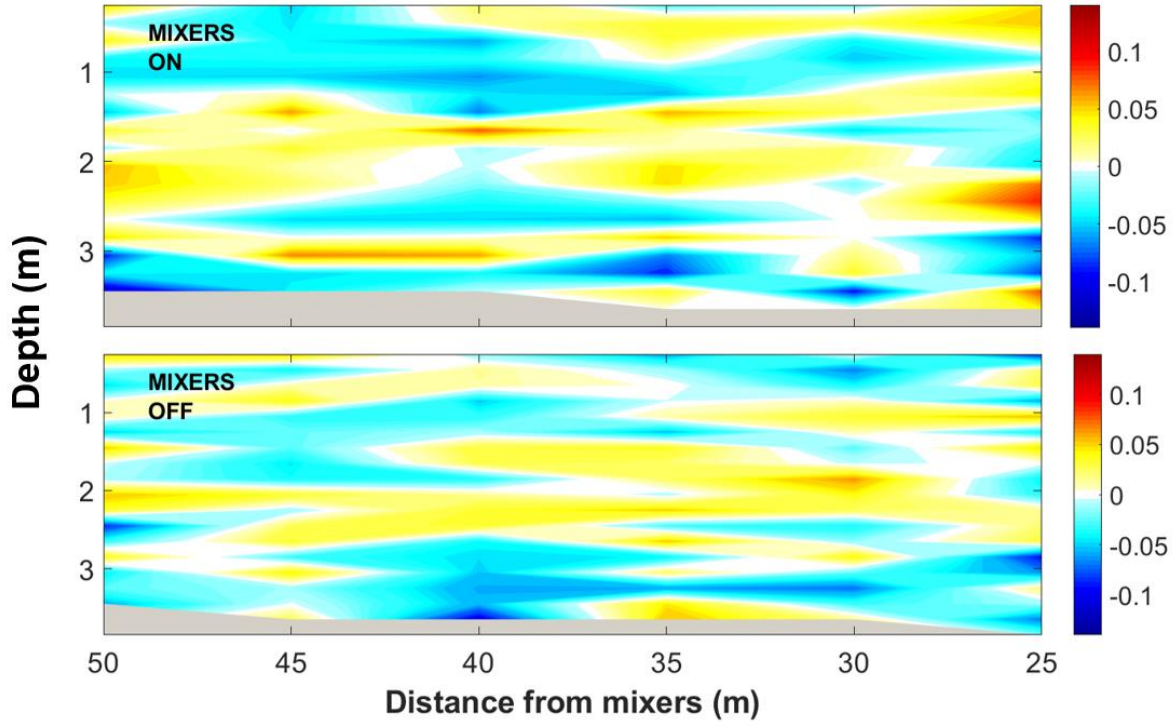

Figure 5.16. Averaged (5 m) E-W velocities from the StreamPro ADCP along Transect (2) moving away from the mixers (25 – 55 m away) when the mixers were on (top panel) and off (bottom panel).

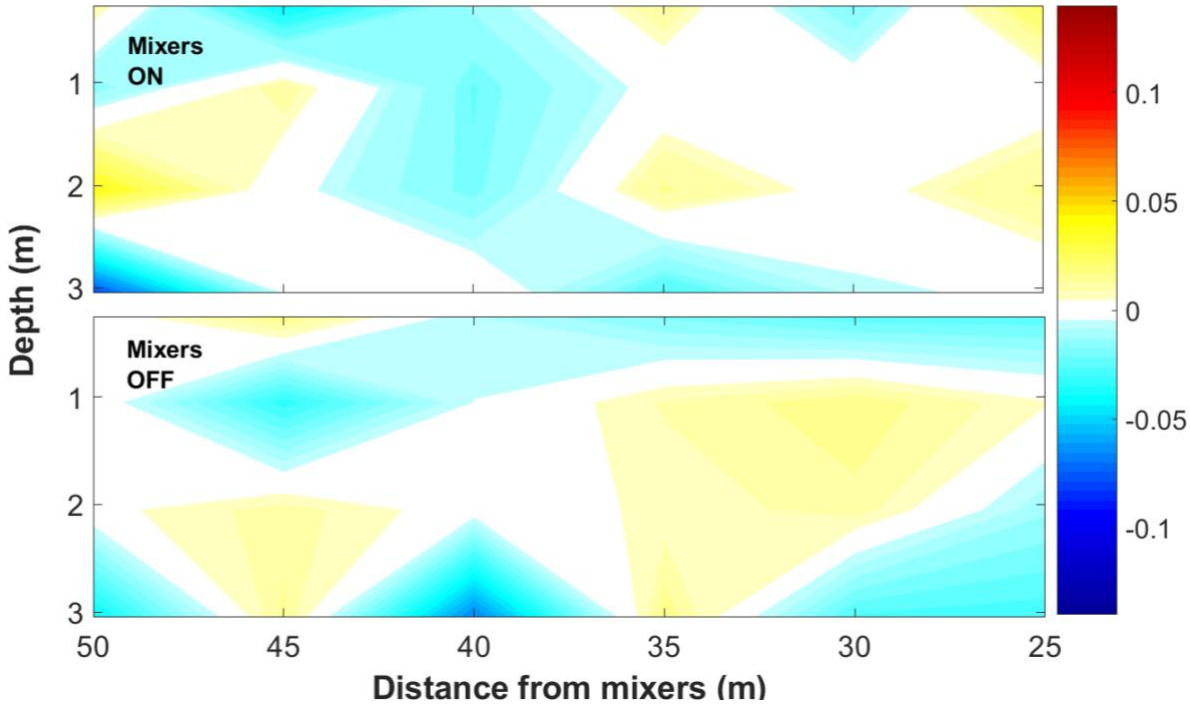

Figure 5.17. Vertically averaged (every 1 m) E-W velocities from the StreamPro ADCP along Transect (2) moving away from the mixers (25 – 55 m away) when the mixers were on (top panel) and off (bottom panel).

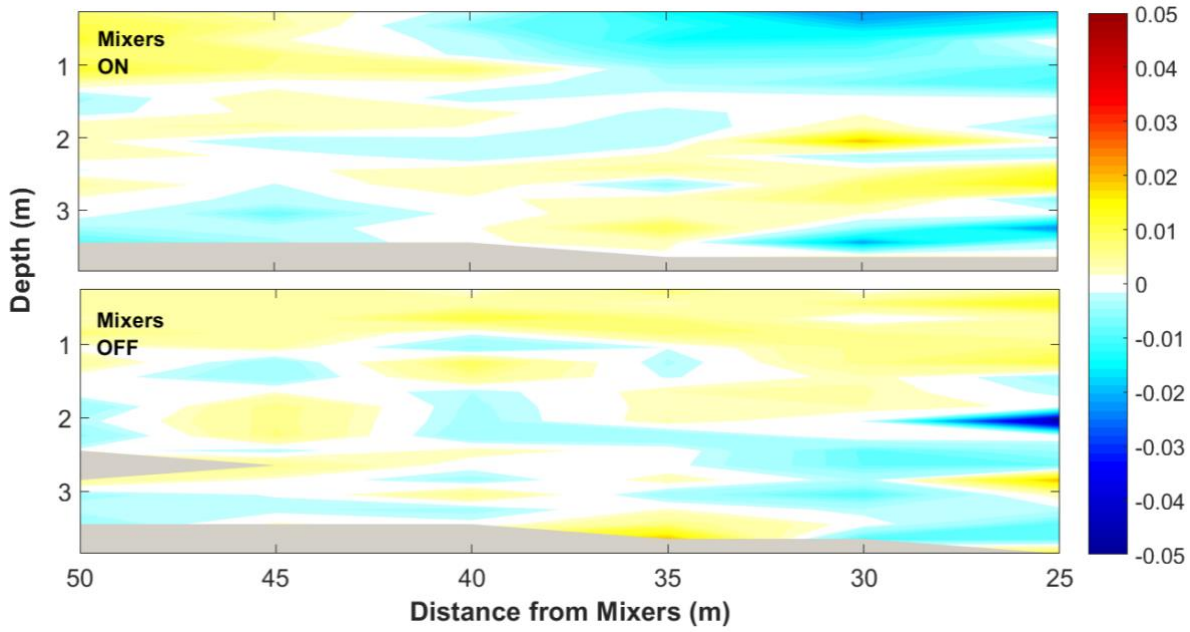

Figure 5.18. Averaged (5 m) up velocities (m s^{-1}) from the StreamPro ADCP along Transect (2) moving away from the mixers (25 – 55 m away) when the mixers were on (top panel) and off (bottom panel).

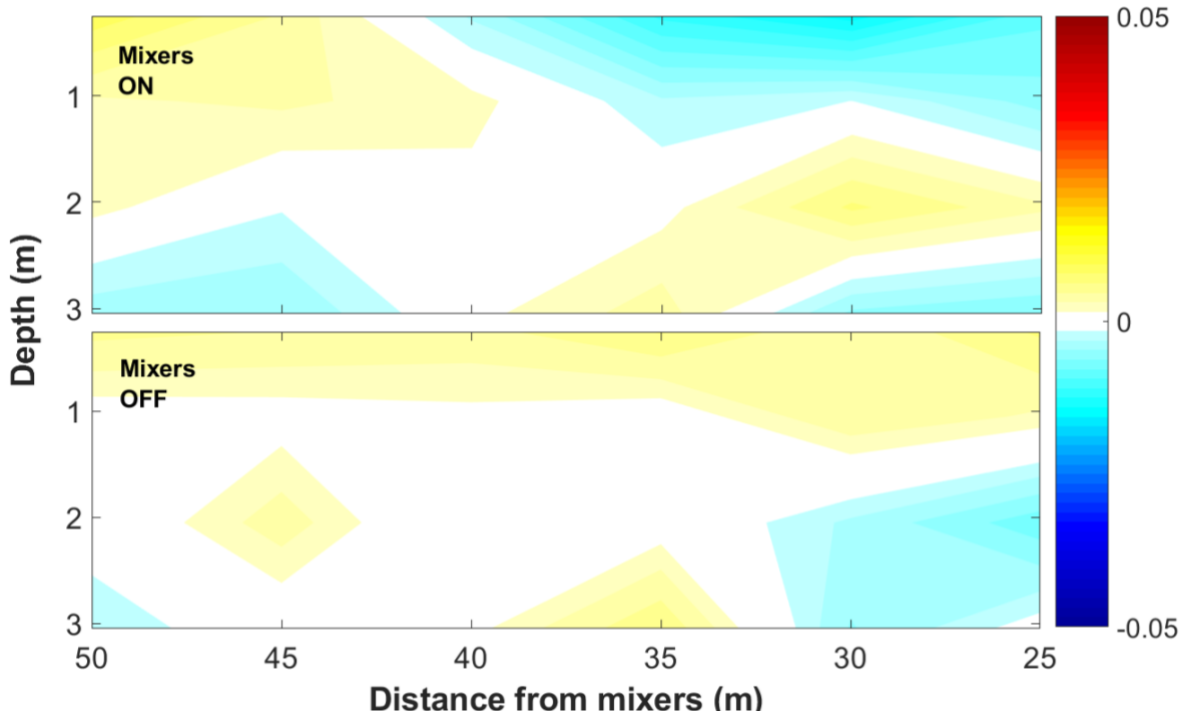

Figure 5.19. Vertically averaged (every 1 m) up velocities (m s^{-1}) from the StreamPro ADCP along Transect (2) moving away from the mixers (25 – 55 m away) when the mixers were on (top panel) and off (bottom panel).

5.4.12 Results Summary

Throughout 2018, daily average ΔT at B1 was significantly lower than ΔT at L2 and L3 when the mixers were operating (Figure 5.9). During both SD-A and SD-B, ΔT at B1 significantly increased, whereas ΔT at L2 and L3 did not appear to change as a result of the mixers being turned on or off. Instead, ΔT at L2 and L3 appeared to respond more to meteorological conditions, indicating that the mixers range of influence may be limited to a localised area. ΔDO at B1 increased significantly during both shutdowns (Figure 5.11; Tables 5.5 and 5.6) but peaks in TKE_{wind} and TKE_{conv} during SD-A and SD-B (Figure 5.3d), respectively, caused a decrease in ΔDO at B1. Inputs of TKE from the wind and convection were shown to be considerably lower than the TKE input from the mixers. The TKE inputs from wind and convection are variable (Figure 5.3) compared to the continuous TKE input generated by each mixer. Therefore, when the mixers were turned off, TKE_{wind} and TKE_{conv} occasionally increased enough to mix the water column at B1 (Figures 5.10 and 5.12). Light penetration at Durleigh was low throughout 2018 (Table 5.2) and diurnal variations in surface temperature were marked (Figure 5.8), especially at the shallowest locations. Profiles of Turbulent diffusivity (Figure 5.7) were similar across all sites and it is possible that the higher wind speeds at the time of sampling may have made it difficult to discern the effects of the mixers from natural mixing processes. ADV data from August 2018 showed a significant reduction in the magnitude of velocities during ADV_OFFB (Figure 5.14 and Table 5.7), indicating that when the mixers were off, the near-bed velocities ~ 30 m north of the mixers were significantly lower. However, all velocities measured between 20 - 24 August 2018 were small compared to the initial flow velocities of 0.15 m s^{-1} from each mixer, which corroborates with the StreamPro ADCP measurements that showed no obvious difference in water velocities at distances > 15 m from the mixers, when the mixers were on compared to when they were off (Figures 5.16 - 5.19). The amplitude from the ADV significantly decreased during ADV_OFFB (Figure 5.15 and Table 5.7) and suggests that sediment resuspension significantly decreased when the mixers were not operating, but changes in wind speed also appeared to influence sediment resuspension ~30 m from the mixers.

5.5 Discussion

Surface mixers are installed with the aim of uniformly mixing the water column to prevent the development of thermal stratification and the associated water quality degradation. However, there is limited peer-reviewed evidence that surface mixers successfully minimise water quality degradation and is particularly lacking for shallow reservoirs. In addition to destratifying (or prevent stratification from forming), a secondary aim for surface mixers is to improve DO concentrations throughout the water column and subsequently reduce nutrient and metal release from the sediments into the overlying water column. Artificial circulation by surface mixers seeks to entrain cyanobacterial cells and reduce the buoyancy advantage of some species by mixing cells out of the euphotic zone long enough to reduce productivity. Understanding the effects of surface mixers on hydrodynamics, temperatures, DO concentration, turbidity, and cyanobacterial cell distributions in shallow eutrophic reservoirs is needed to better inform water quality management decisions. The findings presented in this chapter indicate that principal aims of artificial circulation are limited to a local area around the mixers, beyond which influence of the mixers are not obviously discernible from meteorological effects. Here, we discuss the *in-situ* observations of artificial circulation on the hydrodynamics, dissolved oxygen, phytoplankton cell distribution, sediment resuspension/light penetration, and raw water quality in a shallow, hypereutrophic drinking water reservoir.

5.5.1 Temperature

Artificial circulation with surface mixers seeks to prevent thermal stratification from forming. Lorenzen and Fast (1977) consider temperature differences of 2℃ or less as successful destratification. Generally, ΔT at B1 generally remained below 2℃ (Figure 5.9) only exceeding this value in late May/early June 2018, when wind speeds were lower and net surface heat flux was higher (Figure 5.3). With increasing distance from the mixers and decreasing water column depth, ΔT exceeded 2℃ more frequently, indicating that surface mixer operation is locally more successful at preventing the development of thermal stratification. Although L2 is only ~ 0.5 m shallower than B1, ΔT was significantly larger, which suggests the effects of the mixers are reduced at 60 m away. During OFFA and OFFB, ΔT at B1 increased significantly and was attributed to the mixers being turned off, whereas no obvious influence of mixer operation was

observed at L2 or L3 (Tables 5.5 and 5.6). Similarly, Lawson and Anderson (2007) observed limited effects of mixer operation on stratification in shallow Lake Elsinore, and Upadhyay et al (2013) reported very localised effects of a solar powered updraft pump.

Although not significant, bottom water temperatures at B1 were higher than L2 and L3 (Tables 5.3 and 5.4), indicating the localised effects of the mixers circulating warmer surface waters downwards. However, warmer temperatures in the bottom waters/hypolimnion affects biogeochemical processes at the sediment water interface (SWI, Bell and Ahlgren, 1987; Visser et al., 2016). For example, warmer temperatures at the SWI can increase rates of mineralisation of organic matter and increased microbial respiration, which increase DO demand. Jiang et al. (2008) found that bacterial respiration at the SWI increased with warmer temperatures, which lowered the redox potential and resulted in a release of Fe-P/Al-P from the sediments to the overlying water. Overall, temperature measurements indicate that surface mixer operation locally decreases ΔT (< 20 m from mixers) and may influence thermal structure > 20 m from the mixers, although at distances > 20 m from the mixers, meteorological conditions appear more influential.

5.5.2 Dissolved Oxygen

Theoretically, surface mixer operation moves oxygenated surface waters down the water column, to the hypolimnion and sediments, where DO demand is typically highest (Beutel and Horne, 1999). ΔDO at B1 is large for both OFFA and OFFB, but the difference between surface and bottom DO may not be entirely driven by mixer operation. For example, high concentrations of DO were observed at the surface of B1 during both shutdowns (Figures 5.12 and 5.13). DO concentrations were highest during OFFB, when total phytoplankton and cyanobacteria cell counts were high (Figures 5.4 and 5.5). Similarly, Lawson and Anderson (2007) observed super saturation near the surface and attributed high DO concentrations to photosynthetic oxygen production in conjunction with high algal biomass (CH2M HILL, 2013). During OFFB, entrainment of phytoplankton cells from the surface downwards decreased and thus positively buoyant species such as *Aphanizomenon* and *Dolichospermum* (formerly *Anabaena*) may have capitalized on the reduced mixing to remain in the photic zone for longer (Moreno-Ostos et al., 2016; Visser et al., 2016; data not shown). Therefore, turning off the mixers likely increased DO concentrations at the surface of B1 indirectly through

reducing the transport of phytoplankton cells out of the photic zone. Generally, the increase in DO near the surface appears to be due to phytoplankton productivity and no obvious increase is observed as a result of mixer operation increasing the diffusion of oxygen from the atmosphere. We suggest that surface mixers in shallow eutrophic reservoirs act more as diluters than oxygenators, whereby DO is mixed more uniformly over the water column, and compared to biological production, levels of DO diffusing from the atmosphere are low.

ΔDO at B1 was significantly larger during the mixer shutdowns compared to periods when the mixers were operating, which indicates that locally the mixers are effective at reducing gradients of dissolved oxygen. During the shutdown in June (OFFA) and the shutdown over September, ΔDO converged and demonstrated that turbulent kinetic energy inputs from the wind and convection can mix the water column. TKE_{wind} peaked at the same time as ΔDO converged during OFFA (Figures 5.2 and 5.12, whereas during OFFB, both TKE_{wind} and TKE_{conv} increased over the shutdown but ΔDO increased, indicating that inputs from wind-driven and convective mixing are not always sufficient to overcome dissolved oxygen gradients at B1. Although after the mixers were turned back on in August (ON2B), ΔDO at B1 decreased rapidly (Figure 5.13), which could in part have been helped by the higher TKE_{wind} and TKE_{conv} inputs at the time (Figure 5.2). During OFFB, DO near the bottom of the water column declined significantly, which is partly due to the mixer shutdown reducing transport of DO from the surface waters downwards, but also a result of high oxygen consumption in the bottom waters. At Lake Elsinore, Lawson and Anderson (2007) observed greater DO gradients through the summer despite mixer operation and high sediment oxygen demand (SOD) from increased organic matter remineralisation. Although there are no direct measurements of SOD in Durleigh, the high algal biomass and history of high nutrient loading (Chapter 3; Fallon and Brock, 1979; Beutel, 2003; Environment Agency, 2016) suggest that SOD is probably high, and therefore contributed to the significant decrease in DO near the sediments at B1 during OFFB. Wetzel (2001) highlights that oxygen deficits near the sediments are: positively correlated with phytoplankton productivity; inversely proportional to Secchi disk depth; higher oxygen deficit with higher phosphorus concentrations; and higher deficits with warmer temperatures promoting bacterial metabolic processes. At Durleigh, phytoplankton biomass was high, Secchi disk depth was low, historically phosphorus loading has been high, and mixer operation locally increased near sediment water temperatures.

Therefore, oxygen depletion in Durleigh is likely high. Additionally, the increased DO and currents near the sediments as a result of mixer operation are likely to have increased SOD by increasing diffusion across a smaller diffusive boundary (Beutel, 2003; Valipour et al., 2017). There was no significant decrease in DO near the sediments at L2 and L3 during OFFA and OFFB, and DO was generally lower at these locations, which further suggests that mixer operation is only effective locally. Mixer operation significantly affects the distribution of DO through the water column locally, but at distances > 20 m from the mixers, their effects are indistinct.

5.5.3 Water Velocities

High water velocities generated by surface mixers can lead to localised circulation cells forming around the mixers, but if water velocities are too low, the desired effects of mixing will not be achieved (Punnett, 1991). At Lake Elsinore, Lawson and Anderson (2007) observed vertical velocities of 0.3 m s^{-1} adjacent to the mixers (although 0.72 m s^{-1} is the assumed initial flow velocity) and these high velocities were acknowledged as the cause of localised circulation cells (24 m radius) around the mixers. Horizontal velocities ranged between 0.1 and 0.2 m s^{-1} up to 20 m from the mixers in Lake Elsinore, and ~ 0.02 m s^{-1} beyond 20 m (Lawson and Anderson, 2007). Comparably, each mixer at Durleigh has an initial flow velocity of 0.15 m s^{-1}, which is only half that of the observed mixer velocities in Lake Elsinore, and StreamPro ADCP measurements showed no discernible differences in horizontal and vertical velocities 15 m from the mixers when they were on and off. Generally, ADCP measurements showed horizontal velocities < 0.05 m s^{-1} and vertical velocities < 0.02 m s^{-1} (15 – 55 m from the mixers; Figures 5.13 – 5.16) at Durleigh when the mixers were on/off. However, the uncertainties associated with the ADCP measurements make drawing conclusions from these data difficult (Lee et al., 2014). On the other hand, the ADV data showed a significant decrease in horizontal velocities ~ 30 m north of the mixers during ADV_OFFB. Although velocities again were generally below 0.05 m s^{-1}, the high resolution, single-point ADV data indicates that mixers still influence near sediment water velocities ~ 30 m to the north, which was not picked up in the ADCP measurements. Taking a conservative estimate of the mixers being effective over a 30 m radius area in August 2018, when capacity was ~ 450 ML (surface area 84000 m^2), we suggest that the minimum area over which the mixers were effective was 3.4% of the total surface area of the reservoir.

Additionally, ADV amplitude data from Durleigh showed that the concentration of suspended particles in the water column decreased significantly during ADV_OFFB, which suggests that the mixers may be responsible for increasing sediment resuspension. Sediment resuspension is problematic for water quality due to increased turbidity, and potential release of metals and nutrients from the sediment pore water into the water column (You et al., 2007; Matisoff et al., 2017). The depth of the water column varies significantly over a season in drinking water reservoirs due to abstraction (draw down), inflows, and evaporation, and shallower water levels further increases the risk of sediment resuspension (Effler and Matthews, 2007). Lawson and Anderson (2007) observed scouring of the bed directly beneath the axial flow pumps in Lake Elsinore. However, surface mixers were deemed successful in a case study reported by Wagner (2015), where a deflection plate was fitted directly beneath the mixers to reduce sediment resuspension. At Durleigh, the decrease in amplitude during ADV_OFFB occurred overnight (Figure 5.15), coinciding with a drop in wind speeds (Figure 5.14a). The decline in suspended particles during ADV_OFFB was likely due to a combination of the mixers being turned off and reduced meteorological forcing. However, an aerial photograph (Figure 3.5, Chapter 3) shows localised sediment plumes formed at the surface from mixer operation, indicating that the mixers do cause sediment resuspension. Another potential contribution to sediment resuspension is bioturbation from the benthic feeding fish, of which there are many at Durleigh (Appendix 1; Barton et al., 2000). Although likely to contribute to sediment resuspension to some extent, bioturbation from fish is more likely to be sporadic and would not reflect an obvious decrease when the mixers were turned off during ADV_OFFB. The effects of mixer operation on sediment resuspension ~30 m north of the mixers is likely caused by a combination of wind-induced mixing and mixer operation, but immediately adjacent to the mixers (Figure 3.5, Chapter 3), mixer operation increases sediment resuspension. To reduce localised sediment resuspension when the mixers are operating, installing a deflection plate, reducing mixer flow rate, or varying the mixer flow rate according to water level could be trialled to see if resuspension decreases.

5.5.4 TKE Inputs and Meteorological Effects

Field observations show that at 20 m from the mixers, temperature and DO concentrations are influenced by mixer operation, but similar effects are not observed at 60 m away. In addition, ADV measurements show significant changes in near-bed

velocities ~ 30 m away from the mixers when they are turned off/on. Therefore, we suggest that mixers are not effective over the entire surface area of the lake. The u*: w* ratio over the study period showed that generally convection was the larger source of TKE into the reservoir, with many values < 0.75 (Figure 5.3), which is in line with observations by Read et al. (2012) who suggested that convective mixing is more likely to dominate in lakes with smaller areas.

One aim of this study was to determine the range of influence of the mixers (the area over which mixer effects are beneficial) and using the results from the field observations (temperature, DO, ADV) it was apparent that the mixers were effective over a radius of 30 m but their effects over 60 m were not obviously discernible from meteorological effects. Therefore, the range of influence of the mixers is considered to cover an area with a radius ranging between 30 – 60 m. When Durleigh is at full capacity, the area of influence ranges between 0.86% and 3.43% of the total surface area or the reservoir. During OFFB, when the depth of the water column was 2 m below full capacity, the area of influence of the mixers ranged between 9% and 34%. Consequently, when the water depth in the reservoir decreases, the mixers influence a greater percentage of the total surface area.

The TKE_{mix} input was 1.67 W m^{-2} calculated over the area of the mixer in eqn. 7. The TKE_{mix} of one mixer at Durleigh is 1.67 W m^{-2}, compared to 195.3 W m^{-2} for one pump from Lake Elsinore (Lawson and Anderson, 2007), calculated using A_0 (equation 7) as the area of the pump. Therefore, the TKE_{mix} of each pump at Lake Elsinore is over 116 times than the TKE_{mix} of one mixer at Durleigh. Despite the greater inputs of energy from the pumps in Lake Elsinore, mixing was still found to be limited.

Using the range of influence of the mixers from the field observations (30 – 60 m radius) as A_0 in the TKE_{mix} calculation gives 2.7 x 10^{-3} W m^{-2} and 6.6 x 10^{-4} W m^{-2} for an area with a 30 m and 60 m radius, respectively. Generally, TKE_{mix} over the maximum estimated area of influence (60 m radius) was greater than the combined inputs of TKE_{wind} and TKE_{conv} indicating that the continuous TKE input from the mixers is always greater than natural inputs over the localised area of influence.

5.5.5 Light Penetration and Phytoplankton Distribution

Profiles of Turbulent diffusivity (Figure 5.7) were similar across all sites and it is possible that the higher wind speeds at the time of sampling may have made it difficult to discern the effects of the mixers from natural mixing processes. However, the

turbulence profiles demonstrate that wind-driven mixing is likely to be sufficient to mix phytoplankton cells through the water column at all locations in Durleigh but the variable nature of wind-driven mixing means that mixing is unlikely to be continuous. On the other hand, the continuous input of energy from the mixers is likely to keep phytoplankton cells passively mixed through the water column over the area that they influence.

Generally, for particles the size of phytoplankton cells, Holland (2010) suggests that vertical velocities of species (0-100 μm s^{-1}) are easily overcome by turbulence and currents. In addition, Huisman et al. (2004) demonstrated that a significant increase in turbulent diffusivity as a result of artificial mixing with air curtains resulted in a shift away from a *Microcystis*-dominated assemblage to a greens/diatoms-dominated phytoplankton community. Turbulent diffusivities at Durleigh were estimated from temperature microstructure profiles and ranged between 10^{-5} and 10^{-3} m^2 s^{-1} (Figure 5.6), which is within a similar range observed by Huisman et al. (2004) when artificial mixing was operational. Walsby and Holland (2006) observed the average sinking velocity of *Planktothrix rubescens* to be 6.21 μm s^{-1}, suggesting that vertical velocities of *Planktothrix* and other cyanobacteria at Durleigh are likely to be easily overwhelmed by the artificial mixing in the reservoir. Additionally, the Peclet number calculated for *Planktothrix* at Durleigh using the turbulent diffusivities and vertical velocities (Walsby and Holland, 2006) stated is 0.037, further demonstrating that turbulent mixing dominates. Therefore, within the range of influence of the mixers, artificial circulation supplements natural mixing mechanisms and together mixing dictates the distribution of phytoplankton cells and filaments through the water column.

Shallow eutrophic reservoirs are typically more turbid, which favours shallower temperature stratification as a larger proportion of solar radiation is absorbed near the water surface (Condie and Webster, 2002; Stepanenko et al., 2013). At Durleigh, turbidity is high and light penetration is low throughout the reservoir with no obvious differences near the mixers (Table 5.2). A large proportion of surface solar radiation was reflected/scattered/absorbed within the top 0.5 m of the water column in 2018, and likely contributed to the diurnal temperature trends observed at L2 and L3 during ON2A (Figure 5.8). Shallow temperature stratification can be sufficient to suppress the depth of penetration of wind-driven mixing (MacIntyre and Melack, 1995). For example, during ON2B, ΔT at L3 was significantly higher than B1 and L2 (Table 5.6).

Rates of dissipation observed at Durleigh were similar to those reported by MacIntyre (1993) that were sufficient to mix phytoplankton in a shallow, eutrophic lake, and expose cells to continuously changing irradiance. Generally, phytoplankton and subsequently cyanobacteria cell distribution is likely combined by a combination of natural and artificial mixing processes. With wind-driven and convective mixing dictating distribution outside of the range of influence of the mixers, resulting in variable levels of mixing dependent on the natural inputs, compared to continuous mixing through the within the range of influence of the mixer that we assume locally circulate the water over a limited area around the mixers. The effect of mixers on cyanobacteria distribution and productivity in a shallow, eutrophic reservoir is explored in more detail in Chapter 6.

5.6 Conclusions

Surface mixer operation at Durleigh appears to be highly localised, but artificial circulation over the localised area is effective at significantly reducing temperature and oxygen gradients. The effects of surface mixer operation on phytoplankton cell distribution was considered for the first time. The turbulent diffusivities observed at Durleigh ranged between 10^{-5} and 10^{-3} m^2 s^{-1}, which were considered sufficient to overwhelm vertical velocities of phytoplankton cells and dictate the transport of cells through the water column, indicating that wind-driven mixing can be sufficient to mix phytoplankton cells through the water column. However, the continual operation of the mixers ensures that within the range of influence, phytoplankton cells are continuously mixed through the water column, which may have implications for productivity and community assemblage and will be discussed further in Chapter 6. Although no exact range of influence was defined, based on temperature and dissolved oxygen observations, it is suggested that surface mixers at Durleigh influence an area over at least a 30 m radius. At ~ 30 m north of the mixers, near-bed water velocities and sediment resuspension significantly decreased during ADV_OFFB, indicating that the mixer may influence water velocities and sediment resuspension at these distances. However, velocities were small, and the effect of the mixers could not be discerned from the effect of naturally induced mixing. Although mixers provide a continuous input of turbulent kinetic energy into the water column at greater magnitudes than wind or convective inputs, they are not effective over the entire surface area of the reservoir and are only likely improve water quality within a localised area. Consequently, to

improve the spatial influence of surface mixers it is suggested that consideration of mixer flow rates and the number and spatial distribution of mixers is required. For water quality purposes, flow rates of mixers in shallow reservoirs should be designed to minimise sediment resuspension but large enough that the plume penetrates to the sediments for oxygen transport. Using a variable flow rate reduces problems when water depth decreases due to abstraction and lower inflows over the summer is desirable. In addition, the installation of a deflection plate directly beneath a mixer in a shallow reservoir may be a more suitable solution in to minimise sediment resuspension while permitting higher flow rates.

CHAPTER 6

THE EFFECTS OF SURFACE MIXERS ON CYANOBACTERIAL PRODUCTIVITY AND MANGANESE CONCENTRATIONS IN A SHALLOW, HYPEREUTROPHIC RESERVOIR

6.1 Introduction

Chapter 2, Section 2.2.2 highlights that the principal aim of artificial circulation with surface mixers is to light-limit phytoplankton to suppress photosynthesis and reduce growth rates. However, in a shallow, hypereutrophic reservoir, light-limitation may not be effective and high biomass does not correlate with T&O metabolite production over time, although the potential for production increases. Therefore, in this chapter, the effects of surface mixers in a shallow, hypereutrophic reservoir will be assessed to determine whether light-limitation of cyanobacteria to reduce biomass is achieved, and if so, influences the production of T&O metabolites (Objectives 3 and 4, Chapter 1).

In addition, Sections 2.2.1 and 2.2.3 (Chapter 2) discussed how the advective transport of DO through the water column by artificial circulation should improve raw water quality, but suggested that for a shallow reservoir, achieving water quality benefits without disturbing the sediments would be difficult. Consequently, this chapter will also discuss whether the advective transport of DO through artificial circulation is sufficient to minimise internal loading of nutrients and metals from the sediments (Chapter 2, Section 2.2.3) with consideration for the management of cyanobacteria and reduction of soluble manganese concentrations at the intake (Objective 1).

6.2 Methods

The measurement campaign and description of Durleigh reservoir are described in detail in Sections 3.3 and 3.2.1 (Chapter 3), respectively. Historical data (between 2010 and 2019) from the intake was provided by Wessex Water and is presented in this chapter (Section 3.4.8, Chapter 3). Table 6.1 outlines the parameters measured and presented in this chapter and refers to the appropriate sections in Chapter 3 where a detailed methodology can be found.

Prior to statistical analysis, autocorrelation (‘autocorr’ function in MATLAB) was employed to determine the appropriate averaging interval of the time series data to ensure that points in the time series were independent of one another and minimise the uncertainty in the statistical analysis. For cyanobacterial cell counts and taste and odour compounds, seasonal averaging showed no autocorrelation and therefore statistical

analysis was conducted on the seasonal average for these parameters. For nutrient, metal and weather time series data (intake and canal), yearly averaging demonstrated no autocorrelation and was used for the statistical analysis.

Statistical analysis was carried out on the raw historical intake, canal, and weather data using the PAST statistical software package (Hammer et al., 2001). Normality was assessed using the Shapiro-Wilk test. For parametric data, a t-test was used to assess whether a significant change in concentration/values had occurred following the installation of mixers at Durleigh. For non-parametric data, the Mann Whitney U-test was used. Correlations between intake and in-reservoir measurements were assessed using Kendall's tau in PAST. The Kruskal Wallis test and Dunn's post hoc test was used to analyse for significant differences between in-reservoir water samples collected during the 2018 measurement campaign.

Table 6.1 Parameters measured for in-reservoir water quality assessment at Durleigh in 2018. Reference to full methods found in relevant sections in Chapter 3.

Parameter	**Equipment Used in the field**	**Dates sampled**	**Method**
Light Penetration	Secchi Disk	Water sampling days	Chapter 3 Section 3.4.5
	HOBO Pendant Temperature/Light 8K Data Loggers (L2 only)	Permanently moored at 0.5, 1.5, and 2.5 m 30 May – 5 October 2018	Chapter 3 Section 3.4.5
Water Quality Profiles	YSI EXO3 sonde	Water sampling days	Chapter 3, Section 3.4.1
Total and Soluble Metals (Iron and Manganese)	Van Dorn water Sampler	Water sampling days	Chapter 3 Section 3.4.8
Phytoplankton cell counts	Van Dorn water Sampler	Water sampling days	Chapter 3 Section 3.4.8
Chlorophyll-*α*	Van Dorn water Sampler	Water sampling days	Chapter 3, section 3.4.8
Nutrient concentrations	Van Dorn water Sampler	Water sampling days	Chapter 3 Section 3.4.8
Geosmin and 2-MIB concentrations	Van Dorn water Sampler	Water sampling days. Between 20 and 24 August only surface and bottom of water column samples collected	Chapter 3 Section 3.4.8
Biochemical Oxygen Demand	Van Dorn water Sampler	Surface and bottom of B1 AM and PM of 21 – 23 August 2018	Chapter 3 Section 3.4.8.3
Weather	Delta T WS-GP1 Weather Station	Permanently installed 5 April – 5 October 2018	Chapter 3 Section 3.4.3

6.3 Results

6.3.1 Historical Data

In this section, historical water sample measurements from the Durleigh intake are presented for cyanobacteria, taste and odour, nutrients, and metal concentrations. Cyanobacteria cells counts are shown to have significantly increased since the installation of the surface mixers, but changes in taste and odour concentrations showed no significant change. Concentrations of soluble metals are also shown to have significantly decreased. Historical nutrient concentrations from the canal inflow and regional weather data are then analysed to consider whether other environmental variables may be responsible for these observed changes. However, Sections 6.3.1.3 and 6.3.1.4 demonstrate that nutrient concentrations from internal/external sources and weather conditions have not changed significantly since mixers were installed, indicating that the operation of surface mixers are the most probable cause of decreased soluble metal concentrations at the intake and significantly higher cyanobacterial biomass. Section 6.3.9 gives a summary of the results presented in this section.

6.3.1.1 Cyanobacteria cell counts and T&O metabolites

Since the installation of mixers at Durleigh, cyanobacterial cell counts have appeared to have increased (Figure 6.1). In addition, statistical analysis of seasonally averaged (months: MAM; JJA; SON; DJF) cell counts from the intake at Durleigh showed that since the mixers have been installed, cyanobacterial cell counts have significantly increased ($U = 90$; $n_1 = 21$, $n_2 = 16$; $p = 0.02$; Figure 6.1). The frequency of counts exceeding 1,000,000 cells ml^{-1} has increased since the mixers were installed (Figure 6.1), although the highest cyanobacterial cell count recorded was 3.54×10^6 cells ml^{-1}, on 10 July 2011 and has not been exceeded since. In the following sections we explore historical nutrient and weather data to determine whether the significant increase in cyanobacterial biomass is attributable to the installation of the mixers, or another environmental variable.

The significant increase in seasonally averaged cyanobacteria was largely attributed to a significant increase in seasonally averaged *Planktothrix* ($U = 99$; $n_1 = 21$, $n_2 = 16$; $p = 0.03$; Figure 6.2c). *Planktothrix* have appeared more frequently in counts since surface mixer installation at Durleigh, while *Dolichospermum* ($U = 122$) and *Aphanizomenon* ($U = 145$) showed no such increase in frequency ($p = 0.16$ and 0.49,

respectively; Figure 6.2a and b). Other cyanobacteria appear to have benefited from mixer installation, including *Aphanocapsa* and *Pseudanabaena* (data not shown), but contributed considerably less to the total cyanobacterial cell counts compared to *Planktothrix*, *Dolichospermum*, and *Aphanizomenon*. The increase in counts was principally due to a significant increase in *Planktothrix*, which agrees with observations by Reynolds et al. (1983) that artificial mixing benefits *Planktothrix agardhii* (formerly *Oscillatoria*). However, Durleigh was artificially mixed by an air curtain before the surface mixers were installed, so the change in mixing caused by surface mixer operation has benefited *Planktothrix* compared to the air curtain.

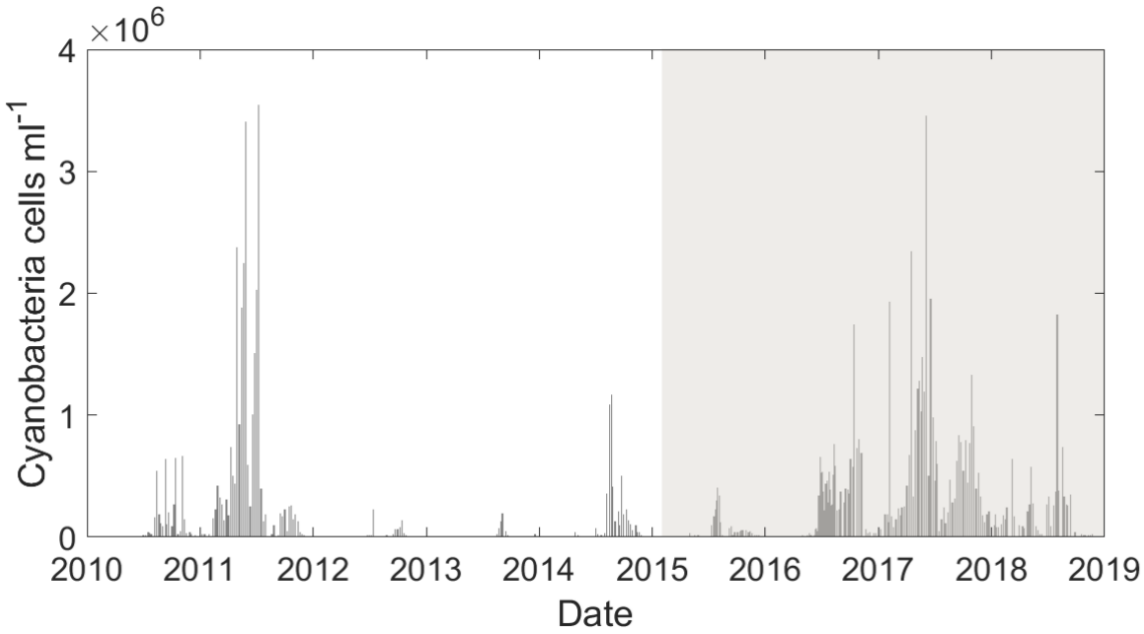

Figure 6.1. Cyanobacterial cell counts from the intake at Durleigh reservoir between 1 Jan 2010 and 1 Jan 2019. Grey shading indicates when the surface mixers were operating in the reservoir.

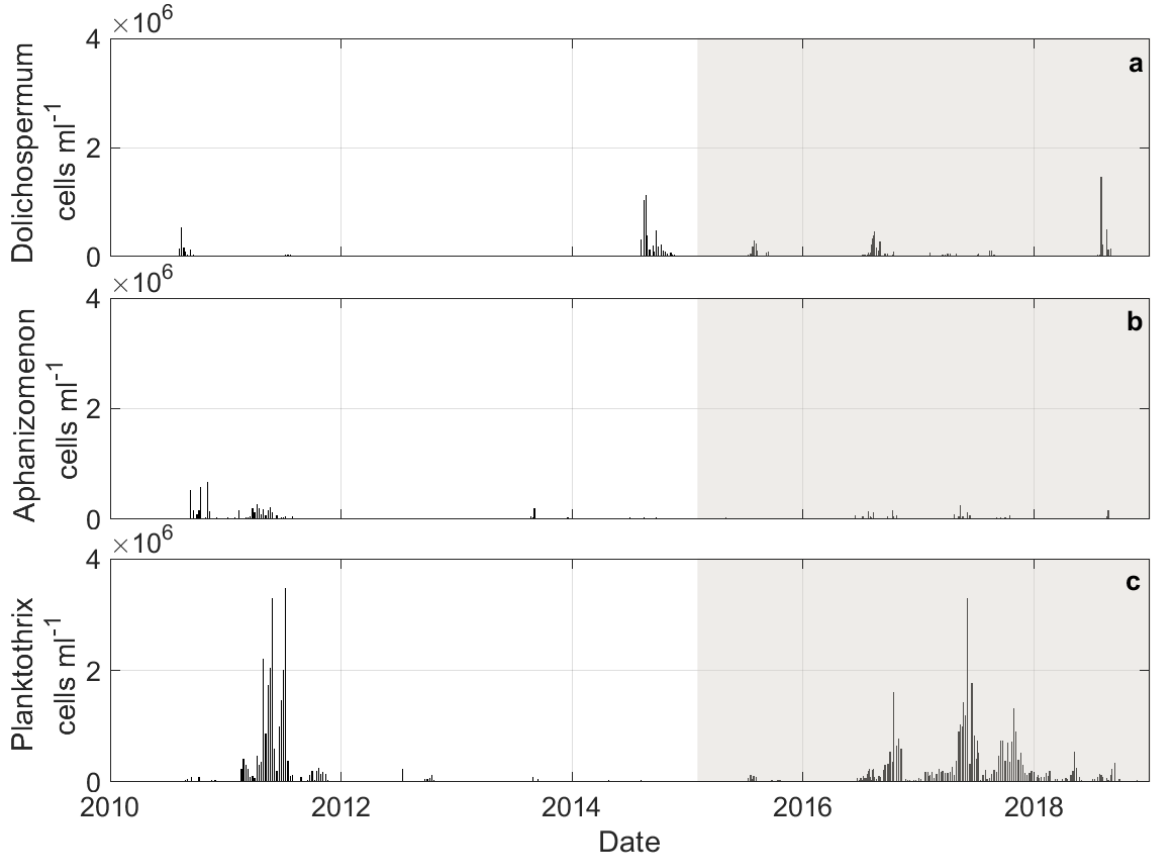

Figure 6.2. Cell counts of Dolichospermum (a), Aphanizomenon (b), and Planktothrix (c) from the intake at Durleigh reservoir between 1 Jan 2010 and 1 Jan 2019. Grey shading indicates when the surface mixers were installed in the reservoir.

Geosmin concentrations from water samples at the Durleigh intake peaked at >700 ng l^{-1} on 27 March 2011 (Figure 6.3a), preceding the peak in cyanobacterial biomass that year (Figure 6.1), which is consistent with findings presented in Chapter 4 that peaks in biomass do not always correlate with peaks in Geosmin concentrations over time. Seasonally averaged Geosmin concentrations have not changed significantly since the mixers were installed ($U = 134.5$; $n_1 = 21$, $n_2 = 16$; $p = 0.31$). Similarly, no significant difference was observed for 2-MIB concentrations ($U = 146$; $n_1 = 21$, $n_2 = 16$; $p = 0.50$, Figure 6.3b). Therefore, mixer operation at Durleigh does not appear to have increased taste and odour concentrations at the intake.

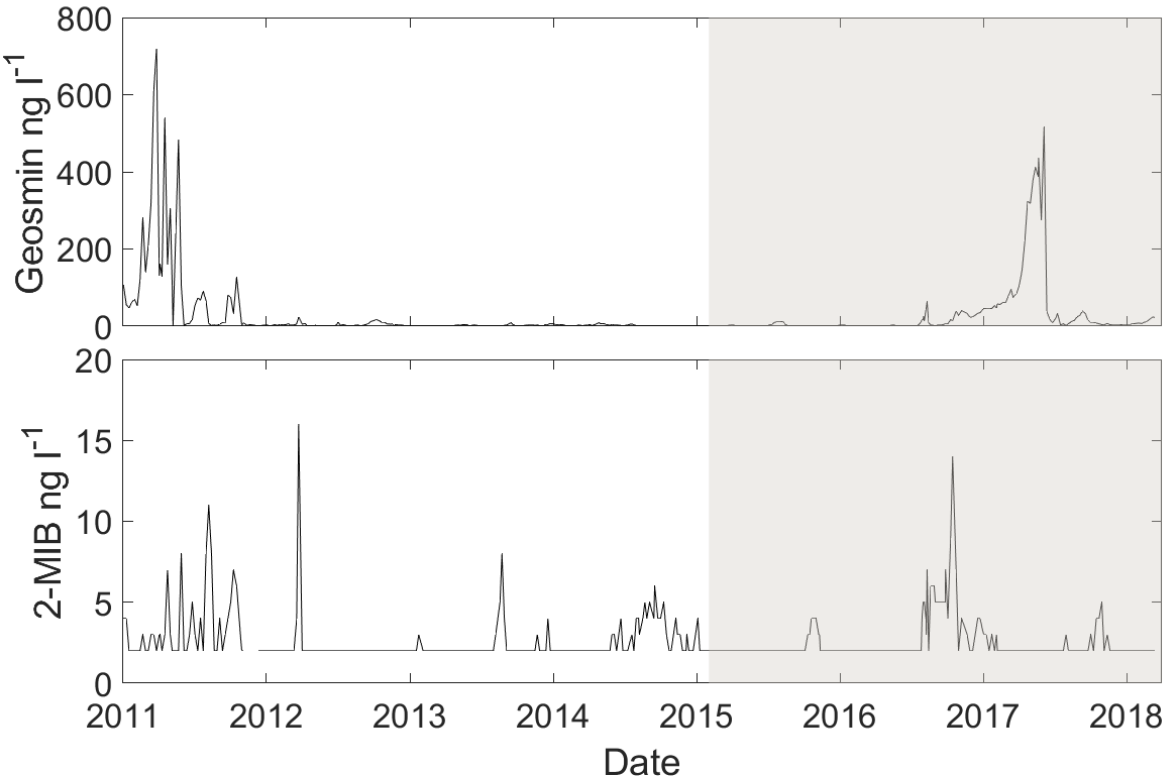

Figure 6.3. a) Geosmin concentrations and b) 2-MIB concentrations from the intake at Durleigh reservoir between 1 Jan 2011 and 23 Mar 2018. Grey shading indicates when the surface mixers were operating. The level of detection for 2-MIB concentrations was 1 ng l^{-1}.

6.3.1.2 Turbidity and metals

Statistical analysis of the annual averages before and after the mixers were installed at Durleigh showed no significant change in turbidity at the intake ($t_{(5)} = 2.55$, $p = 0.91$; Figure 6.4). The installation of mixers at Durleigh do not appeared to have affected the turbidity at the intake despite the increase in cyanobacterial biomass.

Annual averages of total iron ($t_{(5)} = 2.57$, $p = 0.35$; Figure 6.5a) and total manganese concentrations ($t_{(3)} = 3.18$, $p = 0.46$; Figure 6.5c) have not significantly changed at the intake since the mixers were operational. However, concentrations of both soluble manganese (Mn^{2+}; $t_{(6)} = 2.45$, $p = 0.03$; Figure 6.5d) and soluble iron (Fe^{2+}; $t_{(6)} = 2.45$; $p < 0.01$; Figure 6.5b) have significantly decreased at the intake following the installation of the mixers at Durleigh. During September 2018, the mixers were turned off for maintenance work of the silt curtain that caused a sediment disturbance near the intake. Consequently, soluble manganese concentrations peaked > 0.5 mg l^{-1} and constituted a large proportion of the total manganese measured at the intake (Figure

6.5). The installation of the mixers appear responsible for the significant decrease in soluble iron and manganese concentrations at the intake.

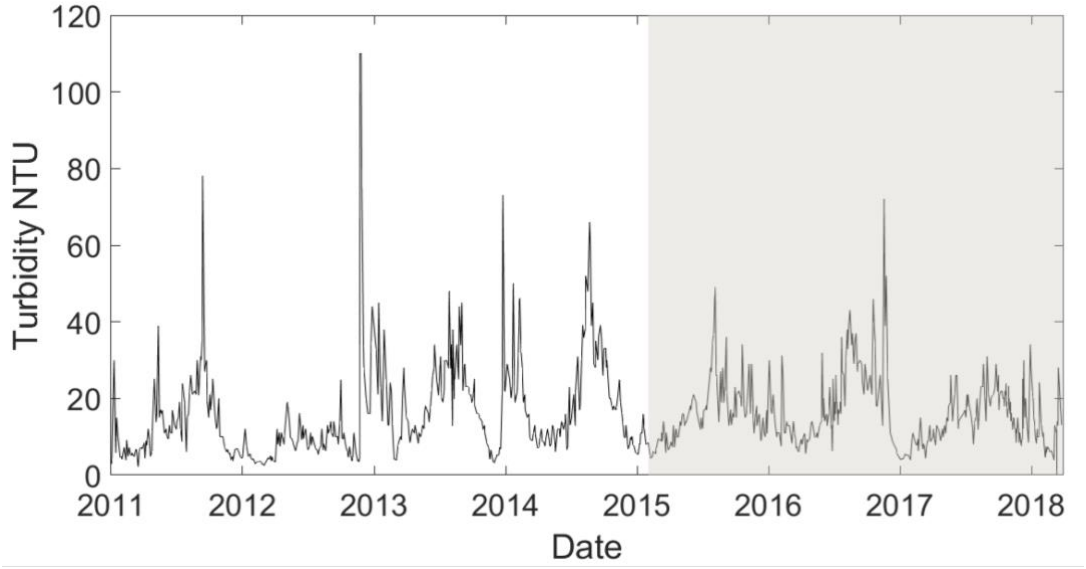

Figure 6.4. Turbidity from the intake at Durleigh between 1 Jan 2011 and 23 Mar 2019. Grey shading indicates when the mixers were installed.

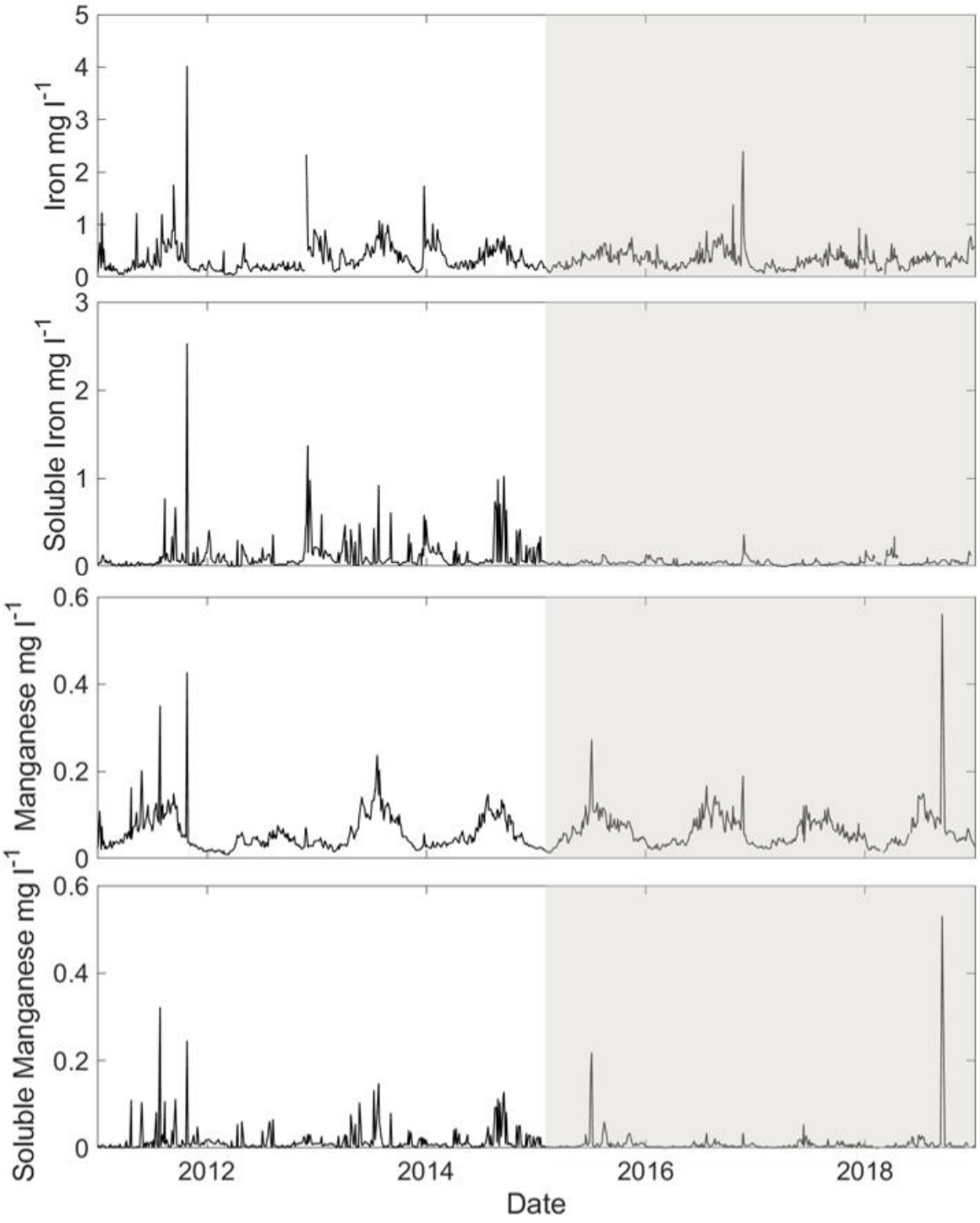

Figure 6.5. a) Total iron concentrations, b) soluble iron concentrations, c) total manganese concentrations, and d) soluble manganese (Mn^{2+}) concentrations from water samples collected at the Durleigh intake between 01/01/2011 and 01/01/2019. Grey shading indicates when the surface mixers were operational.

6.3.1.3 Nutrients

Historical nutrient data from the intake and canal inflow were analysed to determine whether changes in nutrient concentration may have caused the increase in cyanobacterial biomass observed. Statistical analysis of annual average concentrations of ammonium and total phosphorus (TP) at the Durleigh intake showed no significant difference after mixers were installed (ammonium: $t_{(6)} = 2.45$; $p = 0.59$; TP: $t_{(4)} = 2.77$; $p = 0.77$; Figure 6.6a and d). Annual average concentrations of nitrate and orthophosphate (OP) at the intake did not significantly change following the installation of mixers at Durleigh (nitrate: $t_{(5)} = 2.57$; $p = 0.73$; OP: $t_{(3)} = 3.18$; $p = 0.21$; Figure 6.6b and c).

Statistical analysis of annual average concentrations from the canal inflow showed no significant difference after surface mixer installation in concentrations of TOC ($t_{(4)} = 2.78$; $p = 0.67$; Figure 6.7c), TP ($t_{(3)} = 3.18$; $p = 0.4$; Figure 6.7e), OP ($t_{(5)} = 2.57$; $p = 0.47$; Figure 6.7d), and nitrate ($t_{(4)} = 2.78$; $p = 0.18$; Figure 6.7b). Annual average ammonium concentrations at the canal inflow decreased after 2015, but not significantly ($t_{(6)} = 2.45$; $p = 0.16$; Figure 6.7a). Generally, the historical nutrient data from the intake and canal at Durleigh suggests that no significant change in nutrient concentrations has occurred that could explain the significant increase in cyanobacterial biomass observed since the surface mixers were operational.

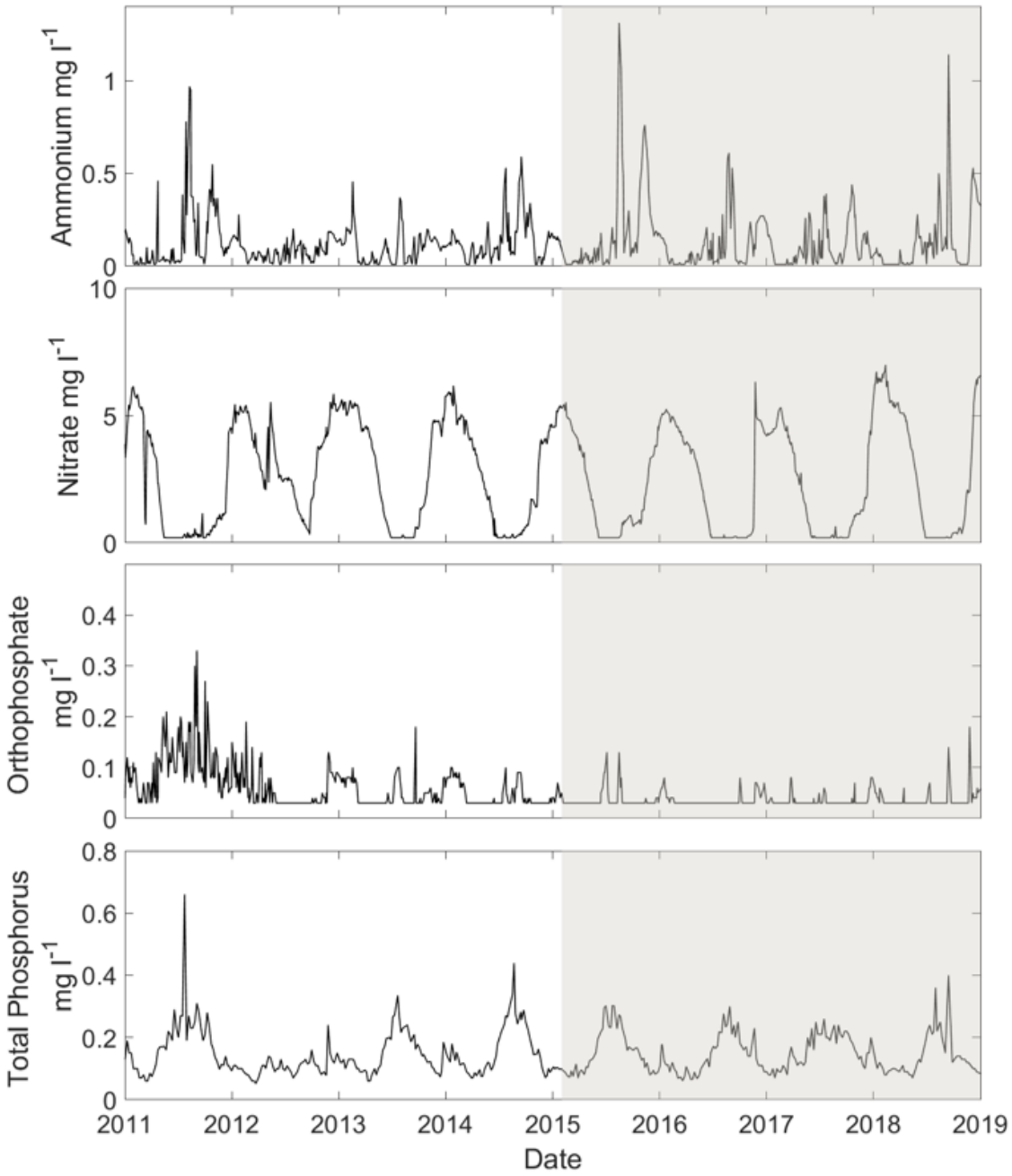

Figure 6.6. a) Ammonium concentrations, b) nitrate concentration, c) orthophosphate concentrations, and d) total phosphorus concentrations from water samples collected at the Durleigh intake between 1 Jan 2011 and 1 Jan 2019. Grey shading indicates when the mixers were operational.

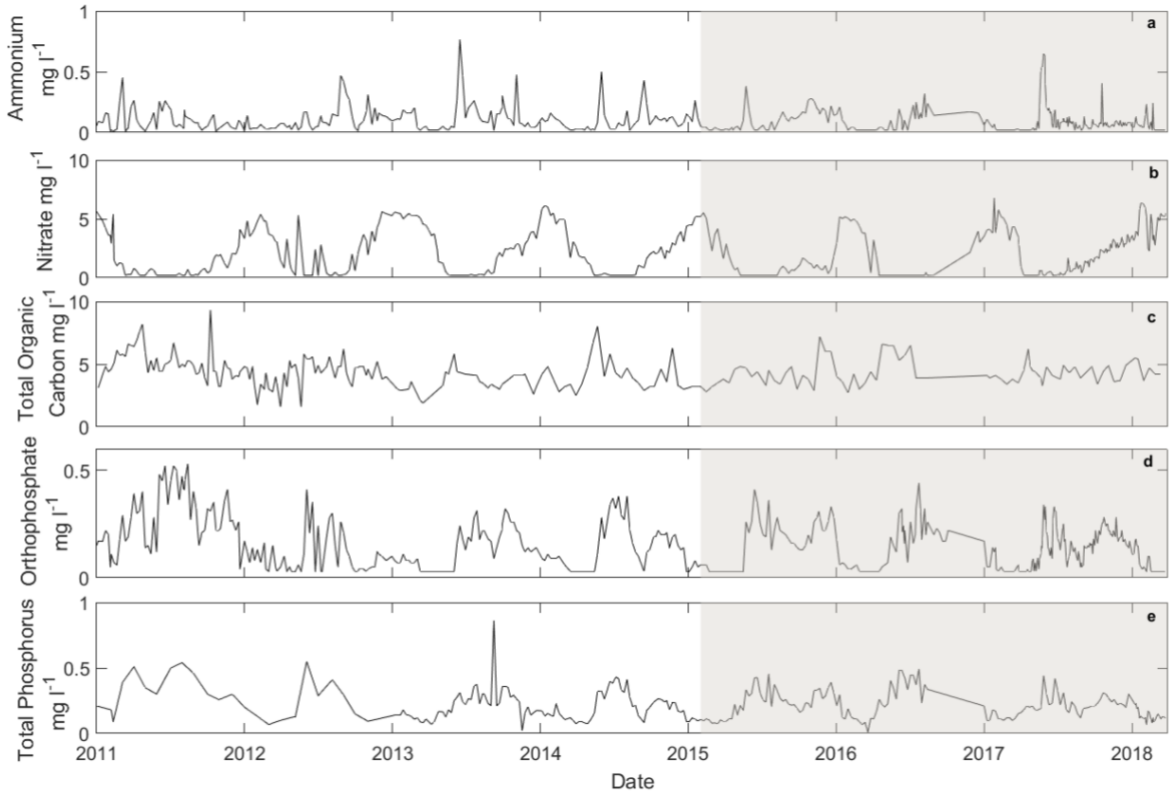

Figure 6.7. a) Ammonium, b) nitrate, c) total organic carbon, d) orthophosphate, and e) total phosphorus concentrations from water samples collected at the Durleigh canal inflow between 1 Jan 2011 and 1 Apr 2018. Grey shading indicates when the surface mixers were operational.

6.3.1.4 Weather and water temperature

Statistical analysis of the annually averaged water temperatures from samples taken at the Durleigh intake were not significantly different following the installation of the mixers ($t_{(6)} = 2.78$; $p = 0.24$; Figure 6.8a). Annually average water temperatures from samples taken at the canal inflow (Figure 6.8b) showed no significant difference since the mixers were installed ($t_{(4)} = 2.45$; $p = 0.16$), indicating that water temperatures are not attributable to the increase in cyanobacterial biomass observed.

Historical weather data were collected from a weather station situated 25 miles north west of Durleigh reservoir, which was the closest freely available historical weather station to the reservoir (Weather Underground, 2019). Generally, air temperatures followed a seasonal trend, while wind speeds and rainfall exhibited greater variability. Statistical analysis of annual average air temperatures showed no significant change between before and after the mixers were installed ($t_{(4)} = 2.78$; $p = 0.10$; Figure 6.9a). There was also no significant change in wind speeds ($t_{(4)} = 2.78$; $p = 0.18$; Figure 6.9c) or rainfall ($t_{(4)} = 2.78$; $p = 0.18$; Figure 6.9c).

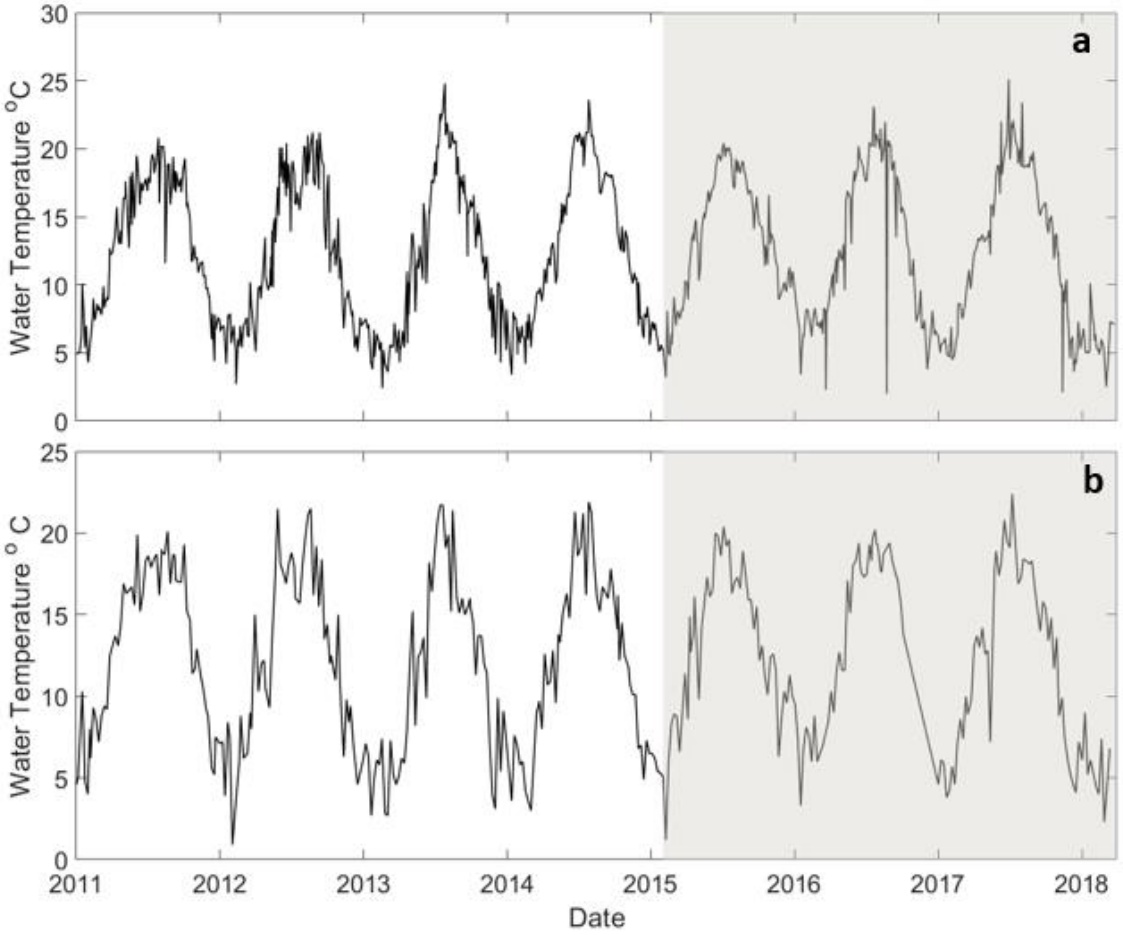

Figure 6.8. Water temperatures of samples collected from the a) Intake and b) canal inflow at Durleigh between 1 Jan 2011 and 1 Apr 2018. Grey shading indicates period mixers were operational.

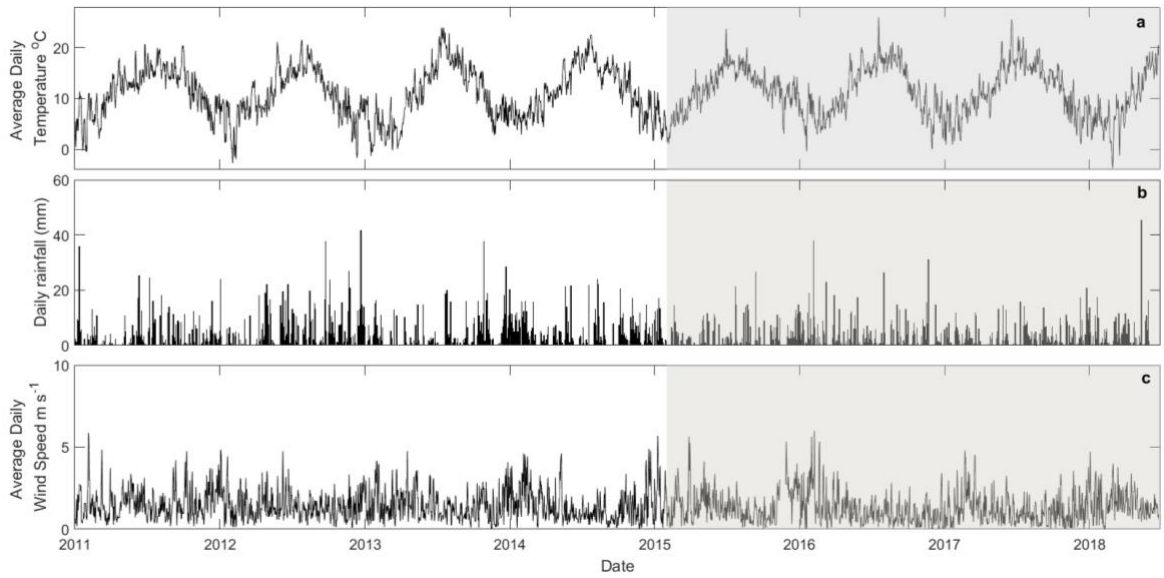

Figure 6.9. a) Daily average air temperatures, b) daily rainfall, and c) daily average wind speeds from a weather station in Somerset between Jan 2011 and Apr 2018. Weather station was located 25 miles north east of Durleigh. Data sourced from Weather Underground (2019).

6.3.2 Light Penetration

Light penetration through the water column in Durleigh is low. Secchi disk depths (Z_{SD}) varied temporally (between 0.2 - 0.7 m) through 2018 but were generally similar between sites on every sampling day (Figure 6.10). Therefore, the average Z_{eu} estimated from Z_{SD} ranged between 0.95 and 1.08 m over 2018 (Table 5.2; Section 5.4.3) and variation was greater temporally compared to spatially. Average Z_{eu} estimated from the SCAMP PAR sensor in 2015 was 1.55 m ± 0.1 m. In general, the Z_{eu} at Durleigh is estimated between the range of 0.74 – 1.74 m over the 2018 season based on both SCAMP PAR sensor data and estimates from Secchi disk measurements (Table 5.2; Section 5.4.3). Low light penetration measurements indicate that there was a high concentration of suspended particles near the surface at Durleigh.

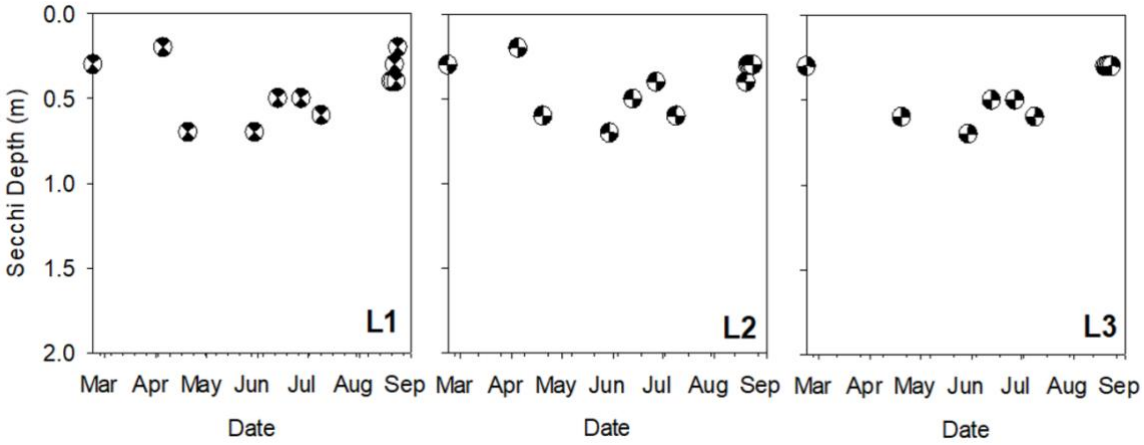

Figure 6.10. Secchi depths recorded on water sampling days at L1 (25 m from mixers), L2 (60 m), and L3 (435 m) through 2018.

Turbidity profiles taken with the EXO3 sonde show that turbidity was high and relatively uniform throughout the water column (data not shown). In addition, ADV data (Section 5.5.9, Chapter 5) and aerial photographs (Figure 3.5, Chapter 3) show that mixer operation increases sediment resuspension locally. Increased sediment resuspension can result in increased turbidity and decrease the depth of light penetration. As the Secchi disk depths are so low at Durleigh, any gradients between sites are likely masked by the accuracy of the measurements themselves, so it cannot be concluded whether light penetration at Durleigh is affected by mixer operation.

6.3.3 Nutrients

Ammonium concentrations in Durleigh were high in May and June 2018 at all 3 locations, although L1 appears to have the highest ammonium concentrations (Figure 6.11). The Kruskal Wallis and Dunn's post hoc test revealed no significant differences in ammonium concentrations between the surface (S), middle (M), and bottom (B) of the water column at each location. However, between locations, surface ammonium concentrations were found to be significantly higher at L1S compared to L3S (p = 0.02). The significant difference could be due to the large (0.4 mg l^{-1}) value reported at L1S on 21 August, there is no evidence suggesting that this value has been misreported. Intake ammonium concentrations during August 2018 (Figure 6.6a) ranged between 0.06 and 0.5 mg l^{-1}, so the value of 0.4 mg l^{-1} at L1S is feasible. In addition, 0.4 mg l^{-1} of ammonium was also recorded at L1M on 21 (AM) and 23 (PM) August, but no significant differences were found in ammonium concentrations between the three measurement locations either in the middle or bottom of the water column. Generally,

in-reservoir measurements suggest that ammonium concentrations varied more temporally than spatially and there were no obvious effects of the mixers.

Nitrate concentrations from in-reservoir measurements (data not shown) showed no significant difference between different depths at the same location, or between the same depth at different locations through 2018. Both in-reservoir measurements and measurements at the intake (Figure 6.6b) show a summer decline in nitrate concentrations, which is likely due to a combination of reduced external loading (reduced runoff), phytoplankton assimilation, and increased denitrification rates (Hill, 1988; David et al., 2006; Bednarek and Zalewski, 2007).

Concentrations of nitrite measured in Durleigh (Figure 6.12) and at the intake (Figure 6.13) follow similar temporal patterns, increasing through spring before a decline in mid-June and increasing again in mid-late August. In October, the in-reservoir nitrite concentrations were lower than concentrations at the intake. Accumulations of nitrite may occur due to varying rates of nitrification by ammonium-oxidising and nitrite-oxidising bacteria, which are dependent on multiple parameters including: dissolved oxygen concentrations, pH, temperature, and light (Wild et al., 1971; Balmelle et al., 1992). The photodegradation of dissolved organic matter has also been reported as a source of nitrite in natural waters (Kieber et al., 1999). There was a peak in nitrite of 0.116 mg l^{-1} at the intake on 14 September 2018 (Figure 6.13), which coincided with a peak in ammonium (Figure 6.6a) at the intake and an increase in ΔDO and ΔT (Chapter 5). These peaks occurred in the middle of a prolonged period of mixer shutdown, suggesting that without mixer operation distributing DO concentrations through the water column, anaerobic conditions developed, which promoted ammonification and decreased nitrification.

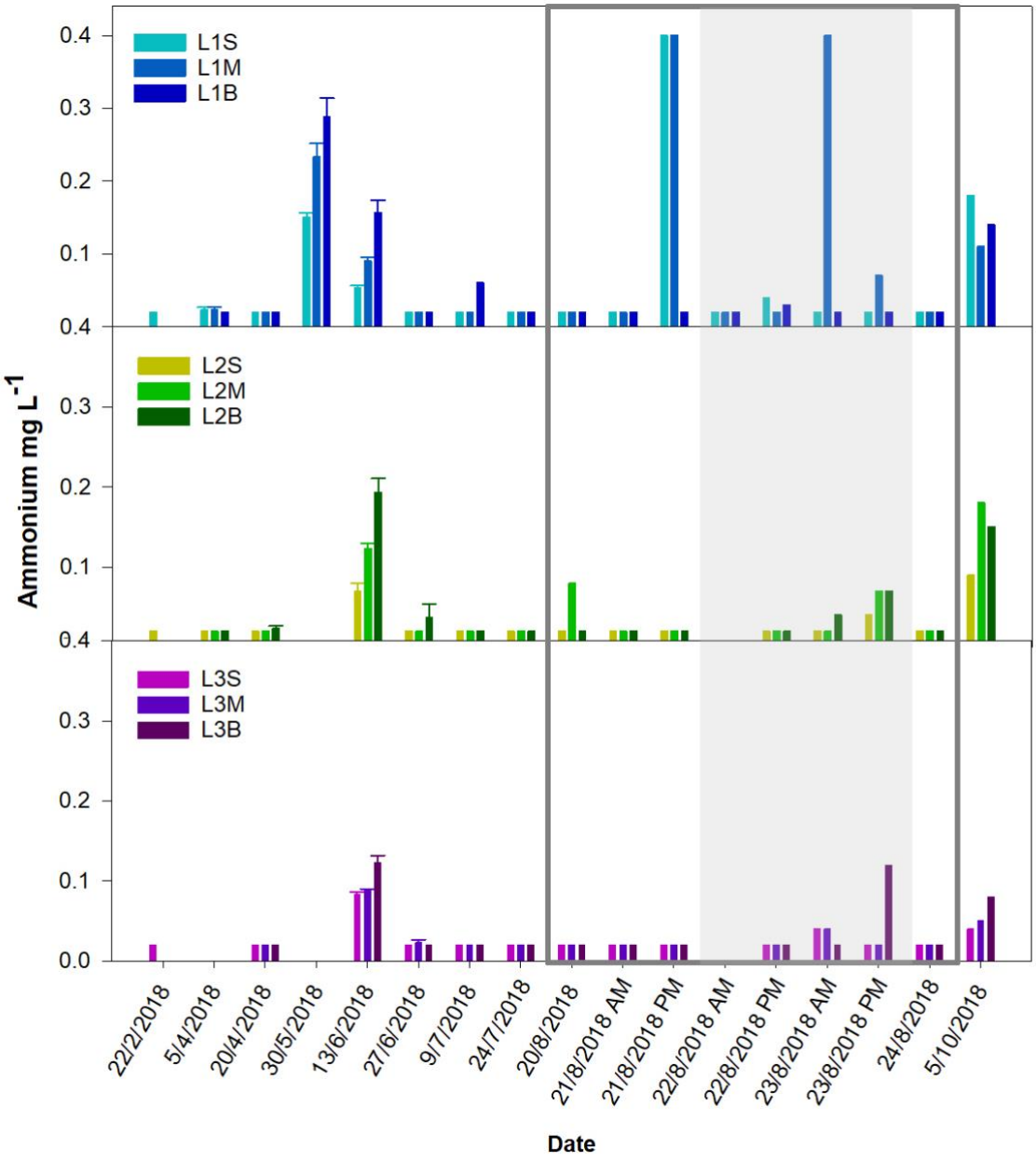

Figure 6.11. Ammonium concentrations from water samples taken at the surface (S), middle (M), and bottom (B) of the water column in Durleigh reservoir at L1, L2, and L3. Error bars for samples taken in triplicate between 5 Apr and 27 Jun 2018 are standard error. After 27 Jun 2018 triplicate samples were not collected due to Wessex Water laboratory demands. Grey box indicates August intensive field sampling and grey patch identifies the period the mixers were off.

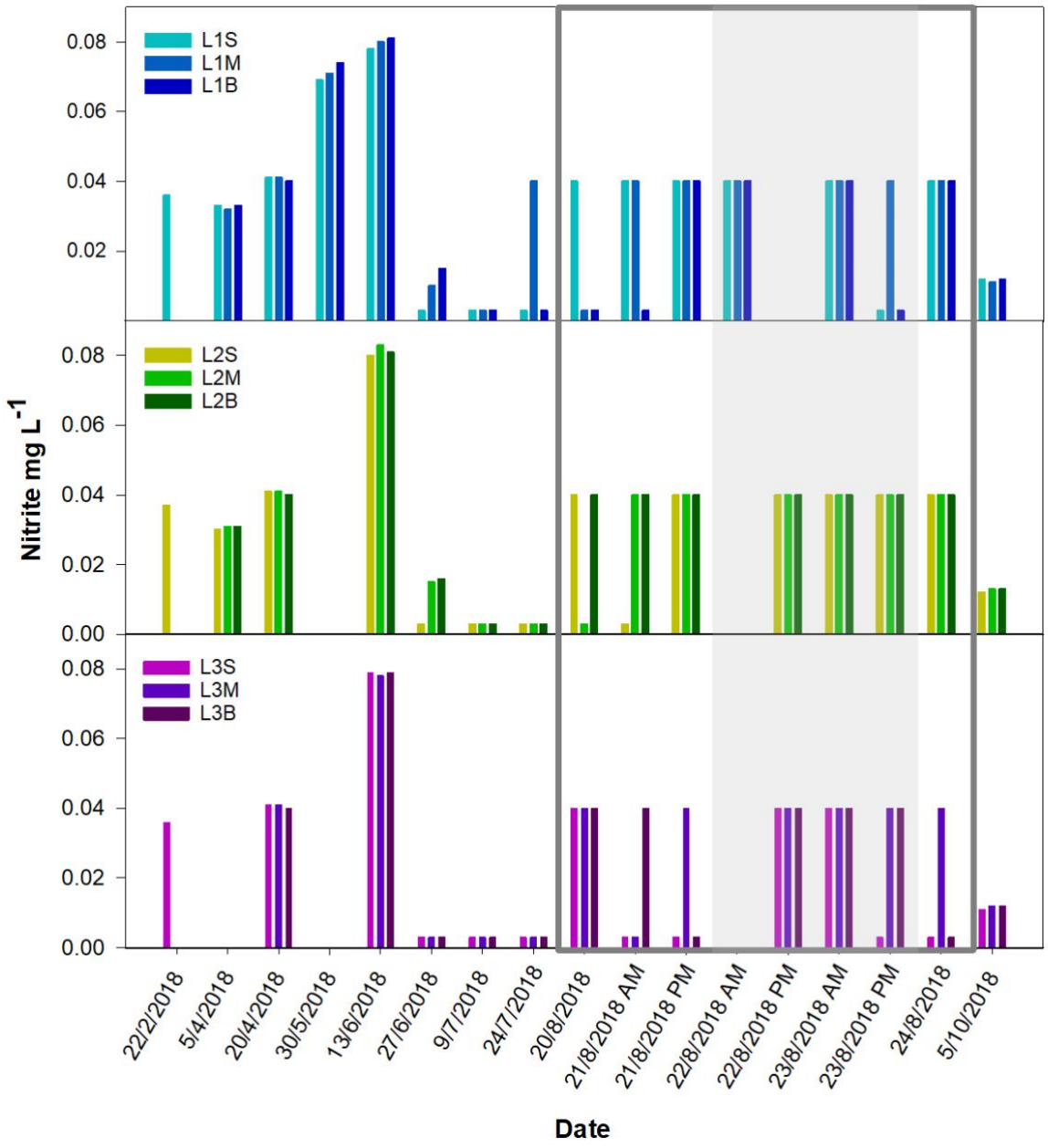

Figure 6.12. In-reservoir nitrite concentrations at L1, L2, and L3 on the water sampling days in 2018. Grey box indicates the more intensive August sampling and the grey shading highlights the period when the mixers were not operating.

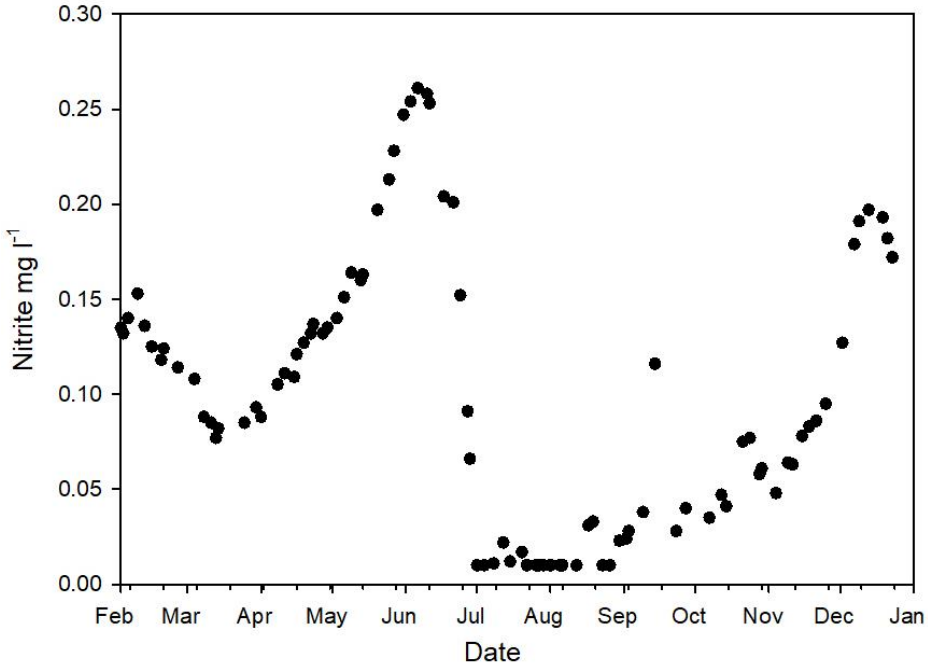

Figure 6.13. Nitrite concentration from the intake at Durleigh between 1 Feb 2018 and 1 Jan 2019.

Orthophosphate concentrations from in-reservoir measurements were at the level of detection (LOD; 0.03 mg l^{-1}) throughout 2018 (data not shown). Concentrations at the intake were also around the LOD through 2018 (Figure 6.6c), but peaked at 0.06, 0.07, and 0.14 mg l^{-1} on 14 April, 10 July, and 13 September, respectively. Total phosphorus (TP) concentrations increased during the summer and peaked at 0.36 mg l^{-1} on 1 August (Figure 6.6d). Another peak of 0.4 mg l^{-1} occurred on 14 September, during the mixer shutdown and sediment disturbance event (when silt curtain anchors were moved), suggesting that TP concentrations in the sediments could lead to internal loading of phosphorus during sediment resuspension events. However, with the existing TP data, robust conclusions about phosphorus dynamics at Durleigh difficult to make.

6.3.4 Biochemical Oxygen Demand

Water samples collected from the surface and bottom of the water column at L1 were filtered and biochemical oxygen demand (BOD) was measured over the period the mixers were shut down in August 2018. Allyl thiourea (atu) was added to BOD samples to suppress nitrification during analysis (Chapter 3) and is subsequently reported at BOD(atu). No water samples were collected from L2 or L3 for BOD measurements, so we cannot comment on the spatial effect of the mixers on BOD at Durleigh. Overall, little difference was observed in BOD(atu) between samples from the surface and bottom of the water column. Usually, 5-day BOD in lakes and streams is around 1 – 2 mg O_2 l^{-1} (CH2M Hill, 2013). In Europe, freshwaters with BOD concentrations > 5 mg O_2 l^{-1} are considered poor quality (Vigiak et al., 2019). At Durleigh, 5-day BOD(atu) ranged between 7 – 10 mg O_2 l^{-1} (Figure 6.14), suggesting that there are high quantities of organic matter (OM) through the water column at L1. However, EXO3 water quality profiles (data not shown) at L1 in August showed that DO concentrations did not drop below 10 mg l^{-1} throughout the profiles, which suggests that the supply of oxygen was sufficient to meet demand. Nevertheless, differing rates of decomposition, microbial respiration, and differences in oxidant concentrations can affect the rate at which oxygen is consumed.

When the mixers were turned off in August, BOD(atu) showed no obvious changes (Figure 6.14). However, during OFFB, DO concentrations declined significantly near the sediments at B1 (Chapter 5), which could reflect the high biochemical oxidation of organic matter near the sediments consuming the available oxygen that is subsequently not replenished because the mixers are not operating. Durleigh is a hypereutrophic reservoir that frequently experiences high cyanobacterial biomass, so the contribution to OM content in the reservoir from settling of dead cyanobacterial cells is likely to be considerable, in addition to loading of OM from allochthonous sources.

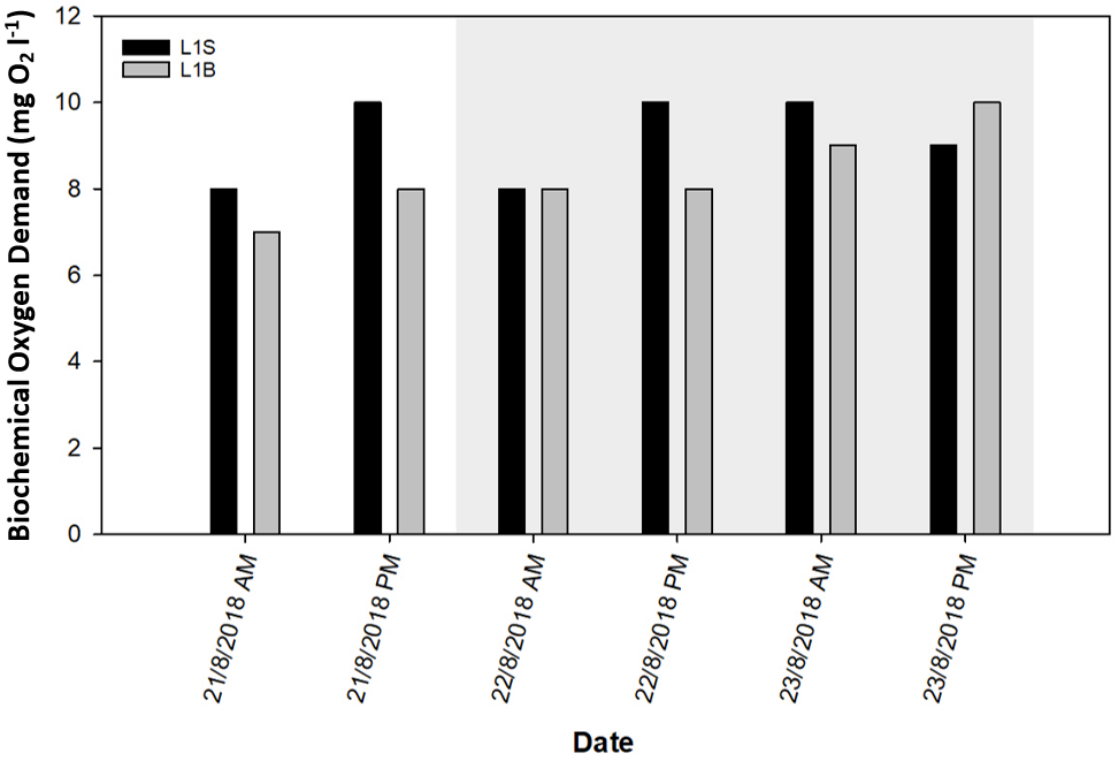

Figure 6.14. Biochemical Oxygen Demand (atu) measurements from the surface (S) and bottom (B) of the water column at Location 1 in Durleigh in the morning and afternoon of 21, 22, and 23 August 2018. Reported in mg O_2 l^{-1}. Grey patch indicates the period the mixers were not operating.

6.3.5 Metals

6.3.5.1. Total Manganese

During 2018, the bottom of the water column at all sites had significantly higher total manganese concentrations than the surface (L1: $p < 0.01$; L2: $p < 0.01$; L3: $p < 0.02$; Figure 6.15), and L2M had significantly lower total manganese concentrations than L2B ($p < 0.03$). The higher concentrations of total manganese at the bottom of the water column may be a consequence of sediment resuspension, which could explain why concentrations are generally higher at the bottom of the water column throughout Durleigh and particularly high near the mixers. Correlation using Kendall's tau between in-reservoir and intake total manganese concentrations revealed that L2M concentrations correlated most strongly with intake samples ($\tau_b = 0.89$, $p < 0.01$).

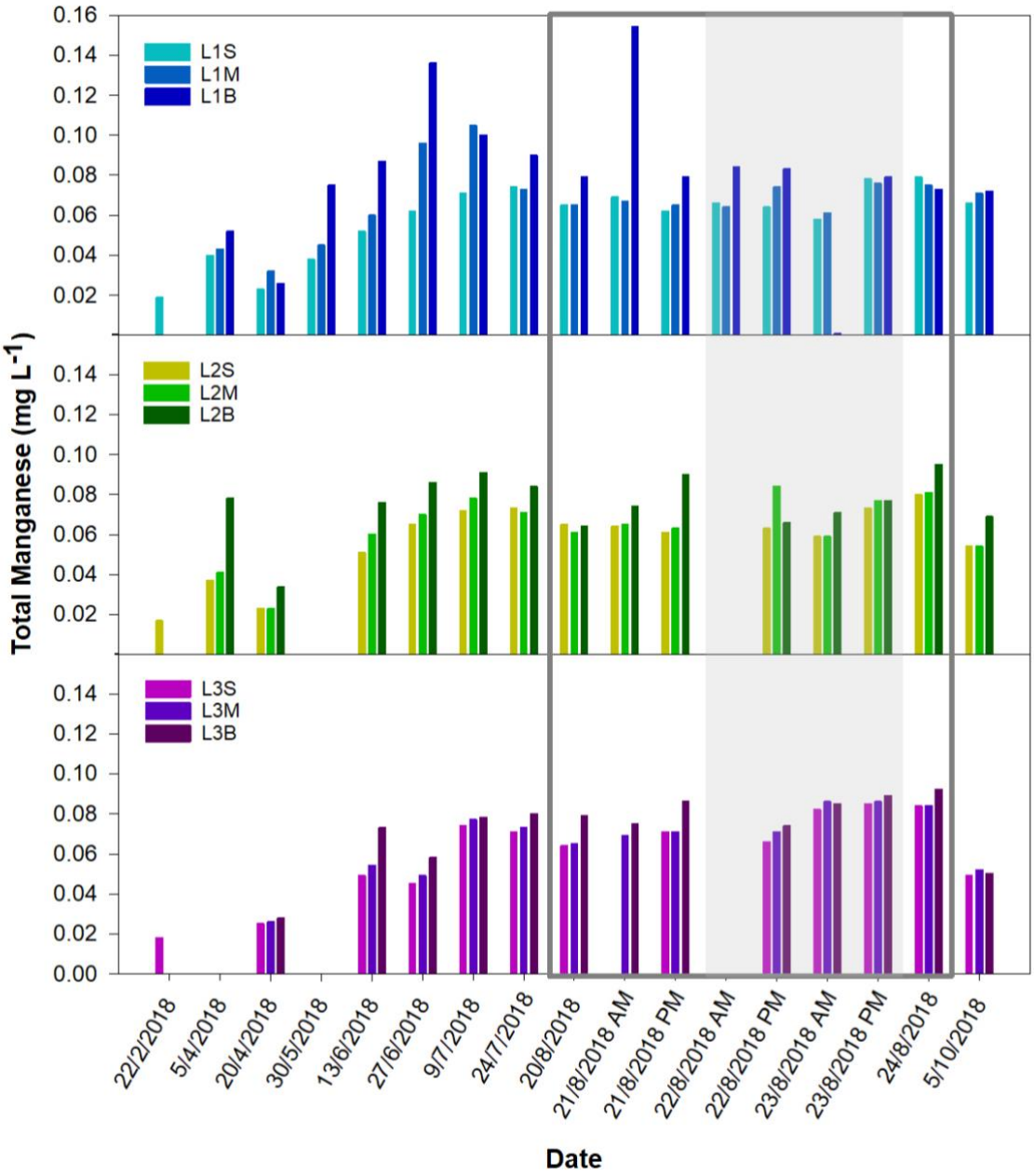

Figure 6.15. Total Manganese (MnO_2) concentrations from water samples taken at the surface (S), middle (M), and bottom (B) of the water column in Durleigh reservoir at L1, L2, and L3. Grey box indicates August intensive field sampling and grey patch identifies the period the mixers were off.

6.3.5.2 Soluble Manganese

Soluble manganese concentrations are high at L1 in May – early July (Figure 6.16), and generally higher at the bottom of the water column at all sites. The Kruskal Wallis and Dunn's post hoc test showed that surface and middle concentrations were significantly lower at all sites than bottom concentrations through 2018 (all $p < 0.05$). The proximity of L1 to the mixers (25 m) suggests that soluble manganese concentrations may be increased by mixer operation, with sediment resuspension resulting in higher concentrations near the bottom of the water column.

Historical data (Section 6.3.1) shows that total manganese concentrations have significantly increased at the intake since the mixers have been installed at Durleigh, but soluble manganese concentrations have significantly decreased (Figure 6.5d). Despite the decrease in soluble manganese at the intake, in-reservoir concentrations of both soluble and total manganese appear highest closest to the mixer (L1), and L1 concentrations correlate well with intake concentrations through 2018 ($\tau_b = 0.78$, $p < 0.01$).

L1 and L2 are similar in depth compared to the much shallower L3, but manganese concentrations (total and soluble) between L2 and L3 exhibit greater similarity than L1 and L2. The difference between L1 and L2 soluble manganese concentrations suggests that mixer operation locally increases soluble manganese. Observations in Chapter 5 suggest that the range of mixer influence is limited, and sediment resuspension occurs due to mixer operation, which may explain the higher concentrations of soluble and total manganese observed at L1 (Abesser and Robinson, 2010). Nevertheless, concentrations of soluble manganese at L1 are still lower compared to soluble manganese concentrations at the intake before the mixers were installed at Durleigh.

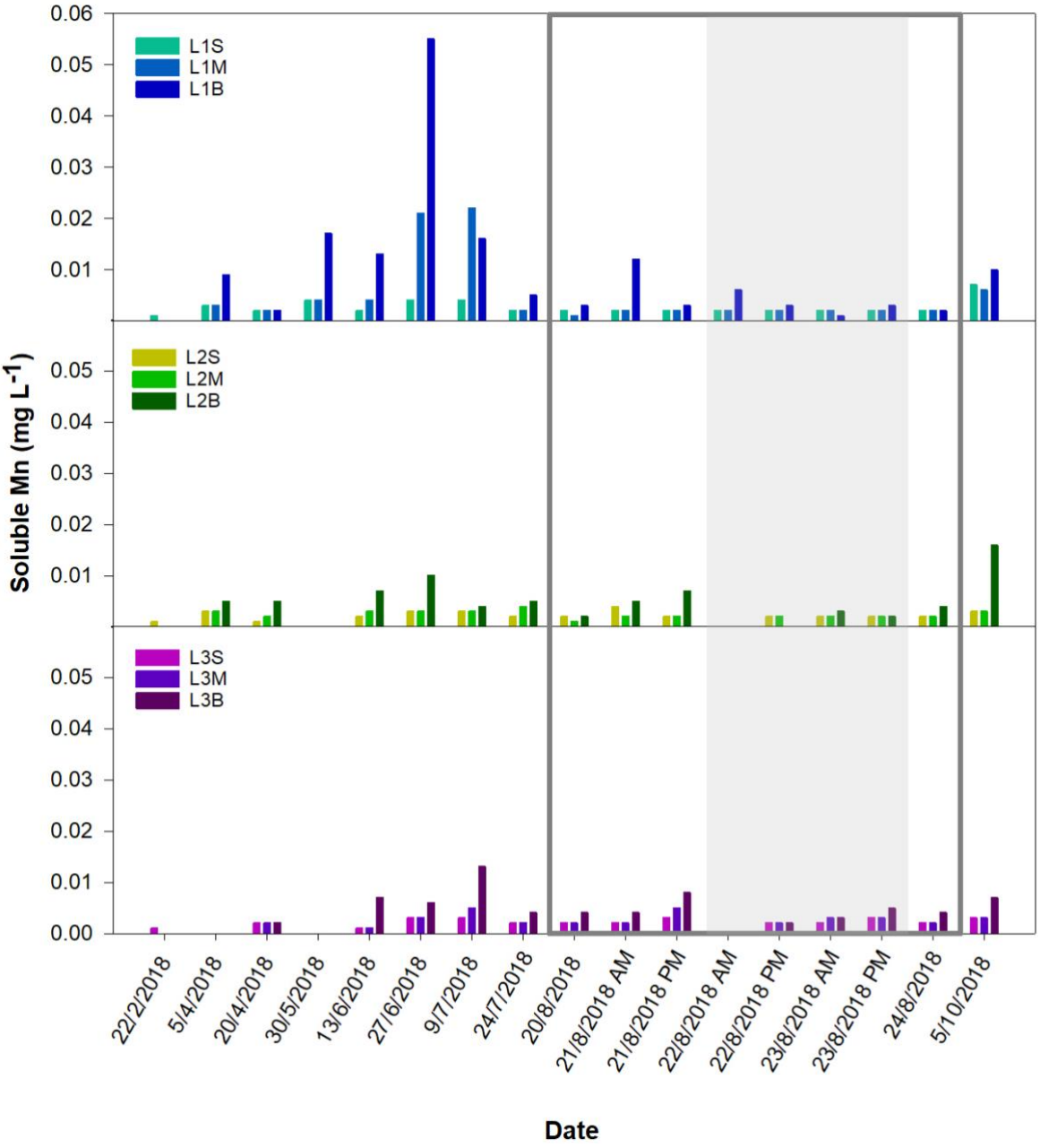

Figure 6.16. Soluble Manganese (Mn^{2+}) concentrations from water samples taken at the surface (S), middle (M), and bottom (B) of the water column in Durleigh reservoir at L1, L2, and L3. Samples for L2 and L3 on 22/08/18 AM and L2B on 22/08/18 PM were lost. Grey box indicates August intensive field sampling and grey patch identifies the period the mixers were off.

6.3.5.3 Iron

Total iron concentrations were typically highest at the bottom of the water column at all sites through 2018 (Figure 6.17), whereas soluble iron concentrations were more uniformly distributed through the water column but varied temporally (Figure 6.18). However, no statistically significant differences were observed in total or soluble iron concentrations both between different locations and between different depths at the same location. In-reservoir concentrations were similar to intake concentrations throughout 2018 for both total and soluble iron (Figure 6.6a and b). Compared to total and soluble manganese concentrations, there are no obvious spatial differences from the in-reservoir measurements. However, oxidation rates of manganese are considerably slower than those of iron (Martin, 2005), which could explain why higher concentrations of soluble manganese are observed at L1 but not elevated concentrations of iron.

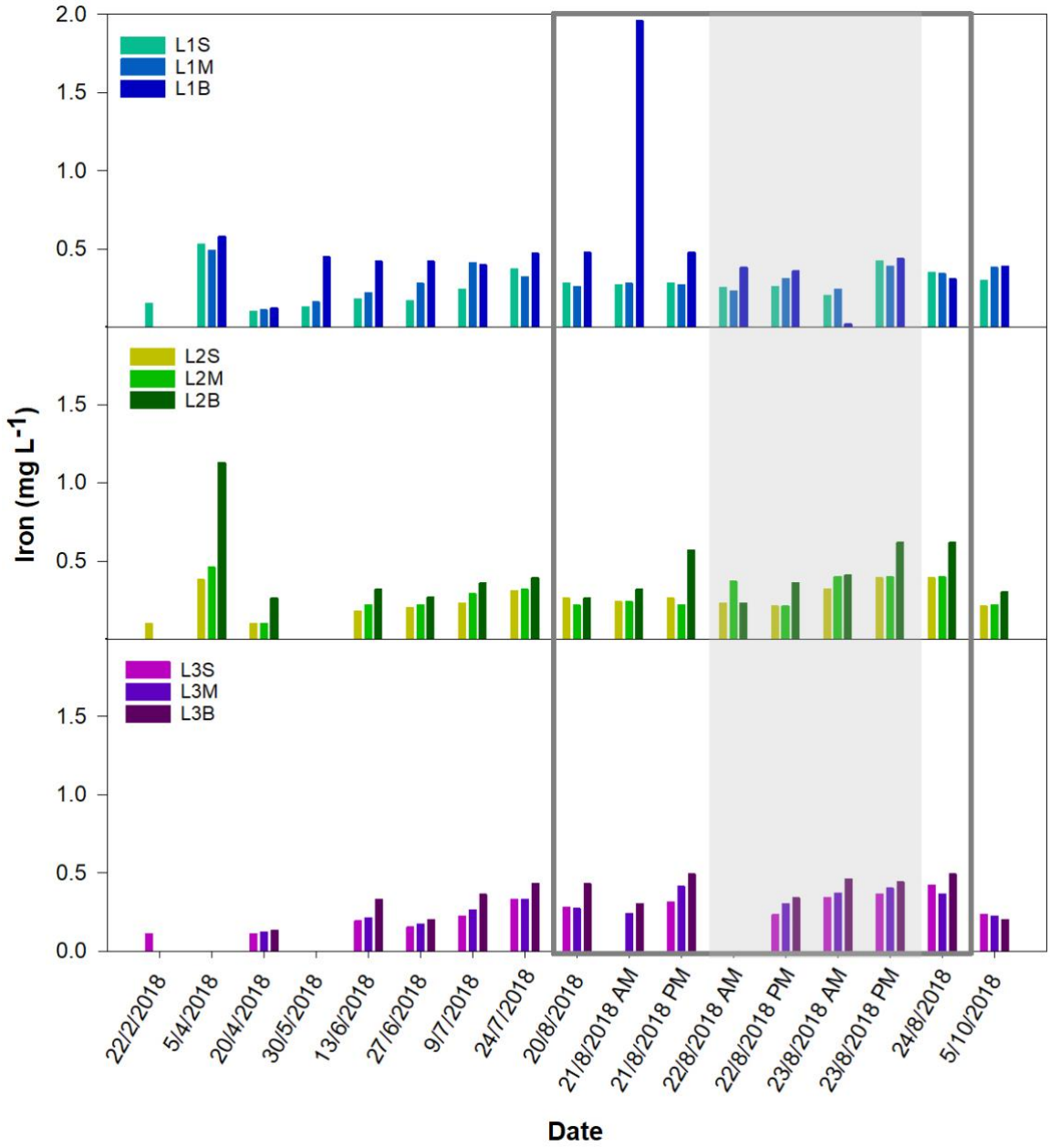

Figure 6.17. Total Iron concentrations from water samples taken at the surface (S), middle (M), and bottom (B) of the water column in Durleigh reservoir at L1, L2, and L3. Grey box indicates August intensive field sampling and grey patch identifies the period the mixers were off.

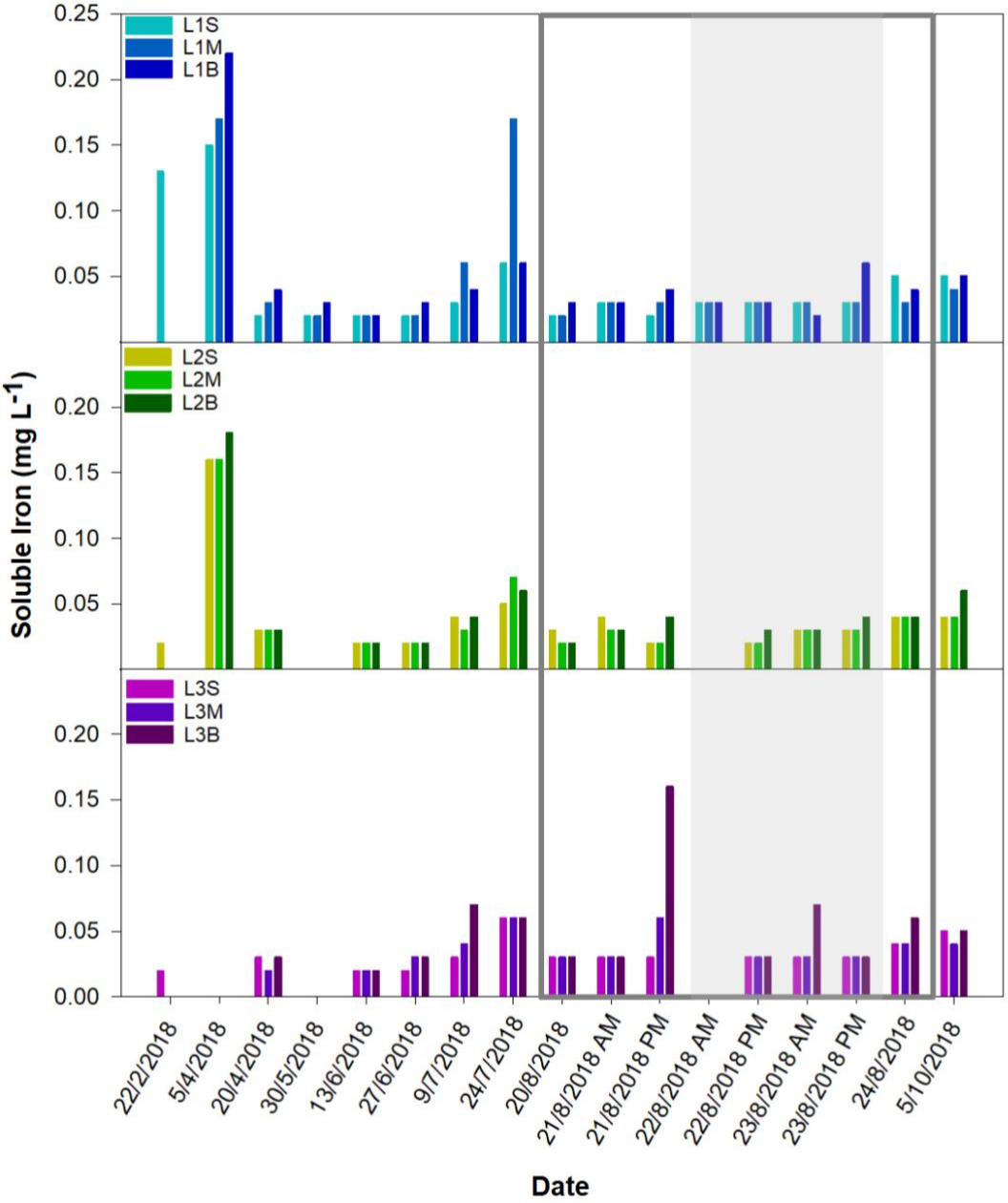

Figure 6.18. Soluble Iron concentrations from water samples taken at the surface (S), middle (M), and bottom (B) of the water column in Durleigh reservoir at L1, L2, and L3. Grey box indicates August intensive field sampling and grey patch identifies the period the mixers were off.

6.3.6 Phytoplankton cell counts

Historical data suggests that total cyanobacteria cell counts have increased significantly since the mixers were installed at Durleigh, which is attributable to a significant increase in *Planktothrix* cell counts (Section 6.3.1). In-reservoir cell count data during 2018 show that despite no statistically significant difference, counts of *Planktothrix* were higher at L1 compared to L2 and L3 through 2018 (Figure 6.19). During August 2018, in -reservoir cell counts of *Dolichospermum* and *Aphanizomenon* were higher than *Planktothrix*. *Aphanizomenon* counts were highest at the surface of L2 (Figure 6.20), whereas *Dolichospermum* counts were higher at L1 (Figure 6.21). However, Planktothrix were generally present throughout 2018 (Figure 6.19; Figure 6.2c), whereas *Aphanizomenon* and *Dolichospermum* were only present in counts during the summer (Figures 6.20 and 6.21). Similarly to the historical data from the intake, the in-reservoir measurements indicate that operation of the mixers at Durleigh appear to benefit cyanobacteria, particularly *Planktothrix.*

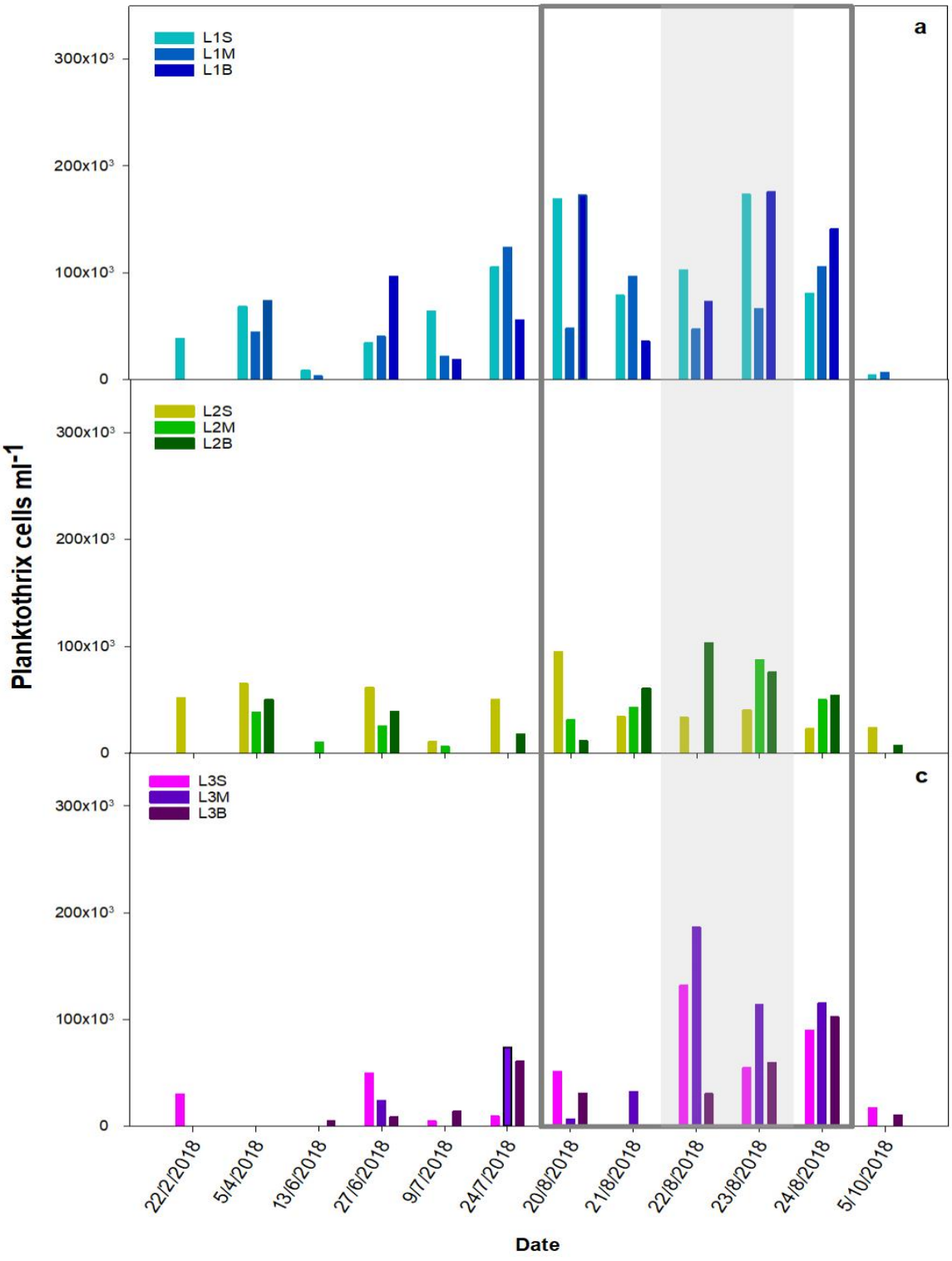

Figure 6.19. Planktothrix cell counts at L1 (a), L2 (b), and L3 (c) on water sampling days in 2018. Counts from the surface (S), middle (M), and bottom (B) of the water column. Grey box indicates August intensive field sampling and grey patch identifies the period the mixers were off.

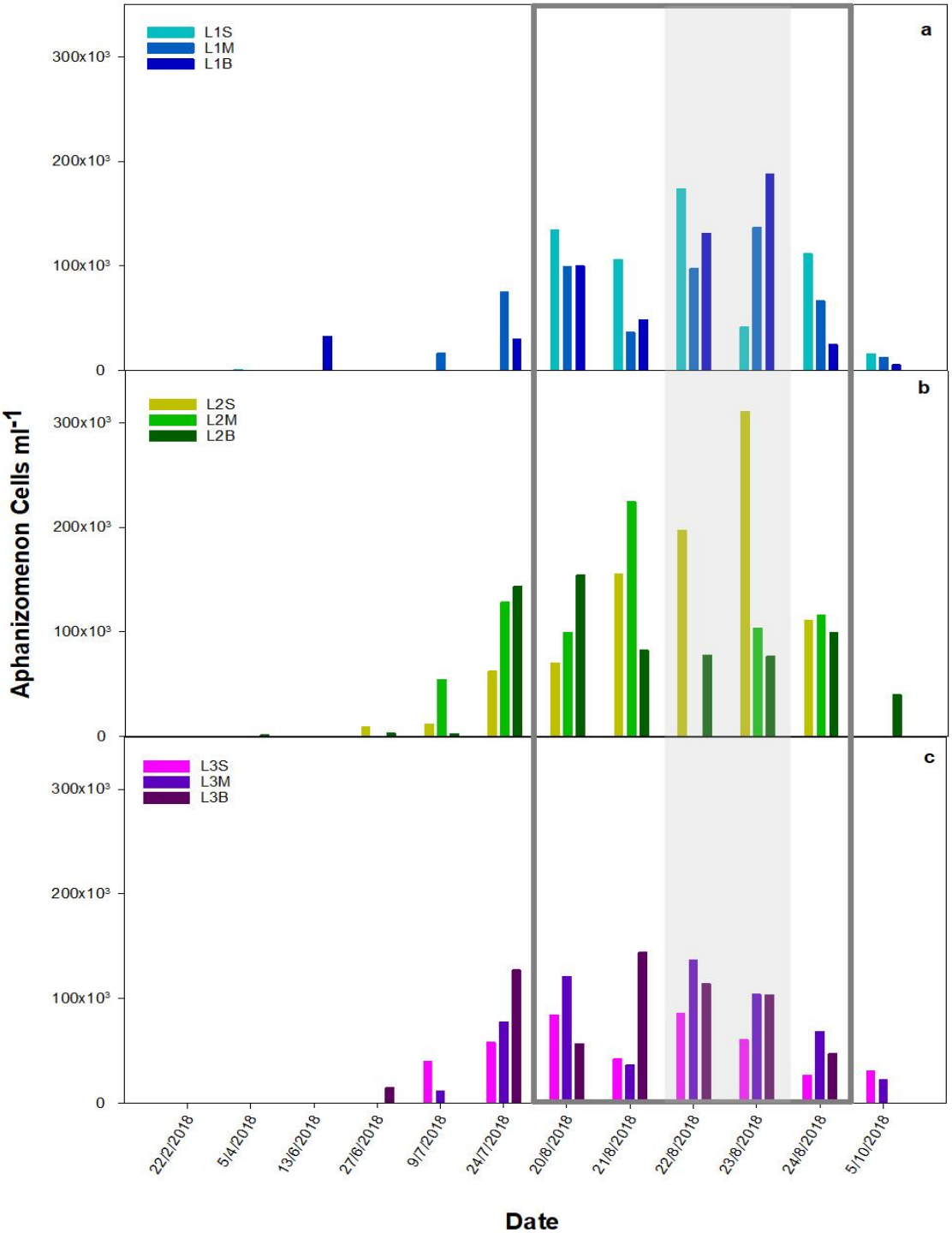

Figure 6.20. Aphanizomenon cell counts at L1 (a), L2 (b), and L3 (c) on water sampling days in 2018. Counts from the surface (S), middle (M), and bottom (B) of the water column. Grey box indicates August intensive field sampling and grey patch identifies the period the mixers were off.

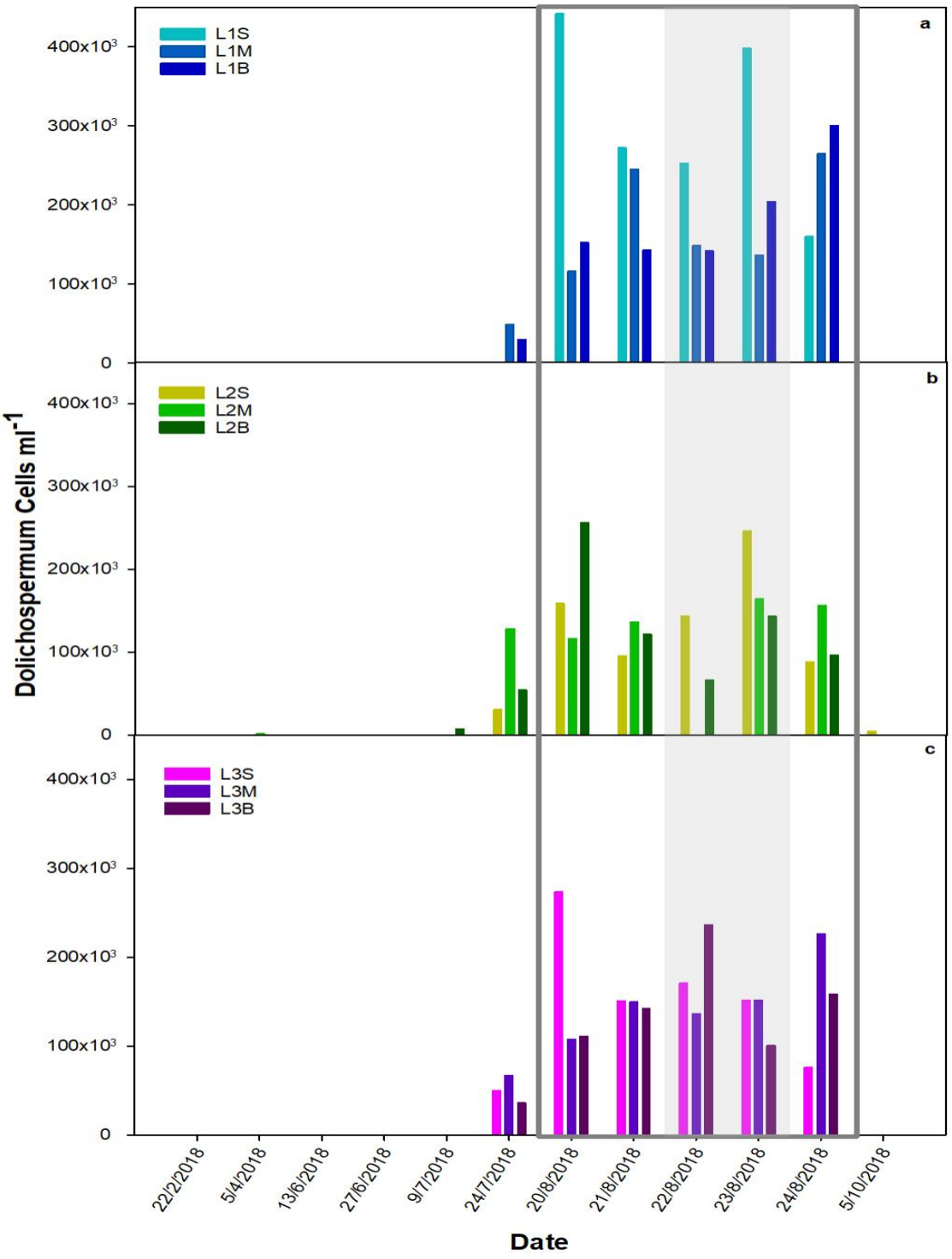

Figure 6.21. Dolichospermum cell counts at L1 (a), L2 (b), and L3 (c) on water sampling days in 2018. Counts from the surface (S), middle (M), and bottom (B) of the water column. Grey box indicates August intensive field sampling and grey patch identifies the period the mixers were off.

6.3.7 Chlorophyll-α Concentrations

Chlorophyll-*α* concentrations are highest at all sites in August 2018 (Figure 6.22), but there were no statistically significant differences between different locations or between different depths at the same location. Concentrations at L1 are consistently highest in the middle of the water column between 21-23 August, which could be due to uncertainties with *in vivo* fluorescence if non-photochemical quenching (NPQ) is occurring in surface samples. NPQ is a mechanism employed by phytoplankton to protect light-harvesting systems from high light intensity damage (Murchie and Lawson, 2013). Excitation of chlorophyll typically emits a photon, which would be measured by fluorescence, however during NPQ, the energy from chlorophyll excitation energy is emitted as heat instead and therefore is not measured through fluorescence (Misumi et al., 2016). At Durleigh, the low light penetration is likely to lead to high light intensity exposure in the surface waters and promote NPQ. Variance in species composition through the vertical profiles could also affect the chlorophyll-*α* fluorescence results (Loftus and Siliger, 1975). However, species composition through the water column at all sites in August was relatively uniform (Figures 6.19 – 6.21) and total phytoplankton counts indicate that surface samples had the highest biomass (Figure 5.3, Chapter 5). Therefore, due to uncertainty in the *in vivo* chlorophyll-*α* measurements, these data will not be considered further in this chapter.

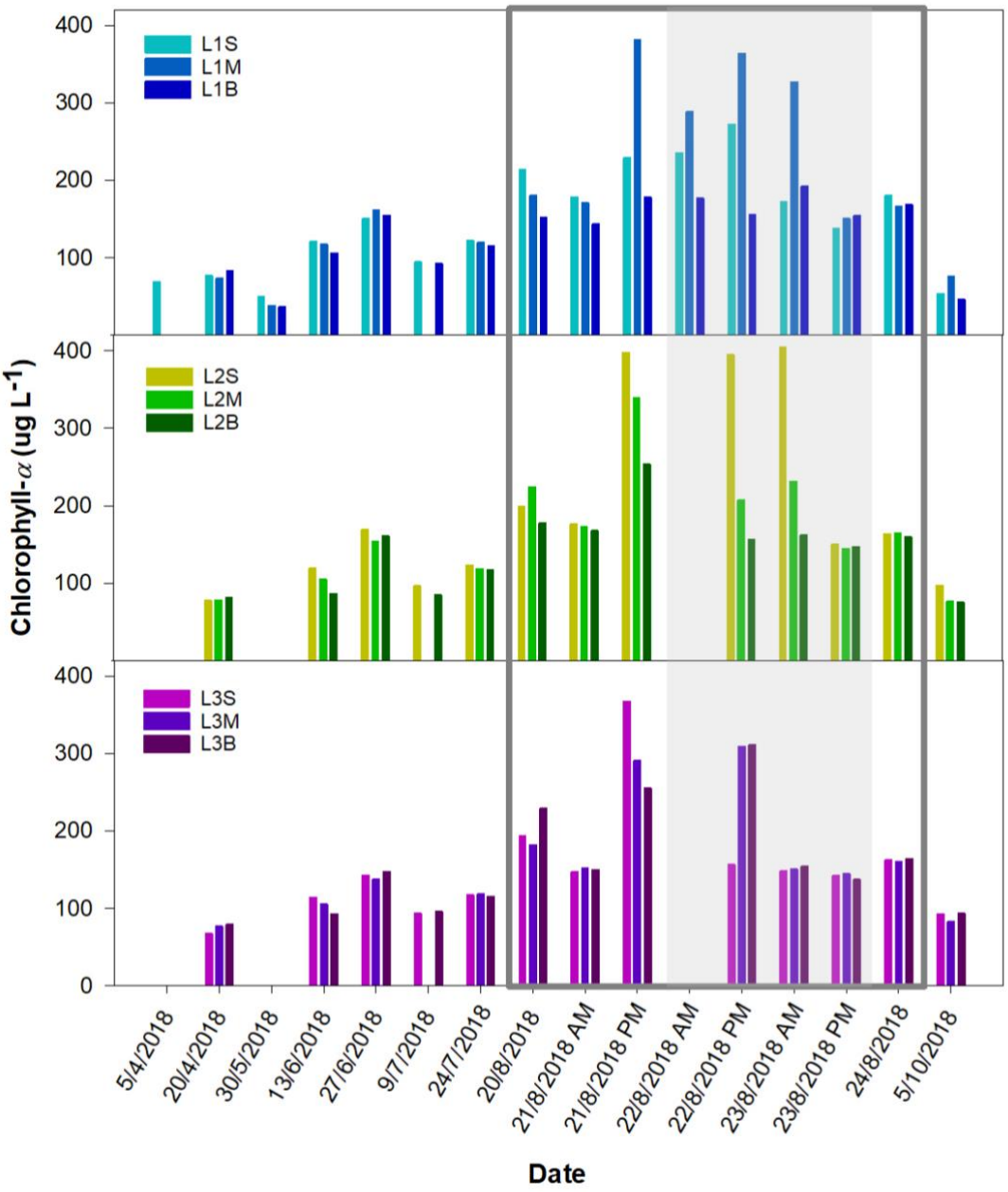

Figure 6.22. Chlorophyll-α concentrations from water samples taken at the surface (S), middle (M), and bottom (B) of the water column in Durleigh reservoir at L1, L2, and L3. Grey box indicates August intensive field sampling and grey patch signifies the period the mixers were off.

6.3.8 Taste and Odour Metabolites

The in-reservoir water samples for taste and odour (T&O) metabolites through 2018 typically exhibited greater temporal variation than spatial differences (Figures 6.23 and 6.24). The Kruskal Wallis and Dunn's post hoc test revealed no significant differences between the same depth and different sites, or between different depths at the same site for both Geosmin and 2-MIB concentrations. On most water sampling days, 2-MIB concentrations were measured at the LOD (2 ng l^{-1}). Concentrations of T&O metabolites at the intake through 2018 show 2 peaks in Geosmin concentration and one peak for 2-MIB (Figure 6.3). Geosmin peaks in early-May and mid-November, whereas 2-MIB peaks in late-October. Both in-reservoir and historical intake measurements of T&O metabolite concentrations suggest that surface mixer operation does not influence their production, which agrees with findings presented in chapter 4 (Perkins et al., 2019).

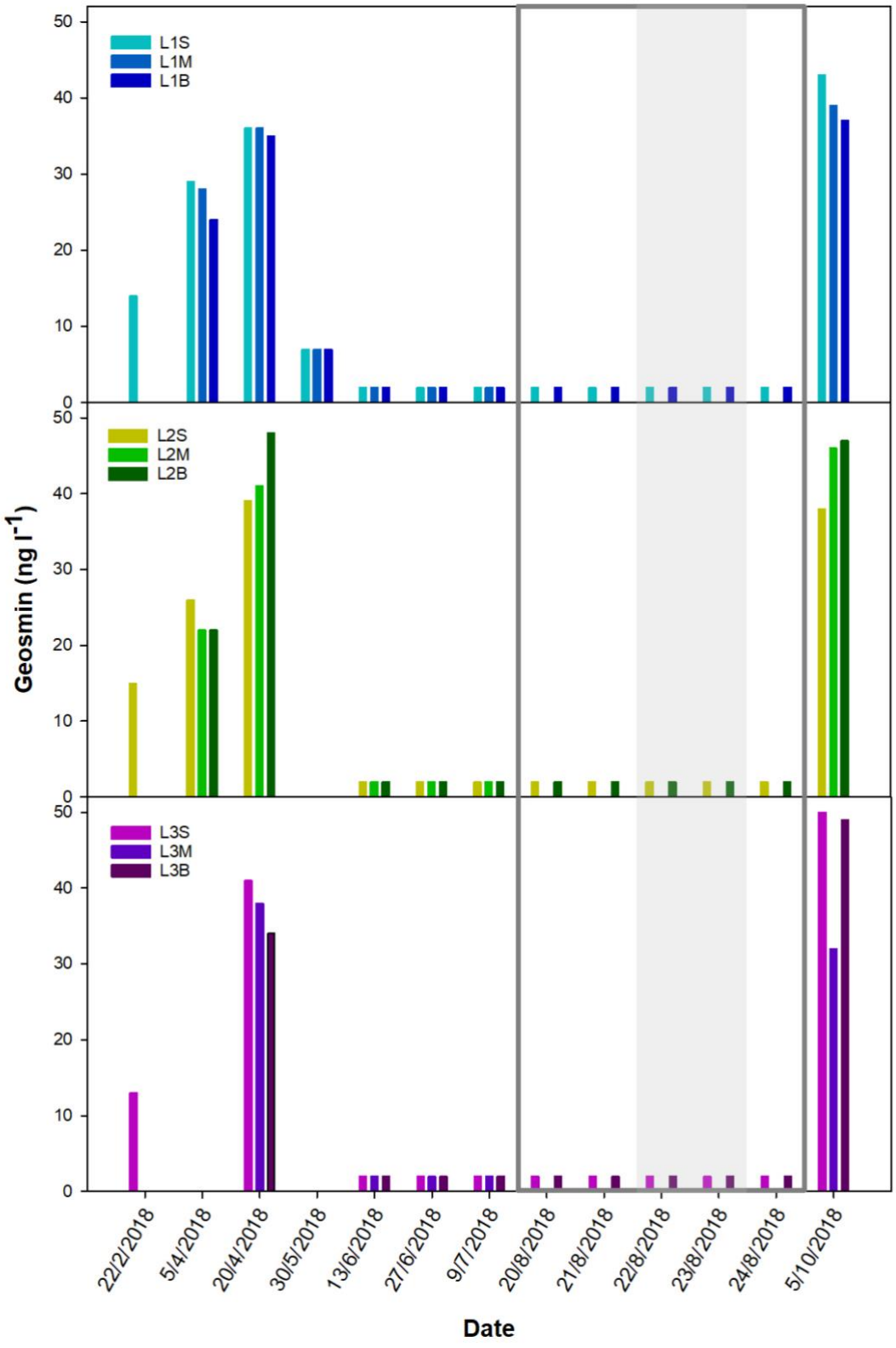

Figure 6.23. Geosmin concentrations from L1, L2, and L3 on water sampling days in 2018. Samples collected from the surface (S), middle (M), and bottom (B) of the water column. Grey box indicates August intensive field sampling and grey patch identifies the period the mixers were off. During the August measurement campaign only surface and bottom samples were collected due to sample processing pressure at the Wessex Water laboratory.

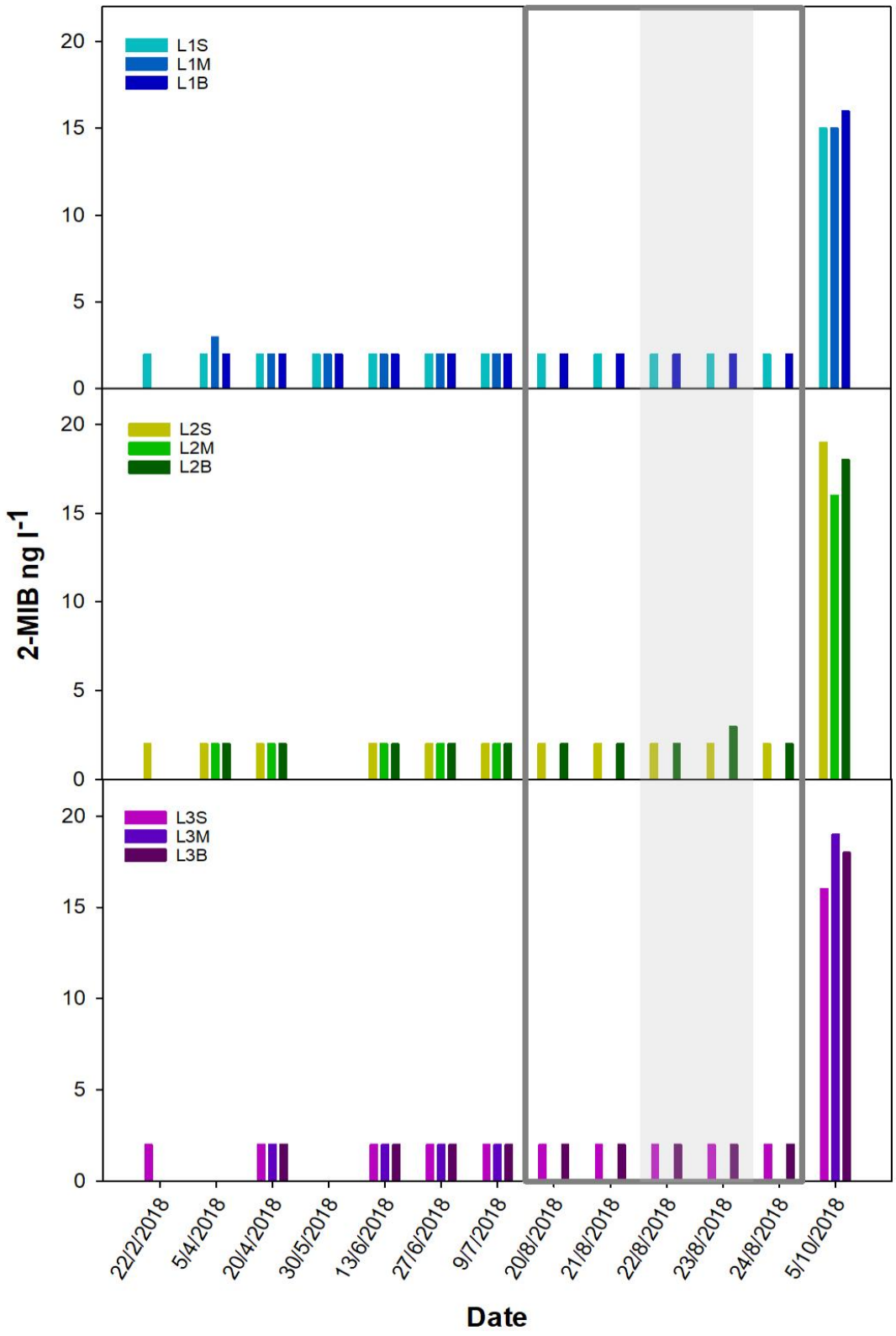

Figure 6.24. 2-MIB concentrations from L1, L2, and L3 on water sampling days in 2018. Samples collected from the surface (S), middle (M), and bottom (B) of the water column. Grey box indicates August intensive field sampling and grey patch identifies the period the mixers were off. During the August measurement campaign only surface and bottom samples were collected due to sample processing pressure.

6.3.9 Results Summary

Since the mixers have been installed at Durleigh, cyanobacterial biomass has increased significantly (Figure 6.1), which is largely due to increased *Planktothrix* cell counts (Figure 6.2c). Analysis of historical weather conditions, water temperatures (canal and intake), and nutrient concentrations (canal and intake) indicate that changes in these variables were not likely to have caused the increased in cyanobacterial biomass (Sections 6.3.1.3 and 6.3.1.4; Figures 6.6 – 6.9). Therefore, the installation of the surface mixers is considered as the principal cause of the increase in cyanobacterial biomass. The installation of the surface mixers did not significantly alter concentrations of 2-MIB or Geosmin (Figure 6.3, 6.23 and 6.24). In-reservoir cell counts show *Planktothrix* counts are higher at L1 (Figure 6.19), closer to the mixers, whereas *Dolichospermum* and *Aphanizomenon* cell counts are more evenly distributed at all sites (Figures 6.20 and 6.21). Light penetration is low throughout the reservoir (Figure 6.10) and turbidity appears relatively uniform. Biochemical oxygen demand is high at the surface and bottom of the water column at L1 (Figure 6.14), suggesting that organic matter content is high in these areas. During OFFB, high BOD near the sediments likely cause the rapid decline in DO near the sediments at B1 (Chapter 5).

Concentrations of total manganese and total iron showed no statistical difference after the installation of the mixers (Figure 6.5a and c). However, soluble iron and soluble manganese concentrations have significantly decreased since the mixers were installed at Durleigh (Figure 6.5b and d). Similarly to the observed increase in cyanobacteria, the installation of the mixers appear to be the principal cause of the decreased soluble metal concentrations at the intake (Figure 6.5). However, in-reservoir measurements show concentrations of total and soluble manganese were significantly higher at the bottom of the water column at all locations, and concentrations at L1 were higher than L2 and L3 (Figures 6.15 and 6.16). Although L1 concentrations are still lower than concentrations at the intake before the mixers were installed, mixer operation may contribute to increased concentrations of both soluble and total manganese through localised resuspension of sediments as observed in Chapter 5.

6.4 Discussion

Principally, artificial circulation aims to reduce cyanobacterial biomass through light-limitation and therefore minimise the risk of T&O events and high toxin concentrations (Elliott and Swan, 2003; Hobson et al., 2012). The findings presented in this Chapter have demonstrated that surface mixers appear responsible for a significant increase cyanobacterial biomass, but there was no significant difference in 2-MIB or geosmin concentrations. In this section, it is proposed that continuous growth conditions provided by mixer operation benefits *Planktothrix* through light-limitation, but mixer operation does not influence T&O metabolite production in cyanobacteria. Instead, variability in environmental conditions appears to influence nutrient concentrations that trigger T&O production in cyanobacteria. Although the principal aim of light-limiting phytoplankton was not achieved, an alternate benefit occurred, whereby surface mixers have significantly decreased soluble manganese concentrations at the intake, despite the highest in-reservoir concentrations being observed near the mixers. Water quality managers need to consider the cost effectiveness of reduced soluble manganese at the intake compared to the risk associated with a T&O producing cyanobacteria-dominated environment that could result in a T&O event if a pulse of ammonium or phosphorus loading occurs under variable environmental conditions.

The operation of the surface mixers at Durleigh appear to be the most likely cause of increased cyanobacterial biomass and decreased soluble metal concentrations at the intake. Analysis of historical weather conditions for the region showed that there has been no significant change in air temperatures, rainfall, or wind speeds since the mixers were installed (Figure 6.9). Nonetheless, the variability in weather conditions, with more extreme weather patterns predicted with climate change could influence T&O metabolite production (Wood et al., 2017). For example, Uwins et al. (2007) reported that increased Geosmin concentrations were typically triggered by large rainfall events that caused a pulse of nutrients to enter the reservoir that trigger T&O production (Perkins and Slavin et al., 2019). On the other hand, Winston et al. (2014) found that mean annual rainfall was negatively correlated with mean annual 2-MIB concentrations. At Durleigh, Geosmin concentrations at Durleigh were high through the winter of 2016/17 and this was likely associated with environmental variability at the time rather than the operation of the surface mixers at Durleigh. The Met Office (2016a) reported a heatwave between 12 and 15 September 2016, accompanied with flash flooding across

the southwest of England that may have increased external loading of nutrients into Durleigh to trigger cyanobacterial productivity and the subsequent increase in Geosmin and 2-MIB concentrations that began in the last week of September 2016 (Figure 6.3). A peak in 2-MIB concentrations occurred on 14 October 2016 (14 ng l^{-1}; Figure 6.3b), but Geosmin concentrations remained high through winter 2016 and spring 2017, peaking at 516 ng l^{-1} on 4 June 2017 (Figure 6.3a). During the winter, *Dolichospermum*, *Aphanizomenon, Planktothrix,* and *Pseudanabaena* were present in the counts and although *Planktothrix* were the most abundant, all genera have been reported to produce Geosmin (Watson et al., 2016). Although peaks in geosmin concentrations were observed in 2011, the prolonged high Geosmin concentrations through the winter of 2016/17 were not observed in any year prior to the installation of the mixers. Therefore, we suggest that the operation of the surface mixers at Durleigh may prolong taste and odour events as the increased biomass feedback to provide an autochthonous source of nutrients that maintains cyanobacterial productivity for longer (Chaui et al., 2011). Consequently, the operation of the surface mixers in a shallow hypereutrophic reservoir increases the risk of high T&O metabolite concentrations by favouring a cyanobacterial community able to utilise nutrient pulse events during variable environmental conditions.

Artificial circulation aims to entrain cyanobacterial cells and transport them out of the euphotic zone to prolong the time cells spend in darkness (Visser et al., 2016), which potentially suppresses growth rates and reduces biomass (Oksam, 1978). But mixing has also been deemed successful when shifts in dominant phytoplankton species have been achieved, despite no observed decreases in biomass (Huisman et al., 2004; Visser et al., 2016). Generally, Visser et al. (2016) reported aeration to successfully reduce cyanobacterial biomass in 7 out of 12 case studies, although Wagner (2015) suggests that for mechanical mixing to effectively light-limit phytoplankton, water column depths need to exceed 10 m in depth. Surface mixers are a relatively novel technique for artificial mixing, so there are few peer-reviewed studies into the effects of surface mixers on cyanobacteria biomass. But the findings presented in this Chapter highlight that in a shallow, hypereutrophic reservoir, surface mixer operation has significantly increased cyanobacterial biomass (Figure 6.1).

At Durleigh, light penetration is very low (Figure 6.10), due to a combination of increased sediment resuspension and total phytoplankton biomass. One measure typically used to assess light availability for phytoplankton is the ratio between mixed

layer depth and euphotic depth (Z_m:Z_{eu}), whereby the higher the ratio, the more light-limited phytoplankton will be (Zohary et al., 2010; Budzyńska et al., 2019). Reynolds et al. (1983) suggest that *Oscillatoria agardhii* (now *Planktothrix agardhii*) can tolerate higher values of Z_m:Z_{eu} (> 2), which could explain why cell counts of *Planktothrix* increased significantly since the mixers were installed at Durleigh. *Planktothrix agardhii* is also a known producer of 2-MIB and Geosmin (Jüttner and Watson, 2007). As light penetration in the reservoir is low, the surface mixers entrain *Planktothrix* filaments and mix them between the euphotic and aphotic zones at higher frequency. In-reservoir cell counts show that near the mixers, *Planktothrix* were generally found at all depths, whereas at L2 and L3 no consistent distribution through the water column was observed (Figure 6.19), which demonstrates that mixers homogenise the distribution of cells through the water column. Additionally, the localised sediment resuspension observed in Chapter 5 (Figure 5.12; Figure 3.5, Chapter 3) indicates that mixing at Durleigh penetrates to the sediments, which could provide *Planktothrix* access to nutrients, helping to maintain higher biomass. Z_{eu} at Durleigh varied in the range 0.5 – 1.75 m (Table 5.3, Chapter 5) and if we assume that the mixed layer depth is the depth of the water column in the range 4 – 6.6 m at Durleigh in 2018, then Z_m:Z_{eu} is 2.3 - 8 (for the shallowest depth: 4 m), which is consistently higher than the threshold of 2 regarded by Reynolds et al. (1983) as beneficial for *Oscillatoria agardhii* (now *Planktothrix agardhii*). Furthermore, Reynolds (1994) suggests that constant mixing in shallow, turbid water bodies benefits *Planktothrix* due to their ability to maintain zero buoyancy and remain in suspension, and filament size that reduces predation likelihood by zooplankton. Constant mixing reduces the risk of photoinhibition and the low light adaptation of *Planktothrix* provides a competitive advantage in light-limited conditions. Therefore, the higher cell counts observed at the intake and L1 at Durleigh indicate that surface mixer operation in a turbid reservoir creates a more constant mixing environment that benefits T&O producing *Planktothrix*.

In addition to benefiting from constant mixing, *Planktothrix* have been reported to be well adapted to low-light intensities (Wood et al., 2010; de Araujo Torres et al., 2016; Pancrace et al., 2017). For example, Post et al. (1985) demonstrated that *Planktothrix agardhii* (formerly *Oscillatoria agardhii*) adapt well to pulsed light conditions over an 8/16-hour light-dark cycle. Under these conditions, cells rapidly accumulated carbohydrates (polyglucose) in the light phase, which were subsequently used as an energy source during the dark phase. Despite a 66% decrease in light

irradiance per 24 hr compared to the continuous light regime, growth rates only decreased by 35%, indicating that *Planktothrix agardhii* can maintain higher growth rates in the dark due to metabolism of stored polyglucose (Post et al., 1985). Further research is required to define the rate at which entrained cells are mixed through the water column at Durleigh. Nevertheless, artificial circulation likely introduces entrained cells to a light-dark cycle, which enables *Planktothrix* to outcompete other cyanobacteria in an already light-limited environment.

Moreover, increases in both C-phycocyanin and chlorophyll-α pigments were observed in the pulsed light regime compared to the continuous light regime, which suggests that under the light-dark cycle, *Planktothrix* photosynthetic performance increases (Post et al., 1985). Production of T&O compounds occur along the same metabolic pathways as pigment synthesis (Bentley and Meganathan, 1981; Jüttner and Watson, 2007). For example, Naes and Post (1988) examined the changes in Geosmin and pigment synthesis (chlorophyll-α and β-carotene) in *Oscillatoria brevis* when exposed to light-limited and nitrogen-limited conditions and reported increased Geosmin when demand for pigments was reduced (nitrogen-limited). Similarly, Zhang et al. (2009) observed highest Geosmin productivity and concentrations in *Lyngbya kuetzingii* at lower light intensities, when pigment demand was lower. Wang et al. (2011) suggest that genes associated with 2-MIB production in cyanobacteria are less active at lower light levels. More recently, Jia et al. (2019) suggested that increased turbidity reduced 2-MIB production in *Planktothrix* in Miyun Reservoir. Both the in-reservoir and intake observations from 2018 suggest that despite high cyanobacterial biomass, T&O metabolites remained low. During 2018, the weather conditions were generally warm and stable, which promotes continuous growing conditions with limited environmental variability. Therefore, at Durleigh under a light-dark cyclic environment generated by artificial circulation, it is hypothesised that the demand for pigments increases in *Planktothrix* and subsequently production of T&O metabolites was reduced. In terms of water quality management, although mixers have increased overall cyanobacteria biomass, it is suggested that the light-limited conditions promote pigment synthesis along isoprenoid pathways over T&O metabolite production during stable environmental conditions. However, any change in environmental conditions or a pulse in nutrients, such as ammonium, may promote accelerated metabolism along these pathways and subsequently increase T&O metabolite production (Chapter 4; Perkins and Slavin et al., 2019).

Decomposition of cyanobacteria has been demonstrated to release soluble inorganic nutrients into the overlying water that could maintain growth rates (Chaui et al., 2011; Ma et al., 2013). For example, Hampel et al. (2019) found that *Planktothrix* blooms in Lake Erie were fuelled by ammonium inputs from ammonification between June and August, as *Planktothrix* typically have a higher affinity for ammonium at low concentrations compared to other cyanobacteria (Zevenboom et al., 1980). At Durleigh, orthophosphate concentrations remained around the LOD throughout the summer of 2018 at Durleigh, but cyanobacteria counts were high (and BOD was high at L1 in August), which suggests that mineralisation and subsequent release of orthophosphate was enough to help sustain cyanobacterial productivity through the summer. Alkaline phosphatase activity may also have contributed to phosphate availability for phytoplankton (Chróst and Overbeck, 1987; Lin et al., 2018). Microbial activity is promoted by warmer water temperatures (Gudasz et al., 2015) and in Chapter 5, mixer operation was demonstrated to significantly increase bottom water temperatures (Tables 5.3 and 5.4, Chapter 5). In addition, ammonium concentrations at the intake were higher during the summer of 2018, which could reflect increased ammonification. However, observations from the shallow, eutrophic, Lake Taihu suggest that sediment resuspension can introduce nutrients into the overlying water column from the pore waters, which contained considerably higher nutrient concentrations (Qin et al., 2004). Perkins and Underwood (2001) demonstrated that sediment resuspension at Alton Water contributed to the internal loading of phosphorus into the overlying water column and was observed even during light wind conditions. Further research into the concentrations of nutrients in the sediments and pore water at Durleigh is required to conclude whether resuspension due to artificial circulation introduces nutrients into the water column, but observations from other shallow eutrophic systems suggest that this is a likely internal source (Hansen et al., 2009; Tammeorg et al., 2013). Mixer operation appears to create a beneficial environment for cyanobacterial productivity, where cells are entrained and transported from the euphotic zone to the sediments continuously, allowing access to both light and nutrients over a time scale that is sufficient for productivity to be maintained.

Microbial decomposition and respiration deplete oxygen, but other oxidants can be used as electron acceptors (e.g. nitrate, MnO_2 and Fe^{3+}; Reddy et al., 1986). Variations in decomposition rates, mineralisation rates, microbial respiration, and differences in oxidant concentrations can affect the redox potential, which may

influence the internal loading of soluble metals and nutrients into the overlying water (Nealson and Myers, 1992; Balistrieri et al., 1992; Lloyd, 2003). Concentrations of soluble manganese are consistently higher at the bottom of the water column throughout 2018, particularly at L1 (Figure 6.16), which may be due to localised sediment resuspension introducing soluble manganese from interstitial pore water into the overlying water column (Eggleston, 2012). Microprofiler data from Durleigh in September 2015 shows that DO concentrations at the sediment water interface (SWI) were higher closer to the mixers (Amani et al., in prep), indicating that operation of the surface mixer locally improves the transport of oxygen through the water column. However, Löfgren and Boström (1989) found that phosphate and soluble forms of iron and manganese were mobilised from interstitial waters in a shallow, eutrophic lake in Sweden despite high bottom water oxygen concentrations, which was attributed to microbial activity (Trimble and Ehrlich, 1970; De Schamphelaire et al., 2007). On the contrary, Li et al. (2019) found that despite operation of water-lifting aerators improving DO concentrations near the sediments, concentrations of Mn^{2+} remained high in the bottom waters, which was attributed to an increased concentration gradient across the SWI that increased the diffusive flux of Mn^{2+}, but no sediment resuspension was observed. Therefore, at Durleigh, surface mixer operation appears to increase transport of DO locally through the water column and effectively oxygenate the SWI, but concentrations of soluble manganese remain high at L1B due to sediment resuspension and microbial activity.

Before mixer installation, peaks in Mn^{2+} occurred during the summer months, which could be attributed to lower DO concentrations at the bottom waters (Betancourt et al., 2010). Chapter 5 demonstrated that mixer operation decreases ΔDO locally and studies have suggested that warmer temperatures, stirring, and higher alkalinity can facilitate manganese oxidation and or adsorption to other particles over time (Zaw and Chiswell, 1999; Nijjer et al., 2000). Despite the improved distribution of DO through the water column, oxidation rates of Mn^{2+} are slow (Gantzer et al., 2009), indicating that it is unlikely to be oxidised before entering the intake. However, Kawashima et al. (1988) found adsorption rate of Mn^{2+} to suspended solids was more appreciable than the oxidation rate and Bryant et al (2011) suggest that increased DO concentrations near the sediments can help facilitate adsorption to suspended particles. The decrease in soluble manganese concentrations occurred rapidly after the mixers were installed (Figure 6.5d). Manganese oxidation is typically slow in natural waters (Gantzer et al., 2009) and

often requires manganese-oxidising microbial communities at the sediment water interface (Nealson and Saffarini, 1994). Therefore, the decrease in Mn^{2+} concentrations at the intake since the mixers were installed is likely caused by adsorption and co-precipitation of soluble manganese with organic detritus (from increased phytoplankton/cyanobacterial biomass), which is facilitated by the available DO from surface mixer operation. Analysis of annual average total manganese concentrations indicates that since surface mixers were installed at Durleigh, there has been no obvious change in total manganese concentrations at the intake. Therefore, soluble manganese concentrations contribute a smaller fraction of the total manganese concentrations since the mixer have been installed at Durleigh. Further work is required to fully determine the contribution of microbial metal reduction and sediment resuspension to increased concentrations of soluble metals in the water column. The results presented in this Chapter strongly suggest that local effects of mixer operation decrease concentrations of soluble iron and manganese at the intake. For management purposes reduced concentrations of soluble iron and manganese at the intake lowers treatment and distribution network concerns of MnO_2 build up in pipes (Tobiason et al., 2016).

Before installing surface mixers into drinking water reservoirs for artificial circulation, identification of the principal water quality problem is necessary. Here, mixers have reduced concentrations of soluble manganese entering the intake, but led to an increase in cyanobacterial biomass, which introduces other concerns for drinking water supply. It is possible that one mixer would effectively transport oxygen through the water column near the intake to reduce soluble manganese concentrations without increasing sediment resuspension and benefiting cyanobacterial productivity. Moreover, abstraction, changes in pumping, and runoff through the year lead to changes in the water level at Durleigh, but the pumps are operated at the same flow rate all year. Therefore, the sustained cyanobacterial productivity could be reduced if flow rates of the mixers were lowered as the water column depth dropped through the summer.

The mixers appear to create a beneficial environment for cyanobacteria, particularly *Planktothrix*, productivity by providing a cyclic link between light and nutrients through entrainment and transport of cells through the water column. Chapter 5 showed that artificial circulation penetrated to the sediments over a limited range of influence, with turbulent diffusivities indicating that artificial mixing dictated phytoplankton cells distribution through the water column. Nevertheless, further investigation into the flow generated by the surface mixers is needed to help understand

in more detail the environment the entrained filaments are subjected to. The weather conditions on site during the measurement campaign were relatively stable (Figure 5.1, Chapter 5), with low levels of rainfall. The relatively stable weather conditions combined with continuous mixing by artificial circulation promote steadier growth rates in cyanobacteria, and consequently pigment synthesis was favoured over T&O production along the pathways of isoprenoid synthesis. However, in the event of a pulse of ammonium into the system, for example through an external/internal loading event, accelerated metabolism along isoprenoid pathways could be stimulated and subsequently increase T&O production (Chapter 4). Effectively, the mixers have created perfect growing conditions for a taste and odour producing cyanobacteria, which increases the risk of a T&O event occurring.

6.5 Conclusions

The results presented in this chapter show that mixer operation has significantly increased overall cyanobacterial biomass but do not appear to have such influenced T&O metabolite production, corroborating the findings of Chapter 4, where it is demonstrated why biomass and T&O concentrations do not always correlate over time. Mixer operation appears to benefit *Planktothrix* due to entraining filaments that are low light adapted and transporting them from the euphotic zone, to nutrients near the sediments at a relatively continuous rate. It is hypothesised that in a light-limited environment with a sustained growth cycle, pigment synthesis takes precedent over T&O metabolite production. However, it is suggested that the environment created by mixing increases the risk of prolonged T&O events in variable environmental conditions that lead to pulses of nutrients, such as ammonium. Since the installation of the mixers, concentrations of soluble iron and soluble manganese have significantly decreased at the intake. Although considerably lower than pre-mixer intake concentrations, the concentrations near the mixers at L1 are notably higher than other sites within the reservoir and was attributed to localised sediment resuspension cause by the mixers. Concentrations of total manganese have not significantly changed since the installation of the mixers at Durleigh, which demonstrated that the fraction of soluble manganese in total manganese concentrations has decreased. It is suggested that sediment resuspension introduces soluble manganese from interstitial pore waters to the overlying water column near the mixers, but the improved distribution of DO through

the water column as a result of artificial circulation, increases likelihood of oxidising soluble manganese to MnO_2. Although concerns over soluble manganese entering treatment and distribution networks has been reduced by localised artificial circulation in a shallow drinking water reservoir, consideration of the negative impacts of increased cyanobacterial biomass need to be weighed against these benefits. Overall, the main aim of surface mixers to light-limit cyanobacteria does not appear to be achieved in shallow, hypereutrophic/eutrophic drinking water reservoirs, but the advective transport of DO through the water column has led to reduced concentrations of undesirable soluble metals entering the intake.

CHAPTER 7

DISCUSSION AND CONCLUSIONS

7.1 Discussion

The findings presented in this thesis consist of both historical data analysis and in-reservoir measurements from a comprehensive field campaign over a typical stratification season at a shallow, hypereutrophic reservoir that is artificially mixed. In this section, the hydrodynamics of surface mixers in a shallow, hypereutrophic reservoir are discussed before findings from all results chapters are summarised and discussed together. Conceptual models of the feedback loops are presented and the effects of the surface mixers on these feedbacks are highlighted. These models have been developed as guidance tools (within practical limits due to necessary simplification of some processes) to help inform management decisions around the use of artificial circulation for water quality management in shallow, hypereutrophic/eutrophic reservoirs.

7.1.1 Hydrodynamics of surface mixers in a shallow reservoir

Using the shutdowns during the 2018 measurement campaign as no-mixing controls, results in Chapter 5 demonstrated that the changes in hydrodynamics from surface mixer operation in a shallow reservoir are highly localised. Although no exact range of influence was defined (Objective 1, Chapter 1), the research showed that within a 30 m radius, surface mixer operation improves the distribution of dissolved oxygen (DO) through the water column and creates a more uniform temperature profile by increasing bottom water temperatures significantly. These observations contrast those from Lawson and Anderson (2007) who observed temperature and DO gradients during the summer at Lake Elsinore, despite axial flow pump operation. However, Lawson and Anderson (2007) reported scouring of the sediments and sediment resuspension, which was also observed at Durleigh with localised clouds of sediment resuspension around the surface mixers (Figure 3.5, Chapter 3) and from ADV data ~ 30 m north of the mixers (Figure 5.12, Chapter 5). Water velocity measurements from the StreamPro ADCP were inconclusive, but velocity measurements from the ADV showed a significant decrease in in horizontal velocities ~ 30 m north of the mixers during ADV_OFFB, indicating the mixers influenced an area with at least a 30 m radius (Chapter 5).

In this thesis, the effects of surface mixer operation on phytoplankton was considered for the first time. The turbulent diffusivities at Durleigh ranged between 10^{-5}

and 10^{-3} m^2 s^{-1} (Figure 5.6, Chapter 5), which is enough to overwhelm vertical velocities of phytoplankton cells and dictate the transport of cells through the water column. Within the range of influence of the mixers, where the turbulent energy input from the mixers remains continuous, cyanobacterial cells and filaments are likely to be entrained within the flow generated by the mixers and transported between the euphotic zone and the bottom waters. The circulation mixes cells between access to light (surface) and nutrient (sediments) at a relatively continuous rate, which sustains growth. Although the passive transport of cyanobacteria cells through the water column reduces the competitive advantage of buoyancy regulating cyanobacteria, the localised mixing environment generated by surface mixer operation benefits other cyanobacteria, such as *Planktothrix* (Reynolds et al., 1983), which is a taste and odour producing genera. Despite the limited range of influence of the surface mixers, their positioning at Durleigh means that significant the increase in *Planktothrix* biomass as a result of their operation has been observed at the intake (Chapter 6).

Overall, the operation of surface mixers at Durleigh locally alter the water quality in the reservoir. However, due to the position of the mixers near the intake of the reservoir, mixer operation does influence the quality of the abstracted water (Chapter 6). Although a large range of influence from surface mixer operation may be desired, water quality managers are ultimately concerned about the quality of the water entering the intake for treatment purposes. Therefore, in the following section, the localised effects of surface mixer operation on water quality at the intake are discussed and conceptual models are presented as guidance tools for management based on these observed effects.

7.1.2 Effects of surface mixers in a shallow, hypereutrophic reservoir

Consensus within literature suggest that although there is increased potential for T&O metabolite production with high cyanobacterial biomass, the production of T&O metabolites does not correlate over time with changes in biomass. Therefore, in this thesis it was hypothesised that artificial circulation designed to address biomass issues will not be successful, and potentially worsen T&O problems in drinking water supply reservoirs. Additionally, research has shown that what triggers production of T&O metabolites along metabolic pathways in cyanobacteria is poorly understood, leading to an aim of this thesis that was to identify the key triggers of production.

In Chapter 4, analysis of historical data using Self-Organising Maps and *in situ* observations from Perkins and Slavin et al. (2019) demonstrated that high concentrations of ammonium relative to nitrate is associated with higher T&O metabolite concentrations across a range of drinking water reservoirs. A key consideration here is that increased ammonium concentrations stimulate rapid growth in cyanobacteria and production of T&O metabolites, whereas if growth rates are sustained, T&O production is less likely (Seto et al., 1996). Observations from Chapters 5 and 6 showed that turbulence from artificial circulation dominates over vertical velocities of phytoplankton, promoting passive transport of cells through the water column. The continuous, localised mixing conditions generated by the surface mixers, combined with low light penetration at Durleigh encourages a continuous growth environment for cyanobacterial, in particular *Planktothrix*. Additionally, the relatively stable weather conditions during 2018 do not favour T&O production, which is why in-reservoir and intake concentrations of 2-MIB and Geosmin were generally at the level of detection (LOD). Nevertheless, combining findings of Chapters 4 and 6, it is recognised that T&O metabolite production could increase if a pulse of ammonium or phosphorus occurs, which would likely stimulate rapid growth involving the pathways of isoprenoid synthesis in the cyanobacteria. Therefore, artificial circulation with surface mixers in a shallow reservoir may increase T&O metabolite risk by favouring a cyanobacterial community able to utilise nutrient pulse events during variable environmental conditions.

Using the findings presented in Chapters 5 and 6, a conceptual model was developed (Figure 7.1) that shows the effects of artificial circulation in a shallow, hypereutrophic reservoir on cyanobacterial biomass and the associated feedbacks. Operation of the mixers at Durleigh creates localised sediment resuspension (Figure 5.12, Chapter 5; Figure 3.5, Chapter 3). Consequently, light penetration decreases, which benefits *Planktothrix* productivity (Post et al., 1985), where the filaments are entrained into a more constant flow generated by the mixers. The enhanced cyanobacterial biomass negatively feeds back by increasing particles suspended in the water column and reducing light penetration to further benefit *Planktothrix*. Although high biomass may influence T&O metabolite concentrations through cell lysis releasing intracellular 2-MIB and Geosmin into the surrounding water (Rosen et al., 1992), no significant changes in T&O concentrations were observed at Durleigh, despite the increased cyanobacterial biomass. Instead, it was suggested that variable environmental

conditions may trigger T&O production through external loading of nutrients followed by favourable growing conditions. The in-reservoir observations in Chapter 6 led to the hypothesis that decreased light penetration and the light-dark environment promoted by artificial circulation encourages pigment synthesis in cyanobacteria over T&O metabolite production during periods of warm, sunny, and stable weather conditions. Therefore, a decrease in T&O metabolite concentrations is shown in Figure 7.1. Artificial circulation in a shallow, hypereutrophic reservoir creates a negative feedback loop were mixing decreases light penetration that benefits low light adapted, T&O producing cyanobacteria, which increase in biomass and further reduce light penetration and proliferating the problem.

Elevated cyanobacterial biomass increases autochthonous inputs of organic matter (CH2M Hill, 2013). Subsequent decomposition of organic matter increases biochemical oxygen demand (BOD), but the improved distribution of dissolved oxygen as a result of artificial circulation generally meets such a demand (Figures 5.10 and 5.11; Tables 5.6 – 5.9, Chapter 5). Artificial circulation was shown to locally decrease temperature gradients by significantly increasing bottom water temperatures (Tables 5.4 and 5.5, Chapter 5), which benefits microbial activity (Gudasz et al., 2015) and raises BOD (Figure 7.1). Decomposition of organic matter introduces inorganic nutrients to the overlying water column through mineralisation and microbial reduction (Fallon and Brock, 1979), which has been shown to sustain growth rates of cyanobacteria during blooms (Chaui et al., 2011). In Chapter 6, both in-reservoir and intake measurements of orthophosphate concentrations were reported to be generally at the LOD throughout 2018, but high cyanobacterial biomass was sustained, suggesting that assimilation of bioavailable phosphorus occurred rapidly after mineralisation and release. When concentrations of bioavailable phosphate are low, alkaline phosphatase activity can increase concentrations of bioavailable phosphate (Lin et al., 2018). However, alkaline phosphatase activity was not assessed in this thesis so its contribution as a source of bioavailable phosphate cannot be quantified. Due to increased cyanobacterial biomass, enhanced alkaline phosphatase activity may provide a more constant supply of bioavailable phosphorus and presents an interesting hypothesis for future work. Despite artificial circulation improving DO distribution through the water column, the increased autochthonous inputs of organic matter from higher cyanobacterial biomass fuels microbial decomposition, which raises biochemical oxygen demand and releases nutrients back into the water column, sustaining cyanobacterial growth and prolonging

water quality problems. Therefore, surface mixer operation in a shallow, hypereutrophic reservoir favours cyanobacterial growth and creates a negative feedback loop where greater cyanobacterial biomass increases autochthonous sources of organic matter and warmer bottom water temperatures from mixer operation promote microbial decomposition, which both enhance the availability of nutrients and helps to sustain cyanobacterial growth.

Localised sediment resuspension may also contribute to increased availability of inorganic nutrients for assimilation by phytoplankton (Figure 7.1). For example, Löfgren and Boström (1989) found that phosphate and soluble forms of iron and manganese were mobilised from interstitial waters in a shallow, eutrophic lake in Sweden despite high bottom water oxygen concentrations, which they attributed to microbial activity. At Durleigh, higher concentrations of soluble iron were observed at L1B (Figure 6.18, Chapter 6), indicating the potential release of reduced iron from the sediments through resuspension. The presence of soluble iron at L1B could be used as a proxy for phosphate concentrations, assuming that Fe^{3+} has been reduced to Fe^{2+}, subsequently releasing phosphate. Although not assessed in this thesis, observations from other shallow eutrophic systems suggest that resuspension introduces nutrients into the overlying water column (Hansen et al., 2009; Tammeorg et al., 2013). For example, Perkins and Underwood (2001) demonstrated that sediment resuspension at Alton Water contributed to the internal loading of phosphorus into the overlying water column and was observed even during light wind conditions. The operation of surface mixers in shallow reservoirs increases sediment resuspension and subsequently the internal loading of bioavailable nutrients into the overlying water column, which aids the growth of cyanobacteria. Although risk of T&O metabolite production is greater, the constant operation of surface mixers in a shallow, hypereutrophic reservoir is likely to maintain continuous growth conditions and promote pigment synthesis over T&O production in cyanobacteria.

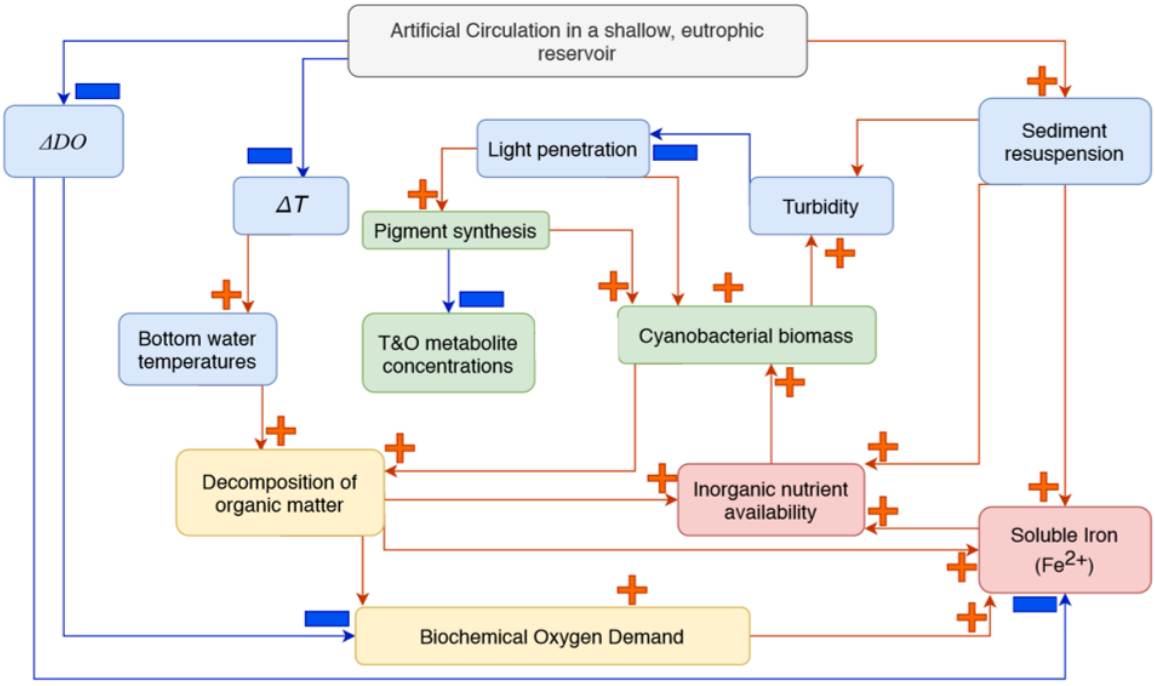

Figure 7.1 Conceptual diagram of the effects of artificial circulation with surface mixers on cyanobacterial biomass and T&O metabolite production in a shallow, hypereutrophic reservoir. Orange arrows and pluses represent increases and blue arrows and minuses represent decreases. Different categories of parameters are colour coded: blue = physical, yellow = biochemical, red = chemical, green = biological.

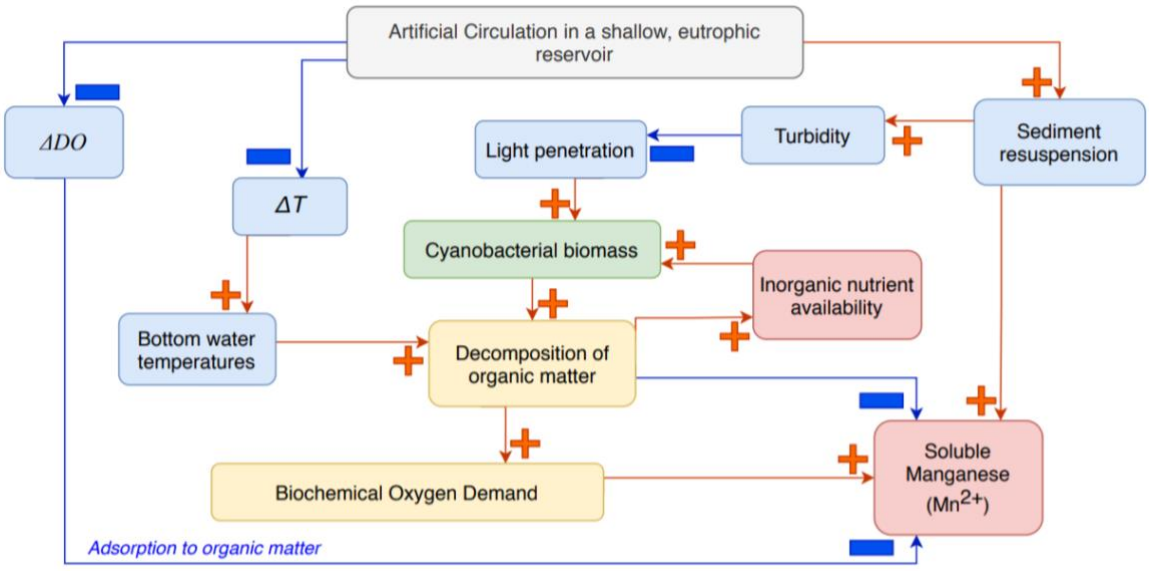

Figure 7.2 Conceptual diagram of the effects of artificial circulation with surface mixers on soluble manganese concentrations in a shallow, hypereutrophic reservoir. Orange arrows and pluses represent increases and blue arrows and minuses represent decreases. Different categories of parameters are colour coded: blue = physical, yellow = biochemical, red = chemical, green = biological.

Despite increased concentrations of soluble iron and soluble manganese at L1B, concentrations at the intake have significantly decreased since the air curtain at Durleigh was replaced with surface mixers (Figures 6.16 and 6.18, Chapter 6). Results from chapters 5 and 6 suggest that sediment resuspension introduces soluble iron and soluble manganese from interstitial water into the overlying water column (Figure 7.2; Eggleston, 2012). Elevated decomposition of organic matter can lead to microbial reduction of iron and manganese despite high concentrations of dissolved oxygen in the bottom waters due to artificial circulation (Trimble and Ehrlich, 1970; Löfgren and Boström, 1989). However, more uniform DO distribution through the water column created by artificial circulation likely promotes the adsorption of soluble manganese onto suspended solids and available organic matter in the water column (Chapter 6; Figure 7.2). For example, Kawashima et al. (1988) found adsorption rate of Mn^{2+} to suspended solids was faster than the oxidation rate. Nonetheless, a decrease in concentrations of soluble manganese at the intake is beneficial for management at it minimises concerns over MnO_2 build up in pipes, which can negatively affect treatment and distribution (Tobiason et al., 2016). Artificial circulation with surface mixers in a shallow, hypereutrophic reservoir locally increases soluble manganese concentrations but potentially promotes adsorption of soluble manganese to suspended solids which reduces concentrations at the intake, which benefits the treatment process and reduces potential build-up of MnO_2 in the distribution network.

The conceptual models presented here show that these seemingly positive effects of artificial circulation influence other processes, which negatively feedback and contribute to increased nutrient availability for phytoplankton assimilation, therefore contributing to the increased cyanobacterial biomass observed. For example, temperature and dissolved oxygen gradients are locally reduced and artificial circulation creates a more homogenous water column, which could be considered beneficial for water treatment processes. Continuous operation of surface mixers in a shallow reservoir locally homogenises the water column near the intake so generally water with the same properties will be treated, which aids the treatment process as less variation in treatment is needed. But warmer bottom water temperatures promote microbial activity and increased decomposition of organic matter reintroduces nutrients back into the water column, which sustains cyanobacterial growth. The operation of surface mixers in a shallow reservoir favours cyanobacterial growth and increases biomass, which increases the potential for a T&O event, however lower light penetration and transport

of cells from the surface to the sediments promotes pigment synthesis over T&O metabolites during warm stable weather conditions. During more variable environmental conditions, the risk of a T&O event is even greater as such conditions are likely to cause nutrient pulses that the cyanobacterial community favoured by mixer operation can capitalise on. Increased sediment resuspension decreases light penetration and introduces nutrients and metals into the overlying water column. For example, soluble manganese concentrations were higher near the mixers. However, soluble manganese concentrations at the intake were significantly lower due to increased adsorption to suspended solids. The decrease in soluble manganese at the intake reduces the potential build-up of MnO_2 through the treatment works and distribution network, which helps water companies maintain assets. On the other hand, the increased T&O metabolite risk as a result of artificial circulation with surface mixers in a shallow reservoir, particularly during variable environmental conditions, raises the potential for customer contacts concerning the wholesomeness of their water. Overall, the higher risk of a T&O event due to artificial circulation with surface mixers suggests that they should not be recommended for in-reservoir water quality management solutions for shallow, hypereutrophic reservoirs.

7.2 Conclusions and further work

In this thesis, ammonium was identified as a key trigger of taste and odour (T&O) metabolite production in cyanobacteria, contributing to the understanding of T&O production with applications for raw water quality management. For the first time, the effects of surface mixers on T&O metabolite production has been assessed. A comprehensive field campaign across the typical thermal stratification season has examined the effects of surface mixers in a shallow, eutrophic reservoir and provided insight into their effectiveness for in-reservoir water quality management. In this section, the findings are summarised and discussed with respect to the aims and objectives of this thesis. The applications for water quality management and possible recommendations are considered, including potential avenues for further work.

7.2.1 Range of influence of surface mixers in shallow reservoirs

The range of influence of the surface mixers in a shallow reservoir was shown to be highly localised (Chapter 5), but an exact area of influence could not be defined (Objective 1, Chapter 1). Using the no-mixing control periods in August 2018, ADV

measurements showed that mixer operation significantly increased near-bed water velocities ~ 30 m north of the mixers (Chapter 5). In addition, the differences between temperatures and dissolved oxygen concentrations at the surface and bottom of the water column were significantly reduced at 20 m from the mixers due to their operation. Despite the limited range of influence of the surface mixers, their position within the reservoir meant their effects were observed at the intake and were identified as the cause of significant increases in cyanobacterial biomass and total manganese concentrations at the intake and significant decreases in soluble metal concentrations (Chapter 6).

For shallow drinking water reservoirs, where water level changes throughout the year with variable inflows and summer drawdown, the risk of sediment resuspension is high with surface mixer operation. Localised sediment resuspension was observed at Durleigh (Figure 3.5; Figure 5.12), and as demonstrated in the conceptual models (Figures 7.1 and 7.2) increased sediment resuspension results in negative feedback loops that lead to water quality deterioration. Variable flow rates through the year to accompany changes in water level, may reduce the risk of sediment resuspension, but are unlikely to improve the range of influence of the mixers.

Project deliverable: For shallow drinking water reservoirs, the limited range of influence of surface mixers restricts their effectiveness as an in-reservoir management technique to improve raw water quality. Even if the reservoir intake was within the mixers range of influence, water quality can still be impacted by inputs from the catchment and water movement through the reservoir before reaching the intake. Additionally, the high risk of sediment resuspension as a result of mixer operation and low water level with summer drawdown reduces the likelihood of surface mixers success.

7.2.2 Key triggers of T&O metabolite production in cyanobacteria

Generally, there is a consensus that T&O metabolite production occur along pathways of isoprenoid synthesis by cyanobacteria (Jüttner and Watson, 2007), it was identified that there was a need to better understand the triggers of T&O production along these pathways to better advise management (Objective 2, Chapter 1). In-reservoir observations at Plas Uchaf (Chapter 4; Perkins and Slavin et al., 2019) showed that ammonium was responsible for a significant decrease in 2-MIB and Geosmin concentrations, which led to the hypothesis that ammonium is a key trigger of cyanobacterial productivity and the production of T&O metabolites. In Chapter 4, this

hypothesis was tested at six reservoirs across a trophic gradient using the relatively novel method of self-organising map analysis that revealed ammonium concentrations relative to nitrate were important determinants of T&O production in cyanobacteria for all sites. Therefore, high concentrations of ammonium relative to nitrate convincingly appear to stimulate rapid growth and subsequent production of T&O metabolites. Further work investigating the mechanisms involved in T&O production is still required, particularly into how the metabolisms of different cyanobacteria taxa respond to changes in nutrient availability and produce 2-MIB and Geosmin, but future investigations can be better informed now that ammonium has been identified as a key trigger.

Project deliverable: For water quality management of 2-MIB and Geosmin production in drinking water supply reservoirs, it is advised that internal and external sources of ammonium are identified and monitored alongside phosphorus. Proactive reduction in ammonium concentrations from all sources is recommended for mitigating against T&O events. In addition, hindcasting to ground truth feedbacks using historical monitoring and weather data should be considered for predictive modelling (e.g. predicting when pulses of ammonium from external sources could stimulate T&O production) as a step forward in Smart Catchment Management. This is currently of key importance for the water companies involved in this project.

7.2.3 Increased cyanobacterial biomass with surface mixers

In this thesis, the hypothesis that surface mixers cannot successfully control cyanobacteria by light-limitation in shallow reservoirs was demonstrated. Historical data analysis in Chapter 6 showed that since the switch from an air curtain to surface mixers as a means of artificial circulation at Durleigh, cyanobacterial biomass has increased. A large proportion of the increase was attributed to significantly higher counts of *Planktothrix*, which agrees with work by Reynolds et al. (1983) that demonstrated *Oscillatoria agardhii* (now *Planktothrix agardhii*) benefit from artificial mixing.

In Chapters 5 and 6, light penetration at Durleigh was shown to be very low and the Z_m:Z_{eu} ratio was consistently > 2 through 2018, further benefiting the low light adapted *Planktothrix*. Chapter 5 showed that artificial circulation dominated over vertical velocities of cells, resulting in the passive transport of cells through the water column that favours cyanobacterial species such as *Planktothrix*. Increased

cyanobacterial biomass through artificial mixing creates interlinked feedbacks (Figure 7.1) that contribute to sustained high cyanobacterial biomass. Therefore, in shallow, eutrophic drinking water reservoirs, artificial circulation is unlikely to effectively light-limit phytoplankton and suppress photosynthesis (Objective 3, Chapter 1). Instead an increase in biomass and community change to favour cyanobacteria was observed as a consequence of artificial circulation with surface mixers, which is an important consideration for water quality managers seeking in-reservoir solutions to control cyanobacterial productivity.

Some studies with bubble plumes and diffusers have shown that intermittent operation of these artificial mixing techniques have effectively reduced cyanobacterial biomass or shifted community assemblage away from those dominated by cyanobacteria (Visser et al., 2016). For artificial circulation with surface mixers, it is unlikely that intermittent operation will achieve a reduction in biomass or shift away from cyanobacteria-dominated assemblages. Changing the flow rates of the mixers with the changing water level throughout the year could reduce sediment resuspension, and potentially reduce the internal loading of inorganic nutrients from interstitial water to the overlying water column, so there is need to find the optimal surface mixer power to depth ratio. However, establishing the correct flow rate for a specific water depth to transport DO to the sediment water interface without disturbing the sediments will be very difficult, especially in reservoirs that are also exposed to naturally induced mixing processes, summer drawdown, and variable pumped filling. Therefore, further investigation into optimal operational conditions for surface mixers could be conducted, but the viability of maintaining optimal conditions throughout the year in a drinking water reservoir needs to be considered.

Project Deliverable: It is recommended that if water companies aim to reduce cyanobacterial biomass or shift phytoplankton community structure away from an assemblage dominated by cyanobacteria, in shallow, hypereutrophic reservoirs, then artificial circulation with surface mixers is unlikely to be successful. Instead, surface mixer operation favours low light adapted cyanobacteria, such as *Planktothrix*, which increases T&O metabolite risk during variable environmental conditions that are likely to be more unpredictable with climate change. Therefore, water companies are advised against the use of surface mixers to address issues associated with high cyanobacterial biomass in shallow, hypereutrophic, drinking water reservoirs and alternate solutions should be sought instead.

7.2.4 Effects of surface mixers on the production of T&O metabolites

An innovative aspect of this work was the examination of the effects of artificial circulation on the production of taste and odour (T&O) metabolite production in cyanobacteria. Identification that cyanobacterial biomass and T&O metabolite concentrations are not always correlated led to the development of the research question: do surface mixers affect the production of T&O compounds in cyanobacteria if their primary aim is to reduce cyanobacterial biomass (Objective 4, Chapter 1). Findings presented in Chapter 6 suggest that mixer operation does not directly influence T&O production. Despite the significant increase in T&O-producing *Planktothrix* since the mixers were installed, no change in T&O was observed through 2018 when continuous favourable weather conditions prevailed, and no external pulses of nutrients occurred.

In Chapter 6, building on the work of Post et al. (1985), it is proposed that pigment synthesis is favoured over T&O metabolite production along the pathways of isoprenoid synthesis in *Planktothrix* due to the light-dark cycle induced by the mixers. Moreover, the environment created by the mixers at Durleigh entrains *Planktothrix* filaments and mixes them between the euphotic zone and bottom waters, where sediment resuspension and mineralisation of organic matter appears to be introducing interstitial inorganic nutrients into the water column. Therefore, a stable and continuous growth environment for *Planktothrix* is created, which reduces the risk of rapid growth and subsequent production of T&O metabolites. However, the *Planktothrix*-dominated environment created by the mixers is effectively the perfect petri dish for a perturbation, such as an increase in ammonium concentration or changing environmental conditions, to provoke rapid growth and trigger T&O production.

In terms of water quality management, artificial circulation with surface mixers will not effectively reduce cyanobacterial biomass in shallow, eutrophic reservoirs. If T&O metabolite (and toxin) concentrations are the primary concern relating to cyanobacteria for water quality managers, then using in-reservoir management techniques that aim to control biomass are unlikely to be successful.

Here, we have presented an interesting hypothesis that under light-limiting, continuously mixed conditions promoted by artificial circulation, pigment synthesis is favoured over T&O metabolite production in *Planktotrhix.* Although not mechanistic proof, this hypothesis lends itself to further work. For example, cultures of *Planktothrix*

could be subjected to different conditions (light availability/nutrient availability) where T&O and pigment production could be assessed.

Project Deliverable: Artificial circulation with surface mixers increases cyanobacterial biomass and favourable conditions for T&O producing cyanobacteria, which raises the potential for T&O events, particularly during environmentally variable conditions that can lead to nutrient pulses that trigger production. Consequently, there is increased potential for customer contacts about wholesomeness, which is a more immediate pressure for water companies than saving money in the treatment process and reducing potential build-up of MnO_2 in the distribution network to maintain assets over the longer term.

7.2.5 Decreased soluble manganese concentrations with surface mixers

In Chapter 5, artificial circulation with surface mixers was shown to have a limited range of influence in a shallow reservoir, which agrees with Lawson and Anderson (2007). However, contrary to Lawson and Anderson (2007), artificial circulation at Durleigh successfully reduced dissolved oxygen (DO) gradients. Improved distribution of DO through the water column locally is attributed to the significant reduction in soluble manganese observed at the intake since the air curtain was replaced with surface mixers. The reduction in soluble manganese occurred immediately after the installation of the surface mixers at Durleigh, which suggests the improved DO distribution through the water column facilitates the adsorption of Mn^{2+} to organic matter suspended in the water column. A reduction in soluble manganese concentrations at the intake is a benefit of artificial circulation with surface mixers as it minimises concerns regarding the build-up of manganese oxides in the treatment works and the network.

Project Deliverable: In chapters 4 and 6, it was shown that although cyanobacterial biomass increases the potential for T&O production, it does not correlate with T&O metabolite concentrations over time and therefore artificial circulation that aims to address biomass is unlikely to minimise risk of T&O events in drinking water reservoirs. Therefore, the water treatment works will need to have GAC/PAC facilities to deal with potential T&O events, which is counterintuitive for having both in-reservoir management and expensive treatment. The benefits of significantly decreasing soluble metal concentrations at the intake need to be weighed against the negative effects of increased cyanobacterial biomass and risk of T&O events to determine whether

artificial circulation in a shallow eutrophic drinking water reservoir is a good in-reservoir management technique.

7.3 Further Work

In addition to both the valuable applications of this research for water quality management and improved scientific understanding of how surface mixers affect raw water quality in shallow drinking water reservoirs, this current work has also highlight new research questions and presented new hypotheses that require further investigation. In this section, the key research directions from the current work are discussed.

7.3.1 Pigment synthesis over T&O metabolite production in cyanobacteria

In Chapter 6, a significant increase in cyanobacterial biomass was observed and attributed to surface mixer operation, although surface mixer operation did not appear to affect T&O metabolite concentrations in the reservoir or at the intake. It was hypothesised that the light-dark cycle cyanobacterial cells are subjected to as a result of mixer operation tends to favour pigment synthesis over T&O synthesis along the pathways of isoprenoid synthesis in *Planktothrix*. To investigate this hypothesis further, mesocosm experiments would provide a good opportunity to test these complex interactions between mixing, light availability, nutrient availability, and T&O metabolite production. For example, with multiple mesocosms filled with water with a culture of *Planktothrix*, mixing regimes can be configured to imitate surface mixer operation and light-dark cycling can be manipulated, with no-mixing controls for comparison. To advance work by Post et al. (1985), nutrient availability can be altered between mesocosms, with continuous supply and pulsed supply, which would enable the assessment of whether pulsed supply of ammonium can trigger T&O metabolite production over pigment synthesis in *Planktothrix* and test the hypotheses developed from this thesis (Chapters 4 and 6).

7.3.2 Variable flow rate of surface mixers with level change

In Chapter 5, localised sediment resuspension was observed as a result of surface mixer operation, which was attributed to the increased turbidity and total metal concentrations at the intake (Chapter 6). The risk of sediment resuspension is high in

shallow drinking water reservoirs and has been associated with negative feedbacks contributing to elevated cyanobacterial biomass (Figure 7.1) and higher concentrations of total metals (Figure 7.2). These surface mixers have variable flow rates so there is the potential to investigate how changing the flow rates of the mixers affects the water quality at the intake. Although the risk of sediment resuspension may be reduced with lower mixer flow rates, the distribution of dissolved oxygen through the water column may be compromised, which could lead to other water quality issues, such as internal loading of nutrients and soluble metals. Based on the findings from this research, Wessex Water have been trialling different flow rates for their surface mixers at Durleigh to see whether water quality improves if flow rates are varied through the year with summer drawdown.

7.4 Summary

This project has shown that artificial circulation using surface mixers in a shallow, turbid, hypereutrophic reservoirs favours cyanobacterial dominance and increased biomass rather than controlling cyanobacteria through light-limitation. Instead the cycling of cells between light and dark conditions is advantageous for the low light adapted and T&O producing *Planktothrix.* Enhanced biomass and favourable conditions increase the potential for T&O metabolite production, although under warm, stable weather conditions, pigment synthesis is likely favoured over T&O production. Nevertheless, with the changing climate, increased variability in weather conditions could prompt nutrient pulses from external or internal sources (or both) that trigger T&O metabolite production in cyanobacteria. Ammonium appears to be important in the production of T&O metabolites and should be monitored more closely to help with predicting T&O events in drinking water reservoirs, whether artificially mixed or not. Overall, it is suggested that because surface mixer operation in shallow reservoirs promote favourable conditions for T&O producing cyanobacteria and increases the risk of T&O events that impact the wholesomeness of water provided to the customer, these devices are unsuitable for in-reservoir water quality management in shallow drinking water reservoirs.

8.0 BIBLIOGRAPHY

Abesser, C. Robinson, R. 2010. Mobilisation of iron and manganese from sediments of a Scottish upland reservoir, *Journal of Limnology*, 69, 12. https://doi.org/10.3274/JL10-69-1-04.

Achmad, M. 2009. Predicting the Effects of Mechanical Destratifiers on Water Quality in Toowoomba's Reservoirs, PhD Thesis, University of Southern Queensland.

Adams, D.D., Matisoff, G., Snodgrass, W.J. 1982. Flux of reduced chemical constituents (Fe^{2+}, Mn^{2+}, NH_4^+ and CH_4) and sediment oxygen demand in Lake Erie, *Hydrobiologia*, 92, 405-414. https://doi.org/10.1007/PL00020031.

Alghanmi, H.A., Alkam, F.M., Al-Taee, M.M. 2018. Effect of light and temperature on new cyanobacteria producers for geosmin and 2-methylisoborneol, *J. Appl. Phycol.*, 30, 319-328. https://doi.org/10.1007/s10811-017-1233-0.

Andersen, I.M., Williamson, T.J., Gonzalez, M.J., Vanni, M.J. 2019. Nitrate, ammonium, and phosphorus drive seasonal nutrient limitation of chlorophytes, cyanobacteria, and diatoms in a hypereutrophic reservoir, *Limnology and Oceanography*, https://doi.org/10.1002/lno.11363.

Ashby, S.L., Kennedy, R.H. 1993. *Effects of Artificial Destratification on Water Quality at East Sidney Lake, New York*, Final Report, Army Engineer Waterways Experiment Station, U.S.

Ashitani, K., Hishida, Y., Fujiwara, K. 1988. Behaviour of musty odorous compounds during the process of water treatment, *Water Sci. Technol.*, 20, 261-267. https://doi.org/10.2166/wst.1988.0251.

Aubriot, L., Bonilla, S. 2012. Rapid regulation of phosphate uptake in freshwater cyanobacterial blooms, *Aquatic Microbial Ecology*, 67, 251-263. https://doi.org/10.3354/ame01596.

Bai, X., Zhang, T., Wang, C., Zong, D., Li, H. Yang, Z. 2017. Occurrence and distribution of taste and odor compounds in subtropical water supply reservoirs and their fates in water treatment plants, *Enrivon. Sci. Pollut. R.*, 24, 2904-2913. https://doi.org/10.1007/s11356-016-7966-5.

Balistrieri, L.S., Murray, J.W., Paul, B. 1992. The cycling of iron and manganese in the water column of Lake Sammamish, Washington, *Limnology and Oceanography*, 37, 510-528.

Balmelle, B., Nguyen, K.M., Capdeville, B., Cornier, J.C., Deguin, A. 1992. Study of factors controlling nitrite build-up in biological processes for water nitrification, *Water Science and Technology*, 26, 1017-1025.

Barton, D.R., Kelton, N., Edey, R.I. 2000. The effects of carp (*Cyprinus carpio* L.) on sediment export from a small urban impoundment, *Journal of Aquatic Ecosystem Stress and Recovery*, 8, 155-159. https://doi.org/10.1023/A:1011423432727.

Batchelor, G.K., 1959. Small-scale variation of convected quantities like temperature in turbulent fluid, *J. Fluid Mech.*, 5, 113-133. https://doi.org/10.1017/S0022112059000106.

Bates, B.C., Kundzewicz, Z.W., Wu, S., Palutikof, J.P. 2008. Climate change and water, *Technical paper of the Intergovernmental Panel on Climate change, IPCC Secretariat*, Geneva 2008. http://hdl.handle.net/123456789/552.

Beale, R., Jackson, T. 1990. Kohonen Self-Organising Networks, In: Beale and Jackson (eds.), *Neural Computing: An Introduction*, Taylor and Francis Group, New York.

Beaver, J.R., Tausz, C.E., Scotese, K.C., Pollard, A.I., Mitchell, R.M. 2018. Environmental factors influencing the quantitative distribution of microcystin and common potentially toxigenic cyanobacteria in U.S. lakes and reservoirs, *Harmful Algae*, 78, 118-128. https://doi.org/10.1016/j.hal.2018.08.004.

Bednarek, A., Zalewski, M. 2007. Potential effects of enhancing denitrification rates in sediments of the Sulejow reservoir, *Environmental Protection Engineering*, 33, 35.

Behr, M., Serchi, T., Cocco, E., Guignard, C., Sergeant, K., Renaut, J., Evers, D., 2014. Description of the mechanisms underlying geosmin production in *Penicillium expansum* using proteomics, *J Proteomics*, 96, 13-28. https://doi.org/10.1016/j.jprot.2013.10.034.

Bell, R.T., Ahlgren, I. 1987. Thymidine incorporation and microbial respiration in the surface sediment of a hypereutrophic lake, *Limnology and Oceanography*, 32, 476-482.

Bentley, R., Meganathan, R. 1981. Geosmin and methylisoborneol biosynthesis in Streptomyces, *FEBS Letters*, 125, 220-222.

Betancourt, C., Jorge, F., Suarez, R., Beutel, M., Gebremariam, S. 2010. Manganese sources and cycling in a tropical eutrophic water supply reservoir, Paso bonito Reservoir, Cuba, *Lake and Reservoir Management*, 26, 217-226. https://doi.org/10.1080/07438141.2010.519856.

Beutel, M.W., Horne, A.J. 1999. A Review of the effects of hypolimnetic oxygenation on lake and reservoir water quality, *Journal of Lake and Reservoir Management*, 15, 285-297. https://doi.org/10.1080/07438149909354124.

Beutel, M., 2006. Inhibition of ammonia release from anoxic profundal sediments in lakes using hypolimnetic oxygenation, *Ecol. Eng.*, 28, 271-279. https://doi.org/10.1016/j.ecoleng.2006.05.009.

Beutel, M., Hannoun, I., Pasek, J., Kavanagh, K.B. 2007. Evaluation of Hypolimnetic Oxygen Demand in a Large Eutrophic Raw Water Reservoir, San Vicente Reservoir, Caif., *Journal of Environmental Engineering*, 133. https://doi.org/10.1061/(ASCE)0733-9372(2007)133:2(130).

Blomqvist, P., Pettersson, A., Hyenstran, P., 1994. Ammonium-nitrogen – a key regulatory factor causing dominance of non-nitrogen-fixing cyanobacteria in aquatic systems, *Arch. Hydrobiol.*, 132, 141-164.

Bormans, M., Jančula, D., Maršálek, B. 2016. Controlling internal phosphorus loading in lakes by physical methods to reduce cyanobacterial blooms: a review, *Aquatic Ecology*, 50, 407-422. https://doi.org/10.1007/s10452-015-9564-x.

Boros, G., Søndergaard, M., Takács, P., Vári, Á., Tátri, I. 2011. Influence of submerged macrophytes, temperature, and nutrient loading on the development of redox and nutrient loading on the development of redox potential around the sediment-water interface in lakes, *Hydrobiologia*, 665, 117-127. https://doi.org/10.1007/s10750-011-0609-4.

Boström, B., Andersen, J.M., Fleischer, S., Jansson, M., 1988. Exchange of phosphorus across the sediment-water interface, *Hydrobiologia*, 170, 229-244. https://doi.org/10.1007/BF00024907.

Breard, G.T., 2017. Evaluating Self-Organising Map Quality measure as convergence criteria, Open access master's thesis paper 1033. http://digitalcommons.uri.edu/theses/1033.

Bryant, L.D., Hsu-Kim, H., Gantzer, P.A., Little, J.C. 2011. Solving the problem at the source: Controlling Mn release at the sediment-water interface via hypolimnetic oxygenation, *Water Research*, 45, 6381-6392. https://doi.org/10/1016/j.watres.2011.09.030.

Budzyńska, A., Rosińska, J., Pełechata, A., Toporowska, M., Napiórkowska-Krzebietke, A., Kozak, A., Messyasz, B., Pęczuła, W., Kokociński, M., Szeląg-Wasielewska, E., Grabowska, M., Mądrecka, B., Niedźwiecki, M., Alcaraz Parraga, P., Pełechaty, M., Karpowicz, M., Pawlik-Skowrońska, B. 2019. Environmental factors driving the occurrence of the invasive cyanobacterium *Sphaerospermosis aphanizomenonoides* (Nostocales) in temperate lakes, *Science of the Total Environment*, 650, 1338-1347. https://doi.org/10.1016/j.scitotenv.2018.09.144.

Carlson, R.E., 1977. A trophic state index for lakes, *Limnol. and Oceanogr.*, 22, 361-369.

Chaffin, J.D., Bridgeman, T.B., Bade, D.L. 2013. Nitrogen constrains the growth of late summer cyanobacterial blooms in Lake Erie, *Advances in Microbiology*, 3, 16-26. https://dx.doi.org/10.4236/aim.2013.36A003.

Chanson, H., Takeuchi, M., Trevethan, M. 2008. Using turbidity and acoustic backscatter intensity as surrogate measures of suspended sediment concentration in a small subtropical estuary, *Journal of Environmental Management*, 88, 1406-1416. https://doi.org/10.1016/j.jenvman.2007.07.009.

Chapnick, S.D., Moore, W.S., Nealson, K.H. 1982. Microbially mediated manganese oxidation in a freshwater lake, *Limnology and Oceanography*, 27, 1004-1014. https://doi.org/10.4319/lo.1982.27.6.1004.

Chaui, X., Ding, W., Chen, X., Wang, X., Miao, A., Xi, B., He, L., Yang, L. 2011. Phosphorus release from cyanobacterial blooms in Meiliang Bay of Lake Taihu, China, *Ecological Engineering*, 37, 842-849. https://doi.org/10.1016/j.ecoleng.2011.01.001.

Chen, X., Yang, L., Xiao, L., Miao, A., Xi, B., 2012. Nitrogen removal by denitrification during cyanobacterial bloom in Lake Taihu, *J Freshwater Ecol.*, 27, 243-258. https://doi.org/10.1080/02705060.2011.644405.

Chong, S., Lee, H., An, K.-G. 2018. Predicting taste and odor compounds in a shallow reservoir using a three-dimensional hydrodynamic ecological model. *Water*, 10, https://doi.org/10.3390/w10101396.

Chowdhury, S., Jafar Mazumder, M.A., Al-Attas, O., Husain, T. 2016. Heavy metals in drinking water: Occurrences, implications, and future needs in developing countries, *Science of the Total Environment*, 569-570, 476-488. https://doi.org/10.1016/j.scitotenv.2016.06.166.

Chröst, R.J., Overbeck, J. 1987. Kinetics of Alkaline Phosphatase activity and phosphorus availability for phytoplankton and bacterioplankton in Lake Plußsee (North German Eutrophic Lake), *Microb. Ecol.*, 13, 229-248. https://doi.org/10.1007/BF02025000.

CH2M Hill, 2013. Assessment of Technologies for Dissolved Oxygen Improvement in J.C. Boyle Reservoir, Final Report, Prepared for PacifiCorp Energy, Portland, Oregon.

Chung, E.G., Bombardelli, F.A., Schladow, S.G. 2009. Modelling linkages between sediment resuspension and water quality in a shallow, eutrophic, wind-exposed lake, *Ecologcial Modelling*, 220, 1251-1265. https://doi.org/10.1016/j.ecolmodel.2009.01.038.

Collos, Y., Berges, J.A. 2009. Nitrogen metabolism in phytoplankton, In: Duarte, C.M., Lot Helgueras, A. (eds.), *Marine Ecology*, Encyclopaedia of Life Support Systems (EOLSS).

Colter, A., Mahler, R.L. 2006. *Iron in drinking water*, Moscow, Idaho: University of Idaho.

Condie, S.A., Webster, I.T. 2002. Stratification and circulation in a shallow turbid waterbody, *Environ. Fluid Mech.*, 2, 177-196. https://doi.org/10.1023/A:101989.

Cooke, G.D., Welch, E.B., Peterson, S.A., Newroth, P.R. 1993. Artificial Circulation, In: Cooke, G.D., Welch, E.B., Peterson, S.A., Newroth, P.R. (eds.), *Restoration and Management of lakes and reservoirs*, Lewis Publishers, London.

da Silva Brito, M.T., Duarte-Neto, P.J., Molica, R.J.R. 2018. *Cylindrospermopsis raciborskii* and *Microcystis aeruginosa* competing under different conditions of pH and inorganic carbon, *Hydrobiologia*, 815, 253-266. https://doi.org/10.1007/s10750-018-3567-2.

David, M.B., Wall, L.G., Royer, T.V., Tank, J.L. 2006. Denitrification and the nitrogen budget of a reservoir in an agricultural landscape, *Ecological Applications*, 16, 2177-2190. https://doi.org/10.1890/1501-0761(2006)016[2177:DATNBO]2.0.CO;2.

Davison, W. 1993. Iron and Manganese in lakes, *Earth-Science Reviews*, 34, 119-163. https://doi.org/10.1016/0012-8252(93)90029-7.

De Araujo Torres, C., Lurling, M., Marinho, M.M. 2016. Assessment of the effects of light availability on growth and competition between strains of PLanktothrix agardhii and Microcystis aeruginosa, *Microbial Ecology*, 71, 802-813. https://doi.org/10.1007/s00248-015-0719-z.

De Schamphelaire, L., Rabaey, K., Boon, N., Verstraete, W., Boeckx, P. 2007. Minireview: the potential of enhanced manganese redox cycling for sediment oxidation, *Geomicrobiology Journal*, 24, 547-558. https://doi.org/10.1080/01490450701670137.

Delpla, I., Jung, A.-V., Baures, E., Clement, M., Thomas, O. 2009. Impacts of climate change on surface water quality in relation to drinking water production, *Environment International*, 35, 1225-1233. https://doi.org/10.1016/j.envint.2009.07.001.

den Heyer, C., Kalff, J. 1998. Organic matter mineralisation rates in sediments: A within- and among-lake study, *Limnology and Oceanography*, 43, 695-705. https://doi.org/10.4319/lo.1998.43.4.0695.

Dokulil, M.T., Teubner, K. 2003. Steady state phytoplankton assemblages during thermal stratification in deep alpine lakes. Do they occur? *Hydrobiologia*, 502, 65-72. https://doi.org/10.1023/B:HYDR.0000004270.70364.f3.

Dunlap, C.R., Sklenar, K., Blake, L. 2015. A costly endeavour: addressing algae problems in a water supply, *J. Am. Water Work. Assoc.*, 107, E255-E262. https://doi.org/10.5942/jawwa.2015.107.0055.

Effler, S.W., Matthews, D.A. 2007. Sediment resuspension and drawdown in a water supply reservoir, *Journal of the American Water Resources Association*, 40, 251-264. https://doi.org/10.1111/j.1752-1688.2004.tb01023.x.

Eggleston, M. 2012. Impact of Sediment resuspension events on the availability of heavy metals in freshwater sediments, PhD Thesis, University of Michigan. http://hdl.handle.net/2027.42/89962.

Elçi, S. 2008. Effects of thermal stratification and mixing on reservoir water quality, *Limnology*, 9, 135-142. https://doi.org/10.1007/s10201-008-0240-x.

Elliott, S., Swan, D. 2013. Source Water Management – Deep Reservoir Circulation, 7th Annual WIOA NSW Water Industry Operations Conference, Exhibition Park in Canberra, 84-91. http://www.wioa.org.au/conference_papers/2013_nsw/documents/Stephen_Elliott.pdf.

Environment Agency (EA) 2016. Nitrate Vulnerable Zone (NVZ) designation, 2017 Eutrophication (lakes), Durleigh Reservoir, [Online]. Available: http://apps.environment-agency.gov.uk/static/documents/nvz/NVZ2017_EL135_Durleigh_Reservoir_Datasheet.pdf. [Accessed 18 June 2019].

Falconer, I.R. 1999. An overview of problems caused by toxic blue-green algae (cyanobacteria) in drinking and recreational water, *Envion. Toxicol.*, 14, 5-12. https://doi.org/10.1002/(SICI)1522-7278(199902)14:1<5::AID-TOX3>3.0.CO;2-0.

Fallon, R.D., Brock, T.D. 1979. Decomposition of blue-green algal (cyanobacterial) blooms in Lake Mendota, Wisconsin, *Applied and Environmental Microbiology*, 37, 820-830.

Fernández, C., Estrada, V., Parodi, E.R. 2015. Factors triggering cyanobacteria dominance and succession during blooms in a hypereutrophic drinking water supply reservoir, *Water Air & Soil Pollution*, 226. https://doi.org/10.1007/s11270-014-2290-5.

Fischer, H.B., List, E.J., Koh, R.C., Imberger, J., Brooks, N.H. 1979. *Mixing in inland and coastal waters*, Academic Press, New York. https://doi.org/10.1016/B978-0-08-051177-1.50010-6.

Flores, E., Herrero, A., 2005. Nitrogen assimilation and nitrogen control in cyanobacteria, *Biochem. Soc. T.*, 33, 164-167. https://doi.org/10.1042/BST0330164.

Frisbie, S.H., Mitchell, E.J., Dustin, H., Maynard, D.M., Sarkar, B. 2012. World Health Organisation discontinues its drinking water guideline for manganese, *Environmental Health Problems*, 120, 775-778. https://doi.org/10.1289/ehp.1104693.

Gantzer, P.A., Bryant, L.D., Little, J.C. 2009. Controlling soluble iron and manganese in a water supply reservoir using hypolimnetic oxygenation, *Water Research*, 43, 1285-1294. https://doi.org/10.1016/j.watres.2008.12.019.

Gao, L., Zhang, L., Hou, J., Wei, Q., Fu, F., Shao, H. 2013. Decomposition of macroalgal blooms influences phosphorus release from the sediments and implications for coastal restoration in Swan Lake, Shandong, China, *Ecological Engineering*, 60, 19-28. https://doi.org/10.1016/j.ecoleng.2013.07.055.

Gilbert, P.M., Wilkerson, F.P., Dugdale, R.C., Raven, J.A., Dupont, C.L., Leavitt, P.R., Parker, A.E., Burkholder, J.M., Kana, T.M. 2016. Pluses and minuses of ammonium and nitrate uptake and assimilation by phytoplankton and implications for productivity and community composition, with emphasis on nitrogen-enriched conditions, *Limnol. Oceanogr.*, 61, 165-197. https://doi.org/10.1002/lno.10203.

Golden, J.W., Yoon, H.-S. 2003. Heterocyst development in *Anabaena*, *Current Opinion in Microbiology*, 6, 557-563. https://doi.org/10.1016/j.mib.2003.10.004.

Gons, H.J., Burger-Wiersma, T., Otten, J.H., Rijkeboer, M. 1992. Coupling of phytoplankton and detritus in a shallow, eutrophic lake (Lake Loosdrecht, The Netherlands), *Hydrobiologia*, 233, 51-59. https://doi.org/10.1007/BF00016095.

Graham, J.L., Loftin, K.A., Meyer, M.T., Ziegler, A.C. 2010. Cyanotoxin mixtures and taste and odour compounds in cyanobacterial blooms from the Midwestern United States, *Environ. Sci. Technol.*, 44, 7361-7368. https://doi.org/10.1021/es1008938.

Gray, E., Mackay, E., Elliott, A., Folkard, A.M., Jones, I. 2020. Wide-spread inconsistency in estimation of lake mixed depth impacts interpretation of limnological processes, *Water Research*, 168, 115136. https://doi.org/10.1016/j.watres.2019.115136.

Greenwald, M.J., Redding, A.M., Cannon, F.S. 2015. A rapid kinetic dye test to predict the adsorption of 2-methylisoborneol onto granular activated carbons and to identify the influence of pore volume distributions, *Water Res.*, 68, 784-792. https://doi.org/10.1016/j.watres.2014.10.022.

Gudasz, C., Sobek, S., Bastviken, D., Koehler, B., Tranvik, L.J. 2015. Temperature sensitivity of organic carbon mineralisation in contrasting lake sediments, *Journal of Geophysical Research: Biogeosciences*, 120. https://doi.org/10.1002/2015JG002928.

Gurney Environmental Ltd. 2018. Raw Water Storage Conditioning with the ResMix System, [Online]. Available: https://gurneyenvironmental.com/index.php/news/item/68-gurney-environmental-ltd-provides-new-treatment-facility-at-windsor-estate [Accessed 8 August 2019].

Ha, H.K., Hsu, W.-Y., Maa, J.P.-Y., Shao, Y.Y., Holland, C.W. 2009. Using ADV backscatter strength for measuring suspended cohesive sediment concentration, *Continental Shelf Research*, 29, 1310-1316. https://doi.org/10.1016/j.csr.2009.03.001.

Hafeman, D., Factor-Litvak, P., Cheng, Z., van Geen, A., Ahsan, H. 2007. Association between manganese exposure through drinking water and infant mortality in Bangladesh, *Environmental Health Perspectives*, 115, 1107-1112. https://doi.org/10.1289/ehp.10051.

Hall, S.R., Smith, V.H., Lytle, D.A., Leibold, M.A. 2005. Constraints on primary producer N:P stoichiometry along N:P supply ratio gradients, *Ecology*, 86, 1894-1904. https://doi.org/10.1890/04-1045.

Hammer, O., Harper, D.A.T., Ryan, P.D. 2001. PAST: Paleontological statistics software package for education and data analysis. https://palaeo-electronica.org/2001_1/past/past.pdf (Accessed 27 March 2019).

Hammer, K.J., Kragh, T., Sand-Jensen, K. 2019. Inorganic carbon promotes photosynthesis, growth, and maximum biomass of phytoplankton in eutrophic water bodies, *Freshwater Biology*, 64, 1956-1970. https://doi.org/10.1111/fwb.13385.

Hampel, J.J., McCarthy, M.J., Neudeck, M., Bullerjahn, G.S., McKay, R.M.L., Newell, S.E. 2019. Ammonium recycling supports toxic *Planktothrix* blooms in Sandusky Bay, Lake Erie: Evidence from stable isotope and metatranscriptome data, Harmful Algae, 81, 42-52. https://doi.org/10.1016/j.hal.2018.11.011.

Hansen, P.S., Philps, E.J., Aldridge, F.J. 2009. The effects of sediment resuspension on Phosphorus Available for algal growth in a shallow subtropical lake, Lake Okeechobee, *Lake and Reservoir Management*, 13, 154-159. https://doi.org/10.1080/0743814970354306.

Harris, T.D., Smith, V.H., Graham, J.L., Van de Waal, D.B., Tedesco, L.P., Clercin, N., 2016. Combined effects of nitrogen to phosphorus and nitrate to ammonia ratios on cyanobacterial metabolite concentrations in eutrophic Midwestern USA reservoirs, *Inland Waters*, 6, 199-210. https://doi.org/10.5268/IW-6.2.938.

Heath, M., Wood, S.A., Young, R.G., Ryan, K.G. 2016. The role of nitrogen and phosphorus in regulating *Phormidium* sp. (cyanobacteria) growth and anatoxin production, *FEMS Microbiol. Ecol.*, 92. https://doi.org/10/1093/femsec/fiw021.

Heo, W.M., Kim, B. 2004. The effect of artificial destratification on phytoplankton in a reservoir, *Hydrobiologia*, 524, 229-239. https://doi.org/10.1023/B:HYDR.0000036142.74589.a4.

Hill, A.R. 1988. Factors influencing nitrate depletion in a rural stream, *Hydrobiologia*, 160, 111-122. https://doi.org/10.1007/BF00015474.

Ho, L., Hoefel, D., Bock, F., Saint, C.P., Newcombe, G. 2007. Biodegradation rate of 2-methylisoborneol (2-MIB) and geosmin through sand filters and in bioreactors, *Chemosphere*, 66, 2210-2218. https://doi.org/10.1016/j.chemosphere.2006.08.016.

Hobson, P., Dickson, S., Burch, M., Thorne, O., Tsymbal, L., House, J., Brookes, J., Chang, D., Kao, S.-C., Lin, T.-F., Bierlein, K., Little, J. 2012. Alternative and Innovative Methods for Source Water Management of Algae and Cyanobacteria, Water Research Foundation, Report 4094.

Højerslev, N.K. 1986. Visibility of the sea with special reference to the Secchi disc, *Society of Photo-Optical Instrumentation Engineers (SPIE)*, Ocean Optics VIII, 637, 294-305.

Højerslev, N.K. 1987. Daylight measurement appropriate for photosynthetic studies in natural sea water, *J. Cons. Int. Explor. Mer*, 38, 131-146.

Holland, D.P. 2010. Sinking rates of phytoplankton filaments oriented at different angles: theory and physical model, *Journal of Plankton Research,* 32, 1327-1336. https://doi.org/10.1093/plankt/fbq044.

Hollister, J.W., Kreakie, B.J. 2016. Associations between chlorophyll *α* and various microcystin -health advisory concentrations, F1000Research, 5. https://doi.org/10.12688/f1000research.7955.2.

Holmes, R.W. 1970, The Secchi disk in turbid coastal waters, *Limnol. Oceanogr.*, 15, 688-694.

Howarth, R.W., Swaney, D.P., Billen, G., Garnier, J., Hong, B., Humborg, C., Johnes, P., Mörth, C.-M., Marino, R. 2012. Nitrogen fluxes from the landscape are controlled by net anthropogenic nitrogen inputs and by climate change, *Frontiers in Ecology and the Environment,* 10, 37-43. https://doi.org/10.1890/100178.

Huisman, J., Sharples, J., Stroom, J.M., Visser, P.M., Kardinaal, W.E.A., Verspagen, J.M.H., Sommeijer, B. 2004. Changes in turbulent mixing shift competition for light between phytoplankton species, *Ecology*, 85, 2960-2970. https://doi.org/10.1890/03-0763.

IBM Corp. Released 2017. IBM SPSS Statistics for Windows, Version 25.0. Armonk, NY: IBM Corp.

Imberger, J. 1985. The diurnal mixed layer[1], *Limnology and Oceanography*, 30, 737-770. https://doi.org/10.4319/lo.1985.30.4.0737.

Imboden, D.M. 1980. The impact of pumped storage operation on the vertical temperature structure in a deep lake: a mathematical model. In: Clugston, J.P. (Ed.), Proceedings of the Clemson Workshop on Environmental Impacts of Pumped Storage Hydroelectric Operations. Fish and Wildlife Services, US Department of the Interior, FWS/OBS-80/28, 125-146.

Imteaz, M.A., Asaeda, T. 2000. Artificial mixing of lake water by bubble plume and effects of bubbling operations on algal bloom, *Water Research*, 34, 1919-1929. https://doi.org/10.1016/S0043-1354(99)00341-3.

Ivey, G.N., Imberger, J. 1991. On the nature of turbulence in a stratified fluid. Part I: The energetics of mixing, *J. phys. Oceanogr.*, 21, 650-658. https://doi.org/10.1175/1520-0485(1991)021<0650:OTNOTI>2.0.CO;2.

Ivey, G.N., Winters, K.B., Koseff, J.R. 2008. Density stratification, turbulence, but how much mixing?, *Annu. Rev. Fluid Mech.*, 40, 169-184. https://doi.org/annurev.fluid.39.050905.110314.

James, T.R., Chimney, M.J., Sharfstein, B., Engstrom, D.R., Schottler, S.P., East, T., Jin, K.R. 2008. Hurricane effects on a shallow lake ecosystem, Lake Okeechobee, Florida (USA), *Fundamental and Applied Limnology*, 172, 273-287. https://doi.org/10.1127/1863-9135/2008/0172-0271.

Jeppesen, E., Kronvang, B., Olesen, J.E., Audet, J., Søndergaard, M., Hoffman, C.C., Andersen, H.E., Lauridsen, T.L., Liboriussen, L., Larsen, S.E., Beklioglu, M., Meerhoff, M., Özen, A., Özkan, K., 2011. Climate change effects on nitrogen loading from cultivated catchments in Europe: implications for nitrogen retention, ecological state of lakes and adaptation, *Hydrobiologia*, 663, 1-21. https://doi.org/10.1007/s10750-010-0547-6.

Jia, Z., Su, M., Liu, T., Guo, Q., Wang, Q., Burch, M., Yu, J., Yang, M. 2019. Light as a possible regulator of MIB-producing *Planktothrix* in source water reservoir, mechanism and *in-situ* verification, *Harmful Algae,* 88. https://doi.org/10.1016/j.hal.2019.101658.

Jiang, X., Jin, X., Yao, Y., Li, L., Wu, F. 2008. Effects of biological activity, light, temperature and oxygen on phosphorus release processes at the sediment and water interface of Taihu Lake, China, Water Research, 42, 2251-2259. https://doi.org/10.1016/j.watres.2007.12.003.

Jöhnk, K.D., Huisman, J., Sharples, J., Sommeijer, B., Visser, P.M., Stroom, J.M. 2008. Summer heatwaves promote blooms of harmful cyanobacteria, *Global Change Biology*, 14. https://doi.org/10.1111/j.1365-2486.2007.01510.x.

Jørgensen, K.S. 1989. Annual pattern of denitrification and nitrate ammonification in estuarine sediment, *Applied and Environmental Microbiology*, 55, 1841-1847.

Jüttner, F. 1984. Dynamics of the volatile organic substances associated with cyanobacteria and algae in a eutrophic shallow lake, *Appl. Environ. Microbiol.*, 47, 814-820.

Jüttner, F., Watson, S.B. 2007. Biochemical and ecological control of geosmin and 2-methylisoborneol in source waters, *Appl. Environ. Microbiol.*, 73, 4395-4406. https://doi.org/10.1128/AEM.02250-06.

Karlson, A.M.L., Duberg, J., Motwani, N.H., Hogfors, H., Klawonn, I., Ploug, H., Svedén, J.B., Garbaras, A., Sundelin, B., Hajdu, S., Larsson, U., Elmgren, R., Gorokhova, E. 2015. Nitrogen fixation by cyanobacteria stimulates production in Baltic food webs, *AMBIO*, 44, 413-426. https://doi.org/10.1007/s13280-015-0660-x.

Kawashima, M., Takamatsu, T., Koyama, M. 1988. Mechanisms of precipitation of manganese(II) in Lake Biwa, a fresh water lakes, *Water Research*, 22, 613-618. https://doi.org/10.1016/0043-1354(88)90062-0.

Ke, Z., Xie, P., Guo, L. 2008. Controlling factors of spring-summer phytoplankton succession in Lake Taihu (Meiliang Bay, China), *Hydrobiologia*, 607, 41-49. https://doi.org/10.1007/s10750-008-9365-5.

Keene, B. 2002. Bay of Quinte remedial action plan update on impaired beneficial use No. 9: restriction on drinking water consumption, taste and odour. Quinte Conservation Authority, Belleville, Ontario, Canada.

Kennedy, R.H., Walker, W.W. 1999. Reservoir nutrient dynamics, In: *Reservoir limnology: ecological perspectives*, 109-131.

Kerimoglu, O., Rinke, K. 2000. Stratification dynamics in a shallow reservoir under different hydro-meteorological scenarios and operational strategies, *Water Resources Research*, 49, 7518-7527 https://doi.org/10.1002/2013WR013520.

Kieber, R.J., Li, A., Seaton, P.J. 1999. Production of nitrite from the photodegradation of dissolved organic matter in natural waters, *Environ. Sci. Technol.*, 33, 993-998. https://doi.org/10.1021/es980188a.

Kim, J., Jung, S. 2008. Soluble manganese removal by porous media filtration, *Environmental Technology*, 29, 1265-1273. https://doi.org/10.1080/09593330802306139.

Kim, K., Park, C., Yoon, Y., Hwang, S.-J., 2018. Harmful cyanobacterial material production in the North Han River (South Korea): Genetic potential and temperature-dependent properties, *Int. J. Environ. Res. Public Health*, 15. https://doi.org/10.3390/ijerph15030444.

Kirk, J.T.O. 1994. *Light and Photosynthesis in Aquatic Ecosystems*, Cambridge University Press, Cambridge, UK.

Kirk, J.T.O 2011. *Light and Photosynthesis in Aquatic Ecosystems*, 3rd edn., Cambridge University Press, Cambridge, UK.

Knoppert, P.L., Rook, J.J., Hofker, T.J., Oskam, G. 1970. Destratification experiments at Rotterdam, *J. Am. Water Works Ass.*, 62, 448-454. https://doi.org/10.1002/j.1551-8833.1970.tb03940.x.

Köhler, J., Wang, L., Guislain, A., Shatwell, T. 2017. Influence of vertical mixing on light-dependency of phytoplankton growth, *Limnology and Oceanography*, 63, 1156-1167. https://doi.org/10.1002/lno.10761.

Kohonen, T., Honkela, T. 2007. Kohonen Network. *Scholarpedia Journal*, 2, 1568.

Komatsu, E., Fukushima, T., Harasawa, H. 2007. A modelling approach to forecast the effect of long-term climate change on lake water quality, *Ecol. Model.*, 209, 351-366. https://doi.org/10.1016/j.ecolmodel.2007.07.021.

Kortmann, R.W., Knoecklein, G.W., Bonnell, C.H. 1994. Aeration of stratified lakes: Theory and Practice, *Lake Reser. Manage.*, 8, 99-120. https://doi.org/10.1080/07438149409354463.

Lawson, R., Anderson, M.A. 2007. Stratification and mixing in Lake Elsinore, California: An assessment of axial flow pumps for improving water quality in a shallow eutrophic lake, *Water Research*, 41, 4457-4467. https://doi.org/10.1016/j.watres.2007.06.004.

Lee, Z., Weidemann, A., Kindle, J., Arnone, R., Carder, K.L., Davis, C. 2007. Euphotic zone depth: Its derivation and implication to ocean-color remote sensing, *Journal of Geophysical Research*, 112. https://doi.org/10.1029/2006JC003802.

Lee, J., Rai, P.K., Jeon, Y.J., Kim, K.-H., Kwon, E.E. 2017. The role of algae and cyanobacteria in the production and release of odorants in water, *Environmental Pollution*, 227, 252-262. https://doi.org/10.1016/j.envpol.2017.04.058.

Lee, K., Ho, H.-C., Marian, M., Wu, C.-H. 2014. Uncertainty in open channel discharge measurements acquired with StreamPro ADCP, *Journal of Hydrology*, 509, 101-114. https://doi.org/10.1016/j.jhydrol.2013.11.031.

Lesven, L., Gao, Y., Billon, G., Leermarkers, M., Oudanne, B., Fischer, J.C., Bayens, W. 2008. Early diagenetic processes aspect controlling the mobility of dissolved trace metals in three riverine sediment columns, *Science and the Total Environment*, 407, 447-459. https://doi.org/10.1016/j.scitotenv.2008.08.003.

Lewis, W.M., Wurtsbaugh, W.A., Paerl, H.W. 2011. Rationale for control of anthropogenic nitrogen and phosphorus in inland waters, *Environ. Sci. Technol.*, 45, 10030-10035. https://doi.org/10.1021/es202401p.

Li, Z., Zhao, Y., Xu, X., Han, R., Wang, M., Wang, G. 2018, Migration and transformation of dissolved carbon during accumulated cyanobacteria decomposition in shallow eutrophic lakes: a simulated microcosm study, *PeerJ* 6(G1):e5922; DOI 10.7717/peerj.5922.

Li, N., Huang, T., Mao, X., Zhang, H., Li, K., Wen. G., Lv, X., Deng, L. 2019. Controlling reduced iron and manganese in a drinking water reservoir by hypolimnetic aeration and artificial destratification, *Science of the Total Environment*, 658, 497-507. https://doi.org/10.1016/j.scitotenv.2019.05.445.

Lin, W., Zhao, D., Luo, J. 2018. Distribution of alkaline phosphatase genes in cyanobacteria and the role of alkaline phosphatase on the acquisition of phosphorus from dissolved organic phosphorus for cyanobacterial growth, *j. Appl. Phycol.*, 30, 839-850. https://doi.org/10.1007/s10811-017-1267-3.

Lindenschmidt, K.E., Hamblin, P.F. 1997. Hypolimnetic aeration in Lake Tegel, Berlin, *Water Research*, 31, 1619-1628. https://doi.org/10.1016/S0043-1354-(96)00407-1.

Lindenschmidt, K.E., Chorus, I. 1998. The effect of water column mixing on phytoplankton succession, diversity and similarity, *Journal of Phytoplankton Research*, 20, 1927-1951.

Lloyd, J.R. 2003. Microbial reduction of metals and radionuclides, *FEMS Microbiology Reviews*, 27, 411-425. https://doi.org/10.1016/SO168-6445(03)00044-5.

Löfgren, S., Boström, B. 1989. Interstitial water concentrations of phosphorus, iron and manganese in a shallow, eutrophic Swedish lake – Implications for phosphorus cycling, *Water Research*, 23, 1115-1125. https://doi.org/10.1016/0043-1354(89)90155-3.

Loftus, M.E., Seliger, H.H. 1975. Some limitation of the *in vivo* fluorescence technique, *Chesapeake Science*, 16, 79-92. https://doi.org/10.2307/1350685.

Lorenzen, M.W., Fast, A. 1977. A guide to aeration/circulation techniques for lake management, EPA-600/3-77-004, U.S. Environmental Protection Agency, Washington D.C.

Luhtala, H., Tolvanen, H. 2013, Optimizing the Use of Secchi Depth as a Proxy for Euphotic Depth in Coastal Waters: An empirical Study from the Baltic Sea, *ISPRS Int. J. Geo-Inf*, 2, 1153-1168. https://doi.org/10.3390/ijgi2041153.

Lund, J.W., Kipling, G., Le Cren, E.D. 1958. The inverted microscope method of estimating algae numbers and the statistical basis of estimation by counting, *Hydrobiologia*, 11, 143-170.

Ma, Z., Niu, Y., Xie, P., Chen, J., Tao, M., Deng, X. 2013. Off-flavour compounds from decaying cyanobacterial blooms of Lake Taihu, *Journal of Environmental Sciences*, 25, 495-501. https://doi.org/10.1016/S1001-0742(12)60101-6.

MacIntyre, S. 1993. Vertical mixing in a shallow, eutrophic lake: Possible consequences for the light climate of phytoplankton, *Limnology and Oceanography*, 38, 798-817. https://doi.org/10.4319/lo.1993.38.4.0798.

MacIntyre, S., Melack, J.M. 1995. Vertical and Horizontal Transport in Lakes: Linking Littoral, Benthic, and Pelagic Habitats, *Journal of the North American Benthological Society*, 14, 599-615. https://doi.org/10.2307/1467544.

Mackay, D., Yeun, A.T.K. 1983. Mass transfer coefficient correlations for volatization of organic solutes from water, *Environ. Sci. Technol.*, 17, 211-217.

Mackay, E., Jones, I., Thackery, S., Folkard, A. 2011. Spatial heterogeneity in a small, temperate lake during archetypal weak forcing conditions, *Fundam. Appl. Limnol.*, 179, 27-40. https://doi.org/10.1127/1863-9135/2011/0179-0027.

Martin, S.T. 2005. Precipitation and Dissolution of Iron and Manganese Oxides, Environmental Catalysis. https://doi.org/10.1201/9781420027679.ch3.

Matisoff, G., Watson, S.B., Guo, J., Duewiger, A., Steely, R. 2017. Sediment and nutrient distribution and resuspension in Lake Winnipeg, *Science of the Total Environment*, 575, 173-186. https://doi.org/10.1016/j.scitotenv.2016.09.227.

McCarthy, M.J., James, R.T., Chen, Y., East, T.L., Gardner, W.S. 2009. Nutrient ratios and phytoplankton community structure in the large, shallow, eutrophic, subtropical Lakes Okeechobee (Florida, USA) and Taihu (China), *Limnology*, 10, 215-227. https://doi.org/10.1007/s10201-009-0277-5.

McGinnis, D.F., Lorke, A., Wüest, A., Stöckli, A., Little, J.C. 2004. Interaction between a bubble plume and the near field in a stratified lake, *Water Resources Research*, 40, W10206. https://doi.org/10.1029/2004WR003038.

McGinnis, D.F., Wüest, A. 2005. Lake Hydrodynamics, *McGraw-Hill Yearbook of Science and Technology*, The McGraw-Hill Companies, Inc.

Melack, J.M. 1985. Interaction of detrital particulates and plankton. In: Davies, B.R., Walmsley, R.D. (eds.), *Perspectives in Southern Hemisphere Limnology. Developments in Hydrobiology*, 28, Springer, Dordrecht. http://doi.org/10/1007/978-94-009-5522-6_15.

Met Office 2016a. Exceptional warmest, September 2016, [Online]. Available: https://www.metoffice.gov.uk/binaries/content/assets/metofficegovuk/pdf/weather/learn-about/uk-past-events/interesting/2016/exceptional-warmth-september-2016---met-office.pdf. [Accessed 20 April 2020].

Met Office 2016b. Exceptionally warm and dry Spring 2011, [Online]. Available: https://www.metoffice.gov.uk/binaries/content/assets/metofficegovuk/pdf/weather/learn-about/uk-past-events/interesting/2011/exceptionally-warm-and-dry-spring-2011---met-office.pdf. [Accessed 20 April 2020].

Met Office, 2016c. Snow and low temperatures, December 2010, [Online]. Available: https://www.metoffice.gov.uk/binaries/content/assets/metofficegovuk/pdf/weather/learn-about/uk-past-events/interesting/2010/snow-and-low-temperatures-december-2010---met-office.pdf. [Accessed 20 April 2020].

Misumi, M., Katoh, H., Tomo, T., Sonoike, K. 2016. Relationship between photochemical quenching and non-photochemical quenching in six species of cyanobacteria reveals species difference in redox state and species commonality in energy dissipation, *Plant and Cell Physiology*, 57, 1510-1517. https://doi.org/10.1093.pcp/pcv185.

Morabito, G., Rogora, M., Austoni, M., Ciampittiello, M. 2018. Could the extreme meteorological events in Lake Maggiore watershed determine a climate-driven eutrophication process?, *Hydrobiologia*, 824, 163-175. https://doi.org/10.1007/s10750-018-3549-4.

Moreno-Ostos, E., Palomino-Torres, R.L., Escot, C., Blanco, J.M. 2016. Planktonic metabolism in a Mediterranean reservoir during a near-surface cyanobacterial bloom, *Limnetica*, 35, 117-130.

Morillo, S., Imberger, J., Antenucci, J.P., Copetti, D. 2009. Using Impellers to Distribute Local Nutrient Loadings in a stratified Lake: Lake Como, Italy, *Journal of Hydraulic Engineering*, 135, 564-574. https://doi.org/10.1061/(ASCE)HY.1943-7900.0000048.

Mueller, D.S., Abad, J.D., Garcia, C.M., Gartner, J.W., 2007, Errors in Acoustic Doppler Profiler Velocity Measurements Caused by Flow Disturbance, *Journal of Hydraulic Engineering*, 133. https://doi.org/10.1061/(ASCE)0733-9429(2007)133:12(1411).

Munger, Z.W., Carey, C.C., Gerling, A.B., Hamre, K.D., Doubek, J.P., Klepatzki, S.D., McClure, R.P., Schreiber, M.E. 2016. Effectiveness of hypolimnetic oxygenation of Fe and Mn in a drinking water reservoir, *Water Research*, 106, 1-14. https://doi.org/10.1016/j.watres.2016.09.038.

Murchie, E.H., Lawson, T. 2013. Chlorophyll fluorescence analysis: a guide to good practice and understanding some new applications, *J. Exp. Bot.*, 64, 3983-3998. https://doi.org/10.1093/jxb/ert208.

Naes, H., Aarnes, H., Utkilen, H.C., Nilsen, S., Skulberg, O.M. 1985. Effect of photon fluence rate and specific growth rate on Geosmin production of the cyanobacterium *Oscillatoria brevis* (Kütz.) Gom, *Appl. Environ. Microbiol.* 49, 1538-1540.

Naes, H., Post, A.F. 1988. Transient states of geosmin, pigments, carbohydrates, and proteins in continuous cultures of Oscillatoria brevis induced by changes in nitrogen supply, *Arch. Microbiology*, 150, 333-337. https://doi.org/10.1007/BF00408303.

Nealson, K.H., Myers, C.R. 1992. Microbial reduction of manganese and iron: New approaches to carbon cycling, *Applied and Environmental Microbiology*, 439-443.

Nealson, K.H., Saffarini, D. 1994. Iron and manganese in anaerobic respiration – environmental significance, physiology, and regulation, *Annual Review of Microbiology*, 48, 311-343. https://doi.org/10.1146/annurev.mi.48.100194.001523.

Nijjer, S., Thonstad, J., Haarberg, G.M. 2000. Oxidation of manganese(II) and reduction of manganese dioxide in sulphuric acid, *Electrochimica Acta*, 46, 395-399. https://doi.org/10.1016/S0013-4686(00)00597-1.

Oberholster, P.J., Botha, A.-M., Cloete, T.E. 2006. Toxic cyanobacterial blooms in a shallow, artificially mixed urban lake in Colorado, USA, *Lakes and Reservoirs: Science, Policy and Management for Sustainable Use*, 11, 111-123. https://doi.org/10.1111/j.1440-1770.2006.00297.x.

O'Neil, J.M., Davis, T.W., Burford, M.A., Gobler, C.J. 2012. The rise of harmful cyanobacteria blooms: the potential roles of eutrophication and climate change, *Harmful Algae*, 14, 313-334. https://doi.org/10.1016/j.hal.2011.10.027.

Onset, 2019. HOBO Pendant Tamperature/Light Data Logger (UA-002-xx) Manual, [Online]. Available: https://www.onsetcomp.com/files/manual_pdfs/9556-M%20UA-002%20Manual.pdf. [Accessed 2020, 21st February].

Örnólfsdóttir, E.B., Lumsden, S.E., Pickney, J.L. 2004. Phytoplankton community growth-rate response to nutrient pulses in a shallow turbid estuary, Galveston Bay, Texas, *J. Plankton Res.*, 26, 325-339F. https://doi.org/10.1093/plankt/fbh035.

Osborn, T.R. 1980. Estimates of the local rate of vertical diffusion from dissipation measurements, *J. Phys. Oceanogr.*, 10, 83-89. https://doi.org/10.1175/1520-0485(1980)010<0083:EOTLRO>2.0.CO;2.

Oulhote, Y., Mergler, D., Barbeau, B., Bellinger, D.C., Bouffard, T., Bordeur, M.-E., Saint-Amour, D., Legrand, M., Sauvé, S., Bouchard, M.F. 2014. Neurobehavioural function in school-age children exposed to manganese in drinking water, *Environmental Health Perspectives*, 122, 1343-1350. https://doi.org/10.1289/ehp.1307918.

Paerl, H.W., Ustach, J.F. 1982. Blue-green algal scums: an explanation for their occurrence during freshwater blooms, *Limnology and Oceanography*, 27, 212-217. https://doi.org/10.4319/lo.1982.27.2.0212.

Paerl, H.W., Huisman, J. 2008. Blooms like it hot, *Science*,320, 57-58. https://doi.org/10.1126/science.1155398.

Paerl, H.W., Gardner, W.S., Havens, K.E., Joyner, A.R., McCarthy, M.J., Newell, S.E., Qin, B., Scott, J.T. 2016. Mitigating cyanobacterial harmful algal blooms in aquatic ecosystems impacted by climate change and anthropogenic nutrients, *Harmful Algae*, 54, 213-222. https://doi.org/10.1016/j.hal.2015.09.009.

Pancrace, C., Barny, M.-A., Ueoka, R., Calteau, A., Scalvenzi, T., Pedron, J., Barbe, V., Piel, J., Humbert, J.-F., Gugger, M. 2017. Insights into the *Planktothrix* genus: Genomic and metabolic comparison of benthic and planktic strains, *Scientific Reports*, 7, 41181. https://doi.org/10.1038/srep41181.

Park Y.-S., Chon T.-S., Kwak I.-S., Lek S. 2004. Hierarchical community classification and assessment of aquatic ecosystems using artificial neural networks, *Sci. Total Environ.*, 327, 105-122. https://doi.org/10.1016/j.scitotenv.2004.01.014.

Park, T.-J., Yu, M.-N., Kim, H.-S., Cho, H.-S., Hwang, M.Y., Yang H.-J., Lee, J.-C., Lee, J.-K., Kim, S.-J. 2014. Characteristics of actinomycetes producing geosmin in Paldang Lake, Korea, *Desalin. Water Treat.*, 57, 888-899.

Perkins, R.G., Underwood, G.J.C. 2001. The potential for phosphorus release across the sediment-water interface in an eutrophic reservoir dosed with ferric sulphate, *Wat. Res.*, 35, 1399-1406. https://doi.org/10.1016/S0043-1354(00)00413-9.

Perkins, R.G., Slavin, E.I., Andrade, T.M.C., Blenkinsopp, C., Pearson, P., Froggatt, T., Godwin, G., Parslow, J., Hurley, S., Luckwell, R., Wain, D.J. 2019. Managing taste and odour metabolite production in drinking water reservoirs: The importance of ammonium as a key nutrient trigger, *Journal of Environmental Management*, 244, 276-284. https://doi.org/10.1016/j.jenvman.2019.04.123.

Peter, A., Köster, O., Schildknecht, A., von Gunten, U. 2009. Occurrence of dissolved and particle-bound taste and odour compounds in Swiss lake waters, *Water Res.*, 43, 2191-2200. https://doi.org/10.1016/j.watres.2009.02.016.

Phlips, E.J., Aldridge, F.J., Schelske, C.L., Crisman, T.L. 1995. Relationships between light availability, chlorophyll a, and tripton in a large, shallow, subtropical lake, *Limnology and Oceanography*, 40, 416-421. https://doi.org/lo.1995.40.2.0416.

Post, A.F., Loogman, J.G., Mur, L.R. 1985. Regulation of growth and photosynthesis by *Oscillatoria agardhii* grown with a light/dark cycle, *FEMS Microbiology Ecology*, 31, 97-102. https://doi.org/10.1016/0378-1097(85)90005-9.

Precision Measurement Engineering Inc. 2017. Model SCAMP – Self-contained Autonomous Microprofiler, [Online]. Available: https://www.environmental-expert.com/products/pme-model-scamp-self-contained-autonomous-microprofiler-62608 [Accessed 2020, February 24].

Punnett, R.E. 1991. Design and Operation of Axial Flow Pumps for Reservoir Destratification, U.S. Army Corps of Engineers, Huntington, West Virginia.

Qin, B., Hu, W., Gao, G., Luo, L., Zhang, J. 2004. Dynamics of sediment resuspension and the conceptual schema of nutrient release in the large shallow Lake Taihu, China, *Chinese Science Bulletin*, 49, 54-64. https://doi.org/10/1007/BF02091743.

Radermacher, M., Van der Goot, F., Rijks, D.C., De Wit, L. 2013. The art of screening: Effectiveness of silt screens, *Terra et Aqua*, 132. http://resolver.tudelft.nl/uuid:47d189ec-7487-48b0-a2bd-80f512e3d817.

Rashash, D.M.C., Dietrich, A.M., Hoehn, R.C., Parker, B.C. 1995. The influence of growth conditions on odor-compound production by two chrysophytes and two cyanobacteria, *Water Sci. Technol.*, 31, 165-172. https://doi.org/10.1016/0273-1223(95)00472-Y.

Raveendran, R., Ashworth, B., Chatelier, B. 2001. Manganese removal in drinking water systems, In: *64th Annual Water Industry Engineers and Operators Conference*, 92-100.

Read, J.S., Hamilton, D.P., Desai, A.R., Rose, K.C., MacIntyre, S., Lenters, J.D., Smyth, R.L., Hnason, P.C., Cole, J.J., Staehr, P.A., Rusak, J.A., Pierson, D.C., Brookes, J.D., Laas, A., Wu, C.H. 2012. Lake-size dependency of wind shear and convection as controls on gas exchange, *Hydrology and Land Surface Studies*, 39. https://doi.org/10.1029/2012GL051886.

Reddy, K.R., Feijtel, T.C., Patrick, W.H. 1986. Effect of soil redox conditions on microbial oxidation of organic matter, In: Chen, Y., Avnimelech, Y. (eds.), *The role of Organic Matter in Modern Agriculture (Developments in Plant and Soil Sciences)*, 25, Springer, Dordrecht. https://doi.org/10.1007/978-94-009-4426-8_6.

Redfield, A.C. 1958. The biological control of chemical factors in the environment, *Am. Scientist*, 46, 1-221.

Rehmel, M.S. 2006. Field Evaluation of shallow-water acoustic Doppler current profiler discharge measurements. In: Proceedings of ASCE-EWRI Congress, May 21-25, Omaha, NE.

Reinart, A., Arst, H., Noges, P., Noges, T. 2000. Comparison of Euphotic Layer Criteria in Lakes, *Geophysica*, 36, 141-159.

Reynolds, C.S., Wiseman, S.W., Godfrey, B.M., Butterwick, C. 1983. Some effects of artificial mixing on the dynamics of phytoplankton populations in large limnetic enclosures, *Journal of Plankton Research*, 5, 203-234. https://doi.org/10.1080/00288330.1987.9516234.

Reynolds, C.S., Oliver, R.L., Walsby, A.E. 1987. Cyanobacterial dominance: The role of buoyancy regulation in dynamic lake environments, *New Zealand Journal of Marine and Freshwater Research*, 21, 379-390. https://doi.org/10.1080/00288330.1987.9516234.

Reynolds, C.S. 1994. The long, the short, and the stalled: on the attributes of phytoplankton selected by physical mixing in lakes and rivers, *Hydrobiologia*, 289, 9-21.

Richardson, L.L., Aguilar, C., Nealson, K.H. 1988. Manganese oxidation in pH and O_2 microenvironments produced by phytoplankton, *Limnology and Oceanography*, 33, 352-363. https://doi.org/10.4319/lo.1988.33.3.0352.

Richardson, J., Feuchtmayr, H., Miller, C., Hunter, P.D., Maberly, S.C., Carvalho, L. 2019. Response of cyanobacteria and phytoplankton abundance to warming, extreme rainfall events and nutrient enrichment, *Global change Biology*, 25, 3365-3380. https://doir.org/10.1111/gcb.14701.

Rogers, H.R. 2001. Factors causing off-taste in waters, and methods and practices for the removal of off-taste and its causes, Final report to the Department of the Environment, Transport and the Regions pp. 105-122 DETR/DWI 5008/1., 327.

Rosen, B.H., MacLeod, B.W., Simpson, M.R. 1992. Accumulation and release of geosmin during the growth phases of *Anabaena circinalis* (kutz.) rabenhorst. *Water Sci. Technol.*, 25, 185-190. https://doi.org/10.2166/wst.1992.0051.

Ruddick, B., Anis, A., Thompson, K. 2000. Maximum likelihood spectral fitting: The Batchelor Spectrum, *J. Atmos. Oceanic Technol.*, 17, 1541-1555. https://doi.org/10.1175/1520-0426(2000)017<1541:MLSFTB>2.0.CO;2.

Rukminasari, N., Redden, A. 2011. Growth response of natural phytoplankton to enrichment of urea and other forms of dissolved nitrogen, *Afr. J. Environ. Sci. Technol.*, 5, 1100-1116. https://doi.org/10.5897/AJEST11.192.

Rumsby, P., Clegg, H., Jonsson, J., Benson, V., Harman, M., Doyle, T., Rushton, L., Warwick, P., Wilkinson, D. 2014. Speciation of manganese in drinking water, *Toxicology Letters*, 229, S120. https://doi.org/10.1016/j.toxlet.2014.06.431.

Saadoun, I.M.K., Schrader, K.K., Blevins, W.T. 2001. Environmental and nutritional factors affecting geosmin synthesis by *Anabaena* sp., *Water Research*, 35, 1209-1218. https://doi.org/10.1016/S0043-1354(00)00381-X.

Saber, A., James, D.E., Hayes, D.F. 2018. Effects of seasonal fluctuations of surface heat flux and wind stress on mixing and vertical diffusivity of water column in deep lakes, *Advances in Water Resources*, 119, 150-163. https://doi.10.1016/j.advwatres.2018.07.006.

Sahoo, G.B., Schladow, S.G., Reuter, J.E., Coats, R. 2011. Effects of climate change on thermal properties of lakes and reservoirs, and possible implications, *Stoch Environ. Res. Risk Assess.*, 25, 445-456. https://doi.org/10.1007/s00477-010-0414-z.

Scanlan, D.J., Post, A.F. 2008. Aspects of marine cyanobacterial nitrogen physiology and connection to the nitrogen cycle, In: Capone, D.G., Bronk, D.A., Mulholland, M.R., Carpenter, E.J. (eds.), Nitrogen in the marine environment, Elselvier, 1073-1096.

Scheffer, M. 2004. *Ecology of Shallow Lakes*, Kluwer Academic Publishers, Dordrecht.

Selim, S.Z., Ismail, M.A. 1984. K-Means-Type Algorithms: A Generalized Convergence Theorem and Characterisation of Local Optimality, *IEEE Transactions on Pattern Analysis and Machine Intelligence*, PAMI-6. https://doi.org/10.1109/TPAMI.1984.4767478.

Seto H., Watanabe H., Furihata K. 1996. Simultaneous operation of the mevalonate and non-mevalonate pathways in the biosynthesis of isopentenyl diphosphate in *Streptomyces aeriouvifer, Tetrahedron Lett.*, 37, 7979-7982. https://doi.org/10.1016/0040-4039(96)01787-X.

Sherman, B., Whittington, J., Oliver, R. 2000. The impact of artificial destratification on water quality in Chaffey Reservoir. *Limnology and Lake Management*, 55, 15-29.

Skupin, A., Agarwal, P., 2008. Introduction: What is a Self-Organising Map? In: Agarwal, P., Skupin, A. (Eds.), Self-Organising Maps Applications in Geographic Information Science, John Wiley & Sons Inc., Chichester.

Sly, L.I., Hodgkinson, M.C., Arunpairojana, V. 1990. Deposition of manganese in a drinking water distribution system, *American Society for Microbiology Journals*, 56, 628-639.

Smith, V.H. 1983. Low nitrogen to phosphorus ratios favour dominance by blue-green algae in lake phytoplankton, *Science*, 221, 669-671. https://doi.org/10.1126/science.221.4611.669.

Stefanovič, P., Kurasova, O. 2011. Visual analysis of self-organising maps, *Nonlinear Analysis: Modelling and Control*, 16, 488-504. https://www.mii.lt/na/issues/NA_1604/NA16409.pdf.

Stepanenko, V.M., Martynov, A., Johnk, K.D., Subin, Z.M., Perroud, M., Fang, X., Beyrich, F., Mironov, D. Goyette, S. 2013. A one-dimensional model intercomparison study if thermal regime of a shallow, turbid midlatitude lake, *Geosci. Model Dev.*, 6, 1337-1352. https://doi.org/10.5194/gmd-6-1337-2013.

Sun, Y. 2000. On quantization error of self-organizing map network, *Neurocomputing*, 34, 169-193. https://doi.org/10.1016/S0925-2312(00)00292-7.

Suffet, I.H., Corado, A., Chou, D., McGuire, M.J., Butterworth, S. 1996. Taste and odour survey, *J. Am. Water Work Assoc.*, 88, 168-180. https://doi.org/10.1002/j.1551-8833.1996.tb06542.x.

Tammeorg, O., Niemistö, J., Möls, T., Laugaste, R., Panksep, K., Kangur, K. 2013. Wind-induced sediment resuspension as a potential factor sustaining eutrophication in large and shallow Lake Peipsi, *Aquatic Sciences*, 75, 559-570. https://doi.org/10.1007/s00027-013-0300-0.

Texas Boom Company (TBC), 2018. Permeable silt curtain vs. impermeable silt curtain, [Online]. Available: https://www.texasboom.com/news/permeable-and-impermeable-silt-curtain-comparison. [Accessed 14 October 2019].

Teledyne RD Instruments, 2015, StreamPro ADCP Guide, [Online]. Available: http://www.teledynemarine.com/Documents/Brand%20Support/RD%20INSTRUMENTS/Technical%20Resources/Manuals%20and%20Guides/StreamPro/StreamPro_ADCP_Guide_Sep15.pdf. [Accessed 30 October 2019].

Tobiason, J.E., Bazilio, A., Goodwill, J., Mai, X., Nguyen, C. 2016. Manganese removal from drinking water sources, *Current Pollution Reports*, 2, 168-177. https://doi.org/10/1007/s40726-016-0036-2.

Trimble, R.B., Ehrlich, H.L. 1970. Bacteriology of manganese nodules, *Applied Microbiology*, 19, 966-972.

Tsukada, H., Tsujimura, S., Nakahara, H. 2006. Seasonal succession of phytoplankton in Lake Yogo over 2 years: effect of artificial manipulation, *Limnology*, 7, 3-14. https://doi.org/10.1007/s10201-005-0159-4.

Upadhyay, S., Bierlein, K.A., Little, J.C., Burch, M.D., Elam, K.P., Brookes, J.D. 2013. Mixing potential of a surface-mounted solar-powered water mixer (SWM) for controlling cyanobacterial blooms, *Ecological Engineering*, 61, 245-250. https://doi.org/10.1016/j.ecoleng.2013.09.032.

Uriarte, E.A., Martín, F.D., 2005. Topology preservation in SOM, *Int. J. Math. Comput., Sci.*, 1, 19-22. https://doi.org/10.5281/zenodo.1062819.

USGS, 2011. Exposure time for ADCP moving-boat Discharge Measurements made during steady flow conditions. USGS Office of Surface Water technical Memorandum 2001.08.

Uwins, H.K., Teasdale, P., Stratton, H. 2007. A case study investigating the occurrence of geosmin and 2-methylisoborneol (MIB) in the surface waters of the Hinze Dam, Gold Coast, Australia, *Water Science and Technology*, 55, 231-238. https://doi.org/10.2166/wst.2007.184.

Valipour, R., Boegman, L., Bouffard, D., Rao, Y.R. 2017. Sediment resuspension mechanisms and their contributions to high-turbidity events in a large lake, *Limnology and Oceanography*, 62, 1045-1065. https://doi.org/10.1002/lno.10485.

Van der Ploeg, M., Dennis, M.E., de Regt, M.Q., 1995. Biology of *Oscillatoria* cf. *chalybea*, a 2-methylisoborneol prodavisoncducing blue-green alga of Mississippi catfish ponds, *Water Sci. Technol.*, 31, 173-180. https://doi.org/10.1016/0273-1223(95)00473-Z.

Vestano, J., Alhoniemi, E., 2000. Clustering of the self-organizing map, *IEEE Trans. Neural Netw.*, 11, 586-600.

Vigiak, O., Grizzetti, B., Udias-Moinelo, A., Zanni, M., Dorati, C., Bouraoui, F., Pistocchi, A. 2019. Predicting biochemical oxygen demand in European freshwater bodies, *Science of the Total Environment*, 666, 1089-1105. https://doi.org/10.1016/j.scitotenv.2019.02.252.

Visser, P.M., Ibelings, B.W., Bormans, M., Huisman, J. 2016. Artificial mixing to control cyanobacterial blooms: a review, *Aquatic Ecology*, 50, 423-441. https://doi.org/10.1007/s10452-015-9534-0.

Vu, T.T., Tan, S.K. 2010. Laboratory investigation of hydraulic performance of silt screens, *Journal of Hydrodynamics*, 22 (Suppl 1), 312-317. https://doi.org/10.1016/S1001-6058(09)60212-2.

Wagner, C., Adrian, R. 2009. Cyanobacteria dominance: Quantifying the effects of climate change, *Limnology and Oceanography*, 54, 2460-2468. https://doi.org/10.4319/lo.2009.54.6_part_2.2460.

Wagner, K.J. 2015. *Oxygenation and Circulation to Aid Water Supply Reservoir Management*, Water Resource Foundation, Denver.

Wallace, B.B., Bailey, M.C., Hamilton, D.P. 2000. Simulation of vertical position of buoyancy regulating *Microcystis aeruginosa* in a shallow eutrophic lake, *Aquatic Sciences*, 62, 320-333. https://doi.org/10.1007/PL00001338.

Walsby, A.E., Holland, D.P. 2006. Sinking velocities of phytoplankton measured on a stable density gradient by laser scanning, *Journal of the Royal Society Interface*, 3, 429-439. https://doi.org/10.1098/rsif.2005.0106.

Wang, Z., Xu, Y., Shao, J., Wang, J., Lli, R. 2011. Genes associated with 2-methylisoborneol biosynthesis in cyanobacteria: isolation, characterisation, and expression in response to light, *PLoS One*, 6, e18665. https://doi.org/10.1371/journal.pone.0018665.

Wang, Z., Huang, S., Li, D. 2019. Decomposition of cyanobacterial bloom contributes to the formation and distribution of iron-bound phosphorus (Fe-P): Insight for cycling mechanism of internal phosphorus loading, *Science of the Total Environment*, 652, 696-708. https://doi.org/10.1016/j.scitotenv.2018.10.260.

Watson, S.B. 2003. Cyanobacterial and eukaryotic algal odour compounds: signals or by products? A review of their biological activity, *Phycologia*, 42, 332-350.

Watson, S.B. 2004. Aquatic taste and odour: a primary signal of drinking water integrity, *J. Toxicol. Environ. Health A*, 67, 1779-1795. https://doi.org/10.1080/15287390490492377.

Watson, S.B., Ridal, J. 2004. Periphyton: a primary source of widespread and severer taste and odour, *Water Sci. Technol.*, 49, 33-39. https://doi.org/10.2166/wst.2004.0527.

Watson, S.B., Ridal, J., Boyer, G.L. 2008. Taste and odour and cyanobacterial toxins: impairment, prediction, and management in the Great Lakes, *Can. J. Fish. Aquat. Sci.*, 65, 1779-1796. https://doi.org/10.1139/F08-084.

Watson, S.B., Monis, P., Baker, P., Giglio, S. 2016. Biochemistry and genetics of taste- and odor-producing cyanobacteria, *Harmful Algae*, 54, 112-127. https://doi.org/10.1016/j.hal.2015.11.008.

WEARS Australia, 2019. ResMix 1000. [Online]. Available: https://www.wears.com.au/resmix-product-range/resmix-1000-2/. [Accessed 14 December 2019].

Weather Underground 2019. Weather Underground, [Online], Available: https://www.wunderground.com/ [Accessed 18 December 2019].

Webber, M.A., Atherton, P., Newcombe, G. 2015. Taste and odour and public perceptions: what do our customers really think about their drinking water? *Journal of Water Supply: Research and Technology-Aqua*, 64, 802-811. https://doi.org/10.2166/aqua.067.

Welch, E.B., Cooke, G.D. 2005. Internal phosphorus loading in shallow lakes: importance and control, *Lake and Reservoir Management*, 21, 209-217. https://doi.org/10.1080/07438140509354430.

Wert, E.C., Korak, J.A., Trenholm, R.A., Roasario-Oritz, F.L. 2014. Effect of oxidant exposure on the release of intracellular microcystin, 2-MIB, and geosmin from three cyanobacteria species, *Water Res.*, 52, 251-259. https://doi.org/10.1016/j.watres.2013.11.001.

Wetzel, R.G. 1983, *Limnology*, 2nd edn., CBS College Publishing, U.S.A.

Whitton, B.A., Potts, M. 2012. Introduction to the cyanobacteria, *Ecology of Cyanobacteria II*, 1-13. https://doi.org/10.1007/978-94-007-3855-3_1.

Wood, S.A., Heath, M.W., Holland, P.T., Munday, R., McGregor, G.B., Ryan, K.G. 2010. Identification of a benthic microcystin-producing filamentous cyanobacterium (Oscillatoriales) associated with a dog poisoning in New Zealand, *Toxicon*, 55, 897-903. https://doi.org/10.1016/j.toxicon.2009.12.019.

Wood, S.A., Borges, H., Puddick, J., Biessy, L., Atalah, J., Hawes, I., Dietrich, D.R., Hamilton, D.P. 2017. Contrasting cyanobacterial communities and microcystin concentration in summers with extreme weather events: insights into potential effects of climate change, *Hydrobiologia*, 785, 71-89. https://doi.org/10.1007/s10750-016-2904-6.

Woolway, R.I., Jones, I.D., Hamilton, D.P., Maberly, S.C., Muraoka, K., Read, J.S., Smyth, R.L., Winslow, L.A. 2015. Automated calculation of surface energy fluxes with high-frequency lake buoy data, *Environmental Modelling & Software*, 70, 191-198. https://doi.org/10.1016/j.envsoft.2015.04.013.

Wild, Jr., H.E., Sawyer, C.N., McMahon, T.C. 1972. Factors affecting nitrification kinetics, *Journal (Water Pollution Control Federation)*, 43, 1845-1854. www.jstor.org/stable/25037179.

Winston, B., Hausmann, S., Scott, J.T., Morgan, R. 2014, The influence of rainfall on taste and odour production in a south-central USA reservoir, *Freshwater Science*, 33, 755-764. https://doi.org/10.1086/677176.

Winter, J.G., DeSellas, A.M., Fletcher, R., Heintsch, L., Morely, A., Nakamoto, L., Utsumi, K. 2011. Algal blooms in Ontario, Canada: increase in reports since 1994, *Lake Reservoir Manag.*, 27, 107-114. https://doi.org/10.1080/07438141.2011.557765.

Wnorowski, A.U., Scott, W.E. 1990. Case histories of algal caused taste and odor problems in South African improvements, *Symposium of Southern African Society for Aquatic Scientists*, Bloemfontein, South Africa.

Wolk, C.P., Ernst, A., Elhai, J. 1994. Heterocyst metabolism and development. In: Bryant, D.A. (eds.), *The Molecular Biology of Cyanobacteria. Advances in Photosynthesis*, Springer, Dordrecht. https://doi.org/10.1007/978-94-011-0227-8_27.

Wu, J.-T., Jüttner, F. 1988. Differential partitioning of geosmin and 2-methlyisoborneol between cellular constituents in *Oscillatoria tenuis*, *Acrh. Microbiol.*, 150, 580-583. https://doi.org/10/1007/BF00408253.

Xuwei, D., Min, Q., Ren, R., Jiarui, L., Xiaoxue, S., Ping, X., Jun, C. 2019. The relationships between odors and environmental factors at bloom and non-bloom area in Lkae Taihu, China, *Chemosphere*, 218, 569-576. https://doi.org/10.1016/j.chemosphere.2018.11.121.

Xylem, 2019. EXO User Manual. [Online]. Available: https://www.ysi.com/File%20Library/Documents/Manuals/EXO-User-Manual-Web.pdf. [Accessed 27 February 2020].

Yang, Y., Wang, Y., Zhang, Z., Wang, W., Ren, X., Gao, Y., Liu, S., Lee, X. 2018. Diurnal and Seasonal variations of thermal stratification and vertical mixing in a shallow freshwater lake, *Journal of Meteorological Research*, 32, 219-232. https://doi.org/10.1007/s13351-018-7099-5.

You, B.-S., Zhong, J.-C., Fan, C.-X., Wang, T.-C., Zhang, L., Ding, S.-M. 2007. Effects of hydrodynamics on phosphorus fluxes from sediment in large, shallow Tiahu Lake, *Journal of Environmental Sciences*, 19, 1055-1060. https://doi.org/10.1016/S1001-0742(07)60172-7.

Zaw, M., Chiswell, B. 1999. Iron and Manganese dynamics in lake water, *Water Research*, 33, 1900-1910. https://doi.org/10.1016/S0043-1354(98)00360-1.

Zevenboom, W., de Groot, G.J., Mur, L.R. 1980. Effects of light on nitrate *limited Oscillatoria agardhii* in chemostat cultures, *Archives of Microbiology*, 125, 59-65. https://doi.org/10.1007/BF00403198.

Zhang, T.Z., Song, L., Chen, W. 2009. Effects of temperature and light on the growth and geosmin production of *Lyngbya kuetzingii* (Cyanophyta), *Journal of Applied Phycology*, 21, 279-285. https://doi.org/10.1007/s10811-008-9363-z.

Zhang, Y., Wu, Z., Liu, M., He, J., Shi, K., Zhou, Y., Wang, M., Liu, X. 2015. Dissolved oxygen stratification and response to thermal structure and long-term climate change in a large and deep subtropical reservoir (Lake Qiandaohu, China), *Water Research*, 75, 249-258. https://doi.org/10.1016/j.watres.2015.02.052.

Zic, K., Stefan, H.G. 1994. Destratification induced by bubble plumes, Turner, H.O., Wilhelms, S.C. (eds.), Technical Report W-94-3, U.S. Engineer Waterways Experiment Station, Vicksburg, MS.

Zimmerman, W.J., Soliman, C.M., Rosen, B.H. 1995. Growth and 2-methylisoborneol production by the cyanobacterium *Phormidium* LM689, *Water Sci. Technol.*, 31, 181-186. https://doi.org/10.2166/wst.1995.0433.

Zohary, T., Padisák, J., Naselli-Flores, L. 2010. Phytoplankton in the physical environment: beyond nutrient, at the end, there is some light, *Hydrobiologia*, 639, 261-269.

APPENDIX A.

Interview with Durleigh Reservoir Ranger

Interview conducted on 19 November 2019 with Paul Martin, a ranger who has worked at Durleigh Reservoir since 1989.

1. History of the reservoir

The reservoir was constructed in the 1930s just used as raw water for the cellophane factory, it initially was not used for drinking water purposes. When it was used as water supply for the factory the water level did not drop as considerably as it does now, with abstraction for drinking water supply. The water used in the factory was not treated, the raw water was abstracted and used in the factory (just filtered).

The water quality in Durleigh originally was clear water, with lots of weeds/underwater plants. Maintaining the higher water levels helped sustained underwater plant life. The water was clear enough you could see basically to the sediments. Down the shallower end of the reservoir, there were lots of weeds, the water was crystal clear, and it was a very good trout fishery. There would only have been the natural run off and the Durleigh Brook inflow, so it was pretty clean and there was no silt build up.

The canal inlet was installed in the 1970s. The canal is filled with River Tone water. The problems for the water quality and the fishing began in the 1970s when the reservoir was altered from drinking water use and started pumping in canal water. The pumped canal inlet was installed when the reservoir was upgraded to drinking water as the levels were going to drop due to abstraction in the summer. The levels needed to be maintained to a certain extent as the flow into the treatment works is gravity fed and requires sufficient head, so if the levels dropped too low, water wouldn't push through to the treatment works effectively.

Keeping the lake level high, even though it is expensive to pump from the canal, dilutes the effect of high nutrient loading when mixed with a greater water volume than when mixed with a lake of reduce level and volume. Also, the weed died from the drop in water level and a bit from the turbidity. Primarily the weed diminished because the level dropped so much from abstraction and not enough pumping.

Pumping of the canal is expensive and turning the canal inlet on is only really done when it is needed to save costs. By the mid-1980s the reservoir had already changed from a clear water, macrophyte environment to a turbid, no under water plant environment. This affected the trout fishing, which became no longer viable. The 1980s was probably the worse water quality the reservoir has ever experienced.

Although the water quality from the canal inlet has improved marginally from what it used to be, certainly since the 1990's when more legislation came in about what farmers could and couldn't put on the fields, and at what time of year they could do certain processes. There have still been years of high nutrient loading before that. Compared to

the 1970s the water entering via the canal inlet is a lot cleaner. Although the canal water still has high loadings of nitrates and phosphates.

There is a concrete channel that runs perpendicular from the dam out across around 1/3 of the lake. The purpose of the channel is for the scour valve, whereby the scour valve would open and draw through the built-up sediments within that channel and flush them out. To reduce the build-up of silt and sediments in the deepest part of the reservoir. Over the years the use of the scour valve has reduced due to legislation on letting silt downstream. They can now only open the scour twice a year now and that must relate to dam inspections and checking. We also know from the divers that there is around 3-4 ft of silt built up in the deeper parts of the reservoir.

The brook water entering the reservoir is considerably cleaner than that entering via the canal inlet. The brook has been at lower levels over more recent years compared with when I started. It has never fully dried out, the flow does reduce to just a trickle in the summer, but it has never completely dried up. Since I have started there is now less water naturally coming through from the Brook. There have been no obvious changes in the Durleigh Brook catchment. There is no obvious pressure from the catchment for the brook, it is mainly an arable catchment with some livestock but not very much.

2. Artificial mixing of the reservoir

The airline has been installed for the entire time I have been here. It was turned off for a while and I think the algae numbers increased when the airline was not on, and from what the scientist at the time said, they also confirmed that was likely the case. When the airline was installed, they had to have a concrete block that raised the pipeline up about 4 ft to prevent it being sat in the silt. The airline was only operated when required due to the expense of operating. Because of the amount of power and energy the airline used was one of the reasons why it fell out of favour.

When the mixers were installed, and the airline was operating until the mixers were turned off. The airline was turned off as the mixers were turned on. Since the mixers were installed, other than the silt clouds around the mixers that appeared, there were no other notable changes in the visible water quality.

When the mixers were turned on, there were 3 obvious sediment clouds at the surface really close to each of the mixers. It looked like the mixers were causing sediment resuspension to the surface.

I think the algae problem has got worse since the mixers were installed, and I spoke to a scientist and they also indicated that was the case. Yes, the mixers did resolve some problems, but they also encouraged algal growth. Especially near the dam. They are not as good on the algae as the airline was and I have also heard that from several people now. The airline was much more effective at turning the lake over and reducing algae blooms. The mixers have not been as effective as that and algae have been more prominent as a result.

Moving one mixer inside the silt curtain, it was decided to move one inside the curtain to reduce the soluble manganese entering the water treatment plant. Since the installation of the silt curtain, there was also a massively noticeable colour difference between the water inside the silt curtain with that outside. Even when the algae in the main reservoir had declined there is sometimes still a noticeable green colour to the

water inside the silt curtain. Also putting your hand in the water inside the silt curtain compared to outside, you can feel a notable difference in temperature too, with it being warmer inside the silt curtain. In the (treatment) plant they have noticed there are more algae on the filters now and they clog a lot quicker than before.

3. Water quality issues

When I started there used to be massive algae blooms of both blue-green and brown algae, and they were much more visual, much more obvious, with scums on the surface. So, although the water quality is still poor, Durleigh is currently a lot cleaner and better water quality now compared with back when I started. The water quality has started to gradually improve because of the increased legislation about what farmers can put on their fields in the catchment (canal catchment mainly). What time of year fertilisers went on and calculate the best times of year to pump around these events so as to reduce the nutrient loading. Although it gets trickier in drier years when water is scarce anyway and the pumping is needed regardless.

Since I started the algae problem seems to have improved, although in the last few years it has started to get worse again. Not as bad as it was but I do think it has got worse.

Since the installation of the silt curtain, the algae population inside has exploded. The coarse fish remain inside the curtain. The water quality of the raw water entering the treatment works is worse since the silt curtain went in.

Removing the silt has become such a big problem because it is expensive to remove and get it taken away as the silt is classified as contaminated now. The silt/sediments from Durleigh used to be removed from the reservoir and given back to farmers to put on their land. Effectively returning the fertilisers back to where they came from. That has stopped due to the contaminated status of the silt now.

A scientist studied the sediments at Durleigh and reported there are so many nutrients locked up in the silt/sediments at Durleigh now it will take years and years for that to break down. The high content in the sediments is most probably due to high nutrient loading from the canal inflow. What is actually in the silt and what it is made up of was the focus of a previous study in Durleigh.

Problems with the sediments have been recognised for some time, with the build-up of sediments/silt, but how to deal with the problem is very complicated.

4. Meteorological patterns and climate

Refilling of the reservoir needs prolonged rain events to make notable increases in water level. Run off into the reservoir at the beginning of the year typically occurs up until ~April from which it slows down as the water table drops and rain after that doesn't really have much of an effect, unless there is a really large storm event. Generally, the trend in the summer is for the level to continue dropping. It used to be around June that the canal inlet would be turned on. At that point in time the level would have dropped about 5-6 ft and pumping would be needed to maintain the level, particularly as demand has increase over the years too, there was need to hold it at that level.

In the last few years weather patterns have seem to have changed and although it is hard to nail down, I do think we have seen more extreme weather in more recent years.

Generally, we are in quite a dry period and are getting slightly drier over time. At the end of the year after pumping and abstraction, in the last 4/5 years we seem to be at record low water levels. With the dry periods too. At the end of the year in the autumn for the last 4/5 years we have had very low water levels and as well as pumping and abstraction, I think that's also down to drier summers in general too.

Generally, the water quality always seems to be much better during windy conditions compared to still days.

The large algae blooms in the 90's were much bigger than now a days, but they were more freak events, for example only occurring during really hot summers.

5. Recreation: fisheries and sailing

Before they put the canal inlet in, there was virtually no silver fish in the lake or coarse fish, which is another reason why it was such a successful trout fishery, as they basically had it to themselves (apart from a few pike). Clean water and a full reservoir also benefited the trout. The silver fish and coarse fish probably got in because of the canal inlet. As the water quality deteriorated, where the waters got warmer and dissolved oxygen concentrations declined, the trout struggled to survive, and they couldn't compete with the growing abundance of coarse fish. Predation now helps to keep a level of coarse fish, but there is still a lot of coarse fish in there now. Before, when they didn't allow any predation the roach took over and potentially caused water quality decline too as the pressure from the fish number on zooplankton populations won't have helped in terms of grazing phytoplankton and keeping those numbers down.

At times in the past there have been fish kills.

There were ideas that the fish might have been responsible for re-suspending the sediments. They do re-suspend the sediments to a certain extent but nowhere near the scale of the mixers and the fish do not increase the turbidity to change the levels entering the treatment works significantly.

Since the installation of the silt curtain and operation of the surface mixer inside the silt curtain the rangers and scientists have seen more of the bottom feeding fish frequently at the surface feeding, indicating that the food is at the surface of the water column.

Activity on the lake in terms of recreation has increased. Fishing has become more popular and the sailing club has grown in numbers, which keeps species like the geese and great crested grebes at lower levels.

6. Wildlife

There has been an increase in the number of waders in the reservoir, for example, herons and egrets. There has been a big increase in the number of waders, and I think that is a result of the general trend of lower water levels, which increases their access to available habitat. As the level drops, there is a larger area for the waders to wade in. Also, as the level drops you are condensing the area in which the fish are. There are a lot of fish in the reservoir anyway, but by reducing the level and the volume of the water they are in, that increases fish per unit water. So it makes it easier for the birds to catch fish too.

7. Other changes in the reservoir

In the past there was an experiment where barley straw was installed in the reservoir. The amount of barley straw that was proposed to combat the phytoplankton cell counts would have been so much, there would be no way that sailing or fishing could have taken place. The compromise was to put a line of barley straw at the shallower end of the reservoir to not impede on fishing and sailing activities so much and use the prevailing wind to mix the decomposed chemicals into the reservoir. But in the summer the drop in water level left the barley straw dispensers out of the water, in the summer when it is needed the most.

There has been some erosion around the banks, but no more than what you would expect over time. Where the old road used to be in the shallow part of the reservoir, when the level dropped it used to be much more prominent. But now there seems to be a lot more silt over it and it's a lot less obvious when the level drops. Since I've been here it looks to me as if there is about half a foot of silt more that has built up from the old road back. Over the years there has been a little bit of bank erosion.

8. Other comments

The ideal situation would be to maintain higher water levels in the reservoir, have underwater plants. But when it comes down to producing water for the best possible price and to keep regulators happy, it is a hard sell to keep pumping water in when the level has only dropped a bit and its expensive to pump water in.

Now the reservoir has been taken offline and the canal inlet is not being used to pump water in because the level should not vary as drastically over the next couple of years while the treatment works is being updated, would be a good time to turn the mixers off and see what happens in the lake when its left as is. To assess what is like in as close to a natural system as you can get now.